

Université de Montréal

**Expanding and Defining Human Hematopoietic Stem
and Progenitor Cells *Ex Vivo* Using Small Molecules**

By

Iman Hatem Fares

Programme de Biologie Moléculaire

Faculté de Médecine

*Thèse présentée à la Faculté de médecine
en vue de l'obtention du grade de Docteur
en biologie moléculaire,
option biologie des systèmes*

April 2016

©Fares, 2016

Résumé

Le terme de cellules souches hématopoïétiques (CSH) désigne une population rare de cellules capables de générer l'ensemble des lignages hématopoïétiques. Cette définition implique une capacité d'auto-renouvellement, ainsi qu'un potentiel de prolifération et de différenciation important. La greffe de cellules souches hématopoïétiques est aujourd'hui une modalité thérapeutique pour le traitement de diverses maladies hématologiques et représente pour de nombreux patients un traitement de dernier recours. Malheureusement, le nombre limité de ces cellules dans une unité de sang de cordon est à l'origine du faible taux de réussite des greffes de sang de cordon chez l'adulte. Plusieurs stratégies sont actuellement mises en place pour permettre la multiplication de ces CSH *ex vivo*. Cependant, Il n'y a jusqu'à ce jour aucun critère ou marqueur phénotypique fiable permettant spécifiquement d'identifier ou d'isoler ces CSH amplifiées, et leur caractérisation reste un défi majeur pour les chercheurs. Dans le laboratoire, nous avons effectué un criblage à haut débit afin de tester le potentiel d'un grand nombre de molécules chimiques à multiplier des cellules souches dérivées de sang de cordon ombilical et nous avons ainsi identifié la molécule UM171, un dérivé pyrimido-indole, qui permet de multiplier par 10 le nombre de CSH et par 100 leur descendance. Nous avons démontré qu'UM171 permet de multiplier les CSH sans affecter la voie de signalisation de la protéine AhR, récemment impliquée dans l'auto-renouvellement des CSH. L'analyse du transcriptome des CSH exposées à la molécule UM171 a permis d'identifier le récepteur endothélial à la protéine C (EPCR), comme marqueur de surface permettant de prédire le nombre et l'activité des CSH en culture et par conséquent de les isoler et de mieux les caractériser. En combinant des techniques de cytométrie de flux et d'ARN interférents avec des expériences de transplantation à long terme dans des souris immuno-déficientes, nous avons pu démontrer qu'EPCR peut être considéré non seulement comme un premier marqueur fiable pour enrichir les CSH en culture mais aussi qu'il est nécessaire pour la fonction de ces CSH *in vivo*. Les résultats de ces travaux représentent une avancée majeure pour accélérer les recherches et les applications cliniques sur l'expansion des CSH *ex vivo* et permettra de comprendre les mécanismes moléculaires qui régissent l'auto-renouvellement des CSH.

Mots-clés: Sang de cordon, cellules souches hématopoïétiques, auto-renouvellement, molécule, marqueur de surface

Abstract

Human hematopoietic stem cells (HSCs) are defined by their capacity to self-renew and to differentiate into all blood lineages during an adult lifetime. Based on these unique properties, HSCs are used in transplantation procedures to treat various hematological diseases. However, the low number of HSCs in a graft limits the use of this treatment. To overcome this restraint, different approaches were established to expand HSCs *ex vivo*; yet, the absence of a reliable surface marker that correlates with HSC activity in culture made the assessment labor-intensive and time-consuming. Using a library of small molecules, we were able to identify pyrimidoin-dole derivative named UM171 as an agonist for HSC self-renewal. UM171 promotes *ex vivo* expansion of hematopoietic and stem cell progenitors (HSPC) independently of AhR suppression- a pathway reported by Boitano et al. to have the greatest effect in HSC expansion. Unlike AhR suppression that targets a hematopoietic population with limited proliferative potential, UM171 targets the long-term HSCs. Transcriptome analysis showed that UM171 reduces the levels of transcripts associated with lineage differentiation and induces the expression of genes encoding for membrane proteins, one of the best differentially expressed being the endothelial protein c receptor (EPCR). Cell sorting and transplantation experiments of EPCR expressing cells showed a high correlation with HSC activity. We demonstrated EPCR as a first reliable marker to enrich for HSC in culture and that it is required for HSPC function *in vivo*. These findings provide a valuable tool for clinical and research applications to optimize further HSPC expansion protocols and understand the molecular machinery that governs the HSC self-renewal.

Keywords: Cord blood, hematopoietic stem cell, self-renewal, small molecule, surface marker

Table of Contents

Chapter 1: Introduction	1
1.1 Model of hematopoiesis	2
1.2 Molecular regulation of HSPC	2
1.3 Origin of human HSPC	5
1.4 Functional assays for human HSPC	6
1.4.1 In vitro assays	6
1.4.1.1 Colony forming unit assay	6
1.4.1.2 Long-term culture initiating cell (LTC-IC) assay	8
1.4.2 In vivo assays	8
1.4.2.1 SCID repopulating cell (SRC)	10
1.4.2.2 Quantifying SRC using limiting dilution assay	10
1.4.2.3 Xenograft models used to assess the SRC	10
1.4.2.4 Distinct classes of SRC	13
1.5 Phenotype of human HSC	13
1.5.1 Lineage depletion (Lin-)	13
1.5.2 CD34 antigen	16
1.5.3 CD38 antigen	16
1.5.4 Rhodamine 123	16
1.5.5 CD45RA antigen	17
1.5.6 CD90 antigens	17
1.5.7 CD49f antigen	17
1.5.8 Other antigens	19
1.6 Phenotype of human hematopoietic progenitor cells	19
1.7 Sources of human HSPCs and their functional differences	19

1.8 Clinical applications of HSPC	20
1.8.1 Cord blood stem cell transplantation	20
1.9 Clinical strategies to improve homing and expansion of CB grafts	22
1.9.1 Homing	22
1.9.1.2 Dipeptidyl peptidase (DDP4 or CD26)	26
1.9.1.2 prostaglandin E2 (PGE2)	26
1.9.1.3 Fucosylation	26
1.9.2 Ex vivo expansion	27
1.9.2.1 Cytokines and growth factors	27
1.9.2.2 Fed batch culture	27
1.9.2.3 Mesenchymal stromal cell coculture	28
1.9.2.4 Delta 1 ligand	28
1.9.2.5 Small molecules	28
1.9.2.5.1 StemRegenin1 (SR1)	29
1.9.2.5.2 Tetraethylenepentamine (TEPA) and Nicotinamide (NAM)	29
1.9.2.3 Other approaches	30
1.10 Impact of improved CB graft	30
1.11 Hypothesis and Main Objectives	32
References	33

Chapter 2: Pyrimido-Indole Derivatives Are Agonists of Human Hematopoietic Stem Cell Self-renewal 46

Abstract 48

2.1 Introduction 49

2.2 Results and Discussion 49

2.2.1 Finding novel agonists that expand human CD34⁺CD45RA⁻ cells 49

2.2.2 Optimizing culture conditions: UM171 and fed-batch system 50

2.2.3 UM171 and SR1 cooperation on CB progenitor cells	50
2.2.4 LT-HSC expansion in presence of UM171	51
2.2.5 Evaluation of UM171 mode of action	52
2.3 Conclusion	53
Acknowledgments	53
References	58
Supporting Material	60
Chapter 3: EPCR expression defines the most primitive subset of expanded human HSPCs and is required for their in vivo activity	84
Abstract	86
3.1 Introduction	87
3.2 Results	87
3.2.1 EPCR ⁺ population exhibits a robust multi-lineage differentiation potential	87
3.2.2 EPCR ⁺ cells provide multi-lineage reconstitution in secondary mice	88
3.2.3 High frequency of human LT-HSCs in EPCR ⁺ fraction	89
3.2.4 EPCR best discriminates expanded CD34 ⁺ HSPC	89
3.2.5 EPCR as a marker of non-expanded LT-HSC	90
3.2.6 EPCR expression is critical for HSPC function	90
3.2.7 HSPC gene signature characterizes EPCR ⁺ cells	90
3.3 Discussion	91
3.4 Conclusion	91
Acknowledgments	91
Reference	101
Supporting Material	103

Chapter 4: Discussion and Future Perspective	130
4.1 Limitation of cord blood HSC transplantation	131
4.2 UM171 mediates expansion of LT- HSC independent of AhR inhibition	131
4.3 UM171 applications	133
4.4 Chemical manipulation of the hematopoietic system is a powerful tool	133
4.5 UM171 treatment induces expression of EPCR, a surface marker that enrich for LT-HSC	137
4.6 EPCR, a stable and reliable LT-HSC surface marker	137
4.7 Human and mouse HSCs, similar need during ex vivo culture	138
4.8 Role of EPCR in HSC activity	138
4.9 Endothelial-related markers of EPCR ⁺ population and origin of HSC	140
4.10 Stemness genetic feature of EPCR population	140
References	143
Conclusion	146

List of Figures

Figure 1.1. Model of human hematopoietic hierarchy.	3
Figure 1.2. Molecular regulation of hematopoietic stem cell.	4
Figure 1.3. Human hematopoiesis during fetal and adult life.	7
Figure 1.4. Assays used to study function of human HSPCs.	9
Figure 1.5. Clonal growth and differentiation dynamic of primitive human hematopoietic cell types in immunodeficient mice.	14
Figure 1.6. Required HSPC activities for a successful cord blood transplantation.	25
Figure 1.7. Schematic view of HSPC expansion.	31
Fig. 2.1. Identification of novel compounds promoting human CD34 ⁺ expansion.	54
Fig. 2.2. UM171 attenuates cell differentiation and promotes ex vivo expansion of primitive human hematopoietic cells.	55
Fig. 2.3. UM171 promotes expansion of LT-HSCs.	56
Fig. 2.4. Summary of UM171 effect on cell expansion and differentiation.	57
Fig. S2.1. Screen setup and hit validation strategy for identifying small molecule(s) that promotes ex vivo expansion of human CD34 ⁺ cells.	67
Fig. S2.2. Chemical structure of two non commercially-available compounds that were selected as hits in the secondary screen.	68
Fig. S2.3. Characterization of UM171 and optimization of fed-batch conditions.	69
Fig. S2.4. UM729 has no effect on expanding murine HSCs.	70
Fig. S2.5. UM729 and UM171 enhance the engraftment potential of macaque CD34 ⁺ CB expanded cells.	71
Fig. S2.6. UM171 is not a mitogen and its effect in expanding CD34 ⁺ and CD34 ⁺ CD45RA ⁻ is reversible.	72

Fig. S2.7. UM171 does not affect division rate of CD34 ⁺ CD45RA ⁻ cells.	73
Fig. S2.8. UM171 expansion protocol is readily reproduced in independent laboratories.	74
Fig. S2.9. UM171-treated CD34 ⁺ cells remain phenotypically primitive in culture.	75
Fig. S2.10. UM171 promotes expansion of LT-HSC in fed-batch culture of CD34 ⁺ CB cells.	76
Fig. S2.11. Comparative transcriptome analysis of CD34 ⁺ cells exposed to UM171 or to SR1.	77
Fig. S2.12. List of differentially expressed genes in CD34 ⁺ CB cells exposed to UM171 or to SR1.	78
Fig. S2.13. PROCR (EPCR or CD201) gene and protein expression in response to UM171.	79
Fig. 3.1. EPCR ⁺ population is enriched with LT-HSC in culture.	94
Fig. 3.2. Frequency of LT-HSC within EPCR ⁻ , EPCR ^{Low} and EPCR ⁺ populations.	95
Fig. 3.3 Expanded EPCR ⁺ progeny retains the most of the ex vivo HSPC expanded cells.	97
Fig. 3.4 Loss of EPCR expression in CD34 ⁺ cells compromise their engraftment ability in NSG mice.	98
Fig. 3.5. Gene expression profiling of cultured EPCR ⁺ population strongly correlates with uncultured HSC-related genes.	100
Fig. S3.1. Cultured CD49 ^{high} CD34 ⁺ CD45RA ⁻ cells lack in vivo repopulation potential.	109
Fig. S3.2. EPCR is a universal surface marker for LT-HSC in culture.	110
Fig. S3.3. CD34 ⁺ CB cells expanded with UM171 retain higher levels of EPCR surface marker expression than those expanded with SR1.	111
Fig. S3.4. Limit dilution assay performed on different EPCR cellular fractions (-, low, and +).	112
Fig. S3.5. In vivo proliferative outcome of different HSPC populations sorted after culture.	113
Fig. S3.6. Uncultured EPCR ^{low} and EPCR ⁺ population are the fractions enriched with LT-HSC.	

	115
Fig. S3.7. Loss of EPCR expression in CD34 ⁺ cells compromise their engraftment ability in NSG mice.	116
Fig. S3.8. EPCR ⁺ population shares genetic features with highly purified primitive hematopoietic cells.	117
Figure 4.1. Schematic representation showing effects of UM171 and SR1 on different cell population.	132
Figure 4.2. Comparing effect of UM171, SR1 and DMSO on hematopoietic stem cell (HSC) and leukemia stem cell (LSC) expansion.	134
Figure 4.3. Phase I/II trial of StemRegenin-1 (SR1) expanded cord blood HSPC.	135
Figure 4.4. UM171 increases lentiviral vector transduction efficiency in human HSPC cells.	136
Figure 4.5. UM171 expands mouse HSCs.	139
Figure 4.6. EPCR ⁺ population retains endothelial phenotype.	141

List of Tables

Table 1.1 Development of immunodeficient mouse models for studying human HSPC function.	12
Table 1.2. SRC frequency of different hematopoietic populations derived from human CB cells.	15
Table 1.3. Cell surface phenotypes of different human hematopoietic stem and progenitor populations.	18
Table 1.4. Comparing frequencies of CD34+ cells, Colony forming unit- granulocyte/monocyte (CFU-GM), long-term culture-initiating cells (LTC-IC) and SCID repopulating cell (SRC) in cord blood (CB), bone marrow (BM), and mobilized peripheral blood (mPB).	21
Table 1.5. . Strategies that enhance HSPC homing and expansion.	23
Table 1.6. Outcome of the approaches used in clinical cord blood transplantation trials.	24
Table S2.1. Limit dilution analysis of NSG engraftment at 20 weeks post-transplantation.	80
Table S2.2 (In vivo data analyzed at week 20 and week30 post-transplantation presented as heat-map)	81
Table S2.3. Limit dilution analysis of NSG engraftment at 30 weeks post-transplantation.	82
Table S2.4. Results from secondary transplantation experiments.	83
Table S3.1: Bone marrow aspiration data of NSG mice injected with different EPCR subsets sorted at day7 from UM171 cultures (page 1/3).	118
Table S3.2: Bone marrow aspiration data of NSG mice injected with different EPCR subsets sorted at day3 from DMSO cultures	121
Table S3.3: EPCR ⁺ cells provide multi-lineage reconstitution in secondary mice.	122
Table S3.4: Limit dilution experiment of different EPCR subsets sorted at day7 (page 1/4).	123
Table S3.5: Limit dilution experiment of uncultured sorted cells (page 1/2).	127
Table S3.6: Differentially expressed genes between EPCR ⁺ and EPCR ^{low/- (Rest)}	129
Table 4.1. EPCR ⁺ population is enriched with transcripts coding for surface markers and tran-	

scription factors that define and regulate HSC activity.

142

Abbreviations

ACE	Angiotensin I Converting Enzyme
Angpt1	Angiopoietin
AGM	Aorta-Gonad-Mesonephros
AhR	Aryl hydrocarbon Receptor
AhRR	Aryl hydrocarbon Receptor Repressor
BFU-E	Burst-Forming Unit–Erythroids
BM	Bone Marrow
BMT	Bone Marrow Transplantation
CB	Cord Blood
CBT	Cord Blood Transplantation
CBU	Cord Blood Unit
CFC	Colony Forming Cell
CFU	Colony Forming Unit
CMP	Common Myeloid Progenitor
DDP4	Dipeptidyl peptidase
EPCR	Endothelial Protein C Receptor
ESC	Embryonic Stem Cell
FB	Fed-Batch
FL	Fetal Liver
FLT3	Fms-Like Tyrosine Kinase 3
FTVI	FucosylTransferase VI
G-CSF	Granulocyte-colony stimulating factor
GDP	Guanosine DiPhosphate
GFI1	Growth Factor Independent 1
GM-CSF	Granulocyte-Macrophage Colony-Stimulating Factor
GMP	Granulocyte monocyte progenitor
GVHD	Graft vs. Host Disease
HES1	Hes Family BHLH Transcription Factor 1
HLA	Human Leukocyte Antigen
HLF	Hepatic Leukemia Factor
HSC	Hematopoietic Stem Cell
HSCT	Hematopoietic Stem Cell Transplant
HSPC	Hematopoietic stem and progenitor cells
IL3	InterLeukin 3
IL6	InterLeukin 6
IGFBP-2	Insulin-like Growth Factor Binding Protein-2
iPS	induced Pluripotent Stem cell

Lin	Lineage
LTC	Long-Term Culture
LTC-IC	Long-Term Culture- Initiating Cell
LT-HSCs	long term-repopulating hematopoietic stem cells
MCP1	Monocyte Chemotactic Protein-1
MDR	MultiDrug Resistance
MEP	Myeloid Erythroid Progenitor
MIP-1 α	Macrophage Inflammatory Protein-1 α
MLP	MultiLymphoid Progenitor
MPP	Multipotent Progenitors
mPB	mobilized Peripheral Blood
NAM	Nicotinamide
NK	Natural Killer
NSG	Nod Scid Gamma
PAX5	Paired box 5
PGE2	ProstaGlandin E2
P-gp	P-glycoprotein
PROM1	Prominin 1
PTN	Pleiotrophin
Rag1	Recombination Activating Gene 1
Rag2	Recombination Activating Gene 2
Rho	Rhodamine 123
SCF	Stem Cell Factor
SCID	Severe Combined ImmunoDeficient
SDF1	Stromal Derived Factor-1
Sh-HSCs	short term- hematopoietic stem cells
SIRPa	Signal Regulatory Protein alpha
SR1	StemRegenin
SRC	SCID Repopulating Cell
TEPA	Tetraethylenepentamine
TGF β	Transforming Growth Factor- β
TNF α	Tumor Necrosis Factor- α
TPO	Thrombopoietin
VCAM1	Vascular Cell Adhesion Molecule-1
YS	Yolk Sac

To my beloved nephew and niece,

Jad and Celine

Acknowledgements

I would to thank my supervisor, Dr. Guy Sauvageau, for his guidance throughout the years spent in his laboratory. His scientific vision has been essential for the success of the work presented in this thesis.

Science is about teamwork as all the pain and joy that accompany this hard work has to be shared with someone. I have been fortunate to be mentored by Dr. Jalila Chagraoui, an exceptional and outstanding scientist. Together, for the last 5 years, we shared our thirst for knowledge and with a lot of fun and excitement; we were constantly developing our scientific learnings to move our research forward. Thank you for bringing the best out of me.

I also want to thank the laboratory assistants especially Nadine Mayotte who was always there to help and the lab members for their scientific discussions and memorable experience.

My wholehearted recognition goes to my family: Hatem, Ghada, Ahmad, Nada, Mohammad, and Abir for constantly believing in me and for their warm support in spite of the vast distance between us. A special thanks for my sweetheart Joseph and my friends Fadi, Gloria, Kamal, Randa, and Aline who shared my PhD journey.

Chapter 1: Introduction

1.1 Model of hematopoiesis

Blood is a highly regenerative tissue where one trillion cells of various lineages are produced daily in human bone marrow (BM). These cells are present at various stages of differentiation and are organized in a cellular hierarchy deriving from one common precursor, a hematopoietic stem cell (HSC) (Figure 1.1). To ensure the blood homeostasis throughout the lifetime of a human being, HSC has to maintain a balance between self-renewal and multi-lineage differentiation. As HSCs differentiate, they give rise to two downstream progenies: multilymphoid progenitor (MLP) and common myeloid progenitor (CMP). The MLP produces all the lymphoid cells (T-, B-, and natural killer (NK)) as well as macrophage-dendritic cell progenitors¹. The CMP generates dendritic cells, monocytes, granulocytes (neutrophils, eosinophils, basophils, and mast cells), erythrocytes and megakaryocytes. The choice in cell fate is controlled by a complex network of signaling pathways and transcription factors.

1.2 Molecular regulation of HSPC

Global transcriptional analysis of different human hematopoietic populations (HSCs, multipotent progenitors MPP, and differentiated cells) shows distinct gene expression patterns as the cells progress from HSC to various blood lineages^{2,3}. A small list of these transcription factors is shown in Figure 1.2. BMI1, a polycomb-group gene, is one of the transcription factors that guard the hematopoietic stem and progenitor cells (HSPC) from apoptosis. Ectopic expression of BMI1 in human HSPCs increases the stem cell pool⁴, while suppressing BMI1 impairs HSC self-renewal potential⁵; thus, highlighting the critical role of BMI1 in maintaining HSPC fate. HLF and HES1 are two other key transcription regulators expressed at high levels in human HSPC. Overexpression of HLF or HES enhances stem-cell frequency by activating cell cycle and inhibiting apoptosis of HSC⁶. The tumor suppressor gene, p53, also plays an essential role in preserving HSC integrity. Human HSCs exhibit enhanced p53-dependent apoptosis after stress conditions of DNA damage to maintain their genomic integrity. Although p53 deletion reduces apoptosis, it significantly compromises the HSC extensive self-renewal capacity possibly due to accumulated DNA damage⁷. GF11 is one of the p53 target genes that restricts HSCs proliferation and maintains their quiescence state⁸. GF11 also has an essential role in lineage specification where it regulates myeloid and lymphoid development⁹.

In mouse, several transcription factors have also been shown to regulate HSC maintenance and self-renewal. Prdm16 is one of the transcription factors that promotes HSC survival by modulating oxidative stress^{10,11}. Also, the homeobox Hoxb4 is of particular interests since it expands

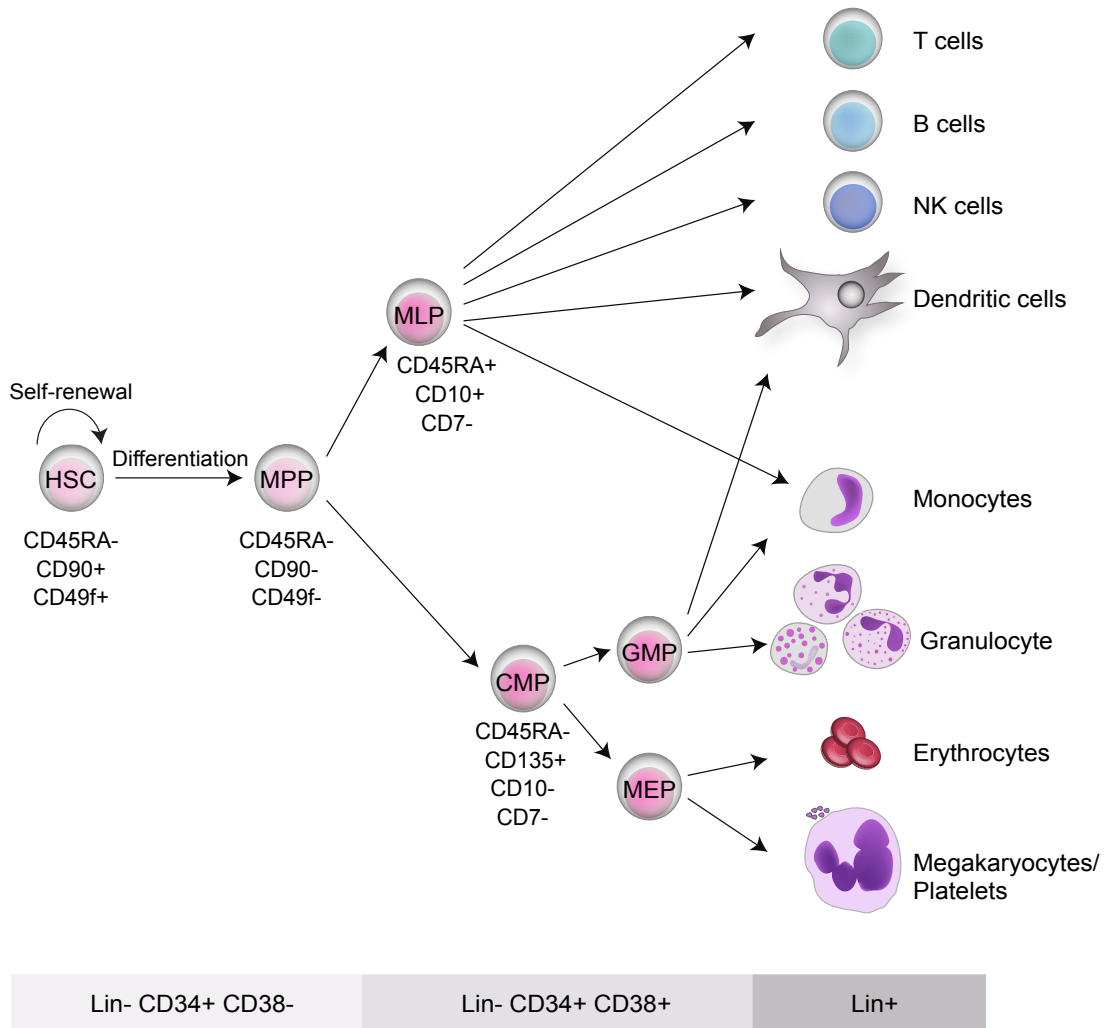


Figure 1.1. Model of human hematopoietic hierarchy.

Human hematopoietic stem cell (HSC) and downstream progenitor populations are defined by the expression of cell surface phenotype. HSC gives rise to multipotent progenitor (MPP) which is defined by loss of CD49f expression. MPP generates multilymphoid progenitor (MLP) and common myeloid progenitor (CMP). The MLP differentiates to T cell, B cell, NK cell, and dendritic cell while the CMP produces granulocyte macrophage progenitor (GMP) and megakaryocyte erythrocyte progenitor (MEP). The figure is Adapted from Doulatov et al., 2010.

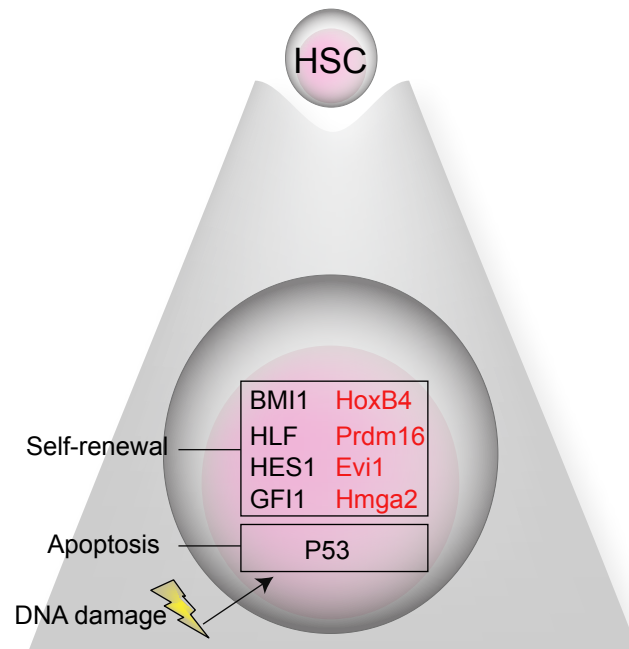


Figure 1.2. Molecular regulation of hematopoietic stem cell.

Some regulators of HSC-self renewal. The transcription factors shown in red are validated in mouse HSCs.

mouse HSC up to 1000-fold by activating their symmetrical self-renewal division¹². Interestingly, human CD34+ (transmembrane phosphoglycoprotein) cells overexpressing HOXB4 barely show any increase in HSC numbers¹³. Hmga2 is another master regulator of HSC self-renewal. It modulates the proliferative potential of HSCs during development where it controls proliferation status that distinguishes fetal HSCs from adult HSCs. Overexpression of Hmga2 in adult HSCs elevates their self-renewal activity and loss of Hmga2 in fetal HSCs compromises their proliferative potential¹⁴. Ecotropic viral integration site 1 (Evi1) is also indispensable for HSC self-renewal in both fetal and adult hematopoietic systems¹⁴. Evi1 expression marks a quiescent state of HSCs with long-term multilineage repopulating activity whereas the absence of Evi1 expression exclusively identifies cells without functional HSC activity. Consistent with other described transcription factors, Evi1 overexpression suppresses differentiation and enhances HSC self-renewal capacity¹⁴. These data settle Evi1 as a central regulator of HSC self-renewal where several transcription factors essential for HSC pool have been identified to be downstream targets such as Gata2^{15,16}, Pbx1¹⁷, and Runx1¹⁸.

Gene expression profiling and bioinformatics analysis of distinct human hematopoietic cell types reveals hundreds of transcription factors differentially expressed in human hematopoietic lineages². For instance, PAX5 and GATA3 are selectively expressed in MLPs while GATA1 is expressed in myeloid erythroid progenitors (MEP) and PU.1 and CEBP α in granulocyte lineage^{1,2}. These transcription factors and others organize the hematopoietic hierarchy from HSC to lineage determination. Mutations in these key factors impair their differentiation fate leading to various hematological diseases¹⁹.

1.3 Origin of human HSPC

Blood cell development progresses in different embryonic sites separated temporally and spatially²⁰ (Figure 1.3). The precursors of HSPC are mainly from mesoderm/hemangioblast cells^{21,22} which transit through different niches where HSPC mature and proliferate to generate a pool of HSC for life. Human hematopoiesis begins at day 16 of embryonic development in the yolk sac (YS) with the early appearance of primitive erythroid cells (primitive hematopoiesis). During the fifth week of development, the first multipotent and myelolymphoid stem cells emerge from the aorta-gonad-mesonephros (AGM) (definitive hematopoiesis)^{23,24}. The differences between the YS vs. AGM hematopoietic outcomes suggest a critical role of the microenvironment that determines the hematopoietic self-renewal potential. These HSPC cells start then to colonize other organs: liver, thymus, spleen then BM²³. At week 13 of gestation, the multilineage hematopoietic progenitors are detected in fetal liver (FL)²⁵ where HSPC expands rapidly. Human

placenta starts to show fetal-derived HSPC from gestating week 8 onward²⁶. Shortly after birth, the bone marrow (BM) becomes the site of permanent adult hematopoiesis at which most of the HSCs are dormant and exhibit a limited proliferative activity to prevent cell exhaustion. The BM niche (endosteal and perivascular regions) provides a unique district for the maintenance of quiescent HSCs. Retention of the HSC in the bone marrow is mediated by adhesion interactions between HSC surface receptors and their respective ligands expressed or secreted by neighboring cells such as stromal derived factor 1 (SDF1), stem cell factor (SCF), Angiopoietin 1 (Angpt1), vascular cell adhesion molecule 1 (VCAM1), and thrombopoietin (TPO)²⁷. Bone marrow is not the final destination of HSPCs; there is a constant exchange of HSPCs between BM and peripheral blood to maintain the hematopoietic hemostasis (Figure 1.3 B). In response to a blood injury, a positive feedback loop induces the HSC to cycle and subsequently replenish the hematopoietic system²⁸.

1.4 Functional assays for human HSPC

Developing assays that distinguish each cell type in the hematopoietic hierarchy into functional cells and evaluating quantitatively their proliferative potential has always been a challenge. Difficulties in developing such assays are mainly due to (a) absence of reliable correlation between the cell phenotype and its function and (b) cell heterogeneity. Two types of assays-*in vitro* and *in vivo* assays- have been developed to study the function of hematopoietic cells. These assays determine the frequencies and the numbers of long and short-term HSCs and progenitor cells in various cell perpetrations and culture conditions.

1.4.1 *In vitro* assays

In vitro assays are used mainly to assess the ability of hematopoietic progenitor cells rather than stem cells to proliferate and differentiate in response to various cytokines, growth factors, and coculture systems.

1.4.1.1 Colony forming unit assay

Colony forming unit (CFU), also known as colony forming cell (CFC) assay, determines the capacity of hematopoietic progenitor cells to form lineage-restricted colonies in a semisolid methylcellulose-based medium supplemented with cytokines. CFU assay detects the proliferation and differentiation of progenitor cells that generate different types of colonies based on their morphology. It distinguishes multilineage progenitor - the cell that gives rise to a colony

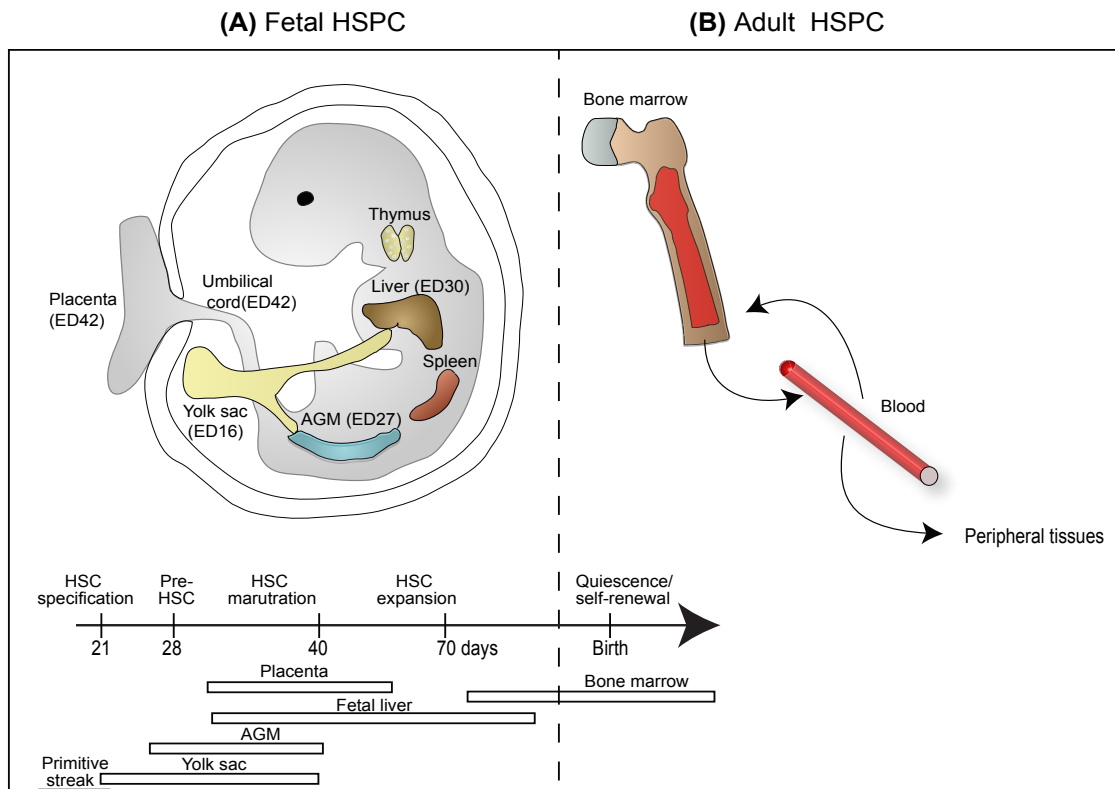


Figure 1.3. Human hematopoiesis during fetal and adult life.

(A) HSPCs originate from yolk sac and migrate to AGM and placenta to colonize later in the fetal liver, the major site of embryonic hematopoiesis where HSPCs proliferate and differentiate. Fetal liver HSPCs then migrate to the thymus, spleen and the bone marrow, the main organ for adult hematopoiesis. (B) A small number of HSPCs circulate between the bone marrow and blood to sustain the hematopoietic homeostasis. AGM: aorta-gonad-mesonephros region, ED: embryonic day. The figure is adapted from Mazo et al., 2011 and Mikkola et al., 2006.

that holds all myeloid lineages (granulocyte/ erythrocyte/ macrophage /megakaryocyte known as CFU-GEMM)- from a lineage-restricted progenitor. Although CFU assay is limited to progenitor cell assessment, it is a useful test to predict the graft quality where high CFU numbers correlate with rapid engraftment and overall survival after HSC transplantation²⁹⁻³².

1.4.1.2 Long-term culture initiating cell (LTC-IC) assay

Dexter et al.³³ are the first to describe a long-term culture (LTC) system that detects primitive hematopoietic cells from unpurified mouse marrow. In this culture, the marrow cells are plated with other cell types that make up the bone marrow niche such as osteoblasts, stromal and endothelial cells named feeder cells. These adherent cells play a role in maintaining and expanding the primitive hematopoietic cells up to several weeks in culture. Consequently, the system was tested on human marrow cells³⁴ where cells that sustain hematopoiesis are cocultured in the presence of irradiated human marrow adherent cells for 5-7 weeks and assessed for their congenic cells for additional 2 weeks (Figure 1.4 A). The long-term cultured cell that is able to generate a myeloid colony in CFU assay is called long-term culture initiating cell (LTC-IC). Thus, LTC-IC assay determines the progenitor cells that are more primitive than CFUs³⁵. LTC-IC assay is a quantitative assay where the clonogenic cell output is linearly related to the input cell number³⁶. Accordingly, starting from different cell doses, the frequency and the number of LTC-IC can be determined. Studies have shown that murine fibroblast or preadipocyte cell lines genetically engineered to secrete human cytokines (such as SCF, colony-stimulating factor (G-CSF), and interleukin 3 (IL3)) can function as efficiently as human adherent marrow cells^{37,38}. In addition to myeloid clonogenic progenitors, several stromal cell culture systems were developed to generate lymphoid and nature killer cells^{39,40}.

LTC-ICs are still functionally heterogeneous since extending the culture for 14 weeks sustain a more primitive subpopulation with distinct proliferation and differentiation capacities than the standard LTC-IC culture⁴¹, which raises the question of the culture period needed to detect the most primitive cells. Accordingly the relationship between LTC-IC and HSC is unclear and *in vivo* experiments are still mandatory for dissociating the two populations.

1.4.2 *In vivo* assays

In vivo assays are the gold standard tests for differentiating long-term HSC from short-term HSC and progenitor cells.

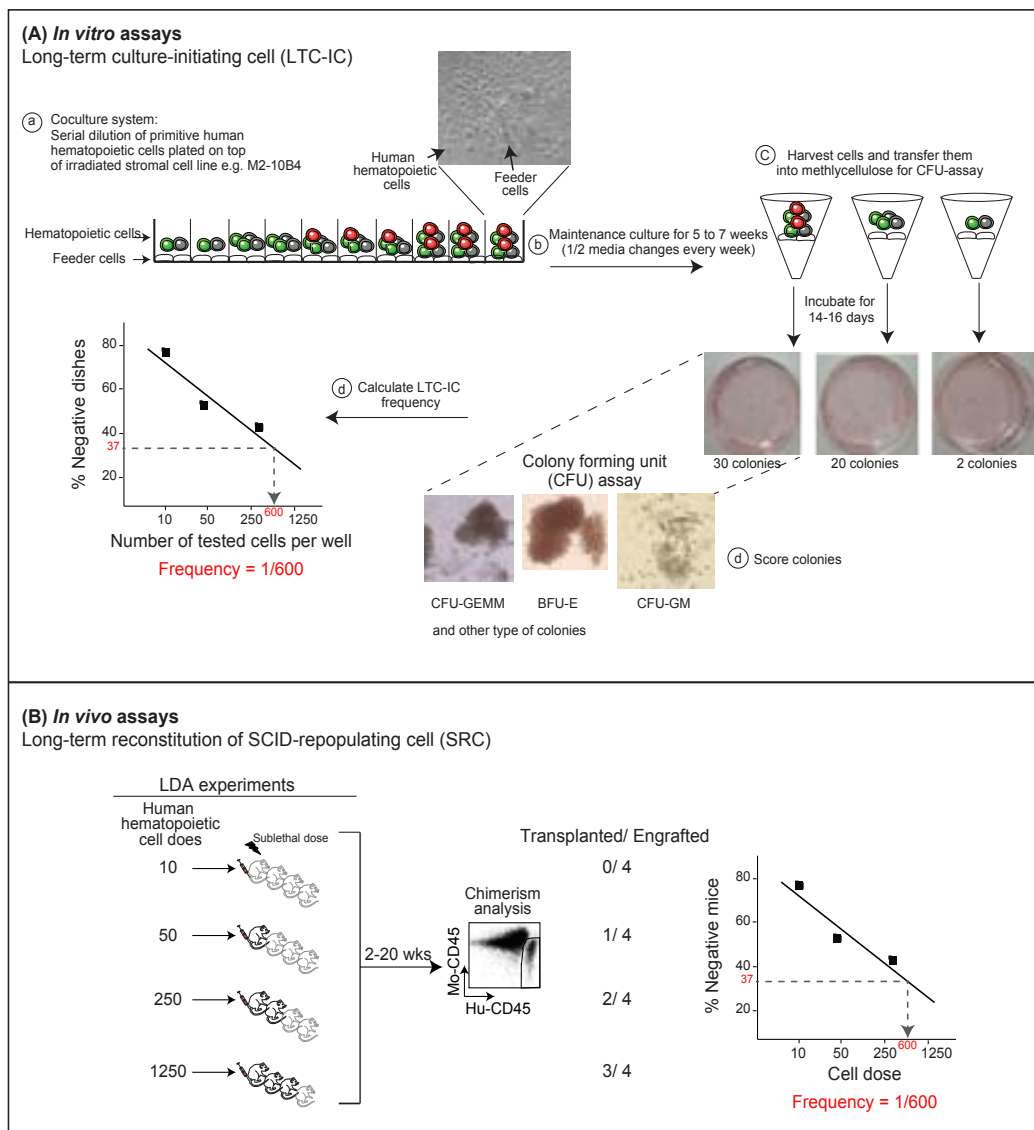


Figure 1.4. Assays used to study function of human HSPCs.

(A) In vitro assays for detecting long-term culture initiating cell (LTC-IC). CFU-GEMM (colony forming unit-Granulocyte/Erythrocyte/Monocyte/macrophage/Megakaryocyte), BFU-E (erythroid burst-forming unit), CFU-GM: (colony forming unit-Granulocyte/macrophage) (B) In vivo assays for detecting SCID-repopulating cell (SRC). Mouse (Mo), Human (Hu).

1.4.2.1 SCID repopulating cell (SRC)

Development of long-term *in vivo* assay for primitive human hematopoietic cells is based on their ability to repopulate the BM of severe combined immunodeficient (SCID) and non-obese diabetic/SCID (NOD/SCID) mice⁴²⁻⁴⁴. Human BM or CB primitive cells can engraft recipient mice where they extensively proliferate and differentiate to myeloid and lymphoid lineages for several weeks – months after transplantation. These engrafting human cells are defined as SCID-repopulating cells (SRCs)⁴⁵. Cell fractionation and retrovirus gene marking experiments show that SRCs are more primitive than CFC or LTC-IC. Most CFCs and LTC-ICs are enriched in the CD34⁺CD38⁺ fraction, highly transduced, and incapable of engrafting NOD/SCID mice; however, SRCs are exclusive in CD34⁺CD38⁻ and poorly infected⁴⁶. Kinetic experiments also supported the hypothesis that SRCs are biologically different from most cells assessed *in vitro*. In these studies, only small fraction (0.1-1%) of injected numbers of CFCs and LTC-ICs is detected in murine BM⁴⁷. Quantitative experiments confirm that SRCs are presented at a lower frequency compared with LTC-ICs (numbers of SRCs in BM or CB cells are lower by ~ 100-200 times than that of LTC-IC)^{36,48,49}. All these data indicate that SRCs are distinct and more primitive than most CFCs and LTC-ICs.

1.4.2.2 Quantifying SRC using limiting dilution assay

Bone marrow is known to be the most radiosensitive tissue. In 1951, Jacobson et al. showed that recovery from irradiation injury is possible by transplanting normal BM cells to the irradiated animal⁵⁰. The normal BM cells replenished the destroyed hematopoietic system where it proliferated and sustained the production of myeloid and lymphoid lineages⁵¹. These observations identify the presence of cells in the BM with a long-term repopulating activity which can be quantified by transplanting different doses of normal BM cells to lethally irradiated recipients⁵²(Figure 1.4 B). This limiting dilution assays (LDA) can determine the minimal number of cells needed to protect the irradiated host. Similarly, LDA can be used in sublethally irradiated immunodeficient mice to determine the number of human cells needed to repopulate SCID mice (SRC) and quantify their frequencies.

1.4.2.3 Xenograft models used to assess the SRC

Severe combined immune-deficient mouse, lacking B and T cells, represents the first murine model to study human hematopoietic system due to the fact that human lymphocytes are able to survive and circulate in a SCID mouse⁴². To suppress further the innate immunity of SCID

model, *Scid* mutation was backcrossed with nonobese diabetic (NOD) mice that have a defective innate immunity^{43,44}. Accordingly, NOD/SCID model shows higher levels of human hematopoietic engraftment than SCID mice (Table 1.1). Additional genetic mutations to impair the immune system were continuously generated to improve the xenograft model. Loss of beta 2-microglobulin allele in NOD/SCID model (NOD/SCID/ $\beta 2m^{null}$), for instance, reduces the activity of murine NK cell and enhances human T cell engraftment⁵³. Others took a different approach to eradicate activity of murine NK cells by either truncating (NOG)⁵⁴ or deleting interleukin 2 receptor common γ chain (NSG)⁵⁵ of NOD/SCID mice. The deletion of this gene results in a complete loss of B, T, and NK cells. NSG model is superior to other models in detecting SRC and showing a lower incidence of thymic lymphoma- one of the major drawbacks of NOS/SCID model that prevented its long-term studies^{55,56}. Thus, NSG represents a new *in vivo* long-lived model with robust engraftment potential (Table 1.1). Other mutations were also studied in NOD/SCID system such as mutations in *recombination-activating gene 1 and 2* (*Rag1 and Rag2*) that cause defects in B and T cell activity; however, none of these mice is better than NSG in engrafting human cells⁵⁷.

Expressing human signal regulatory protein alpha (SIRP α) - a receptor that negatively regulates phagocytosis- in immunodeficient mice induces host macrophage tolerance to human transplanted cells. These SIRP α expressing models lead to significant increase in human engraftment reaching levels comparable to NSG model⁵⁸ (Table 1.1).

Lack of cross-reactivity between the mouse and human myeloid growth factors (IL3, Granulocyte-macrophage colony-stimulating factor (GM-CSF), and SCF cytokines) hinder the long-term production of myeloid cells from HSC. Thus, immunodeficient mice injected in human cytokines or genetically manipulated to express human cytokines show stable engraftment of myeloid lineages for more than 4 months^{59,60} (Table 1.1).

The method of injection is also important in measuring SRC numbers. Intravenous injection of transplanted cells circulates through the blood before anchoring to BM niche. This approach might underestimate the SRC numbers that are incapable of migrating and/or homing to BM. Yahata⁶¹ and McKenzie⁶² show that intratibial and intrafemoral injection provide more robust engraftment than intravenous injection. This optimal injection procedure renders the *in vivo* assay more sensitive to SRC detection.

Interestingly, murine sex difference plays a role in human engraftment. In NSG, it has been reported that female recipients are superior in detecting human chimerism suggesting sex-specific signals that are yet to be identified, in regulating human HSPC engraftment⁶³.

Mouse model	Mouse genetic background	Mouse immunity	Human engraftment
SCID ⁴²	Homozygous for the severe combined immune deficiency spontaneous mutation (Pirk dc <i>scid</i>), referred as <i>scid</i> . C57BL/6J background.	Absence of functional T cells and B cells, lymphopenia, hypogammaglobulinemia, and a normal hematopoietic microenvironment.	B and T cell engraftment.
NOD/SCID ⁴⁴	NOD/ShiLTSz instead of C57BL/6J background.	Low levels of NK cells cytotoxic activity, absence of hemolytic complement, and functionally immature macrophages.	Higher level of human CD45 engraftment when compared with SCID model. Myeloid and erythroid engraftment in addition to B and T cell engraftment.
NOD/SCID/ β 2m ^{null53}	Double homozygous for <i>scid</i> mutation and beta 2-microglobulin null (β 2m) allele.	Impaired NK activity. Characterized by shortened life span due to accelerated thymic lymphomagenesis.	Major increase in human T cell engraftment compared to NOD/SCID.
NOD/Shi-SCID/IL2R γ ^{null} (NOG) ⁵⁴	Scid mutation combined with truncated interleukin-2 receptor gamma chain (IL2R γ) mutation. The targeted IL2R γ mutation used in these crosses is not completely null.	Impaired NK cell activity and severe reduction of interferon γ (IFN- γ) production from the dendritic cells in the NOG mice spleen.	Higher level of human engraftment when compared with NOD/SCID or NOD/SCID/ β 2 ^{null} models.
NOD/SCID/IL2R γ ^{null} (NSG) ^{55, 56}	Scid mutation combined with complete interleukin-2 receptor gamma chain (IL2R γ) null mutation.	Deficient in mature lymphocytes and NK cells and dendritic cell population, do not develop thymic lymphomas, and are long-lived (>16 month of age).	3.6- fold enrichment in detecting SRC and 1.5- fold improvement in the CD45-BM engraftment when compared with NOG model.
NOD-Rag1 ^{-/-} IL2R γ ^{null} (NRG) ⁵⁷	NOD-scid IL2R γ null with Rag1 null mutation.	Defect in functional B and T lymphocytes.	Similar engraftment as NSG model. More radioresistant than NSG model.
NSGS ⁵⁹	NSG mice expressing human IL3, GM-CSF and SCF.	Similar to NSG.	Stable engraftment of myeloid lineages and regulatory T cell populations.
hSIRPa-transgenic Rag2 ^{-/-} γ c ^{-/-58}	Expression of a human signal regulatory protein alpha (hSIRPa), a receptor that negatively regulates phagocytosis, in Rag2 ^{-/-} γ c ^{-/-} mice.	Defect in functional B and T lymphocytes. hSIRPa expression on mouse macrophages lead to decreased phagocytosis of human CD47 (a SIRPa ligand expressed on hematopoietic cells and sends a "do not eat me" signal) cells.	CD45 engraftment levels in hSIRPa-transgenic Rag2 ^{-/-} γ c ^{-/-} were comparable to that of NSG, except for frequency of erythrocyte which was significantly higher in NSG model.
MISTRG ⁶⁰	Expression of a human M-CSF, IL3/GM-CSF, SIRPa, TPO in Rag2 ^{-/-} IL2R γ ^{-/-} mice.	Similar to Rag2 ^{-/-} IL2R γ ^{-/-} .	Efficient development of human innate immune system.

Table 1.1 Development of immunodeficient mouse models for studying human HSPC function.

Continuous development for optimal xenograft models has enabled sensitive detection and better classification of human HSPCs.

1.4.2.4 Distinct classes of SRC

Transplantation experiments are the first to reveal a hierarchy of cell states that enable successive waves of human blood lineage reconstitution⁶⁴. Fluorescent gene marking and DNA barcoding of human HSPC transplanted into immunodeficient mice confirm the existence of different engrafted clones with variable multipotentiality and longevity, illustrated by the presence of both short- and long-term repopulating cells^{65,66}(Figure 1.5). The short-term repopulating clones show a transient and rapid engraftment detectable at 4-5 weeks and sometimes lasting up till 16-20 weeks post-transplantation (Figure 1.5, orange wave) while the long-term repopulating clones become evident after 16-20 weeks and persist beyond 27 weeks post transplantation (Figure 1.5, green wave). Some of these long-term clones are more stable than others where they sustain hematopoiesis in secondary recipients⁶⁵. Cell purification allows us to distinguish between the *in vivo* proliferative potential of the uncultured human transplanted cells. The CD34⁺CD38⁺ cells are known to generate the first transient wave with restrictive lineage output⁶⁷ while the CD34⁺CD38⁻CD45RA⁻CD90⁻CD49f⁻ cells known as multipotent progenitors (MPPs), sustain the multilineage cell production but not longer than 20 weeks⁶⁸. Upstream MPPs is the HSCs with CD34⁺CD38⁻CD45RA⁻CD90⁺CD49f⁺ phenotype that generate stable long-term blood lineages over many months⁶⁸. Detecting and distinguishing the short from the long-term repopulating cell is a time-consuming procedure since only transplantation experiments can differentiate between the two cell types.

1.5 Phenotype of human HSC

Since the frequency of HSC is extremely low in the blood tissue, many studies have identified surface markers or viable dye staining that enable isolation of these rare cells, such as CD34, CD38, CD90, CD133, CD45RA, CD49f, and Rhodamine dye. These surface markers and staining dyes were validated using *in vivo* functional assays (Table 1.2).

1.5.1 Lineage depletion (Lin-)

The first step in the HSC purification is to enrich for cells that do not express lineage-specific antigens. This is achieved by depleting lineage committed cells using a mixture of monoclonal antibodies directed against a variety of lymphoid, myeloid, and erythroid antigens. Lineage de-

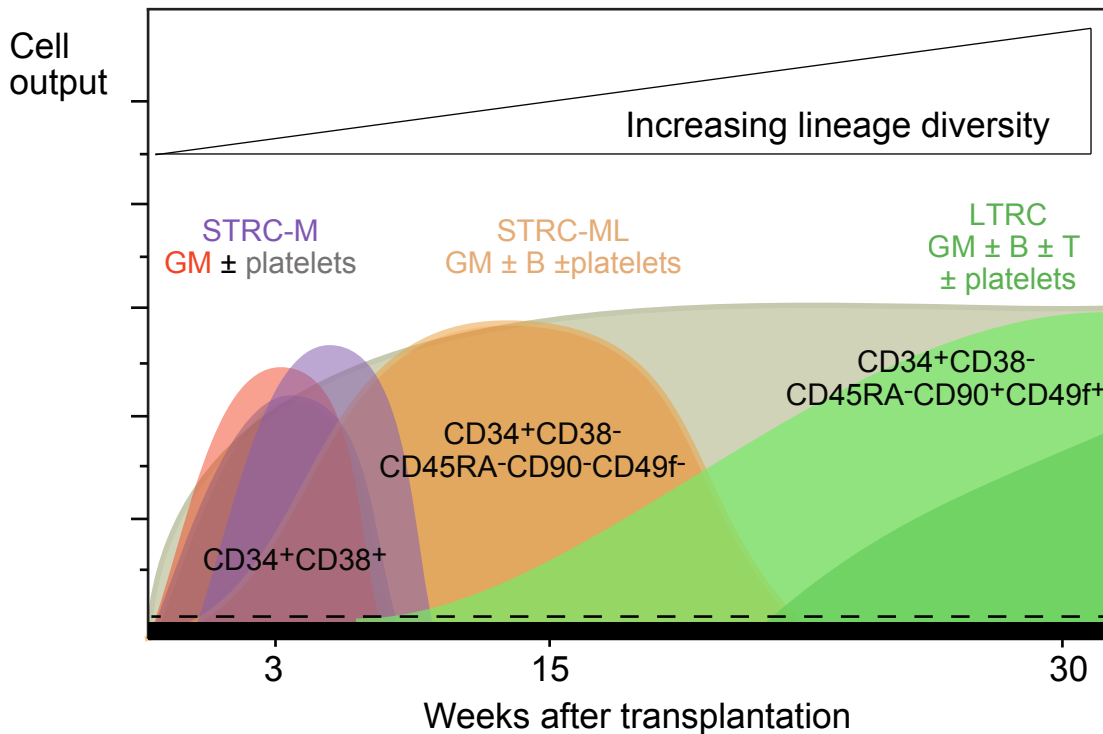
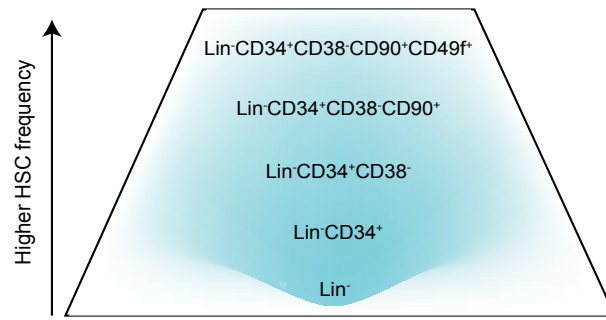


Figure 1.5. Clonal growth and differentiation dynamic of primitive human hematopoietic cell types in immunodeficient mice.

The first repopulating wave derived from $CD34^+CD38^+$ cells produces early transient clones of monocyte (M), granulocyte-monocyte (GM), or platelet restricted cells that disappear within 9 weeks after transplantation. Multiple clones are detected at later time points with multilineage repopulation. Some of these clones have limited self-renewal ability (orange) and do not sustain blood production beyond 16-20 weeks of transplantation. These clones are derived from short-term HSCs (ST-HSC) or multipotent progenitors (MPP) defined as $CD34^+CD38^-CD45RA^-CD90^-CD49f^-$ cells. Others are long-lived clones with high proliferative potential (green). They become evident at week 9 or even later and persist up to 27- 30 weeks. These clones are derived from cells upstream MPPs named long-term HSCs (LT-HSC) and defined as $CD34^+CD38^-CD45RA^-CD90^+CD49f^+$ cells. The figure is adapted from Cheung et al., 2013 and Miller et al., 2013.



Sorted population	SCID repopulating cell (SRC)	Type of injection	Mouse model	Chimerism assessed after (weeks)	Reference
Lin ⁻ CD34 ⁻	1 in 125,000	Tail-vein	NOD/SCID	8-12	76
Lin ⁻ CD34 ⁻	1 in 24,100	Intra-BM	NOD/SCID	12	75
Lin ⁻ CD34 ⁻ CD38 ⁻ CD93 ⁺	1 in 7,500	Tail-vein	NOD/SCID	8-10	77
18Lin ⁻ CD34 ⁻ CD38 ⁻ CD133 ⁺	1 in 142	Intra-BM	NOG	12	78
Lin ⁻ CD34 ⁺	1 in 1,010	Intra-BM	NOD/SCID	12	75
Lin ⁻ CD34 ⁺ CD38 ⁻	1 in 617	Tail-vein	NOD/SCID	6-9	82
Lin ⁻ CD34 ⁺ CD38 ⁻	1 in 121	Intra-femoral	NOD/SCID	7-10	87
Lin ⁻ CD34 ⁺ CD38 ⁻ Rho ^{low}	1 in 30	Intra-femoral	NOD/SCID	7-10	87
Lin ⁻ CD34 ⁺ CD38 ⁻ CD90 ⁻	1 in 100	Intra-femoral	NSG	20 + 2 nd trsp	68
Lin ⁻ CD34 ⁺ CD38 ⁻ CD90 ⁺	1 in 20	Intra-femoral	NSG	20 + 2 nd trsp	68
Lin ⁻ CD34 ⁺ CD38 ⁻ CD90 ⁺ CD45RA ⁻	1 in 10	Tail-vein	NOG	12	92
Lin ⁻ CD34 ⁺ CD38 ⁻ CD90 ⁺ CD45RA ⁻ Rho ^{low} CD49f ⁺	less than 1 in 10	Intra-femoral	NSG	20 + 2 nd trsp	68

Table 1.2. SRC frequency of different hematopoietic populations derived from human CB cells.

pletion is then further enriched for HSPC using a combination of other surface markers (Table 1.2).

1.5.2 CD34 antigen

CD34 antigen is one of the major positive markers for human HSPC^{69,70}. It comprises 1- 4% of marrow mononuclear cells. Berenson and colleagues show that transplantation of enriched CD34⁺ cells derived from BM restores hematopoiesis into lethally irradiated baboons and promotes hematopoietic recovery in human patients after marrow ablative therapy^{71,72}. Functional studies show that CD34⁺ cells exhibit cytoadhesion characteristics caused by a concomitant activation of the β 2 integrin, postulating that CD34⁺ cells home to BM as a result of binding to adhesion proteins⁷³. CD34 expression also has a role in regulating hematopoietic progenitor cell differentiation where silencing of CD34 in HSPCs generates more megakaryocyte and granulocyte precursors at the expense of erythroid cell production⁷⁴.

CD34⁻ fraction exhibits a limited SRC activity when cells are injected intravenously (via tail-vein). However the SRC activity is enhanced when CD34⁻ cells are injected into bone marrow (Table 1.2), possibly because CD34⁻ cells express a low level of homing receptors⁷⁵. Further purification protocols showed that CD34⁻ fraction has a higher SRC frequency when depleted from CD38 and enriched with C1qR1 (CD93) or CD133 surface expression⁷⁶⁻⁷⁸ (Table 1.2).

Since CD34 is also expressed on progenitor cells, additional purification is required to enrich for stem cells^{79,80}.

1.5.3 CD38 antigen

To further enrich for HSC frequency, CD34⁺ cells are fractionated based on CD38 expression, which is correlated with differentiated cells⁸¹. Only 1- 10% of CD34⁺ cells do not express CD38. CD34⁺ CD38⁻ cells are mainly quiescent before cytokine stimulation and are more enriched with LTC-IC compared to CD34⁺CD38⁺ cells⁸⁰. Bhatia and colleagues show that SRC activity is exclusively found in the CD34⁺CD38⁻ fraction, enhancing HSPC frequency by 1,500 folds (HSPC frequency is: 1 in 617 CD34⁺CD38⁻ vs. 1 in 930,000 CB cells)⁸².

1.5.4 Rhodamine 123

Rhodamine 123 (Rho) is a lipophilic fluorescent dye that accumulates in the mitochondria of metabolically active cells⁸³. Rho efflux is mediated by P-glycoprotein (P-gp), a product of mul-

drug resistance (MDR) genes expressed in CD34⁺ cells⁸⁴. Rho uptake is used in purifying stem cell populations where its fluorescent intensity distinguishes the quiescent HSC population (Rho^{low}) from the proliferative progenitor cells (Rho^{high})^{85,86}. Refining HSC based on Rho efflux identifies a long-term self-renewal population and enhances the SRC frequency in CD34⁺CD38⁻ cells by 4 folds⁸⁷ (HSPC frequency is: 1 in 121 CD34⁺ CD38⁻ vs. 1 in 30 in CD34⁺ CD38⁻ Rho^{low}, Table 1.2).

1.5.5 CD45RA antigen

Further studies introduce CD45RA as a marker for differentiated progenitors. Depleting CD45RA expressing cells from CD34⁺ cells retains the primitive cells that initiate hematopoiesis in long-term cultures⁸⁸.

1.5.6 CD90 antigens

CD90 or Thy-1 has been first isolated from human fetal BM where its coexpression with CD34⁺ shows a higher engraftment potential in SCID mice compared to CD34⁺CD90⁻³⁹. CD90 is expressed on 5 to 25% of CD34⁺ cells derived from fetal or adult BM^{39,89}. In human clinical trials, CD34⁺CD90⁺ cells were able to produce rapid and fast hematopoietic reconstitution in autologous bone marrow and peripheral blood cells transplants^{90,91}.

Combining CD90 expression with the previously stated surface makers, Majeti and colleagues refine the hematopoietic hierarchy and describe a new class of primitive cells with limited long-term self-renewal potential known as multipotent progenitors (MPP). These cells- which lack the expression of CD90 in the Lin⁻CD34⁺CD38⁻CD45RA⁻ compartment- lie directly below HSC in the hematopoietic hierarchy⁹². Although MPP cells have lower engraftment capacity when compared with HSCs (Lin⁻CD34⁺CD38⁻CD45RA⁻CD90⁺), they can still engraft secondary recipients^{68,92}. These findings raised some uncertainty about whether CD90 expression is sufficient to separate HSC from MPPs.

1.5.7 CD49f antigen

Notta et al. further characterize the MPP and HSC populations by identifying CD49f (ITGA6), an adhesion molecule that is enriched in HSC (CD90⁺) and depleted in MPP (CD90⁻) compartment⁶⁸ (Table 1.3). HSC cells (Lin⁻ CD34⁺CD38⁻CD45RA⁻CD90⁺CD49f⁺) additionally sorted on low Rho staining improve the stem cell frequency to less than 1 in 10 Lin⁻ CD34⁺CD38⁻

Cell type	Surface markers
HSC ^{68,92}	Lin-CD34 ⁺ CD38 ⁻ CD45RA ⁻ CD90 ⁺ CD49f ⁺
MPP ^{68,92}	Lin-CD34 ⁺ CD38 ⁻ CD45RA ⁻ CD90 ⁻ CD49f ⁻
MLP ¹	Lin-CD34 ⁺ CD38 ⁻ CD45RA ⁺ CD90 ^{-/low}
CMP ^{1, 97-99}	Lin-CD34 ⁺ CD38 ⁺ CD90 ⁻ CD10 ⁻ CD7 ⁻ CD45RA ⁻ CD135 ⁺
GMP ^{1, 97-99}	Lin-CD34 ⁺ CD38 ⁺ CD90 ⁻ CD10 ⁻ CD7 ⁻ CD45RA ⁺ CD135 ⁺
MEP ^{1, 97-99}	Lin-CD34 ⁺ CD38 ⁺ CD90 ⁻ CD10 ⁻ CD7 ⁻ CD45RA ⁻ CD135 ⁻

Table 1.3. Cell surface phenotypes of different human hematopoietic stem and progenitor populations.

CD45RA⁻CD90⁺CD49f⁺ Rho^{low} (Table 1.2). This is the purest population identified so far where HSC can be transplanted in as a single cell and have 14- 28% chance to display a long-term multilineage chimerism⁶⁸.

1.5.8 Other antigens

Other surface molecules were identified to enrich for human fetal and/or adult hematopoietic tissues such as VE-cadherin⁹³, angiotensin converting enzyme (ACE)⁹⁴, and GPI 80⁹⁵.

Identifying all these surface markers helped in characterizing and studying HSPC; however, robust purification of human HSCs at a single-cell resolution is still a challenge especially after *ex vivo* culture conditions where the HSC phenotype is dissociated from HSC activity (Reference⁹⁶ and chapter 3). Once achieved, it will pave the way to understand further the mechanism of HSC development and self-renewal.

1.6 Phenotype of human hematopoietic progenitor cells

Human hematopoietic progenitors are also purified based on surface markers (Table 1.3). Early lymphoid progenitors in adult bone marrow are marked by the expression of CD10 (CD34⁺CD38⁺ CD10⁺), which gives rise to B, NK, T and dendritic cells⁹⁷. In cord blood, while CD10 compartment is highly heterogeneous, CD7 (CD34⁺CD38⁻CD7⁺) expression distinguishes early lymphoid progenitors from myeloerythroid cells⁹⁸. On the other hand, differential expression of CD45RA and CD135 (FLT3) within CD34⁺CD38⁺ fraction identified CMP, GMP, and MEP. CMP (CD135⁺CD45RA⁻) is shown to give rise to both GMP (CD135⁺CD45RA⁻) and MEP (CD135⁻CD45RA⁻)¹. Like CD135, CD123 (ILR α) was important for myeloid but not erythroid development⁹⁹.

Isolating functionally distinct populations provides tools to study the earliest events and the transcription regulation in lineage commitment.

1.7 Sources of human HSPCs and their functional differences

Human HSPCs can be isolated from FL, CB, BM and G-CSF mobilized peripheral blood (mPB). HSPCs purified from various sources have different functional properties concerning proliferation, migration, and repopulating potential. Primitive hematopoietic cells derived from adult BM have shorter telomerase and limited proliferative potential than their counterparts derived from FL or CB^{100,101}. Lansdorp et al. show that proliferative potential of primitive cells is

restricted to early stages of development and declines as the cell ages (from FL to CB to BM)¹⁰⁰. Following studies reveal that although the frequency of progenitor cells is roughly similar in mononuclear cells derived from CB, mPB, and BM (illustrated in CFU-GM and LTC-numbers), the primitive cells identified as SRC are higher in CB compared with the adult tissues (BM, mPB). This data confirms that functional differences exist between the HSPC sources^{48,49} (Table 1.4).

1.8 Clinical applications of HSPC

In 1960, Till and McCulloch made the first breakthrough description of HSPC, showing that bone marrow-derived cells from a healthy mouse can regenerate the hematopoietic system of sub-lethally irradiated mouse recipient¹⁰². Extensive studies were also done by Donnall Thomas, who performed the first human bone marrow transplantation in patients receiving radiation and chemotherapy¹⁰³, widening the use of this procedure for more than 50,000 patients worldwide per year with various hematological diseases, solid tumors and immune disorder¹⁰⁴⁻¹⁰⁶. Mobilized peripheral blood cells (mPB) have since become a better graft source than BM because the procedure is less invasive and more efficient in recovering neutrophils and platelets engraftment^{107,108}.

There are two types of HSC transplantations (HSCT): (i) autologous stem cell transplantation in which patient's stem cell is used. This kind of treatment is preferred in solid tumors, and the main advantage of this procedure is the absence of graft rejection. (ii) Allogenic stem cell transplantation where the patient receives stem cells from a family or unrelated donor. One limitation of this procedure is the development of graft vs. host disease (GVHD) where the patient's body rejects the donor stem cell due to differences in human leukocyte antigens (HLA). Accordingly, the HLA of the patient and donor should be closely matched to minimize the GVHD risk¹⁰⁹. The chance of finding HLA-match significantly varies according to racial and ethnic backgrounds of the patients, where only 60% of patients have the required HLA-matched donor¹¹⁰. Cord blood cells could be an alternative source for the patients that lack HLA-matched donor.

1.8.1 Cord blood stem cell transplantation

First human CB transplantation (CBT) was performed in 1988 for Fanconi anemia patient¹¹¹. Since then CB banks have been recognized worldwide to collect, preserve and distribute the units for allogenic HSCT, allowing more than 30,000 patients worldwide since 1988 to benefit from this treatment¹¹². The cord blood naïve immune system reduces HLA matching requirements, which is not tolerated with unrelated adult donor grafts^{113,114}. This less stringent

Source of MNC	%CD34+ Median (range)	CFU-GM in 10 ⁶ MNC Median (range)	LTC-IC estimated frequency (range)	SRC
CB	1.13 (0.56 - 3.9)	1,825 (520 - 3,400)	1:12,506 - 1:34,546	1 in 930,000
BM	1.48 (0.4 - 8.3)	1,170 (300 - 3,740)	1:13,314 - 1:33,949	1 in 3,000,000
mPB	3.7 (0.5 -18)	4,255 (834 - 9,200)	1:10,302 - 1:12,891	1 in 6,000,000

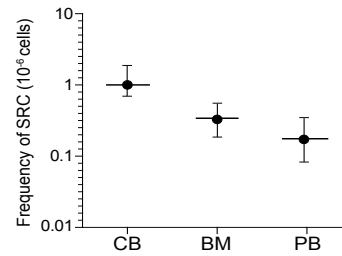


Table 1.4. Comparing frequencies of CD34+ cells, Colony forming unit- granulocyte/ monocyte (CFU-GM), long-term culture-initiating cells (LTC-IC) and SCID repopulating cell (SRC) in cord blood (CB), bone marrow (BM), and mobilized peripheral blood (mPB).

SRC was assessed in NOD/SCID mice after 6 weeks of transplantation. MNC (Mononuclear cell). Data adapted from (Pettengell et al., 1994 and Wang et al., 1997)

requirement in HLA matching increases access to HSCT for almost all patients irrespective of racial and ethnic background¹¹⁵. Additionally, CB transplants show less incidence of GVHD and lower relapse risk of the primary malignancy when compared to other graft sources^{116,117}. Although practiced clinically for more than 28 years, the use of CBT remains limited due to low cell dose of sorted units which results in delayed neutrophils and platelets recovery compared to BM transplantation. More than 21 days of delay in myeloid engraftment leave the patients vulnerable to infection which increases the incidence of morbidity and mortality. To defeat the inadequate cell dose, double-CB units were used in transplantation procedures; however, this approach does not recover the delay in hematopoietic engraftment and shows a higher incidence of GVHD compared to single CB unit¹¹⁸. To improve outcomes of CBT (rapid engraftment and less graft failure rates), several studies have been initiated to find culture conditions that allow *ex vivo* expansion of best HLA-matched CB units.

1.9 Clinical strategies to improve homing and expansion of CB grafts

Defining culture conditions for HSPC expansion is one of the biggest challenges in stem cell biology. HSCs cultured in serum-free media with cytokines lead to expansion of the progenitor cells at the expense of stem cell self-renewal^{119,120}. Culture conditions are known to cause epigenetic modifications in HSCs impairing self-renewal machinery and BM homing^{121,122}. These compromised HSCs are evaluated by the loss of CD34 surface protein expression and failure to improve engraftment. With more knowledge of the hematopoietic niche factors and the key regulators that govern HSC activity, new approaches to enhance BM homing and increase numbers of HSPC have been developed (Figure 1.6 and Table 1.5). These strategies have been tested clinically to evaluate their outcomes in CBT (Table 1.6). Most of the trials used double CB units, one unit that is manipulated in homing/expansion cultures and another left unmanipulated as a backup in the event the expanded graft fail to engraft.

1.9.1 Homing

Efficacious hematopoietic recovery after transplantation depends on migration of HSPCs to the bone marrow and homing into specific niches—a microenvironment that supports the maintenance and self-renewal state of HSCs¹²³ (Figure 1.6). The HSPC journey requires the activity of various components including chemoattractant and adhesion molecules. HSPCs' efficient rolling along the endothelial wall of blood vessels depends on P-selectin, E-selectin, and vascular cell adhesion molecule-1 (VCAM1). HSPCs rolling on endothelial selectin rapidly adhere to BM endothelial surface through SDF1-mediated integrin activation. The attached HSPCs can

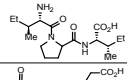
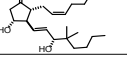
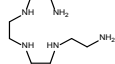
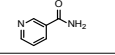
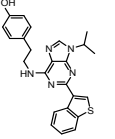
	Compound name	Chemical structure	Target	HSPC starting population	Culture condition	CD34+ expansion	CD34+ CD45RA- expansion	Method used to assessing HSPC expansion	HSPC expansion in vivo
Improve HSPC homing	DPP4/CD26 inhibitor ²⁵		Cleaves N-terminal X-Pro or X-Ala motif	CB-Lin- or CD34+ cells	15 min short-term exposure of diproin A (5nM) in dextran/albumin.	No difference after a brief exposure		% of human CD45 chimerism Mouse model: NOD/SCID Analyzed: 12 wks post-transplantation	Higher level of human CD45 chimerism of diproin A treated cells compared to controls.
	16, 16-Dimethyl prostaglandin (dmPGE2) ²⁹		PGs	CB-unfractionated or CD34+ Cells	1 hour short-term exposure of dmPGE2 (10µM) in dextran/albumin.	No difference after a brief exposure		% of human CD45 chimerism Mouse model: NOD/SCID Analyzed: 13 wks post-transplantation	Higher level of human CD45 chimerism of dmPGE2 treated cells compared to controls.
Enhance HSPC expansion	Fed-batch system ⁵¹		Modulate paracrine signaling	CB-Lin- cells	12 day culture with Fl3L (100ng/ml), SCF (100ng/ml), TPO (50ng/ml), LDL (1µg/ml).	4	ND	SRC frequency Mouse model: NSG Analyzed: 16 wks post-transplantation	11-fold increase in SRC activity of fed-batch cultures compared to uncultured Lin- cells.
	Notch ligand (Delta1) ¹⁶²⁻¹⁶³		Notch receptor	CB-CD34+ cells	17-21 day treatment of immobilized Notch ligand (Delta1), Fl3L (300ng/ml), SCF (300ng/ml), TPO (100ng/ml), IL6 (100ng/ml), IL3(10ng/ml).	3.2	ND	Short-term SRC frequency Mouse model: NSG Analyzed: 9 weeks post transplantation	1.8 and 6.2-fold increase in SRC activity of Delta1 treated cells compared to controls or uncultured CD34+ cells.
	Tetraethylenepentamine (TEPA) ¹⁷²		?	CB-CD34+ cells	21 day treatment of TEPA (5µM), Fl3L (50ng/ml), SCF (50ng/ml), TPO (50ng/ml), IL6 (50ng/ml).	1	ND	% of human CD45 chimerism Mouse model: NOD/SCID Analyzed: 8 wks post-transplantation	Higher short-term engraftment potential of TEPA treated cells compared to control or uncultured CD34+ cells.
	Nicotinamide (NAM) ¹⁷³		?	CB-CD34+ cells	21 day treatment of NAM (5nM), Fl3L (50ng/ml), SCF (50ng/ml), TPO (50ng/ml), IL6 (50ng/ml).	1	ND	Short-term SRC frequency Mouse model: NOD/SCID Analyzed: 8 wks post transplantation	7.6 and 9 -fold increase in short-term SRC activity of NAM treated cells compared to controls or uncultured CD34+ cells.
	StemRegenin (SR1) ^{166,170,168}		AhR	CB-CD34+ cells mPB-CD34+ cells CB-CD34+ cells	21 day treatment of SR1 (1µM), Fl3L (100ng/ml), SCF (100ng/ml), TPO (100ng/ml), IL6 (100ng/ml). 14 day treatment of SR1 (1µM), Fl3L (100ng/ml), SCF (100ng/ml), TPO (100ng/ml), IL6 (100ng/ml). 12 day treatment of SR1 (750nM), Fl3L (100ng/ml), SCF (100ng/ml), TPO (50ng/ml), LDL (10ug/ml), LDL (10ug/ml).	73 7 2.7	ND 2.2 2.4	Short-term SRC frequency Mouse model: NSG Analyzed: 16 wks post transplantation Short-term SRC frequency Mouse model: NSG Analyzed: 8 wks post transplantation Long-term SRC frequency Mouse model: NSG Analyzed: 30 wks post transplantation	17-fold increase in SRC activity of SR1 treated cells compared to controls or uncultured CD34+ cells. Not more than 2-fold increase in short-term SRC numbers of SR1 treated cells compared to controls. SR1 culture had lower stem cell activity when compared to unexpanded cells. No significant increase in long-term SRC activity of SR1 treated cells compared to controls or uncultured CD34+ cells.

Table 1.5. Strategies that enhance HSPC homing and expansion.

Fold expansion of CD34+ and CD34+CD45RA- presented is compared to vehicle-controls. Not determined (ND)), unknown (?). Adapted from Fares et al., 2015.

	Compound name	Transplantation strategy	Number of participants	Median fold of expansion	Median-engraftment recovery (participants vs. historical control groups)	Acute GvHD incidents
Improve HSFC homing	16, 16-Dimethyl prostaglandin (dmPEG2) ¹⁵¹	Patients received two CBUs. One of the CBU was exposed for 2 hours to dmPGE2 (10µM at 37°C in LMD/HAS media) followed by a second unmanipulated CBU.	12	No difference after a brief exposure	Neutrophil (17.5 vs 21 days) Platelet (43 vs 45 days)	Grade II-III in 5 patients
	Sitagliptin (DPP4/CD26 inhibitor) ¹²⁵	Patients received single red cell-deplete CBU (day0). Patients orally received Sitagliptin (600mg) every 24 hours from -1 to +2 days.	17	No difference after a brief exposure	Neutrophil (21 vs 22 days) Platelet (77 vs ND days)	Grade II in 1 patients
	Fucosylation ¹³⁴ (Fucosyltransferase-VI + Guanosine diphosphate fucose)	Patients received two CBUs. One of the CBU was treated for 30 min with (100 mU/ml) FTVI and GDP-fucose (1mM) and infused after a second unmanipulated CBU.	22	No difference after a brief exposure	Neutrophil (17 vs 26 days) Platelet (35 vs 45 days)	Grade II-IV in 9 patients
Enhance HSFC expansion	Cytokins ¹⁴²	Patients received one CBU. A 10-day CD34+ expanded CBU with 100 ng/mL each of SCF, G-CSF, and MGDF. The CD34-, non-cultured fraction of the manipulated CBU was also infused.	37	Total cell count: 56-fold CD34+cells: 4-fold	Neutrophil 28 days Platelet 108 days	Grade II-IV in 20 of 30 evaluable patients
	Mesenchymal stromal cell-coculture ¹⁵⁸	Patients received two CBUs. A 14-day expanded CBU with mesenchymal stromal cell infused after a second unmanipulated CBU.	31	Total cell count: 12-fold CD34+cells: 30-fold	Neutrophil (15 vs 24 days) Platelet (42 vs 49 days)	Grade II-IV in 13 patients
	Tetraethylenepentamine (TEPA) ¹⁷⁴	Patients received single CBU split into two fractions. Fractions ranging from 50-20% of the CBU was sorted for CD 133 cells and expanded for 21 days with TEPA (5µM). The expanded unit was infused after 24 hours from administering the unmanipulated fraction of the CBU.	10	Total cell count: 161-fold CD34+cells: 2.3-fold	Neutrophil (30 vs ND days) Platelet (48 vs ND days)	Grade II in 4 out of 9 patients
	Notch ligand ¹⁶²	Patients received two CBUs. A 16-day CD34+ expanded CBU with immobilized engineered Notch ligand (Delta 1) infused after a second unmanipulated CBU.	10	Total cell count: 562-fold CD34+cells: 164-fold	Neutrophil (16 vs 26 days) Platelet (not reported)	Grade II in 9 patients and Grade III in 1 patient
	Nicotinamide (NAM) ¹⁷⁵	Patients received two CBUs. A 21-day CD133+ expanded CBU with NAM (2.5mM) followed by a second unmanipulated CBU. The CD133-, non-cultured fraction of the manipulated CBU was also infused.	11	Total cell count: 486-fold CD34+cells: 72-fold	Neutrophil (13 vs 25 days) Platelet (33 vs 37 days)	Grade II in 5 patients
	StemRegenin(SR1) ¹⁶⁷	Patients received two CBUs. A 15-day CD34+ expanded CBU with SR1 (750M) infused after a second unmanipulated CBU. The CD34-, non-cultured fraction of the manipulated CBU was also infused.	17	Total cell count: 854-fold CD34+cells: 330-fold	Neutrophil (15 vs 24 days) Platelet (49 vs 89 days)	Similar to historical cohort

Table 1.6. Outcome of the approaches used in clinical cord blood transplantation trials.

Cord blood unit (CBU), fucosyltransferase-VI (FTVI), Guanosine diphosphate (GDP), Stem cell factor (SCF), granulocyte-colony stimulating factor (G-CSF), megakaryocyte growth and differentiation factor (MGDF). Adapted from Fares et al., 2015.

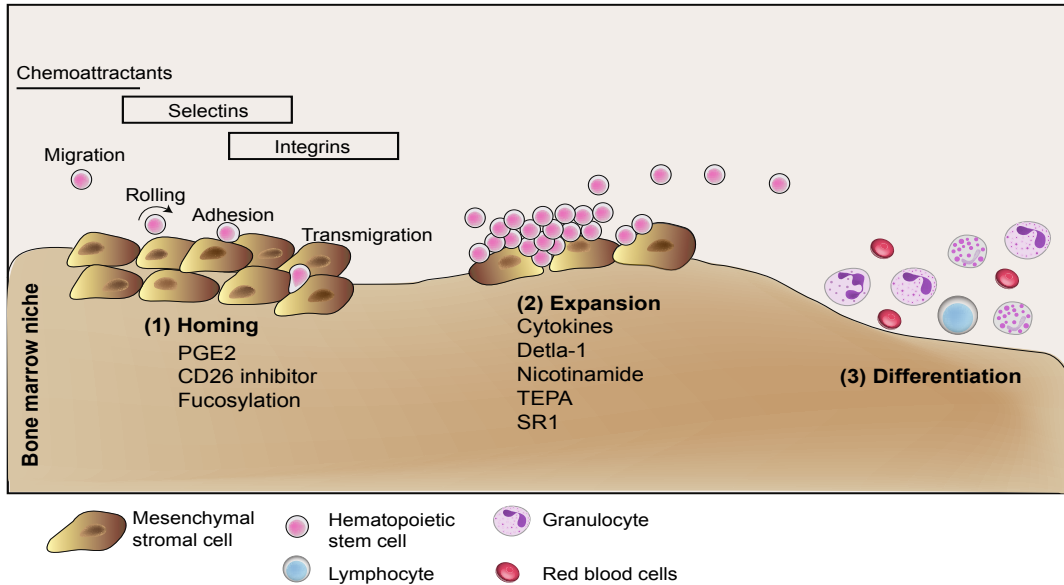


Figure 1.6. Required HSPC activities for a successful cord blood transplantation.

Upon transplantation, hematopoietic stem and progenitor cells (HSPCs) home toward the bone marrow niche (1), expand within the bone marrow environment (2), and differentiate into all blood lineages (3). Listed below the approaches used to improve homing and ex vivo expansion of HSPC. Prostaglandin E2 (PGE2), tetra-ethylenepent-amine (TEPA), stemregenin (SR1). The figure is adapted from Lund et al., 2014.

then transmigrate through endothelial layer where it gets fastened in a specialized BM niche. Accordingly studies were conducted to improve CBT outcomes by optimizing BM homing of the transplanted graft (Figure 1.6). The advantage of these studies is the brief exposure of CB cells to the treatment thereby simplifying and speeding the transplantation procedure.

1.9.1.2 Dipeptidyl peptidase (DDP4 or CD26)

Stromal derived factor 1 (SDF1) is a chemoattractant that binds to CXCR4 of HSPCs inducing their migration and retention to the bone marrow¹²³. Dipeptidyl peptidase (DDP4 or CD26) interferes with HSPC chemotaxis through cleaving SDF1 which no longer can bind and activate the CXCR4 signaling. Small molecule inhibition of DPP4/CD26 enhances human engraftment in immunocompromised mice¹²⁴. The FDA-approved DPP4/CD26 inhibitor (sitagliptin) has been recently evaluated in a pilot clinical trial¹²⁵ with no statistical difference in neutrophil engraftment (Table 1.6).

1.9.1.2 prostaglandin E2 (PGE2)

A stable prostaglandin E2 (PGE2) derivative, 16, 16-dimethyl PGE2 (dmPGE2), was previously demonstrated to be a critical regulator of HSPC homeostasis in both zebrafish and mouse systems^{126,127}. Recent findings extended the conservative role of dmPGE2 in enhancing HSPC function to human and non-human primates¹²⁸. DmPGE2 improves the human HSPC survival and engraftment by increasing expression of survivin and CXCR4, respectively^{127,129}. Furthermore, dmPGE2 treatment elevates the cAMP activity, which regulates HSPC numbers through Wnt signaling pathway thereby controlling cell proliferation and apoptosis^{128,130}. Phase I/II clinical trials showed an earlier neutrophil recovery by 3-4 days vs. controls¹³¹.

1.9.1.3 Fucosylation

Selectin ligands expressed on HSPC have to be fucosylated to bind firmly to endothelial selectins. Inducing fucosylation by treating HSPC with fucosyltransferase VI (FTVI) and its substrate (GDP-fucose) improves binding to selectins thus enhancing CB engraftment in immunocompromised mice recipients^{132,133}. A recent clinical trial showed that *ex vivo* fucosylation of CB units accelerates neutrophil and platelet engraftment¹³⁴ (Table 1.6)

1.9.2 *Ex vivo* expansion

Growing clinical evidence associates the number of total nucleated cells (TNC) and CD34⁺ cells with the rate of engraftment^{135,136}. Studies showed that patients receiving CB grafts with >10⁷ TNC/kg and >10⁵ CD34⁺/kg experience faster engraftment¹³⁷; however most of the CB units cryopreserved in CB banks hold close to 10⁹ TNC indicating that the majority of adult patients will not benefit from CB transplantation. This inspired scientists to develop *ex vivo* liquid or coculture systems that improve expansion of CB graft and allow neutrophil engraftment within ≥15 days, a typical recovery period achieved in BM or mPB grafts.

1.9.2.1 Cytokines and growth factors

Various cytokines have been tested to optimize the culture for HSPC expansion. Many of these cytokines regulate quiescence, cell survival, proliferation, differentiation, and adhesion¹³⁸. The addition of SCF, thrombopoietin (TPO), and Flt-3 ligand (Flt-3L) cytokines into the culture media have shown to enhance hematopoietic cell proliferation and colony forming unit (CFU) expansion¹³⁹. Other cytokines such as IL3, IL6, and G-CSF are also added with a tendency to expand progenitors at the expense of long-term engraftment potential^{140,141}. The safety and the efficacy of cytokine expanded CB cells were tested in phase I clinical trial. Although the safety of this approach is reported, the manipulated graft does not show any improvement in recovering myeloid or platelet engraftment¹⁴² (Table 1.6).

These studies suggest that cytokines alone may not be sufficient to achieve HSPC expansion. Additional growth factors such as insulin-like growth factor binding protein-2 (IGFBP-2)¹⁴³, angiopoietin-like (Angptl) proteins^{144,145}, and pleiotrophin (PTN)¹⁴⁶ might be required to achieve optimal culture conditions.

1.9.2.2 Fed batch culture

A major limitation in HSPC *ex vivo* culture is the rapid generation of differentiated cells that secrete inhibitory paracrine factors. Many of these released components inhibit HSPC expansion such as transforming growth factor-β (TGFβ), tumor necrosis factor-α (TNFα), macrophage inflammatory protein-1α (MIP-1α), monocyte chemotactic protein-1 (MCP1), and chemokines (CCL2, CCL3, CCL4, and CXCL10)¹⁴⁷⁻¹⁵⁰. Strategies to reduce these negative regulators led to the development of fed-batch culture system, which dilute these factors by systematic addition of fresh media. Furthermore, continuous increase in the culture volume leads to a lower

cell density thereby slowing the rate of inhibitory feedback signals¹⁵¹. Accordingly, this culture method enhances the HSPC survival and SRC numbers by 11-folds (Table 1.5). Fed-batch culture is a clinically relevant system for HSC expansion that can also be combined with other expansion protocols like the addition of small molecules.

1.9.2.3 Mesenchymal stromal cell coculture

In bone marrow, HSPCs reside in a unique microenvironment called BM niche where they are in a close contact with several type of stromal cells that provide HSPCs with vital signals for their proliferation and survival¹⁵². Mesenchymal stromal cells (MSC) improve viability of co-culture CB cells through a cell-cell contact and transfer of cytosolic material between the two cell types¹⁵³. One of the documented cytosolic components is SDF1, a chemokine produced by MSCs to promote HSPC engraftment^{154,155}. Insulin-like growth factor binding protein 2 (IGFBP-2), a growth factor known to expand hematopoietic repopulating cells¹⁵⁶, is another example of components that are secreted by stromal-derived cells¹⁵⁷. MSCs have thus been isolated from human donors to provide a co-culture system that mimics the marrow environment for CB expansion. Although CB-MSC co-culture shows an increase in CD34⁺ count, preliminary clinical results do not show any advantage in enhancing early engraftment¹⁵⁸ (Table 1.6).

1.9.2.4 Delta 1 ligand

Notch signaling is known to control cell fate and developmental process¹⁵⁹. Accordingly, Notch gene expression on human HSPC suggested a role in hematopoietic cell fate¹⁶⁰. Forced expression studies of Notch in primitive hematopoietic cells enhance the self-renewal repopulating cells¹⁶¹. Additionally, activating endogenous Notch signaling with soluble or immobilized notch ligand Delta1 boosts the expansion of CD34⁺ and CD34⁺CD38⁻ and increases the SRC frequency by 6- folds^{162,163}(Table 1.5). Clinical studies showed that notch-mediated expansion of CB cells enhances the rate of myeloid engraftment. Most of the patients were not able to retain long-term hematopoiesis/repopulating cells from the expanded cord either due to HSC exhaustion/loss of stem cell self-renewal ability or immune mediated rejection of the expanded unit from the dominant unmanipulated unit^{164,165}.

1.9.2.5 Small molecules

Small molecule-based approach is one of the most attractive strategies since it can be optimized to a more potent and stable molecule thus facilitating its clinical utility. Furthermore, synthe-

sizing small molecules under good manufacturing practice (GMP) is less challenging when compared to other methods such as clinical grade MSCs, which eases their therapeutic use.

1.9.2.5.1 StemRegenin1 (SR1)

StemRegenin1 (SR1), a purine derivative, has been identified in a high throughput chemical screen with primary human HSPCs for CD34 and CD133 cell expansion¹⁶⁶. SR1 treatment retains the HSPC phenotype of expanded cord blood CD34+ cultures with 17- fold increase in SRC numbers. Transcriptome analysis and mechanistic studies reveal that SR1 antagonizes aryl hydrocarbon receptor (AhR) signalling by suppressing two of its downstream target genes: cytochrome P4501B1 (CYP1B1) and the AhR repressor (AhRR)¹⁶⁶. Recent clinical studies using SR1-expanded graft (HSC835) showed rapid hematopoietic recovery with sustained long-term engraftment in 11 of 17 patients¹⁶⁷. Aiming for a better HSPC expansion, various newly identified small molecules or approaches were tested in combination with SR1^{151,168-170}, one of which is eupalinilide E, a plant natural product¹⁷¹. Independent of AhR suppression, eupalinilide E expands myeloid-erythroid progenitors by inhibiting differentiation mainly the erythroid lineage. Combining eupalinilide E with SR1-treatment leads to an additive effect in expanding CD34+ cells indicating that eupalinilide E and SR1 have different molecular targets. This interesting finding suggests that different molecules could improve the outcome of *ex-vivo* stem cell expansion, thereby enhancing their clinical utility.

1.9.2.5.2 Tetraethylenepentamine (TEPA) and Nicotinamide (NAM)

Cu-chelator (tetraethylenepentamine; TEPA)¹⁷² and Sirtuin 1 Deacetylase inhibitor (nicotinamide; NAM)¹⁷³ are two compounds that have been assessed for HSPC expansion. HSPCs treated with TEPA or NAM maintain the immature cell phenotype and show less cell differentiation. Interestingly, after 3 weeks of culture, although the single compound treatment does not show an expansion in CD34+ cells compared to controls, an enhancement in short-term SRC is observed (Table 1.5). This preclinical data led both studies into clinical trials (Table 1.6). Results from TEPA study are not informative in determining any advantage in hematopoietic recovery¹⁷⁴ while NAM-trial shows early neutrophil and platelet engraftment rates when compared to control groups¹⁷⁵. Importantly, although patients demonstrated a long-term engraftment that derived from the NAM-treated cord, a significant enhancement in lymphoid engraftment is not evident suggesting that the culture protocol is not optimal for expanding HSC with the long-term multilineage reconstitution.

1.9.2.3 Other approaches

Additional studies aiming to generate HSPCs from embryonic stem cells (ESCs)^{176,177} and induced pluripotent cells (iPS)^{178,179} were also reported (Figure 1.7). However, due to their availability and clinical relevance, CB cells are still the most common used source for *ex vivo* HSC expansion.

1.10 Impact of improved CB graft

Continuous studies to generate safe and efficient methods for HSPC expansion will lower the cell dose threshold required for cord blood transplantation. This will allow more patients to access such treatment with the use of a single unit that meets the HLA-matching criteria.

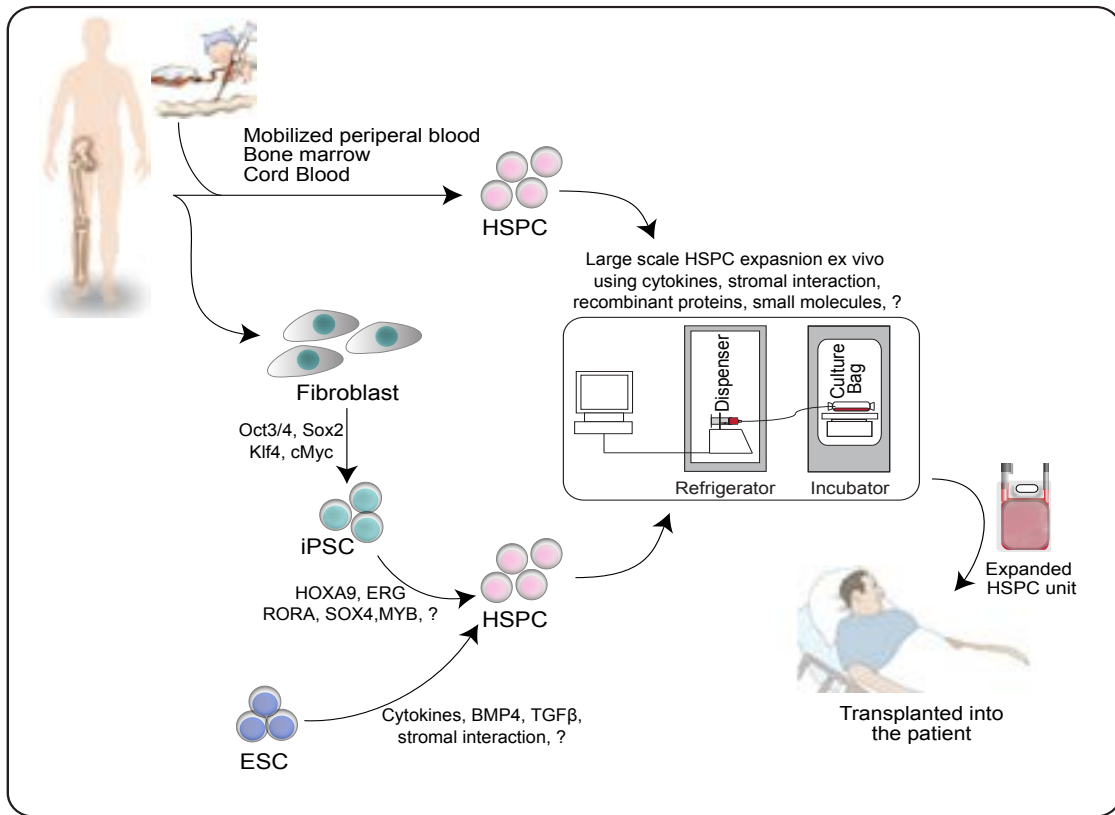


Figure 1.7. Schematic view of HSPC expansion.

Human hematopoietic stem/ progenitor cell (HSPC) derived from mobilized peripheral blood, bone marrow or cord blood, induce pluripotent cells (iPS) or embryonic stem cells (ESC) expanded ex vivo to achieve number of cells required for bone marrow transplantation.

The figure is adapted from Park et al., 2015.

1.11 Hypothesis and Main Objectives

Failure of *ex vivo* HSPCs expansion is due to suboptimal culture condition and that this limitation could be overcome by identifying small molecules that could enhance their activity. Our main objects were:

Objective 1: (a) Identify small molecules that lead to *ex vivo* expansion of human HSC. (b) Optimize activity of best compound by performing structure activity relationship study. (c) Define the responding cellular populations, and determine the impact of the identified small molecule on HSC transcriptome.

Objective 2: Exploit the optimized compound to define the “surfaceome” of expanded human HSC.

References

- 1 Doulatov, S. *et al.* Revised map of the human progenitor hierarchy shows the origin of macrophages and dendritic cells in early lymphoid development. *Nature immunology* **11**, 585-593, doi:10.1038/ni.1889 (2010).
- 2 Novershtern, N. *et al.* Densely interconnected transcriptional circuits control cell states in human hematopoiesis. *Cell* **144**, 296-309, doi:10.1016/j.cell.2011.01.004 (2011).
- 3 Laurenti, E. *et al.* The transcriptional architecture of early human hematopoiesis identifies multilevel control of lymphoid commitment. *Nature immunology* **14**, 756-763, doi:10.1038/ni.2615 (2013).
- 4 Rizo, A., Dontje, B., Vellenga, E., de Haan, G. & Schuringa, J. J. Long-term maintenance of human hematopoietic stem/progenitor cells by expression of BMI1. *Blood* **111**, 2621-2630, doi:10.1182/blood-2007-08-106666 (2008).
- 5 Rizo, A. *et al.* Repression of BMI1 in normal and leukemic human CD34(+) cells impairs self-renewal and induces apoptosis. *Blood* **114**, 1498-1505, doi:10.1182/blood-2009-03-209734 (2009).
- 6 Shojaei, F. *et al.* Hierarchical and ontogenic positions serve to define the molecular basis of human hematopoietic stem cell behavior. *Developmental cell* **8**, 651-663, doi:10.1016/j.devcel.2005.03.004 (2005).
- 7 Milyavsky, M. *et al.* A distinctive DNA damage response in human hematopoietic stem cells reveals an apoptosis-independent role for p53 in self-renewal. *Cell stem cell* **7**, 186-197, doi:10.1016/j.stem.2010.05.016 (2010).
- 8 Zeng, H., Yucel, R., Kosan, C., Klein-Hitpass, L. & Moroy, T. Transcription factor Gfi1 regulates self-renewal and engraftment of hematopoietic stem cells. *The EMBO journal* **23**, 4116-4125, doi:10.1038/sj.emboj.7600419 (2004).
- 9 van der Meer, L. T., Jansen, J. H. & van der Reijden, B. A. Gfi1 and Gfi1b: key regulators of hematopoiesis. *Leukemia* **24**, 1834-1843, doi:10.1038/leu.2010.195 (2010).
- 10 Chuikov, S., Levi, B. P., Smith, M. L. & Morrison, S. J. Prdm16 promotes stem cell maintenance in multiple tissues, partly by regulating oxidative stress. *Nature cell biology* **12**, 999-1006, doi:10.1038/ncb2101 (2010).
- 11 Aguilo, F. *et al.* Prdm16 is a physiologic regulator of hematopoietic stem cells. *Blood* **117**, 5057-5066, doi:10.1182/blood-2010-08-300145 (2011).
- 12 Antonchuk, J., Sauvageau, G. & Humphries, R. K. HOXB4-induced expansion of adult hematopoietic stem cells ex vivo. *Cell* **109**, 39-45 (2002).
- 13 Amsellem, S. *et al.* Ex vivo expansion of human hematopoietic stem cells by direct delivery of the HOXB4 homeoprotein. *Nature medicine* **9**, 1423-1427, doi:10.1038/nm953 (2003).
- 14 Copley, M. R. *et al.* The Lin28b-let-7-Hmga2 axis determines the higher self-renewal potential of fetal haematopoietic stem cells. *Nature cell biology* **15**, 916-925, doi:10.1038/ncb2783

(2013).

- 15 Sato, T. *et al.* Evi-1 promotes para-aortic splanchnopleural hematopoiesis through up-regulation of GATA-2 and repression of TGF- β signaling. *Cancer science* **99**, 1407-1413, doi:10.1111/j.1349-7006.2008.00842.x (2008).
- 16 Yuasa, H. *et al.* Oncogenic transcription factor Evi1 regulates hematopoietic stem cell proliferation through GATA-2 expression. *The EMBO journal* **24**, 1976-1987, doi:10.1038/sj.emboj.7600679 (2005).
- 17 Shimabe, M. *et al.* Pbx1 is a downstream target of Evi-1 in hematopoietic stem/progenitors and leukemic cells. *Oncogene* **28**, 4364-4374, doi:10.1038/onc.2009.288 (2009).
- 18 Senyuk, V. *et al.* Repression of RUNX1 activity by EVI1: a new role of EVI1 in leukemogenesis. *Cancer research* **67**, 5658-5666, doi:10.1158/0008-5472.CAN-06-3962 (2007).
- 19 Tenen, D. G. Disruption of differentiation in human cancer: AML shows the way. *Nature reviews. Cancer* **3**, 89-101, doi:10.1038/nrc989 (2003).
- 20 Mikkola, H. K. & Orkin, S. H. The journey of developing hematopoietic stem cells. *Development* **133**, 3733-3744, doi:10.1242/dev.02568 (2006).
- 21 Oberlin, E., Tavian, M., Blazsek, I. & Peault, B. Blood-forming potential of vascular endothelium in the human embryo. *Development* **129**, 4147-4157 (2002).
- 22 Tavian, M., Biasch, K., Sinka, L., Vallet, J. & Peault, B. Embryonic origin of human hematopoiesis. *The International journal of developmental biology* **54**, 1061-1065, doi:10.1387/ijdb.103097mt (2010).
- 23 Tavian, M. & Peault, B. Embryonic development of the human hematopoietic system. *The International journal of developmental biology* **49**, 243-250, doi:10.1387/ijdb.041957mt (2005).
- 24 Zambidis, E. T., Oberlin, E., Tavian, M. & Peault, B. Blood-forming endothelium in human ontogeny: lessons from in utero development and embryonic stem cell culture. *Trends in cardiovascular medicine* **16**, 95-101, doi:10.1016/j.tcm.2006.01.005 (2006).
- 25 Hann, I. M., Bodger, M. P. & Hoffbrand, A. V. Development of pluripotent hematopoietic progenitor cells in the human fetus. *Blood* **62**, 118-123 (1983).
- 26 Robin, C. *et al.* Human placenta is a potent hematopoietic niche containing hematopoietic stem and progenitor cells throughout development. *Cell stem cell* **5**, 385-395, doi:10.1016/j.stem.2009.08.020 (2009).
- 27 Morrison, S. J. & Scadden, D. T. The bone marrow niche for haematopoietic stem cells. *Nature* **505**, 327-334, doi:10.1038/nature12984 (2014).
- 28 Wright, D. E., Wagers, A. J., Gulati, A. P., Johnson, F. L. & Weissman, I. L. Physiological migration of hematopoietic stem and progenitor cells. *Science* **294**, 1933-1936, doi:10.1126/science.1064081 (2001).
- 29 Hogge, D. E. *et al.* Quantitation of primitive and lineage-committed progenitors in mobilized peripheral blood for prediction of platelet recovery post autologous transplant. *Bone marrow*

- transplantation* **25**, 589-598, doi:10.1038/sj.bmt.1702211 (2000).
- 30 Yang, H. *et al.* Association of post-thaw viable CD34+ cells and CFU-GM with time to hematopoietic engraftment. *Bone marrow transplantation* **35**, 881-887, doi:10.1038/sj.bmt.1704926 (2005).
- 31 Prasad, V. K. *et al.* Unrelated donor umbilical cord blood transplantation for inherited metabolic disorders in 159 pediatric patients from a single center: influence of cellular composition of the graft on transplantation outcomes. *Blood* **112**, 2979-2989, doi:10.1182/blood-2008-03-140830 (2008).
- 32 Page, K. M. *et al.* Total colony-forming units are a strong, independent predictor of neutrophil and platelet engraftment after unrelated umbilical cord blood transplantation: a single-center analysis of 435 cord blood transplants. *Biology of blood and marrow transplantation : journal of the American Society for Blood and Marrow Transplantation* **17**, 1362-1374, doi:10.1016/j.bbmt.2011.01.011 (2011).
- 33 Dexter, T. M., Allen, T. D. & Lajtha, L. G. Conditions controlling the proliferation of haemopoietic stem cells in vitro. *Journal of cellular physiology* **91**, 335-344, doi:10.1002/jcp.1040910303 (1977).
- 34 Sutherland, H. J., Eaves, C. J., Eaves, A. C., Dragowska, W. & Lansdorp, P. M. Characterization and partial purification of human marrow cells capable of initiating long-term hematopoiesis in vitro. *Blood* **74**, 1563-1570 (1989).
- 35 Conneally, E., Cashman, J., Petzer, A. & Eaves, C. Expansion in vitro of transplantable human cord blood stem cells demonstrated using a quantitative assay of their lympho-myeloid repopulating activity in nonobese diabetic-scid/scid mice. *Proceedings of the National Academy of Sciences of the United States of America* **94**, 9836-9841 (1997).
- 36 Sutherland, H. J., Lansdorp, P. M., Henkelman, D. H., Eaves, A. C. & Eaves, C. J. Functional characterization of individual human hematopoietic stem cells cultured at limiting dilution on supportive marrow stromal layers. *Proceedings of the National Academy of Sciences of the United States of America* **87**, 3584-3588 (1990).
- 37 Sutherland, H. J., Eaves, C. J., Lansdorp, P. M., Thacker, J. D. & Hogge, D. E. Differential regulation of primitive human hematopoietic cells in long-term cultures maintained on genetically engineered murine stromal cells. *Blood* **78**, 666-672 (1991).
- 38 Hogge, D. E., Lansdorp, P. M., Reid, D., Gerhard, B. & Eaves, C. J. Enhanced detection, maintenance, and differentiation of primitive human hematopoietic cells in cultures containing murine fibroblasts engineered to produce human steel factor, interleukin-3, and granulocyte colony-stimulating factor. *Blood* **88**, 3765-3773 (1996).
- 39 Baum, C. M., Weissman, I. L., Tsukamoto, A. S., Buckle, A. M. & Peault, B. Isolation of a candidate human hematopoietic stem-cell population. *Proceedings of the National Academy of Sciences of the United States of America* **89**, 2804-2808 (1992).
- 40 Miller, J. S., Verfaillie, C. & McGlave, P. The generation of human natural killer cells from CD34+/DR- primitive progenitors in long-term bone marrow culture. *Blood* **80**, 2182-2187 (1992).

- 41 Hao, Q. L., Thiemann, F. T., Petersen, D., Smogorzewska, E. M. & Crooks, G. M. Extended long-term culture reveals a highly quiescent and primitive human hematopoietic progenitor population. *Blood* **88**, 3306-3313 (1996).
- 42 Bosma, G. C., Custer, R. P. & Bosma, M. J. A severe combined immunodeficiency mutation in the mouse. *Nature* **301**, 527-530 (1983).
- 43 Greiner, D. L. *et al.* Improved engraftment of human spleen cells in NOD/LtSz-scid/scid mice as compared with C.B-17-scid/scid mice. *The American journal of pathology* **146**, 888-902 (1995).
- 44 Shultz, L. D. *et al.* Multiple defects in innate and adaptive immunologic function in NOD/LtSz-scid mice. *Journal of immunology* **154**, 180-191 (1995).
- 45 Vormoor, J. *et al.* Immature human cord blood progenitors engraft and proliferate to high levels in severe combined immunodeficient mice. *Blood* **83**, 2489-2497 (1994).
- 46 Larochelle, A. *et al.* Identification of primitive human hematopoietic cells capable of repopulating NOD/SCID mouse bone marrow: implications for gene therapy. *Nature medicine* **2**, 1329-1337 (1996).
- 47 Cashman, J. D. *et al.* Kinetic evidence of the regeneration of multilineage hematopoiesis from primitive cells in normal human bone marrow transplanted into immunodeficient mice. *Blood* **89**, 4307-4316 (1997).
- 48 Pettengell, R. *et al.* Direct comparison by limiting dilution analysis of long-term culture-initiating cells in human bone marrow, umbilical cord blood, and blood stem cells. *Blood* **84**, 3653-3659 (1994).
- 49 Wang, J. C., Doedens, M. & Dick, J. E. Primitive human hematopoietic cells are enriched in cord blood compared with adult bone marrow or mobilized peripheral blood as measured by the quantitative in vivo SCID-repopulating cell assay. *Blood* **89**, 3919-3924 (1997).
- 50 Jacobson, L. O., Simmons, E. L., Marks, E. K. & Eldredge, J. H. Recovery from radiation injury. *Science* **113**, 510-511 (1951).
- 51 Ford, C. E., Hamerton, J. L., Barnes, D. W. & Loutit, J. F. Cytological identification of radiation-chimaeras. *Nature* **177**, 452-454 (1956).
- 52 McCulloch, E. A. & Till, J. E. The radiation sensitivity of normal mouse bone marrow cells, determined by quantitative marrow transplantation into irradiated mice. *Radiation research* **13**, 115-125 (1960).
- 53 Christianson, S. W. *et al.* Enhanced human CD4+ T cell engraftment in beta2-microglobulin-deficient NOD-scid mice. *Journal of immunology* **158**, 3578-3586 (1997).
- 54 Ito, M. *et al.* NOD/SCID/gamma(c)(null) mouse: an excellent recipient mouse model for engraftment of human cells. *Blood* **100**, 3175-3182, doi:10.1182/blood-2001-12-0207 (2002).
- 55 Shultz, L. D. *et al.* Human lymphoid and myeloid cell development in NOD/LtSz-scid IL2R gamma null mice engrafted with mobilized human hemopoietic stem cells. *Journal of immunology* **174**, 6477-6489 (2005).

- 56 McDermott, S. P., Eppert, K., Lechman, E. R., Doedens, M. & Dick, J. E. Comparison of human cord blood engraftment between immunocompromised mouse strains. *Blood* **116**, 193-200, doi:10.1182/blood-2010-02-271841 (2010).
- 57 Pearson, T. *et al.* Non-obese diabetic-recombination activating gene-1 (NOD-Rag1 null) interleukin (IL)-2 receptor common gamma chain (IL2r gamma null) null mice: a radioresistant model for human lymphohaematopoietic engraftment. *Clinical and experimental immunology* **154**, 270-284, doi:10.1111/j.1365-2249.2008.03753.x (2008).
- 58 Strowig, T. *et al.* Transgenic expression of human signal regulatory protein alpha in Rag2-/-gamma(c)-/- mice improves engraftment of human hematopoietic cells in humanized mice. *Proceedings of the National Academy of Sciences of the United States of America* **108**, 13218-13223, doi:10.1073/pnas.1109769108 (2011).
- 59 Billerbeck, E. *et al.* Development of human CD4+FoxP3+ regulatory T cells in human stem cell factor-, granulocyte-macrophage colony-stimulating factor-, and interleukin-3-expressing NOD-SCID IL2Rgamma(null) humanized mice. *Blood* **117**, 3076-3086, doi:10.1182/blood-2010-08-301507 (2011).
- 60 Rongvaux, A. *et al.* Development and function of human innate immune cells in a humanized mouse model. *Nature biotechnology* **32**, 364-372, doi:10.1038/nbt.2858 (2014).
- 61 Luk'ianenko, N. G., Bogatskii, A. V., Savenko, T. A., Vongai, V. G. & Iaroshchenko, I. M. [Anti-arrhythmia activity of crown-lactone I and its effect on aconitine-modified sodium channels]. *Biofizika* **30**, 427-430 (1985).
- 62 McKenzie, J. L., Gan, O. I., Doedens, M. & Dick, J. E. Human short-term repopulating stem cells are efficiently detected following intrafemoral transplantation into NOD/SCID recipients depleted of CD122+ cells. *Blood* **106**, 1259-1261, doi:10.1182/blood-2005-03-1081 (2005).
- 63 Notta, F., Doulatov, S. & Dick, J. E. Engraftment of human hematopoietic stem cells is more efficient in female NOD/SCID/IL-2Rgc-null recipients. *Blood* **115**, 3704-3707, doi:10.1182/blood-2009-10-249326 (2010).
- 64 Miller, P. H., Knapp, D. J. & Eaves, C. J. Heterogeneity in hematopoietic stem cell populations: implications for transplantation. *Current opinion in hematology* **20**, 257-264, doi:10.1097/MOH.0b013e328360aaf6 (2013).
- 65 Cheung, A. M. *et al.* Analysis of the clonal growth and differentiation dynamics of primitive barcoded human cord blood cells in NSG mice. *Blood* **122**, 3129-3137, doi:10.1182/blood-2013-06-508432 (2013).
- 66 Guenechea, G., Gan, O. I., Dorrell, C. & Dick, J. E. Distinct classes of human stem cells that differ in proliferative and self-renewal potential. *Nature immunology* **2**, 75-82, doi:10.1038/83199 (2001).
- 67 Glimm, H. *et al.* Previously undetected human hematopoietic cell populations with short-term repopulating activity selectively engraft NOD/SCID-beta2 microglobulin-null mice. *The Journal of clinical investigation* **107**, 199-206, doi:10.1172/JCI11519 (2001).
- 68 Notta, F. *et al.* Isolation of single human hematopoietic stem cells capable of long-term multi-

- lineage engraftment. *Science* **333**, 218-221, doi:10.1126/science.1201219 (2011).
- 69 Andrews, R. G., Singer, J. W. & Bernstein, I. D. Monoclonal antibody 12-8 recognizes a 115-kd molecule present on both unipotent and multipotent hematopoietic colony-forming cells and their precursors. *Blood* **67**, 842-845 (1986).
- 70 Krause, D. S., Fackler, M. J., Civin, C. I. & May, W. S. CD34: structure, biology, and clinical utility. *Blood* **87**, 1-13 (1996).
- 71 Berenson, R. J. *et al.* Antigen CD34+ marrow cells engraft lethally irradiated baboons. *The Journal of clinical investigation* **81**, 951-955, doi:10.1172/JCI113409 (1988).
- 72 Berenson, R. J. *et al.* Engraftment after infusion of CD34+ marrow cells in patients with breast cancer or neuroblastoma. *Blood* **77**, 1717-1722 (1991).
- 73 Majdic, O. *et al.* Signaling and induction of enhanced cytoadhesiveness via the hematopoietic progenitor cell surface molecule CD34. *Blood* **83**, 1226-1234 (1994).
- 74 Salati, S. *et al.* Role of CD34 antigen in myeloid differentiation of human hematopoietic progenitor cells. *Stem cells* **26**, 950-959, doi:10.1634/stemcells.2007-0597 (2008).
- 75 Wang, J. *et al.* SCID-repopulating cell activity of human cord blood-derived CD34- cells assured by intra-bone marrow injection. *Blood* **101**, 2924-2931, doi:10.1182/blood-2002-09-2782 (2003).
- 76 Bhatia, M., Bonnet, D., Murdoch, B., Gan, O. I. & Dick, J. E. A newly discovered class of human hematopoietic cells with SCID-repopulating activity. *Nature medicine* **4**, 1038-1045, doi:10.1038/2023 (1998).
- 77 Danet, G. H. *et al.* C1qRp defines a new human stem cell population with hematopoietic and hepatic potential. *Proceedings of the National Academy of Sciences of the United States of America* **99**, 10441-10445, doi:10.1073/pnas.162104799 (2002).
- 78 Takahashi, M. *et al.* CD133 is a positive marker for a distinct class of primitive human cord blood-derived CD34-negative hematopoietic stem cells. *Leukemia* **28**, 1308-1315, doi:10.1038/leu.2013.326 (2014).
- 79 Andrews, R. G., Singer, J. W. & Bernstein, I. D. Precursors of colony-forming cells in humans can be distinguished from colony-forming cells by expression of the CD33 and CD34 antigens and light scatter properties. *The Journal of experimental medicine* **169**, 1721-1731 (1989).
- 80 Hao, Q. L., Shah, A. J., Thiemann, F. T., Smogorzewska, E. M. & Crooks, G. M. A functional comparison of CD34 + CD38- cells in cord blood and bone marrow. *Blood* **86**, 3745-3753 (1995).
- 81 Terstappen, L. W., Huang, S., Safford, M., Lansdorp, P. M. & Loken, M. R. Sequential generations of hematopoietic colonies derived from single nonlineage-committed CD34+CD38- progenitor cells. *Blood* **77**, 1218-1227 (1991).
- 82 Bhatia, M., Wang, J. C., Kapp, U., Bonnet, D. & Dick, J. E. Purification of primitive human hematopoietic cells capable of repopulating immune-deficient mice. *Proceedings of the National Academy of Sciences of the United States of America* **94**, 5320-5325 (1997).

- 83 Johnson, L. V., Walsh, M. L. & Chen, L. B. Localization of mitochondria in living cells with rhodamine 123. *Proceedings of the National Academy of Sciences of the United States of America* **77**, 990-994 (1980).
- 84 Chaudhary, P. M. & Roninson, I. B. Expression and activity of P-glycoprotein, a multidrug efflux pump, in human hematopoietic stem cells. *Cell* **66**, 85-94 (1991).
- 85 Zijlmans, J. M. *et al.* Modification of rhodamine staining allows identification of hematopoietic stem cells with preferential short-term or long-term bone marrow-repopulating ability. *Proceedings of the National Academy of Sciences of the United States of America* **92**, 8901-8905 (1995).
- 86 Kim, M., Cooper, D. D., Hayes, S. F. & Spangrude, G. J. Rhodamine-123 staining in hematopoietic stem cells of young mice indicates mitochondrial activation rather than dye efflux. *Blood* **91**, 4106-4117 (1998).
- 87 McKenzie, J. L., Takenaka, K., Gan, O. I., Doedens, M. & Dick, J. E. Low rhodamine 123 retention identifies long-term human hematopoietic stem cells within the Lin-CD34+CD38- population. *Blood* **109**, 543-545, doi:10.1182/blood-2006-06-030270 (2007).
- 88 Lansdorp, P. M., Sutherland, H. J. & Eaves, C. J. Selective expression of CD45 isoforms on functional subpopulations of CD34+ hemopoietic cells from human bone marrow. *The Journal of experimental medicine* **172**, 363-366 (1990).
- 89 Murray, L. *et al.* Analysis of human hematopoietic stem cell populations. *Blood cells* **20**, 364-369; discussion 369-370 (1994).
- 90 Michallet, M. *et al.* Transplantation with selected autologous peripheral blood CD34+Thy1+ hematopoietic stem cells (HSCs) in multiple myeloma: impact of HSC dose on engraftment, safety, and immune reconstitution. *Experimental hematology* **28**, 858-870 (2000).
- 91 Esber, E., DiNicola, W., Movassaghi, N. & Leikin, S. T and B lymphocytes in leukemia therapy. *American journal of hematology* **1**, 211-218 (1976).
- 92 Majeti, R., Park, C. Y. & Weissman, I. L. Identification of a hierarchy of multipotent hematopoietic progenitors in human cord blood. *Cell stem cell* **1**, 635-645, doi:10.1016/j.stem.2007.10.001 (2007).
- 93 Kim, I., Yilmaz, O. H. & Morrison, S. J. CD144 (VE-cadherin) is transiently expressed by fetal liver hematopoietic stem cells. *Blood* **106**, 903-905, doi:10.1182/blood-2004-12-4960 (2005).
- 94 Jokubaitis, V. J. *et al.* Angiotensin-converting enzyme (CD143) marks hematopoietic stem cells in human embryonic, fetal, and adult hematopoietic tissues. *Blood* **111**, 4055-4063, doi:10.1182/blood-2007-05-091710 (2008).
- 95 Prashad, S. L. *et al.* GPI-80 defines self-renewal ability in hematopoietic stem cells during human development. *Cell stem cell* **16**, 80-87, doi:10.1016/j.stem.2014.10.020 (2015).
- 96 Dorrell, C., Gan, O. I., Pereira, D. S., Hawley, R. G. & Dick, J. E. Expansion of human cord blood CD34(+)/CD38(-) cells in ex vivo culture during retroviral transduction without a corresponding increase in SCID repopulating cell (SRC) frequency: dissociation of SRC phenotype and function.

- Blood* **95**, 102-110 (2000).
- 97 Galy, A., Travis, M., Cen, D. & Chen, B. Human T, B, natural killer, and dendritic cells arise from a common bone marrow progenitor cell subset. *Immunity* **3**, 459-473 (1995).
- 98 Hao, Q. L. *et al.* Identification of a novel, human multilymphoid progenitor in cord blood. *Blood* **97**, 3683-3690 (2001).
- 99 Manz, M. G., Miyamoto, T., Akashi, K. & Weissman, I. L. Prospective isolation of human clonogenic common myeloid progenitors. *Proceedings of the National Academy of Sciences of the United States of America* **99**, 11872-11877, doi:10.1073/pnas.172384399 (2002).
- 100 Lansdorp, P. M., Dragowska, W. & Mayani, H. Ontogeny-related changes in proliferative potential of human hematopoietic cells. *The Journal of experimental medicine* **178**, 787-791 (1993).
- 101 Vaziri, H. *et al.* Evidence for a mitotic clock in human hematopoietic stem cells: loss of telomeric DNA with age. *Proceedings of the National Academy of Sciences of the United States of America* **91**, 9857-9860 (1994).
- 102 Till, J. E. & Mc, C. E. A direct measurement of the radiation sensitivity of normal mouse bone marrow cells. *Radiation research* **14**, 213-222 (1961).
- 103 Thomas, E. D., Lochte, H. L., Jr, Lu, W. C. & Ferrebee, J. W. Intravenous infusion of bone marrow in patients receiving radiation and chemotherapy. *The New England journal of medicine* **257**, 491-496, doi:10.1056/NEJM195709122571102 (1957).
- 104 Appelbaum, F. R. Hematopoietic-cell transplantation at 50. *The New England journal of medicine* **357**, 1472-1475, doi:10.1056/NEJMp078166 (2007).
- 105 Copelan, E. A. Hematopoietic stem-cell transplantation. *The New England journal of medicine* **354**, 1813-1826, doi:10.1056/NEJMra052638 (2006).
- 106 Ljungman, P. *et al.* Allogeneic and autologous transplantation for haematological diseases, solid tumours and immune disorders: definitions and current practice in Europe. *Bone marrow transplantation* **37**, 439-449, doi:10.1038/sj.bmt.1705265 (2006).
- 107 Schmitz, N. *et al.* Randomised trial of filgrastim-mobilised peripheral blood progenitor cell transplantation versus autologous bone-marrow transplantation in lymphoma patients. *Lancet* **347**, 353-357 (1996).
- 108 Korbling, M. & Freireich, E. J. Twenty-five years of peripheral blood stem cell transplantation. *Blood* **117**, 6411-6416, doi:10.1182/blood-2010-12-322214 (2011).
- 109 Howard, C. A. *et al.* Recommendations for donor human leukocyte antigen assessment and matching for allogeneic stem cell transplantation: consensus opinion of the Blood and Marrow Transplant Clinical Trials Network (BMT CTN). *Biology of blood and marrow transplantation : journal of the American Society for Blood and Marrow Transplantation* **21**, 4-7, doi:10.1016/j.bbmt.2014.09.017 (2015).
- 110 Fuchs, E. J., Huang, X. J. & Miller, J. S. HLA-haploidentical stem cell transplantation for hematologic malignancies. *Biology of blood and marrow transplantation : journal of the American Society for Blood and Marrow Transplantation* **16**, S57-63, doi:10.1016/j.bbmt.2009.10.032 (2010).

- 111 Gluckman, E. *et al.* Hematopoietic reconstitution in a patient with Fanconi's anemia by means of umbilical-cord blood from an HLA-identical sibling. *The New England journal of medicine* **321**, 1174-1178, doi:10.1056/NEJM198910263211707 (1989).
- 112 Ballen, K. K., Gluckman, E. & Broxmeyer, H. E. Umbilical cord blood transplantation: the first 25 years and beyond. *Blood* **122**, 491-498, doi:10.1182/blood-2013-02-453175 (2013).
- 113 Garderet, L. *et al.* The umbilical cord blood alphabeta T-cell repertoire: characteristics of a polyclonal and naive but completely formed repertoire. *Blood* **91**, 340-346 (1998).
- 114 Lee, S. J. *et al.* High-resolution donor-recipient HLA matching contributes to the success of unrelated donor marrow transplantation. *Blood* **110**, 4576-4583, doi:10.1182/blood-2007-06-097386 (2007).
- 115 Gragert, L. *et al.* HLA match likelihoods for hematopoietic stem-cell grafts in the U.S. registry. *The New England journal of medicine* **371**, 339-348, doi:10.1056/NEJMsa1311707 (2014).
- 116 Laughlin, M. J. *et al.* Outcomes after transplantation of cord blood or bone marrow from unrelated donors in adults with leukemia. *The New England journal of medicine* **351**, 2265-2275, doi:10.1056/NEJMoa041276 (2004).
- 117 Brunstein, C. G. *et al.* Allogeneic hematopoietic cell transplantation for hematologic malignancy: relative risks and benefits of double umbilical cord blood. *Blood* **116**, 4693-4699, doi:10.1182/blood-2010-05-285304 (2010).
- 118 Wagner, J. E., Jr. *et al.* One-unit versus two-unit cord-blood transplantation for hematologic cancers. *The New England journal of medicine* **371**, 1685-1694, doi:10.1056/NEJMoa1405584 (2014).
- 119 Hofmeister, C. C., Zhang, J., Knight, K. L., Le, P. & Stiff, P. J. Ex vivo expansion of umbilical cord blood stem cells for transplantation: growing knowledge from the hematopoietic niche. *Bone marrow transplantation* **39**, 11-23, doi:10.1038/sj.bmt.1705538 (2007).
- 120 Rice, A. *et al.* Comparative study of the in vitro behavior of cord blood subpopulations after short-term cytokine exposure. *Bone marrow transplantation* **23**, 211-220, doi:10.1038/sj.bmt.1701558 (1999).
- 121 Weidner, C. I. *et al.* Hematopoietic stem and progenitor cells acquire distinct DNA-hypermethylation during in vitro culture. *Scientific reports* **3**, 3372, doi:10.1038/srep03372 (2013).
- 122 Yamagata, Y. *et al.* Lentiviral transduction of CD34(+) cells induces genome-wide epigenetic modifications. *PloS one* **7**, e48943, doi:10.1371/journal.pone.0048943 (2012).
- 123 Sahin, A. O. & Buitenhuis, M. Molecular mechanisms underlying adhesion and migration of hematopoietic stem cells. *Cell adhesion & migration* **6**, 39-48, doi:10.4161/cam.18975 (2012).
- 124 Christopherson, K. W., 2nd, Paganessi, L. A., Napier, S. & Porecha, N. K. CD26 inhibition on CD34+ or lineage- human umbilical cord blood donor hematopoietic stem cells/hematopoietic progenitor cells improves long-term engraftment into NOD/SCID/Beta2null immunodeficient mice. *Stem cells and development* **16**, 355-360, doi:10.1089/scd.2007.9996 (2007).
- 125 Farag, S. S. *et al.* In vivo DPP-4 inhibition to enhance engraftment of single-unit cord blood

- transplants in adults with hematological malignancies. *Stem cells and development* **22**, 1007-1015, doi:10.1089/scd.2012.0636 (2013).
- 126 North, T. E. *et al.* Prostaglandin E2 regulates vertebrate haematopoietic stem cell homeostasis. *Nature* **447**, 1007-1011, doi:10.1038/nature05883 (2007).
- 127 Hoggatt, J., Singh, P., Sampath, J. & Pelus, L. M. Prostaglandin E2 enhances hematopoietic stem cell homing, survival, and proliferation. *Blood* **113**, 5444-5455, doi:10.1182/blood-2009-01-201335 (2009).
- 128 Goessling, W. *et al.* Prostaglandin E2 enhances human cord blood stem cell xenotransplants and shows long-term safety in preclinical nonhuman primate transplant models. *Cell stem cell* **8**, 445-458, doi:10.1016/j.stem.2011.02.003 (2011).
- 129 Frisch, B. J. *et al.* In vivo prostaglandin E2 treatment alters the bone marrow microenvironment and preferentially expands short-term hematopoietic stem cells. *Blood* **114**, 4054-4063, doi:10.1182/blood-2009-03-205823 (2009).
- 130 Goessling, W. *et al.* Genetic interaction of PGE2 and Wnt signaling regulates developmental specification of stem cells and regeneration. *Cell* **136**, 1136-1147, doi:10.1016/j.cell.2009.01.015 (2009).
- 131 Cutler, C. *et al.* Prostaglandin-modulated umbilical cord blood hematopoietic stem cell transplantation. *Blood* **122**, 3074-3081, doi:10.1182/blood-2013-05-503177 (2013).
- 132 Robinson, S. N. *et al.* Ex vivo fucosylation improves human cord blood engraftment in NOD-SCID IL-2Rgamma(null) mice. *Experimental hematology* **40**, 445-456, doi:10.1016/j.exphem.2012.01.015 (2012).
- 133 Xia, L., McDaniel, J. M., Yago, T., Doeden, A. & McEver, R. P. Surface fucosylation of human cord blood cells augments binding to P-selectin and E-selectin and enhances engraftment in bone marrow. *Blood* **104**, 3091-3096, doi:10.1182/blood-2004-02-0650 (2004).
- 134 Popat, U. *et al.* Enforced fucosylation of cord blood hematopoietic cells accelerates neutrophil and platelet engraftment after transplantation. *Blood* **125**, 2885-2892, doi:10.1182/blood-2015-01-607366 (2015).
- 135 Gluckman, E. *et al.* Factors associated with outcomes of unrelated cord blood transplant: guidelines for donor choice. *Experimental hematology* **32**, 397-407, doi:10.1016/j.exphem.2004.01.002 (2004).
- 136 Wagner, J. E. *et al.* Transplantation of unrelated donor umbilical cord blood in 102 patients with malignant and nonmalignant diseases: influence of CD34 cell dose and HLA disparity on treatment-related mortality and survival. *Blood* **100**, 1611-1618, doi:10.1182/blood-2002-01-0294 (2002).
- 137 Barker, J. N. & Wagner, J. E. Umbilical cord blood transplantation: current practice and future innovations. *Critical reviews in oncology/hematology* **48**, 35-43 (2003).
- 138 Zhang, C. C. & Lodish, H. F. Cytokines regulating hematopoietic stem cell function. *Current opinion in hematology* **15**, 307-311, doi:10.1097/MOH.0b013e3283007db5 (2008).

- 139 Levac, K., Karanu, F. & Bhatia, M. Identification of growth factor conditions that reduce ex vivo cord blood progenitor expansion but do not alter human repopulating cell function in vivo. *Haematologica* **90**, 166-172 (2005).
- 140 Sauvageau, G., Iscove, N. N. & Humphries, R. K. In vitro and in vivo expansion of hematopoietic stem cells. *Oncogene* **23**, 7223-7232, doi:10.1038/sj.onc.1207942 (2004).
- 141 Nitsche, A. *et al.* Interleukin-3 promotes proliferation and differentiation of human hematopoietic stem cells but reduces their repopulation potential in NOD/SCID mice. *Stem cells* **21**, 236-244, doi:10.1634/stemcells.21-2-236 (2003).
- 142 Shpall, E. J. *et al.* Transplantation of ex vivo expanded cord blood. *Biology of blood and marrow transplantation : journal of the American Society for Blood and Marrow Transplantation* **8**, 368-376 (2002).
- 143 Zhang, C. C., Kaba, M., Iizuka, S., Huynh, H. & Lodish, H. F. Angiopoietin-like 5 and IGFBP2 stimulate ex vivo expansion of human cord blood hematopoietic stem cells as assayed by NOD/SCID transplantation. *Blood* **111**, 3415-3423, doi:10.1182/blood-2007-11-122119 (2008).
- 144 Fan, X. *et al.* Low-dose insulin-like growth factor binding proteins 1 and 2 and angiopoietin-like protein 3 coordinately stimulate ex vivo expansion of human umbilical cord blood hematopoietic stem cells as assayed in NOD/SCID gamma null mice. *Stem cell research & therapy* **5**, 71, doi:10.1186/scrt460 (2014).
- 145 Zhang, C. C. *et al.* Angiopoietin-like proteins stimulate ex vivo expansion of hematopoietic stem cells. *Nature medicine* **12**, 240-245, doi:10.1038/nm1342 (2006).
- 146 Himburg, H. A. *et al.* Pleiotrophin regulates the expansion and regeneration of hematopoietic stem cells. *Nature medicine* **16**, 475-482, doi:10.1038/nm.2119 (2010).
- 147 Kirouac, D. C. *et al.* Cell-cell interaction networks regulate blood stem and progenitor cell fate. *Molecular systems biology* **5**, 293, doi:10.1038/msb.2009.49 (2009).
- 148 Madlambayan, G. J. *et al.* Dynamic changes in cellular and microenvironmental composition can be controlled to elicit in vitro human hematopoietic stem cell expansion. *Experimental hematology* **33**, 1229-1239, doi:10.1016/j.exphem.2005.05.018 (2005).
- 149 Cashman, J. D., Eaves, C. J., Sarris, A. H. & Eaves, A. C. MCP-1, not MIP-1alpha, is the endogenous chemokine that cooperates with TGF-beta to inhibit the cycling of primitive normal but not leukemic (CML) progenitors in long-term human marrow cultures. *Blood* **92**, 2338-2344 (1998).
- 150 Bonnet, D., Lemoine, F. M., Najman, A. & Guigon, M. Comparison of the inhibitory effect of AcSDKP, TNF-alpha, TGF-beta, and MIP-1 alpha on marrow-purified CD34+ progenitors. *Experimental hematology* **23**, 551-556 (1995).
- 151 Csaszar, E. *et al.* Rapid expansion of human hematopoietic stem cells by automated control of inhibitory feedback signaling. *Cell stem cell* **10**, 218-229, doi:10.1016/j.stem.2012.01.003 (2012).
- 152 Wilson, A. & Trumpp, A. Bone-marrow haematopoietic-stem-cell niches. *Nature reviews. Im-*

- munology* **6**, 93-106, doi:10.1038/nri1779 (2006).
- 153 Chu, P. P. *et al.* Intercellular cytosolic transfer correlates with mesenchymal stromal cell rescue of umbilical cord blood cell viability during ex vivo expansion. *Cytotherapy* **14**, 1064-1079, doi:10.3109/14653249.2012.697146 (2012).
- 154 Gillette, J. M., Larochelle, A., Dunbar, C. E. & Lippincott-Schwartz, J. Intercellular transfer to signalling endosomes regulates an ex vivo bone marrow niche. *Nature cell biology* **11**, 303-311, doi:10.1038/ncb1838 (2009).
- 155 Noort, W. A. *et al.* Mesenchymal stem cells promote engraftment of human umbilical cord blood-derived CD34(+) cells in NOD/SCID mice. *Experimental hematology* **30**, 870-878 (2002).
- 156 Huynh, H. *et al.* Insulin-like growth factor-binding protein 2 secreted by a tumorigenic cell line supports ex vivo expansion of mouse hematopoietic stem cells. *Stem cells* **26**, 1628-1635, doi:10.1634/stemcells.2008-0064 (2008).
- 157 Dumont, N. *et al.* Medium conditioned with mesenchymal stromal cell-derived osteoblasts improves the expansion and engraftment properties of cord blood progenitors. *Experimental hematology* **42**, 741-752 e741, doi:10.1016/j.exphem.2014.04.009 (2014).
- 158 de Lima, M. *et al.* Cord-blood engraftment with ex vivo mesenchymal-cell coculture. *The New England journal of medicine* **367**, 2305-2315, doi:10.1056/NEJMoa1207285 (2012).
- 159 Artavanis-Tsakonas, S., Rand, M. D. & Lake, R. J. Notch signaling: cell fate control and signal integration in development. *Science* **284**, 770-776 (1999).
- 160 Milner, L. A., Kopan, R., Martin, D. I. & Bernstein, I. D. A human homologue of the Drosophila developmental gene, Notch, is expressed in CD34+ hematopoietic precursors. *Blood* **83**, 2057-2062 (1994).
- 161 Varnum-Finney, B. *et al.* Pluripotent, cytokine-dependent, hematopoietic stem cells are immortalized by constitutive Notch1 signaling. *Nature medicine* **6**, 1278-1281, doi:10.1038/81390 (2000).
- 162 Delaney, C. *et al.* Notch-mediated expansion of human cord blood progenitor cells capable of rapid myeloid reconstitution. *Nature medicine* **16**, 232-236, doi:10.1038/nm.2080 (2010).
- 163 Ohishi, K., Varnum-Finney, B. & Bernstein, I. D. Delta-1 enhances marrow and thymus repopulating ability of human CD34(+)CD38(-) cord blood cells. *The Journal of clinical investigation* **110**, 1165-1174, doi:10.1172/JCI16167 (2002).
- 164 Gutman, J. A. *et al.* Single-unit dominance after double-unit umbilical cord blood transplantation coincides with a specific CD8+ T-cell response against the nonengrafted unit. *Blood* **115**, 757-765, doi:10.1182/blood-2009-07-228999 (2010).
- 165 Ramirez, P. *et al.* Factors predicting single-unit predominance after double umbilical cord blood transplantation. *Bone marrow transplantation* **47**, 799-803, doi:10.1038/bmt.2011.184 (2012).
- 166 Boitano, A. E. *et al.* Aryl hydrocarbon receptor antagonists promote the expansion of human hematopoietic stem cells. *Science* **329**, 1345-1348, doi:10.1126/science.1191536 (2010).

- 167 Wagner, J. E., Jr. *et al.* Phase I/II Trial of StemRegenin-1 Expanded Umbilical Cord Blood Hematopoietic Stem Cells Supports Testing as a Stand-Alone Graft. *Cell stem cell* **18**, 144-155, doi:10.1016/j.stem.2015.10.004 (2016).
- 168 Fares, I. *et al.* Cord blood expansion. Pyrimidoindole derivatives are agonists of human hematopoietic stem cell self-renewal. *Science* **345**, 1509-1512, doi:10.1126/science.1256337 (2014).
- 169 Dahlberg, A., Brashem-Stein, C., Delaney, C. & Bernstein, I. D. Enhanced generation of cord blood hematopoietic stem and progenitor cells by culture with StemRegenin1 and Delta1(Ext-IgG.). *Leukemia* **28**, 2097-2101, doi:10.1038/leu.2014.181 (2014).
- 170 Chen, X. *et al.* G9a/GLP-dependent histone H3K9me2 patterning during human hematopoietic stem cell lineage commitment. *Genes & development* **26**, 2499-2511, doi:10.1101/gad.200329.112 (2012).
- 171 de Lichtervelde, L. *et al.* Eupalinilide E inhibits erythropoiesis and promotes the expansion of hematopoietic progenitor cells. *ACS chemical biology* **8**, 866-870, doi:10.1021/cb4000234 (2013).
- 172 Peled, T. *et al.* Linear polyamine copper chelator tetraethylenepentamine augments long-term ex vivo expansion of cord blood-derived CD34+ cells and increases their engraftment potential in NOD/SCID mice. *Experimental hematology* **32**, 547-555, doi:10.1016/j.exphem.2004.03.002 (2004).
- 173 Peled, T. *et al.* Nicotinamide, a SIRT1 inhibitor, inhibits differentiation and facilitates expansion of hematopoietic progenitor cells with enhanced bone marrow homing and engraftment. *Experimental hematology* **40**, 342-355 e341, doi:10.1016/j.exphem.2011.12.005 (2012).
- 174 de Lima, M. *et al.* Transplantation of ex vivo expanded cord blood cells using the copper chelator tetraethylenepentamine: a phase I/II clinical trial. *Bone marrow transplantation* **41**, 771-778, doi:10.1038/sj.bmt.1705979 (2008).
- 175 Horwitz, M. E. *et al.* Umbilical cord blood expansion with nicotinamide provides long-term multilineage engraftment. *The Journal of clinical investigation* **124**, 3121-3128, doi:10.1172/JCI74556 (2014).
- 176 Chadwick, K. *et al.* Cytokines and BMP-4 promote hematopoietic differentiation of human embryonic stem cells. *Blood* **102**, 906-915, doi:10.1182/blood-2003-03-0832 (2003).
- 177 Ledran, M. H. *et al.* Efficient hematopoietic differentiation of human embryonic stem cells on stromal cells derived from hematopoietic niches. *Cell stem cell* **3**, 85-98, doi:10.1016/j.stem.2008.06.001 (2008).
- 178 Takahashi, K. *et al.* Induction of pluripotent stem cells from adult human fibroblasts by defined factors. *Cell* **131**, 861-872, doi:10.1016/j.cell.2007.11.019 (2007).
- 179 Doulatov, S. *et al.* Induction of multipotential hematopoietic progenitors from human pluripotent stem cells via respecification of lineage-restricted precursors. *Cell stem cell* **13**, 459-470, doi:10.1016/j.stem.2013.09.002 (2013).

Chapter 2: Pyrimido-Indole Derivatives Are Agonists of Human Hematopoietic Stem Cell Self-renewal

Publish Manuscript in Science 2014 Sept; 345: 1509-12. doi: 10.1126/ science.1256337 (2014).

Permission from publishing group: This is a License Agreement between Iman Fares and The American Association for the Advancement of Science provided by Copyright Clearance Center (License Number 3832030552745).

Synopsis:

Hematopoietic stem cell (HSC) transplantation is a treatment procedure for various blood diseases; however, the low stem cells numbers in a graft limits the use of such treatment. Aiming at expansion of HSC *ex vivo* to broaden patient's access for HSC transplantation, we initiated a high-throughput screen of small molecules and identified UM171- a pyrimido-indole derivative- as an HSC agonist.

Contribution:

All the data in **Figure 2.1, 2.2, 2.3A-B, 2.4, S2.1-2.4, S2.6, S2.9-2.12, and Table S2.1-2.4** were generated by **Iman Fares (100%)**

Data in **Figure 2.3C and S2.7** were generated by **Jalila Chagraoui**

Data in **Figure S2.5** were generated by **Kori L Watts** from **Hans-Peter Kiem** laboratory

Data in **Figure S2.8A** were generated by **Mor Ngom** and **Suzan Imren** from **R. Keith Humphries** laboratory

Data in **Figure S2.8B** were generated by **David JHF Knapp** and **Paul Miller** from **Connie J. Eaves** laboratory

Pyrimido-Indole Derivatives Are Agonists of Human Hematopoietic Stem Cell Self-renewal

Authors: Iman Fares¹, Jalila Chagraoui¹, Yves Gareau², Stéphane Gingras², Réjean Ruel², Nadine Mayotte¹, Elizabeth Csaszar³, David JHF Knapp⁴, Paul Miller⁴, Mor Ngom⁴, Suzan Imren⁴, Denis-Claude Roy^{5,6}, Kori L Watts⁷, Hans-Peter Kiem^{7,8}, Robert Herrington⁹, Norman N. Iscove^{9,10}, R. Keith Humphries⁴, Connie J. Eaves⁴, Sandra Cohen^{5,6}, Anne Marinier², Peter W. Zandstra³, Guy Sauvageau^{1,5,6}

¹Molecular Genetics of Stem Cells Laboratory, Institute of Research in Immunology and Cancer (IRIC), University of Montreal, Montreal, QC, Canada.

²Medicinal chemistry, Institute of Research in Immunology and Cancer (IRIC), University of Montreal, Montreal, QC, Canada.

³Terrence Donnelly Centre for Cellular and Biomolecular Research, University of Toronto, Toronto, ON, Canada.

⁴Terry Fox Laboratory, British Columbia Cancer Agency and University of British Columbia, Vancouver, BC, Canada.

⁵ Division of Hematology, Maisonneuve-Rosemont Hospital, Montreal, QC, Canada.

⁶Department of Medicine, Faculty of Medicine, University de Montreal, Montreal, QC, Canada.

⁷Clinical Research Division, Fred Hutchinson Cancer Research Center and University of Washington, Seattle, WA, USA.

⁸Department of Medicine and Pathology, University of Washington, Seattle, WA, USA.

⁹Ontario Cancer Institute, University Health Network, Toronto, ON, Canada.

¹⁰Department of Immunology, University of Toronto, Toronto, ON, Canada.

Corresponding Author:

Guy Sauvageau M.D., Ph.D.

Institut de Recherche en Immunologie et Cancérologie

C.P. 6128, succursale Centre-Ville, Montréal, Québec

Canada H3C 3J7

Telephone: (514) 343-7134

Facsimile: (514) 343-7379

E-mail: guy.sauvageau@umontreal.ca

Manuscript: test, figures, supplementary text and figures

(No Data Deposition)

Abstract

The small number of hematopoietic stem and progenitor cells in cord blood units limits their widespread use in human transplant protocols. We have now identified a family of chemically related small molecules that stimulate the expansion *ex vivo* of human cord blood cells capable of reconstituting human hematopoiesis for at least 6 months in immunocompromised mice. The potent activity of these newly identified compounds, UM171 being the prototype, is independent of suppression of the aryl hydrocarbon receptor, which targets cells with more limited regenerative potential. The properties of UM171 make it a potential candidate for hematopoietic stem cell transplantation and gene therapy.

One sentence summary

The pyrimido-indole derivative, UM171, enhances HSC self-renewal *in vitro*.

2.1 Introduction

Allogeneic HSC transplant is the only curative therapy for numerous hematologic malignancies. Unfortunately 30-40% of patients will not have an HLA identical donor and will be excluded from therapy (1). Cord blood (CB) transplants offer several advantages namely the reduced need for HLA matching thereby extending transplantation availability to nearly all patients (2) and the decreased risk of chronic GVHD, the most significant determinant of long term quality of life in transplant patients. However, CB transplants suffer from limited progenitor cell dose leading to delayed neutrophil engraftment and increased mortality (3, 4).

Recent studies in immunodeficient mice have confirmed the existence of human cord blood-derived long term-repopulating hematopoietic stem cells (LT-HSCs) capable of regenerating the lifelong production of all mature blood cells (5). These LT-HSCs show a delayed engraftment pattern, in opposition to short term-HSCs (ST-HSCs) which produce short-lived progenitors responsible for the production of mature blood cells and prompt neutrophil recovery (3, 5). Hence the great interest in the development of conditions for robustly expanding these progenitor cells while maintaining or expanding LT-HSCs. Unfortunately, most expansion systems available to date achieve progenitor cell expansion at the expense of the LT-HSC loss (6), increasing the risk of late graft failure.

Recent studies showed that aryl hydrocarbon receptor (AhR) antagonists and a notch ligand agonist promote the *in vitro* expansion of human CB cells with repopulating activity lasting up to 16 weeks in immunodeficient mice (7, 8). We have developed an automated and continuous medium delivery system which produces an equivalent expansion of CB cells with similar repopulation properties (9). This fed-batch culture system optimizes the balance of stimulatory and inhibitory factors in a small culture volume. We hypothesized that small molecules with potent LT-HSC-stimulating activities might be identified and be potentiated in this fed-batch culture system.

2.2 Results and Discussion

2.2.1 Finding novel agonists that expand human CD34⁺CD45RA⁻ cells

We screened a library of 5,280 low molecular weight compounds for their ability to expand human CD34⁺CD45RA⁻ mobilized peripheral blood (mPB) cells which are enriched in LT-HSCs (10) (fig. S2.1, A and B). Seven hits were identified after excluding the auto-fluorescent compounds (Fig. 2.1A and fig. S2.1C), 5 of which were known (n=4, (11, 12)) or novel (n=1,

UM125454, fig. S2.2) suppressors of the AhR pathway (Fig. 2.1B). The other 2 compounds, UM729 (fig. S2.2) and UM118428 did not suppress the AhR pathway (Fig. 2.1B). Due to its apparent superior activity in expanding CD34⁺CD45RA⁻ cells, UM729 was selected for further characterization and optimization by structure activity relationship (SAR) studies that determine the link between the chemical structure of the compound and its biological activity in expanding CD34⁺CD45RA⁻ cells. More than three hundred newly synthesized analogs of UM729 were examined of which one (UM171, Fig. 2.1C) was 10-20 times more potent than UM729, with effective concentrations of 17-19 nM when tested for its ability to stimulate the expansion of HSC enriched population, CD34⁺CD45RA⁻ cells (10) (Fig. 2.1D and fig. S2.3, A and B). UM729 did not expand mouse HSCs (fig. S2.4). UM729 and UM171 treatment enhanced the engraftment potential of CD34⁺ macaque cells by 3 fold when compared with controls (fig. S2.5).

2.2.2 Optimizing culture conditions: UM171 and fed-batch system

Optimization of fed-batch culture duration indicated that the highest expansion of multipotent progenitors and long-term culture-initiating cells (LTC-ICs) was obtained on day 12 (fig. S2.3, C, D and E). Likewise, the proportion of apoptotic cells was lower at that time when compared to day 16 (fig. S2.3F). We also observed that the effect of UM171 requires its constant presence in the media and that the molecule lacks direct mitogenic activity (fig. S2.6). Cell division tracking further showed that UM171 does not affect the division rate of phenotypically primitive populations (fig. S2.7).

2.2.3 UM171 and SR1 cooperation on CB progenitor cells

We next designed experiments to compare the impact of UM171 and SR1 on outputs of CD34⁺ CB cells introduced in fed-batch cultures. Control (DMSO) fed-batch cultures contained mostly differentiated cells (Fig. 2.2A, DMSO) and a reduced frequency of CD34⁺CD45RA⁻ cells (compare red box of the 2 upper right panels in Fig. 2.2B). In contrast, this phenotype remained prominent in cultures containing UM171 (Fig. 2.2A and red box in Fig. 2.2B). Although CD34⁺ cell frequencies in cultures containing SR1 or UM171 were similar (Fig. 2.2B, middle panels), CD34⁺CD45RA⁻ cells were proportionally more abundant when UM171 was present (Fig. 2.2B, third panels, red box; $p < 0.005$, Mann Whitney test). Determining the absolute numbers of these primitive phenotypes and functionally defined cells confirmed the greater effect of UM171 when compared to control or SR1 (compare UM171 (red) with fed-batch (black) and SR1 (blue) in Fig. 2.2C and fig. S2.8 and S2.6 for fold expansion and absolute cell numbers,

respectively. Furthermore, the effect of UM171 on CFU-GEMM expansion (Fig. 2.2D) and on mature cell output suppression (e.g. CD34⁻ cells in Fig. 2.2B and Fig. 2.2C) was enhanced by the addition of SR1. Together, these observations show that these 2 compounds cooperate to enhance *ex vivo* expansion of progenitor cells and that they suppress mature cell output (differentiation). These data also suggest that UM171 targets phenotypically more primitive cells than those targeted by SR1.

2.2.4 LT-HSC expansion in presence of UM171

Using conditions described in fig S2.10A, we next determined the frequencies (adjusted to numbers of CD34⁺ cells at day 0 hereafter called d0 equivalent) and absolute numbers of LT-HSCs in fed-batch cultures supplemented with DMSO (control), UM171, SR1 or the combination of both (Fig. 2.3A and table S2.1, respectively). When analyzed at 20 weeks post-transplantation, LT-HSC frequencies in fresh (uncultured) CD34⁺ CB were measured at the expected frequency of ~1 per 880 CD34⁺ starting cells (95% confidence interval (CI) of 470-1600; see Fig. 2.3A in which frequencies (red line) and 95% CIs (gray box) are indicated). Similar LT-HSC frequencies were obtained from fed-batch cultures (DMSO) whether or not they contained SR1 (Fig. 2.3A). Frequencies of day 0 equivalent LT-HSCs were 13-fold higher in cultures supplemented with UM171 when compared to DMSO or to fresh (uncultured) controls (Fig. 2.3A). Absolute LT-HSC values determined after 20 weeks post transplantation in all culture conditions are provided in table S1. Simultaneous addition of SR1 to UM171 treated cultures did not significantly change these numbers indicating that the cooperativity between these two molecules is restricted to short-lived progenitors and that LT-HSC output is selectively enhanced in the presence of UM171 (Fig. 2.3A and table S1).

We analyzed the nature of human hematopoietic reconstitution obtained by transplanting fresh or expanded cells in NSG mice. Levels of human cell engraftment, whether total (CD45), myeloid (CD33) and B lymphoid (CD19) were determined for approximately 300 mice and represented in the form of heat-map in Fig. 2.3B (raw data in table S2.2). Analysis of this dataset indicates two emerging patterns of human reconstitution, one from predominantly lympho-myeloid LT-HSC, observed at high cell doses with most conditions, and the other from LT-HSC that display a lymphoid-deficient differentiation phenotype mostly observed with UM171 treatment, with or without SR1 (Fig. 2.3B). However, neither B lymphopoiesis nor the frequency or number of lympho-myeloid LT-HSCs is negatively affected by UM171 (Fig. 2.3B). Interestingly, SR1 treatment appeared to compromise the *in vivo* proliferative potential, although not the number, of lympho-myeloid LT-HSCs (compare color code representing reconstitution

levels of SR1 to uncultured or UM171 conditions in Fig. 2.3B). In support of this, the presence of SR1 in UM171 treated cultures appears to slightly hamper the proliferative potential of the expanded cells (see reduction in red colors in Combi versus UM171 conditions in Fig. 2.3B). The impact of UM171 on LT-HSC was preserved at 30 weeks post-transplantation (fig. S2.10B and table S2.3) at which time multilineage contribution remained obvious at the high cell dose (Fig. 2.3C). At this extended time point post-transplant, we also noted a slight augmentation in myeloid cell output, a phenomenon recently described with normal unexpanded cells (5, 13). The molecular and cellular mechanisms underlying this effect of UM171 on expanding LT-HSCs that show a lymphoid-deficient differentiation pattern is of interest given previous studies of a similar self-perpetuating LT-HSC subset in mice (14) whose prominence is increased in the bone marrow as soon as HSCs begin to migrate from the fetal liver to that site (15).

To further evaluate the impact of UM171 treated LT-HSC population(s), we performed transplantation experiments in secondary recipients. For these studies, 4-6 primary recipients were selected per condition in which human reconstitution ranged between 10-70%. Results presented in table S2.4 indicate that UM171 *ex vivo* treatment did not appear to affect the capability of LT-HSC to expand in primary recipients and hence similarly reconstituted secondary animals for at least 18 more weeks. Thus indicating that cells exposed to the molecule *ex vivo* are still competent in secondary recipients where they show no advantage when compared to unmanipulated CD34⁺ cells.

2.2.5 Evaluation of UM171 mode of action

We next performed RNA-Seq expression profiling experiments to gain insights into the mode of action of UM171. SR1-treated cells were also analyzed for comparison. As expected, SR1, but not UM171, treatment resulted in down-regulation of AhR target genes such as CYP1B1, CYP1A1 and AhRR (Fig. 2.4A and fig. S2.11A) (7, 16). Unlike SR1, UM171 treatment was accompanied by a marked suppression of transcripts associated with erythroid and megakaryocytic differentiation (Fig. 2.4B and fig. S2.11B). Only six to seven genes were commonly up- or down-regulated in cells exposed to UM171 or SR1 (fig. S2.12A). In line with these results, gene expression signatures were very different between cells exposed to UM171 versus those treated with SR1 (fig. S2.11C and fig. S2.12B). Most notably, we found that the transmembrane protein of unknown function TMEM183A was the most up-regulated transcript in both conditions (fig. S2.11, A and B) and, the most highly up-regulated genes in UM171-treated cells encode for surface molecules (fig. S2.11B, highlighted in red). These genes included PROCR or EPCR (also called CD201) which represents a known marker of mouse LT-HSCs (17). Ad-

ditional RNA-Seq experiments and FACS analyses confirmed that expression of this receptor is modulated, in a dose-dependent manner, by UM171 treatment (see fig. S2.13).

2.3 Conclusion

In summary, UM171 enables a robust *ex vivo* expansion of human CB cells with functionally validated long-term *in vivo* repopulating capability (Fig. 2.4C). Based on these findings, we suggest that UM171 acts by enhancing the human LT-HSC self-renewal machinery independently of AhR suppression. Conversely, AhR inhibitors' activity appears restricted to the production of cells with less durable self-renewal activity (Fig. 2.4C). By expanding LT-HSCs and downstream cells *in vitro*, using UM171, it may become possible for small, well HLA-matched CB units to become a prioritized source of cells for transplantation in future donor selection algorithms.

Acknowledgments

The authors acknowledge the help of M. Cooke and A. Boitano in setting up the assay for the primary screen. We also acknowledge the expert help of J. Duchaine at IRIC for assistance with the chemical screen, D. Gagné also at IRIC for technical support with HTS-flow cytometry, and M. Frechette and V. Blouin-Chagnon for assistance with mice experiments. We also thank J. Roy and J. Krosi for scientific support and for critical reading of the manuscript. We thank Héma-Québec and the Women's and Children's Hospital of British Columbia for providing cord blood. Also, Maisonneuve-Rosemont hospital cell therapy laboratory staff for mobilized peripheral blood. Financial support was from a grant to GS and collaborators from the Stem Cell Network of Canada and from IRICoR. DCR is also supported through Fonds de Recherche du Québec Santé – ThéCell. HPK is also supported through NIH HL84345 grant. DJHFK held a Vanier Scholarship and PM a Banting and Best Studentship, both from the Canadian Institutes of Health Research. GS, YG, RR, SG and IF are inventors on a patent application filed by the University of Montreal, Canada that covers pyrimido indoles and their use in expansion of hematopoietic stem and progenitor cells. PZ and EC are inventors on a patent application filed by the University of Toronto, Canada that covers the fedbatch system. Compounds UM729 and/or UM171 can be obtained from GS laboratory under a Material Transfer Agreement with the University of Montreal. Authors reported no conflict of interest.

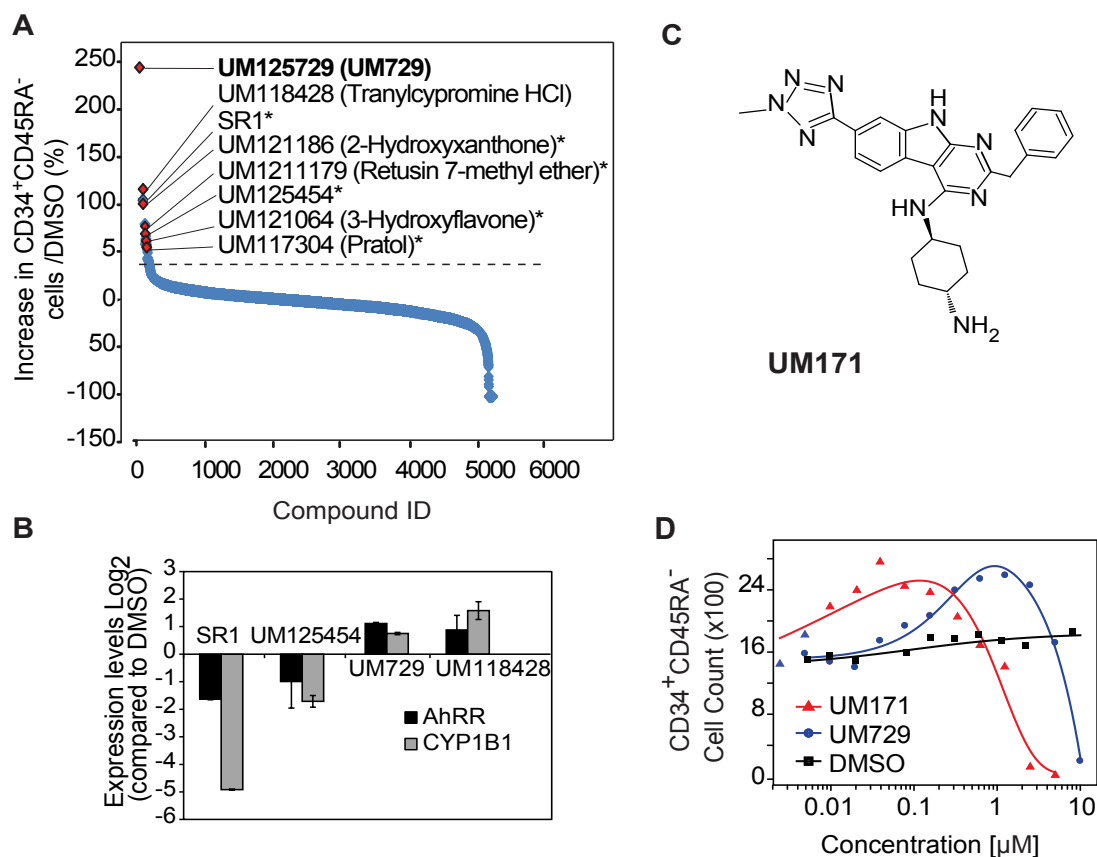


Fig. 2.1. Identification of novel compounds promoting human CD34⁺ expansion.

(A) Results of primary screen, (*) denotes the compounds that suppress the aryl hydrocarbon receptor (AhR) pathway. (B) Changes in expression levels of AhR targets (AhRR, and CYP1B1) measured by q-RT-PCR after a 12-hour incubation with selected compounds compared to DMSO (using GAPDH and HPRT as control, mean ± SD). (C, D) Chemical structure of UM171, the optimized version of UM729 and their comparative activity on expansion of CD34⁺CD45RA⁻ mPB cells after 7 day cultures. Note the cytostatic/cytotoxic effects of UM729 and UM171 were observed at values above 1 μM and 0.125 μM, respectively

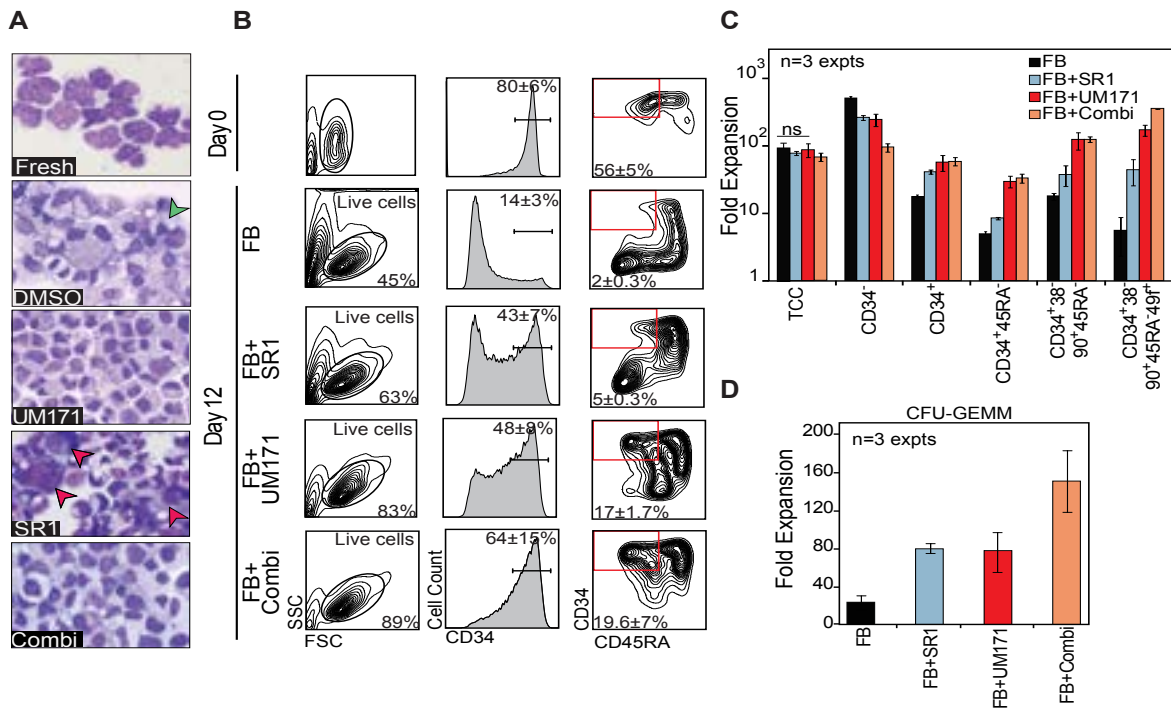


Fig. 2.2. UM171 attenuates cell differentiation and promotes ex vivo expansion of primitive human hematopoietic cells.

(A) Wright-stained cytopsin preparation of CD34+ CB cells at day 0 and after 12 days in fed-batch cultures supplemented with vehicle (DMSO 0.1%), UM171 [35 nM], SR1 [750nM] or combination of SR1 [500 nM] and UM171 [35 nM]. Arrowheads show macrophages (green) and megakaryocyte (red). (B) Representative FACS profiles of CD34+ and CD34+CD45RA-populations in fresh (day0) or cultured (day12) CB cells. (C) Bar graph showing the fold-expansion of phenotypically defined cell subsets after 12 days in fed-batch cultures supplemented with indicated compounds (mean±SD: unless specified (ns, not significant); all values are significant when compared to control (back bars): p<0.05, Mann Whitney test). (D) Fold-expansion of CFU-GEMMs after 12 days in cultures.

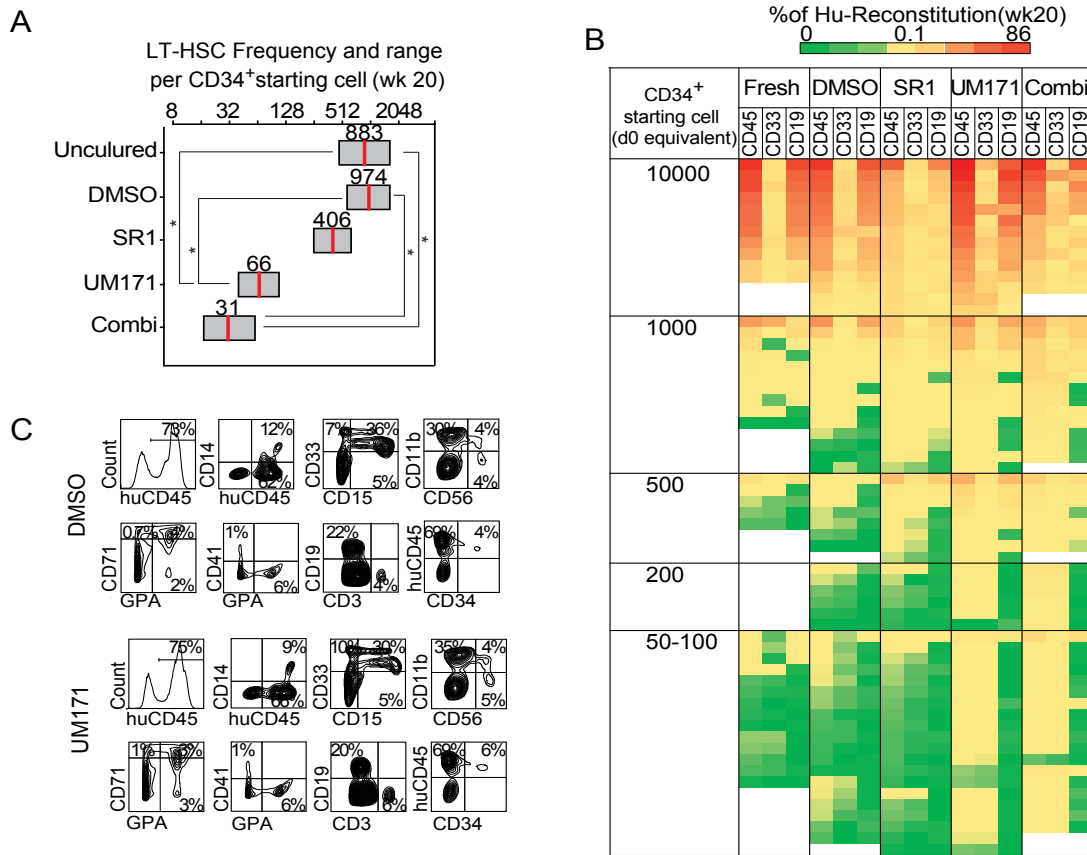


Fig. 2.3. UM171 promotes expansion of LT-HSCs.

(A) LT-HSC frequencies (red line) and 95% CI (gray box) presented as 1/number of starting cell (day 0) equivalent for each condition; n= 5 independent experiments performed with a pool of 2-3 human CB units per experiment. Significance level: * p<0.05 (Mann Whitney test). (B) Color code (from red=86% to green=0%) showing levels of human (Hu) engraftment in NSG mice transplanted with different cell doses (column 1). See table S2 for raw data. (C) Representative FACS profiles showing multilineage repopulation of NSG mice.

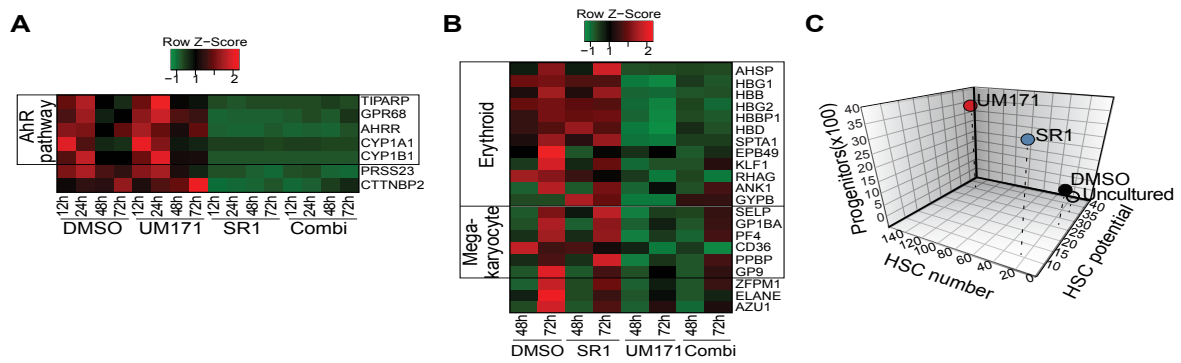


Fig. 2.4. Summary of UM171 effect on cell expansion and differentiation.

(A) Heat-map showing expression of AhR targets (A) or lineage-specific (B) genes (green = low; red = high) in indicated conditions. (C) Comparison of UM171 with SR1 and DMSO on number and quality of LT-HSC and progenitors based on results from expansion of 10,000 fresh CD34+ CB cells.

References

1. L. Gragert, M. Eapen, E. Williams, J. Freeman, S. Spellman, R. Baitty, R. Hartzman, J. D. Rizzo, M. Horowitz, D. Confer, M. Maiers, *The New England journal of medicine* **371**, 339-348 (2014).
2. C. G. Brunstein, J. A. Gutman, D. J. Weisdorf, A. E. Woolfrey, T. E. Defor, T. A. Gooley, M. R. Verneris, F. R. Appelbaum, J. E. Wagner, C. Delaney, *Blood* **116**, 4693-4699 (2010).
3. V. Rocha, M. Labopin, G. Sanz, W. Arcese, R. Schwerdtfeger, A. Bosi, N. Jacobsen, T. Ruutu, M. de Lima, J. Finke, F. Frassoni, E. Gluckman, B. Acute Leukemia Working Party of European, G. Marrow Transplant, R. Eurocord-Netcord, *The New England journal of medicine* **351**, 2276-2285 (2004).
4. P. H. Miller, D. J. Knapp, C. J. Eaves, *Current opinion in hematology* **20**, 257-264 (2013).
5. A. M. Cheung, L. V. Nguyen, A. Carles, P. Beer, P. H. Miller, D. J. Knapp, K. Dhillon, M. Hirst, C. J. Eaves, *Blood* **122**, 3129-3137 (2013).
6. M. Norkin, H. M. Lazarus, J. R. Wingard, *Bone marrow transplantation* **48**, 884-889 (2013).
7. A. E. Boitano, J. Wang, R. Romeo, L. C. Bouchez, A. E. Parker, S. E. Sutton, J. R. Walker, C. A. Flaveny, G. H. Perdew, M. S. Denison, P. G. Schultz, M. P. Cooke, *Science* **329**, 1345-1348 (2010).
8. C. Delaney, S. Heimfeld, C. Brashem-Stein, H. Voorhies, R. L. Manger, I. D. Bernstein, *Nature medicine* **16**, 232-236 (2010).
9. E. Csaszar, D. C. Kirouac, M. Yu, W. Wang, W. Qiao, M. P. Cooke, A. E. Boitano, C. Ito, P. W. Zandstra, *Cell stem cell* **10**, 218-229 (2012).
10. R. Majeti, C. Y. Park, I. L. Weissman, *Cell stem cell* **1**, 635-645 (2007).
11. L. C. Bouchez, A. E. Boitano, L. de Lichtervelde, R. Romeo, M. P. Cooke, P. G. Schultz, *Chembiochem : a European journal of chemical biology* **12**, 854-857 (2011).
12. E. C. Henry, A. S. Kende, G. Rucci, M. J. Tottleben, J. J. Willey, S. D. Dertinger, R. S. Pollenz, J. P. Jones, T. A. Gasiewicz, *Molecular pharmacology* **55**, 716-725 (1999).
13. I. Sloma, P. A. Beer, K. M. Saw, M. Chan, D. Leung, K. Raghuram, C. Brimacombe, B. Johnston, K. Lambie, D. Forrest, X. Jiang, C. J. Eaves, *Experimental hematology* **41**, 837-847 (2013).
14. B. Dykstra, D. Kent, M. Bowie, L. McCaffrey, M. Hamilton, K. Lyons, S. J. Lee, R. Brinkman, C. Eaves, *Cell stem cell* **1**, 218-229 (2007).
15. C. Benz, M. R. Copley, D. G. Kent, S. Wohrer, A. Cortes, N. Aghaeepour, E. Ma, H. Mader, K. Rowe, C. Day, D. Treloar, R. R. Brinkman, C. J. Eaves, *Cell stem cell* **10**, 273-283 (2012).
16. L. Sparfel, M. L. Pinel-Marie, M. Boize, S. Koscielny, S. Desmots, A. Pery, O. Fardel, *Toxicological sciences : an official journal of the Society of Toxicology* **114**, 247-259 (2010).
17. A. B. Balazs, A. J. Fabian, C. T. Esmen, R. C. Mulligan, *Blood* **107**, 2317-2321 (2006).
18. Y. Hu, G. K. Smyth, *Journal of immunological methods* **347**, 70-78 (2009).

19. C. Simon, J. Chagraoui, J. Krosi, P. Gendron, B. Wilhelm, S. Lemieux, G. Boucher, P. Chagnon, S. Drouin, R. Lambert, C. Rondeau, A. Bilodeau, S. Lavalley, M. Sauvageau, J. Hebert, G. Sauvageau, *Genes & development* **26**, 651-656 (2012).

Supporting Material

Material and methods
Supplementary text
Figures S2.1 to S2.13
Tables S2.1 to S2.4

Materials and methods

Human CD34⁺ mobilized peripheral blood and cord blood cell collection and processing

Samples were collected from consenting donors according to ethically approved procedures at St. Justine, Maisonneuve-Rosemont Hospital (Montreal, QC, Canada) and Women's and Children's Hospital of British Columbia (Vancouver, BC). Human CD34⁺ cord blood (CB) cells were isolated using RosetteSep™ CD34 pre-enrichment cocktail followed by CD34 positive selection using EasySep™ (StemCell Technologies). Human CD34⁺ mobilized peripheral blood (mPB) cells were isolated using autoMACS Separator (Miltenyi Biotec), according to the manufacturer's protocol after collecting the mononuclear cells by Ficoll-Paque PLUS (GE).

CD34⁺ cell culture

Human CD34⁺ cells were cultured in HSC expansion media consisting of StemSpan SFEM (StemCell Technologies) supplemented with human 100 ng/ml stem cell factor (SCF, R&D Systems), 100 ng/ml FMS-like tyrosine kinase 3 ligand (FLT3, R&D Systems), 50 ng/ml thrombopoietin (TPO, R&D Systems), and 10 µg/ml low-density lipoproteins (StemCell Technologies). For the screen, human CD34⁺ mPB cells were resuspended in HSC expansion medium (50,000 cells/ml) before being aliquoted in 384 well plates (Greiner Bio-One). Compounds dissolved in DMSO were added directly after plating such that the final concentration of DMSO did not exceed 0.1% (v/v). For transplantation experiments, the fed-batch culture system was used as previously described (9). 1x10⁵ CD34⁺ CB cells/ml were injected into 12 ml or 25 ml bags (American Fluoroseal Corporation) connected to a syringe loaded pumping system and maintained on an orbital shaker at 37°C and 5% CO₂ in air. The pump was set to continuously deliver HSC expansion media supplemented with vehicle (0.1%DMSO), UM171 [35 nM], SR1 (Alichem, 41864) [750 nM] or combination of UM171 [35 nM] + SR1 [500 nM] at a flow rate of 0.7 µl/min.

Chemical library

A total of 5,280 compounds were used in our screen: 2000 compounds from Microsource Discovery Spectrum, 500 compounds from Biomol (natural products), 1120 compounds from Prest-

wick (commercialized products), 1280 compounds from SIGMA Lopac™ and the remaining 380 compounds were non-commercial small molecules synthesized at university of Montreal.

Primary screen and flow cytometry

CD34⁺ mPB cells were seeded at 2000 cells per well in the presence of chemical compounds. Relative and absolute numbers of CD34⁺CD45RA⁻ cells were determined after 7 days of culture using flow cytometry. Primary hits were selected as indicated in Fig. 2.1. The primary screen was performed with a LSRII flow cytometer equipped with a high throughput screening module (Becton Dickinson Biosciences). Cells were stained in PBS supplemented with 2% fetal bovine serum (FBS) at 4°C for 15 minutes with APC-labelled anti-human CD34 (BD Biosciences) and PE-labelled anti-human CD45RA (BD Biosciences).

Cell phenotypes in fresh and expanded cells were measured using a combination of the following antibodies and fluorophores: FITC-labelled anti-human CD34 (BD Biosciences), PE-labelled anti-human CD45RA (BD Biosciences), PE-Cy7-labelled anti-human CD38 (eBioscience), APC-labelled anti-human CD90 (BioLegend), PE-Cy5-labelled anti-human CD49f (BD Biosciences) and APC-labelled anti-human EPCR (eBioscience). Stained cells were washed once with PBS supplemented with 2% FBS and analyzed.

Transplantation and monitoring of human CD34⁺ CB cells in NSG mice

All experiments with animals were conducted under protocols approved by the Animal Care Committee of Université de Montréal. Fresh CD34⁺ CB cells or their progeny present in 12-day cultures were transplanted by tail vein injection into sub-lethally irradiated (250 cGy, <24 hr before transplantation) 8 to 12 week-old female NSG (NOD-*Scid* *IL2Rγ*^{null}, Jackson Laboratory). Human cells in NSG bone marrow (BM) was monitored by flow cytometry 20 and 30 weeks post-transplantation. NSG BM cells were collected by femoral aspiration (at week 20) or by flushing the two femurs, tibias and hips when animals were sacrificed at week 30. For secondary transplants, 25,000 freshly isolated (uncultured) CD34⁺ CB cells or the progeny of the equivalent of 10,000 freshly isolated CD34⁺ CB cells that had been originally cultured in DMSO or UM171 were injected into secondary sub-lethally irradiated NSG mice. BM cells of the secondary mice were harvested and analyzed 18 weeks post-transplantation. Flow cytometry analysis was performed on freshly collected BM cells. Cells were treated with 1x red blood cell lysis buffer (StemCell Technologies), washed and stained with Pacific Blue-labelled anti-human CD45 (BioLegend), APC-eFluo-labelled 780 anti-mouse CD45 (eBioscience), PE-labelled anti-human CD33 (BD Biosciences), PE-Cy5 labelled anti-human CD11b (BD Biosciences), FITC-labelled anti-human CD15 (BD Biosciences), APC-Cy7 labelled anti-human CD14 (Bi-

oLegend), PE-Cy7 labelled anti-human CD19 (BD Biosciences), FITC-labelled anti-human CD3 (BD Biosciences), APC-labelled anti-human CD71 (BioLegend), PE-labelled anti-human glycoprotein A (GPA) (BD Biosciences), FITC-labelled anti-human CD41 (BD Biosciences). Cells then were washed and analyzed using a FACSCanto II (BD Biosciences). BD FACSDiva or FlowJo software were used to analyze the flow cytometry data. The correspondence between antibody labeling and cell populations is as follows: CD11b, CD14, CD15, CD33 (monocytes and granulocytes); CD56 (NK cells); CD71, GPA, CD41 (erythroid and megakaryocyte lineages); CD19, CD3 (B and T cells) and CD34 (stem/progenitor cells)

A total of 300,000 BM cells were analyzed per mouse. Considering current FACS limit of detection of 1 per 20,000 events, a minimum threshold of 15 human cells could be detected in these mice. Because some lymphoid cells are long-lived, their presence after a long time can be potentially misleading for assessing LT-HSC activity, which is more conservatively assessed by relying on detecting the sustained output of short-lived cells (e.g., granulocytes). To detect human LT-HSC contribution to NSG reconstitution, we arbitrarily set the lower limit of human cell engraftment at 10-times the FACS threshold or 150 myeloid cells per 300,000 BM cells.

T-cell reconstitution was not monitored because it correlates poorly with LT-HSC engraftment in other studies (5) and may represent graft versus host disease, a state that could be associated with peripheral amplification of T-cells not reflecting LT-HSC activity. Similarly, low levels of B-cell restricted reconstitution (<0.05%) was not considered for LT-HSC evaluation because of the extended longevity of B lymphocytes *in vivo*. However, these criteria led to the reclassification of only 5 mice in our cohort of 300.

Estimation of LT-HSC numbers by limiting dilution analysis

All limiting dilution analyses were performed using the ELDA software from the Walter and Eliza Hall Institute of Medical Research software <http://bioinf.wehi.edu.au/software/elda/index.html> (18). Differences in HSC frequencies were analyzed by chi-square test. *P values <0.05 were considered significant (Mann Whitney test). Limiting dilution analyses presented in Fig. 2.3 were based on the combined data of 5 independent transplantation studies where 4 to 14 mice were analyzed per dilution (table S2.1 to S2.3).

Transplantation and monitoring of Macaque CD34⁺ CB cells in NSG mice

Macaque CD34⁺ CB cells were expanded for 11 days in the presence of vehicle, SR1 [1 μ M], UM729 [500 nM] or UM171 [40 nM]. Irradiated (275 cGy) NSG mice (n=3 mice / group) were subsequently transplanted with unexpanded CD34⁺ cells or expanded progeny of 250,000

CD34⁺ cells. Average engraftment levels of nonhuman primate CD45⁺ cells in the peripheral blood of NSG mice were determined by flow cytometry at week 4, 7 and 10 after transplantation.

Evaluation of UM729 effect on mouse cells

Lin⁻ckit⁺Sca1⁺CD150⁺CD48⁻ cells from C57Bl/6J-CD45.1-Pep3b x C3H/HeJ donor mice were sorted using the following antibody and fluorophores: for lineage depletion, CD45.1 bone marrow cells were stained with APC-labelled anti-mouse Gr1, Ter119 and B220 (BD-Biosciences) followed by Anti-APC microbeads (MACS miltenyi Biotec). The lin⁻ CD45.1 cells then were stained with PE-Cy7-labelled anti-mouse ckit (eBiosciences), PE-Cy5-labelled anti-mouse Sca1 (eBiosciences), PE-labelled anti-mouse CD150 (BioLegend) and FITC-labelled anti-mouse CD48 (BD-Biosciences) and sorted for the ckit⁺Sca1⁺CD150⁺CD48⁻ subpopulation using a FACSAria (BD Biosciences). The sorted cells were cultured for 7 days in the presence of vehicle (DMSO) or UM729 [500 nM] in StemSpan SFEM (StemCell Technologies) media supplemented with mouse Flt3L (100 ng/ml), SCF (100 ng/ml), IL3 (10 ng/ml) and IL6 (50 ng/ml) from R&D systems. After 7 day culture, the progeny of 20, 100 and 300 Lin⁻ckit⁺Sca1⁺CD150⁺CD48⁻ cells of day0 were transplanted into 2–4 sublethally irradiated (800 cGy) C57Bl/6J-CD45.2 x C3H/HeJ congenic recipient mice along with 2×10^5 CD45.2 competitor cells. The level of CD45.1 donor reconstitution was evaluated 18 weeks by flow cytometric after staining the peripheral blood cells with APC-labelled anti-mouse CD45.1 (BD Biosciences) and FITC-labelled anti-mouse CD45.2 (BD Biosciences).

CFSE labeling

CD34⁺ CB cells (1×10^6 cells/ml) were labeled with 5 μ M carboxyfluorescein diacetate succinimidyl ester (CellTrace, CFSE Cell Proliferation Kit, Molecular Probes/Invitrogen) according to the manufacturer's guidelines. Labeled cells were cultured for 24 hours before they were stained with APC-labelled anti-human CD34 and sorted for CD34⁺CFSE⁺ peaks using a FACSAria (BD Biosciences). Sorted cells were then resuspended in HSC expansion medium supplemented with vehicle (DMSO), UM171 [35 nM], SR1 [750 nM] or a combination of UM171 [35 nM] + SR1 [500 nM]. Cell aliquots after 2 and 4 days in culture were stained with APC-labelled anti-human CD34 and PE-labelled anti-human CD45RA before cells were analyzed for CFSE intensity.

Colony-forming cell assays

Frequencies of colony-forming cells were estimated by plating 250-1000 human CD34⁺ CB

cells in 1 ml of 2% methylcellulose-based media in Iscove's Modified Dulbecco's Medium (IMDM) plus 10% fetal bovine serum (FBS), 2% bovine serum albumin (BSA), 2 mM L-glutamine, 100 ng/ml SCF, 10 ng/ml IL-3, 10 ng/ml IL-6, 5 ng/ml erythropoietin, 200 µg/ml transferrin and 10^{-4} M 2-mercaptoethanol. After 14 days in culture, plates were visually scored for CFU-multilineage colonies (containing granulocytes and erythroid cells at least).

Long-term culture-initiating cell (LTC-IC) assays

LTC-IC frequencies were determined by plating different numbers of fresh human CD34⁺ CB cells and measuring their culture-derived colony in 12-replicate cultures in gelatin-coated plates previously seeded with irradiated (6000 rad) M2-10B4 murine stromal cells in Myelo-Cult H5100 medium containing 10^{-6} M hydrocortisone (Stem Cell Technologies). After 5 weeks in culture with weekly half-media exchanges, the contents of each well were harvested using 0.25% trypsin in PBS, and plated in methylcellulose cultures (described above). Methylcellulose cultures with 1 or more CFC were considered to have been derived from cultures initiated with at least 1 LTC-IC. Limit dilution analysis software <http://bioinf.wehi.edu.au/software/elda/index.html> (18) was used to determine LTC-IC frequencies.

Annexin V staining

Cultured cells adjusted to 1×10^6 cells/ml were stained with APC-labelled anti-human CD34 and PE-labelled anti-human CD45RA and re-suspended in binding buffer (10 mM HEPES/NaOH (PH7.4); 14 mM NaCl, 2.5 mM CaCl₂). Cells were then stained with FITC labelled-Annexin V (BD Biosciences) for 15 minutes at room temperature. Cells were washed with binding buffer before 7ADD viability staining solution was added (Biolegend).

RNA Isolation and q-RT-PCR

RNA was isolated from CD34⁺ mPB and CB cells using Trizol reagent according to the manufacturer's protocol (Invitrogen/Life Technologies). cDNA was synthesized from RNA using MMLV reverse transcriptase and random primers (Invitrogen/Life Technologies). Fast Master Mix (2x) containing primers and probes from the Universal Probe Library (Roche Diagnostics) were used for q-RT-PCR reactions which were amplified in technical replicates on an ABI 7900HT Fast Real-Time PCR System (Applied Biosystems /Life Technologies). Analysis was done with SDS 2.2.2 software (Applied Biosystems /Life Technologies) using the comparative delta CT method and normalized to GAPDH and HPRT. The following primers and probes were used: GAPDH (probe 60): forward: 5'-AGCCACATCGCTCAGACAC-3', re-

verse 5'-GCCCAATACGACCAAATCC-3'; HPRT (probe22): forward 5'-TGATAGATCCATTCCTATGACTGTAGA-3', reverse 5'-CAAGACATTCTTTCCAGTTAAAGTTG-3'; CYP1B1 (probe20): forward 5'-CGGCCACTATCACTGACATC-3', reverse 5'-CTCGAGTCTGCACATCAGGA 3'; AHRR (probe72): forward 5'-TGCTTCATCTGCCGTGTG-3', reverse 5'-AGCTGCCAAGCCTGTGAC-3'.

RNA-sequencing

RNA-Sequencing (RNA-Seq) was performed as previously described (19). Two RNA expression profiling experiments were performed. One experiment was done in dose response of UM171 and another for different time point treatment. For the dose response experiment, CD34⁺ mPB or CB cells were treated with vehicle (DMSO) or UM171 at different concentrations [19, 30, 48, 78 and 125 nM] or SR1 [750 nM] for 16 hours. For the different time point treatment, CD34⁺ CB cells were treated with vehicle (DMSO), SR1 [500 nM], UM171 [35 nM], or combination of SR1 [500 nM]+UM171 [35 nM] for 3, 12, 24, 48, and 72 hours. At each time point, cells were lysed, RNA was extracted using Trizol and RNeasy columns (Qiagen) and mRNA libraries prepared using the TruSeq RNA Sample preparation kit (Illumina). RNA libraries were sequenced on an Illumina HiSeq 2000 machine using paired end reads (2 x 100 bp).

Accession codes

Gene Expression Omnibus: [GSE57299](https://www.ncbi.nlm.nih.gov/geo/query/acc.cgi?token=otibicyuhnuftyn&acc=GSE57299) and [GSE57561](https://www.ncbi.nlm.nih.gov/geo/query/acc.cgi?token=mhkhkckufhwhtoz&acc=GSE57561)

<http://www.ncbi.nlm.nih.gov/geo/query/acc.cgi?token=otibicyuhnuftyn&acc=GSE57299>

<http://www.ncbi.nlm.nih.gov/geo/query/acc.cgi?token=mhkhkckufhwhtoz&acc=GSE57561>

Supplementary online text for fig. S2.6

UM171 washout experiments demonstrated a rapid arrest of CD34⁺ and CD34⁺CD45RA⁻ cell expansion after removal of the compound suggesting that its effect is reversible (fig. S2.6, A and B). To assess whether UM171 acts as a mitogen and compensates for the absence of cytokine(s) such as FLT3L, or SCF, or TPO, we cultured cells with UM171 [35 nM] or DMSO in the presence or absence of one or all the three cytokines. UM171 failed to support expansion of CD34⁺ or CD34⁺CD45RA⁻ in the absence of growth factors (fig. S2.6, C and D) suggesting that our molecule has no inherent mitogenic activity.

Supplementary online text for fig. S2.7

During the 4 day incubation both the UM171- and vehicle-treated cells underwent 4 population doublings (fig. S2.7) indicating that UM171 does not change the rate of division of CD34⁺CD45RA⁻ cells.

Supplementary online text for fig. S2.13

PROCR or EPCR (CD201) transcripts were shown to be up-regulated after UM171 treatment (fig. S2.13A). Interestingly, levels of EPCR transcripts correlated with the dose of UM171 but were not affected by SR1 (fig. S2.13B). EPCR protein levels were also elevated in UM171-treated cells (fig. S2.13C, upper panel). Remarkably, EPCR^{high} cells were enriched for CD34⁺ and CD34⁺CD45RA⁻ expression compared to EPCR^{low} population (fig. S2.13C, mid and lower panel) suggesting that its expression maybe indicative of a more primitive cell type.

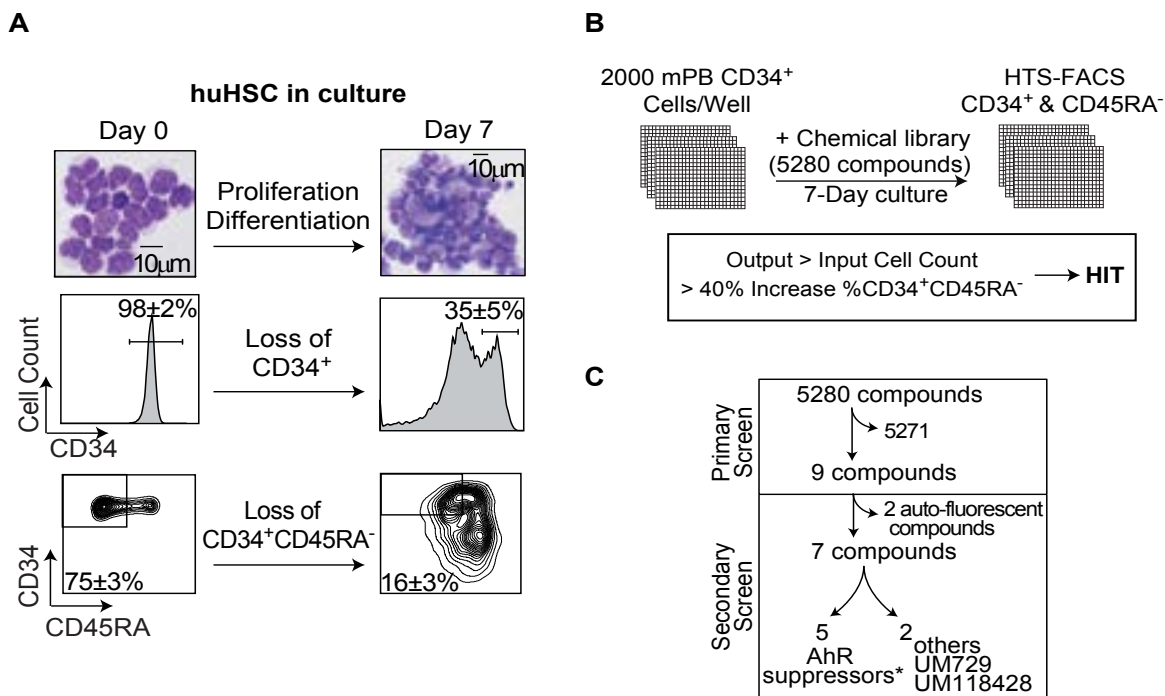


Fig. S2.1. Screen setup and hit validation strategy for identifying small molecule(s) that promotes ex vivo expansion of human CD34⁺ cells.

(A) CD34⁺ mPB cells cultured for 7 days in serum-free medium supplemented with 100 ng/ml Flt3L, 100 ng/ml SCF and 50 ng/ml TPO differentiate as demonstrate by changes in cell morphology (wright staining, upper panel) and flow cytometric analysis showing loss of CD34⁺ (middle panels) and the more primitive CD34⁺CD45RA⁻ population (bottom panels). (B) Primary screen setup and criteria for hit identification. (C) Chemical screen result summary.

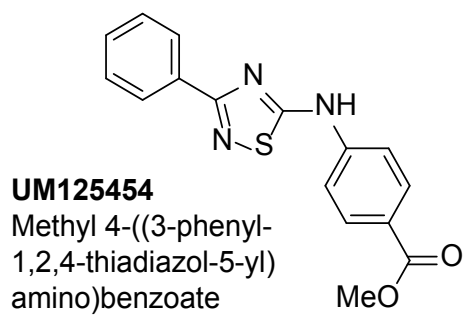
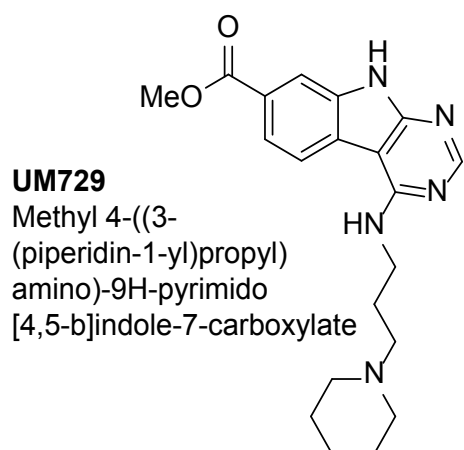


Fig. S2.2. Chemical structure of two non commercially-available compounds that were selected as hits in the secondary screen.

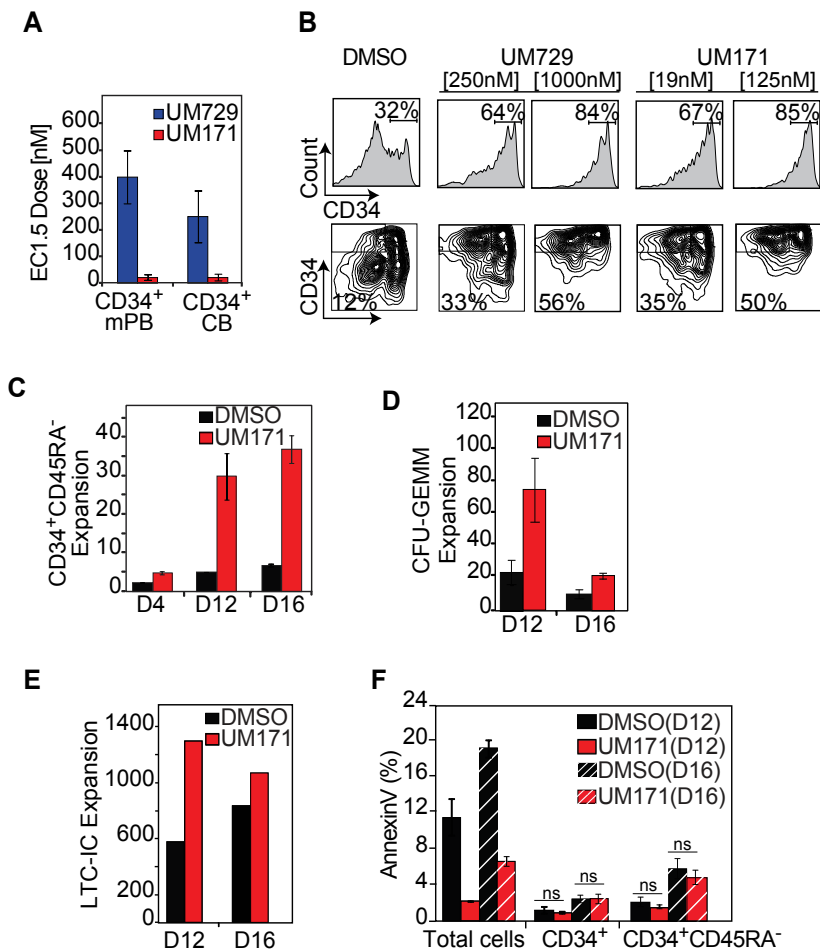


Fig. S2.3. Characterization of UM171 and optimization of fed-batch conditions.

(A) Effective concentration 1.5 (EC1.5) was defined as the concentration that resulted in 1.5-fold expansion of CD34⁺CD45RA⁻ cells starting from CD34⁺ CB- or mPB-derived cells. (B) Representative FACS profile of CD34⁺ mPB cells treated for 7 days with vehicle (DMSO 0.1%), UM729 [250 nM or 1000 nM] or UM171 [19 nM or 125 nM]. (C) Fold-expansion of CD34⁺CD45RA⁻ CB cells cultured for 4, 12, and 16 days in a fed-batch system supplemented with DMSO or UM171 [35 nM]. (D) Fold-expansion of multipotent progenitor cells (CFU-GEMMs, colony-forming unit-granulocytes, erythrocytes, macrophages, megakaryocytes) after 12 and 16 days in culture. (E) Number of LTC-ICs per 10⁵ CD34⁺ CB starting cells (n=1 experiment with 6 replicates). (F) Percentages of apoptotic cells were monitored by AnnexinV staining at different time points. Unless specified, data represent mean ± SD of 3 independent experiments. Unless specified otherwise, all results in panels D and F were statistically significant (p<0.05, Mann Whitney test) when compared with control (DMSO). ns: not significant.

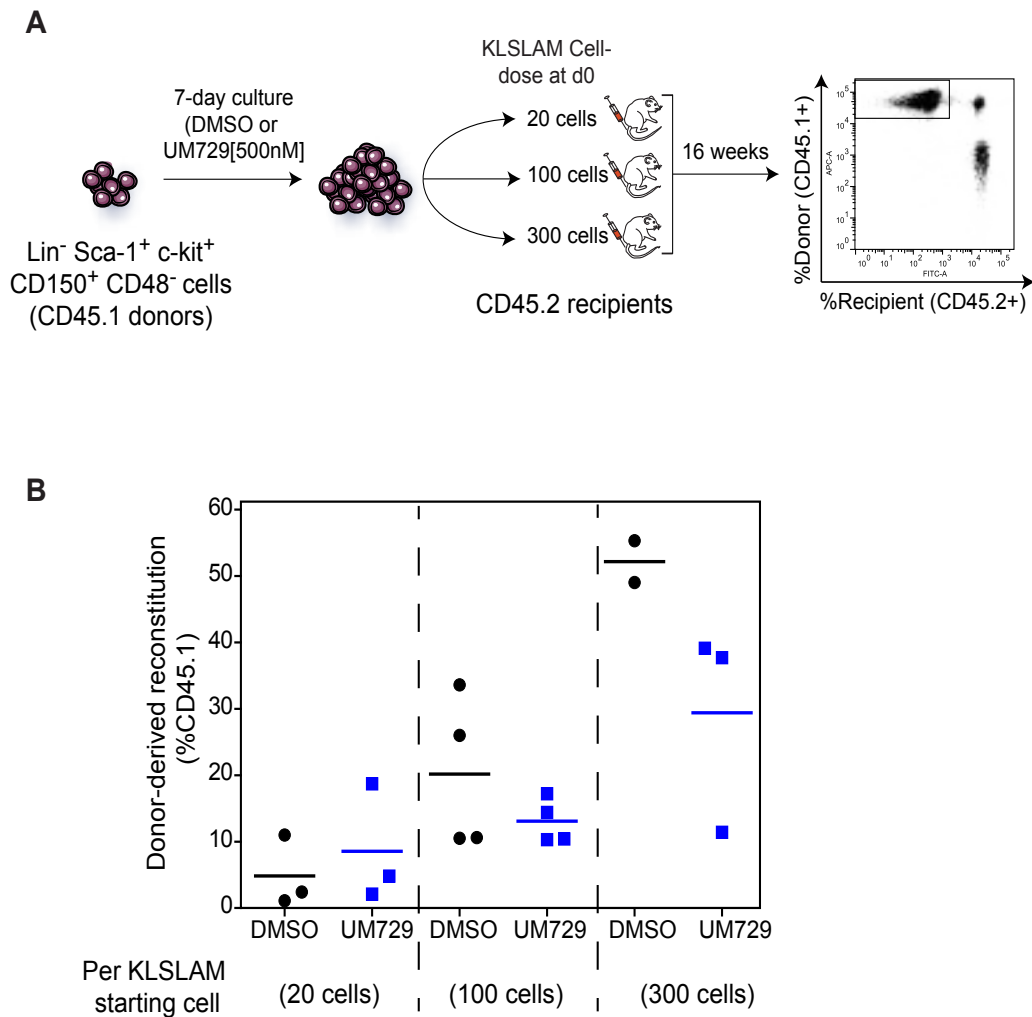


Fig. S2.4. UM729 has no effect on expanding murine HSCs.

(A) Schematic representation of the experiment design. Lin⁻Sca-1⁺c-kit⁺CD150⁺CD48⁻ from CD45.1 donors were expanded for 7 days in the presence of vehicle or UM729 [500 nM]. Sublethally irradiated (800 cGy) CD45.2 recipients (n=2-4mice/group) were transplanted with expanded progeny of 20, 100 and 300 Lin⁻Sca-1⁺c-kit⁺CD150⁺CD48⁻ cells. (B) Average engraftment levels of donor reconstitution (%CD45.1) in the peripheral blood were determined by flow cytometry at week 16 post transplantation.

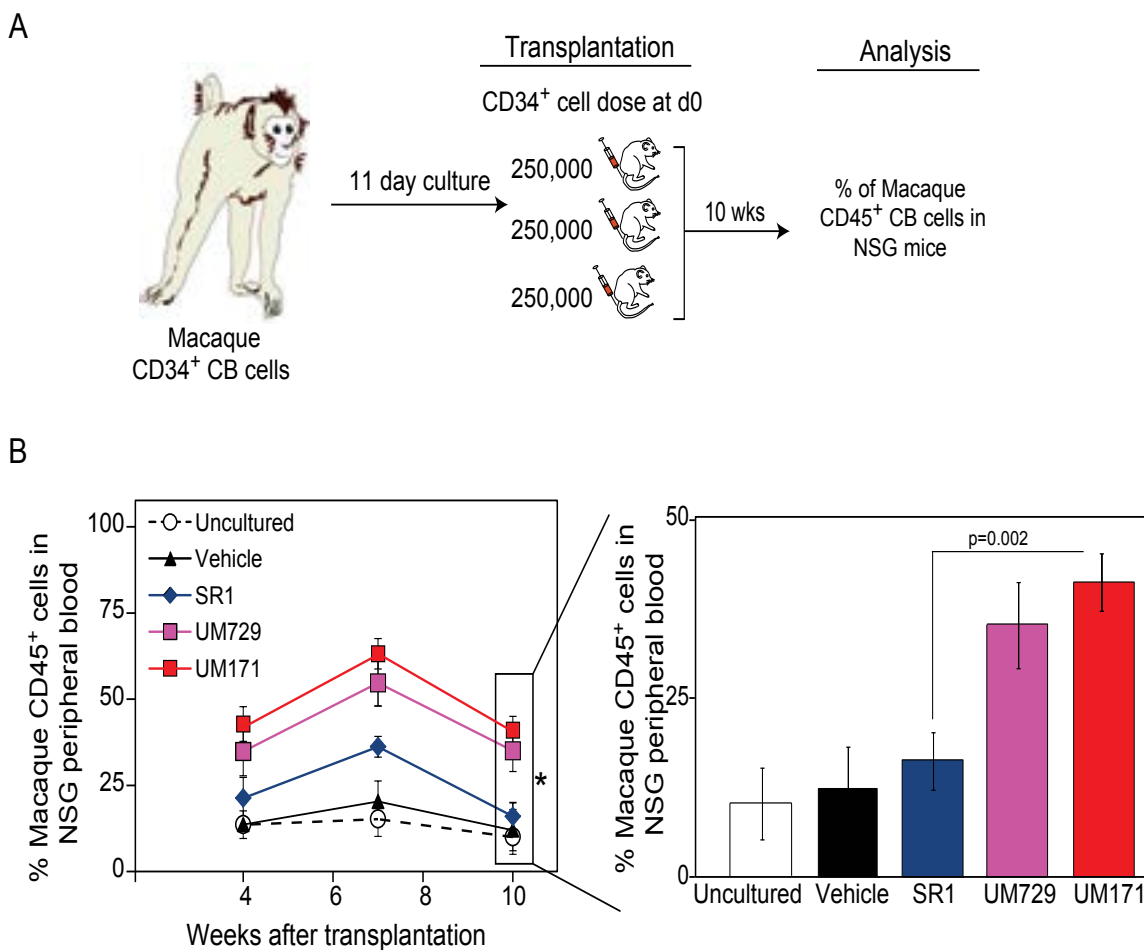


Fig. S2.5. UM729 and UM171 enhance the engraftment potential of macaque CD34⁺ CB expanded cells.

(A) Schematic presentation of the experiment design. Macaque CD34⁺ CB cells were expanded for 11 days in the presence of vehicle, SR1 [1 μ M], UM729 [500 nM] or UM171 [40 nM]. Irradiated (275 cGy) NSG mice (n=3 mice / group) were transplanted with unexpanded CD34⁺ cells or expanded progeny of 250,000 CD34⁺ cells. (B) Average engraftment levels of non-human primate CD45⁺ cells in the peripheral blood of NSG mice were determined by flow cytometry at week 4, 7 and 10 (also left panel) post transplantation. Significance level: *p < 0.05.

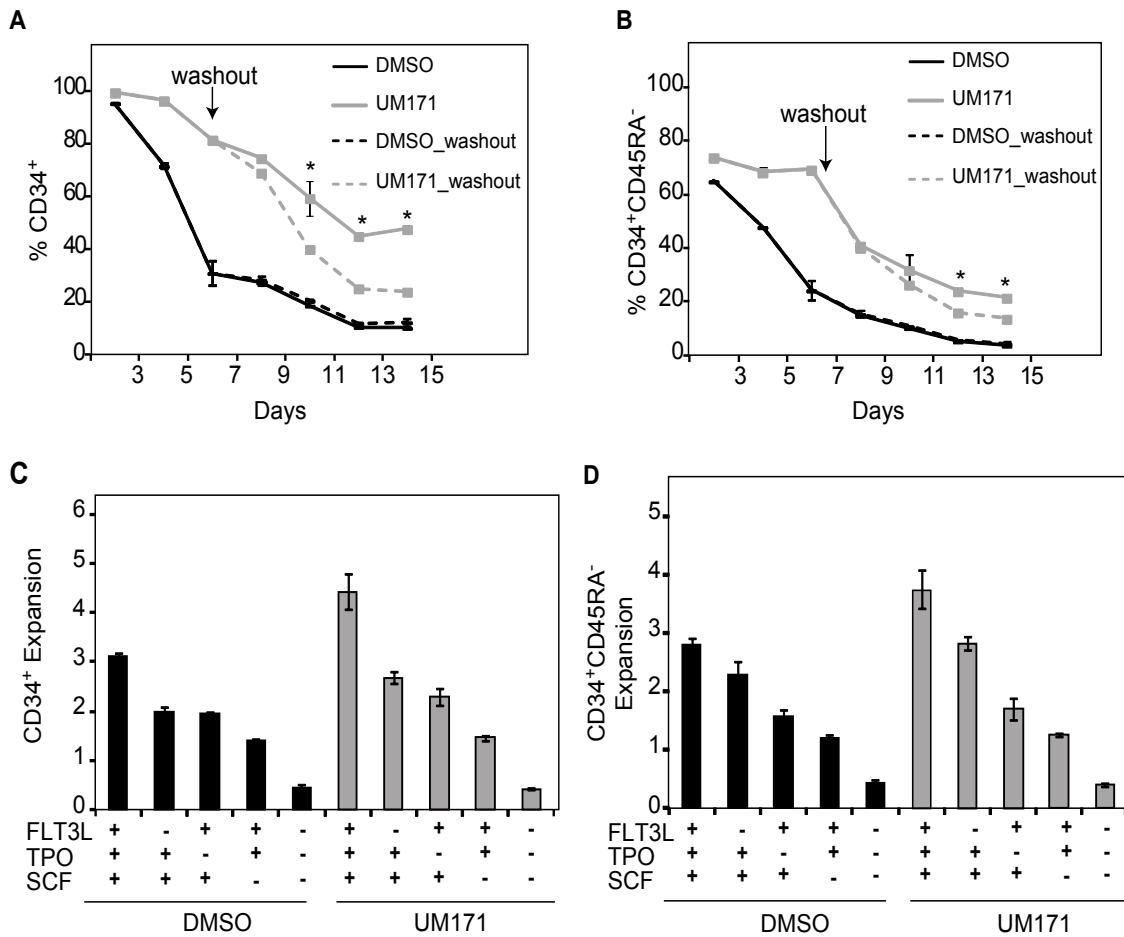


Fig. S2.6. UM171 is not a mitogen and its effect in expanding CD34+ and CD34+C-D45RA- is reversible.

CD34+ (A) or CD34+CD45RA-(B) mPB cells were cultured in the presence of UM171 [35 nM] or vehicle (DMSO). After 7 days of culture, cellular aliquots were washed twice with media lacking UM171 and DMSO and replated in fresh media also lacking UM171 (gray dashed) or DMSO (black dashed) for an additional period of 8 days. The percentages of CD34+ (A) and CD34+CD45RA- (B) populations were monitored every 2 days throughout the cultures. Data are expressed as mean \pm SD of 3 independent experiments. Significance level: *p value <0.05 (Mann Whitney test). Similar results were obtained with cord blood (not shown). (C) and (D) CD34+ mPB cells were cultured with DMSO or UM171 [35 nM] in serum free media in the absence or presence of the indicated cytokines. Fold-expansion of CD34+ (C) and CD34+C-D45RA- (D) populations over input were assessed at day 7 (see supplemental text for fig.S6). Data are given as means \pm SD, n=3 independent experiments. All conditions in (C) and (D) when compared to control (media supplemented with 3 cytokines) were statistically significant with p value <0.05 (Mann Whitney test).

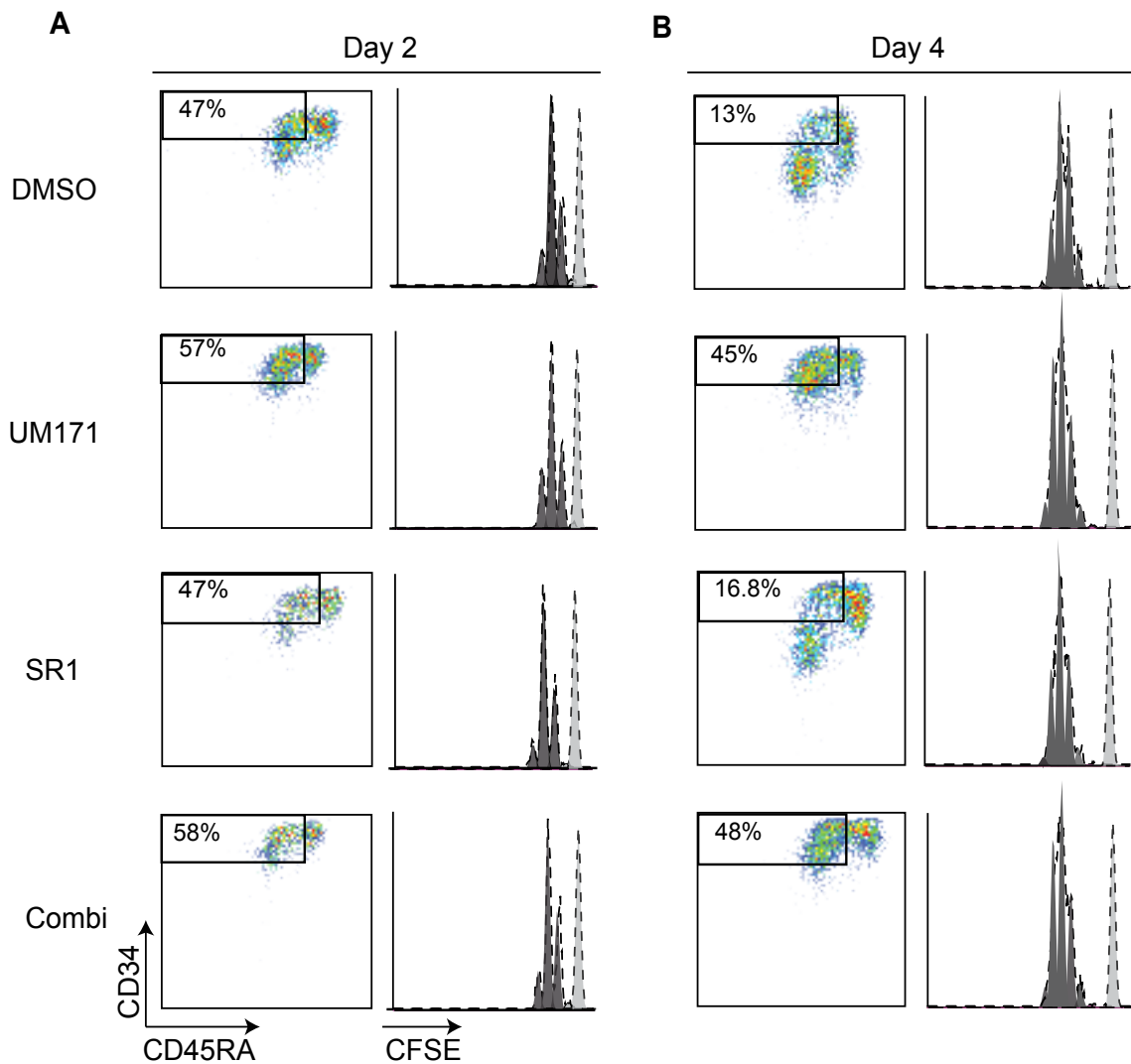


Fig. S2.7. UM171 does not affect division rate of CD34+CD45RA- cells.

CFSE cell labeling was used to characterize the proliferation pattern of CD34+ CB cells. CFSE irreversibly integrates the intracellular environment and is therefore being distributed evenly to daughter cells at each division. As a result fluorescence caused by CFSE activation is precisely halved for each generation. In these experiments, CD34+ CB cells were labeled with CFSE and cultured in presence of DMSO, or UM171 [35 nM], or SR1 [750 nM] or the combination of both compounds (UM171 [35 nM] + SR1 [500 nM]). For analysis, we gated on the primitive CD34+CD45RA- population at indicated time points, day 2 (A) and day 4 (B). FACS profiles are representatives from 3 independent experiments. See also supplementary text for fig. S7.

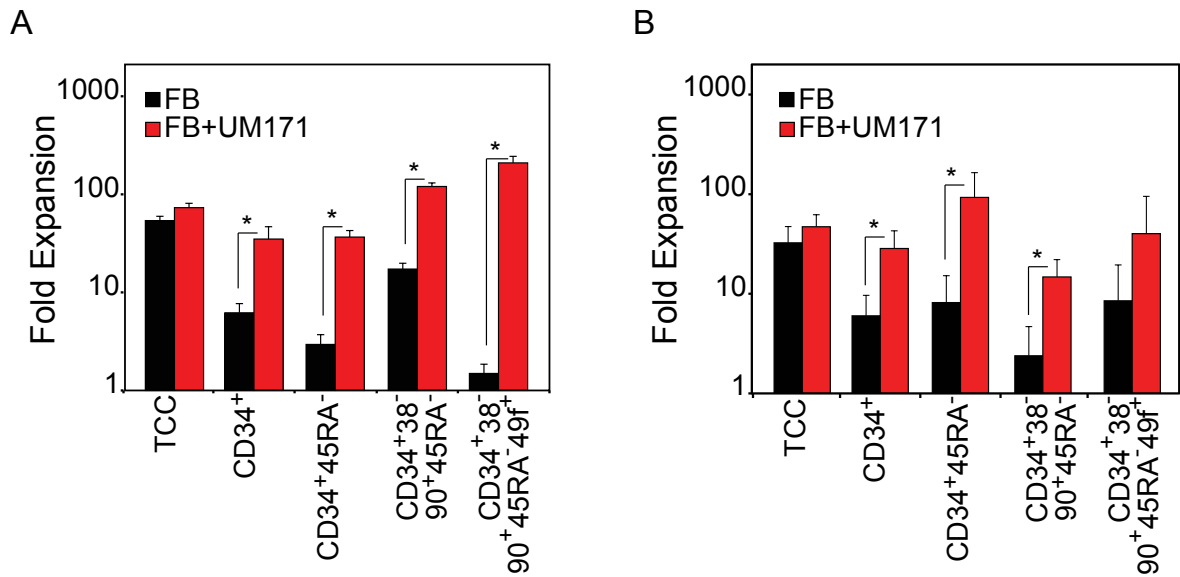


Fig. S2.8. UM171 expansion protocol is readily reproduced in independent laboratories.

(A) and (B) Data from two independent labs (R.K.H., left; C.E., right) confirming that UM171 addition in a fed-batch culture retains the HSC phenotype better than control cultures. Data represent mean \pm SD (n=3 independent experiments). Significance level *p<0.05.

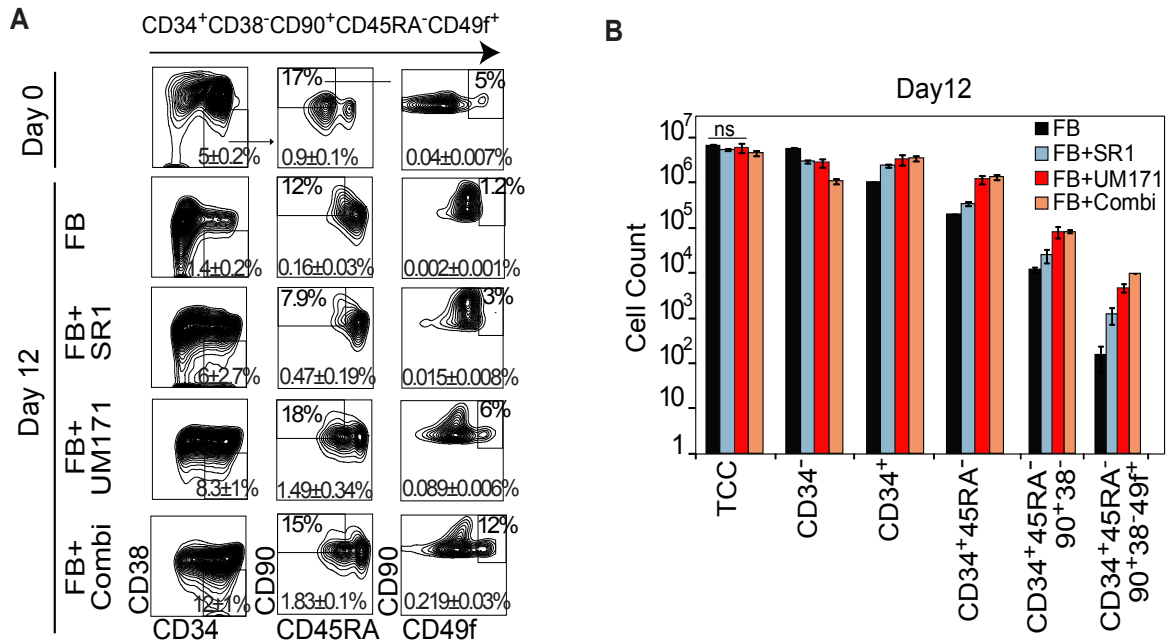


Fig. S2.9. UM171-treated CD34⁺ cells remain phenotypically primitive in culture.

(A) Representative FACS profiles of the most primitive HSC phenotype subset (CD34⁺CD38⁻CD45RA⁻CD90⁺CD49f⁺) at day 0 (fresh cells) and day 12 culture in a fed-batch system supplemented with DMSO, SR1 [750 nM], UM171 [35 nM], or combination of SR1 [500 nM] +UM171 [35 nM]. (B) Bar graph showing cell counts of phenotypically defined cellular subsets determined by flow cytometric analysis after 12 day fed-batch cultures in presence of DMSO (black), SR1 (blue), UM171 (red), or combination (orange). Data represent mean ± SD (n=3 independent experiments). All conditions were statistically significant (p<0.05, Mann Whitney test) when compared to control (FB), unless specified otherwise (ns: not significant, Mann Whitney test).

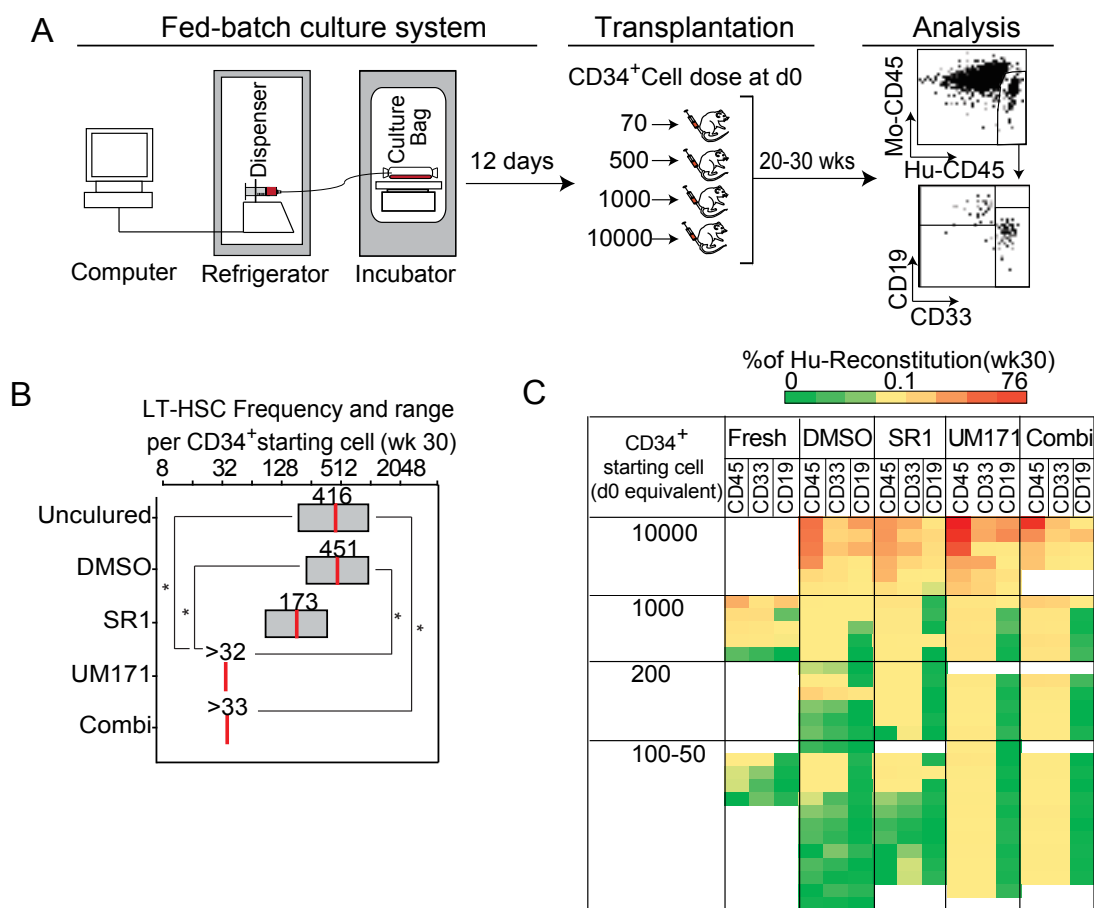


Fig. S2.10. UM171 promotes expansion of LT-HSC in fed-batch culture of CD34⁺ CB cells.

(A) Experimental design. (B) Limiting dilution assays were used to estimate frequencies of LT-HSCs determined at 30 weeks after transplantation. Results presented as 1/number of starting cell (d0) equivalent for each condition. Gray box represent 95% CI. Data are from 5 independent experiments performed with a pool of 2-3 human CB units per experiment. Significance level: * $p < 0.05$ (Mann Whitney test). (C) Levels of human engraftment in the BM of NSG mice 30 weeks after their transplantation with different day 0 equivalent cell doses of fresh (uncultured) CD34⁺ CB cells or their progeny cultured with DMSO, or UM171, or SR1, or UM171+SR1 (Combi). See table S2 for raw data. Color code illustrates human reconstitution levels in NSG mice from 76% (red) to 0% (green). Confidence interval for UM171 and Combi could not be accurately estimated at this time point as all the mice were positive.

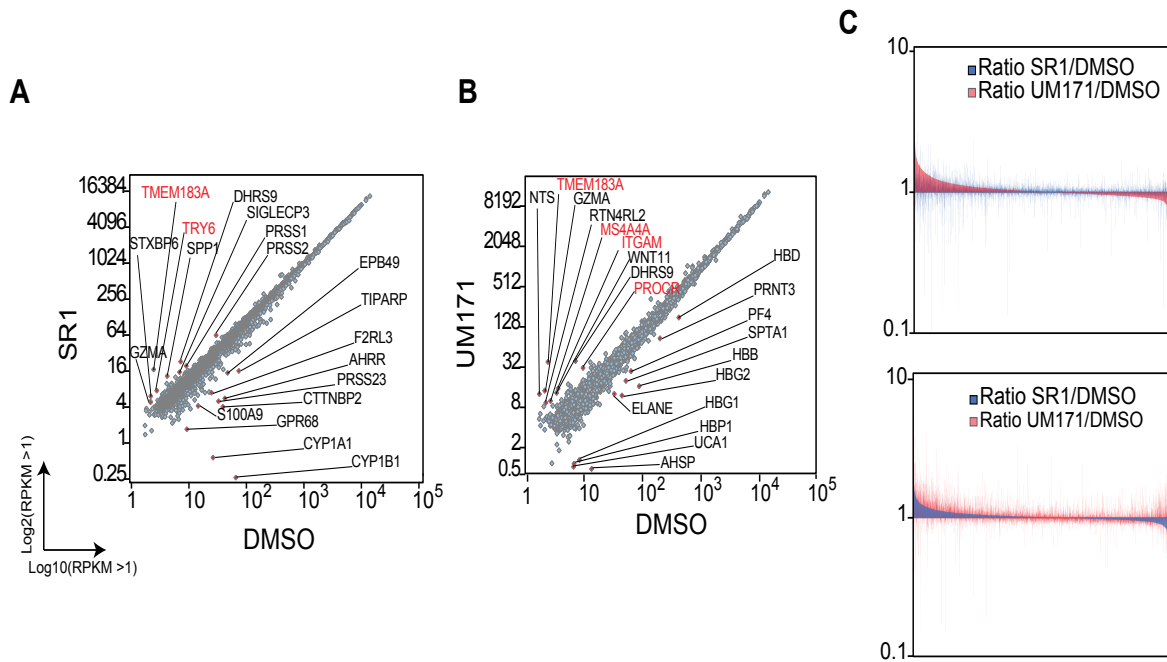
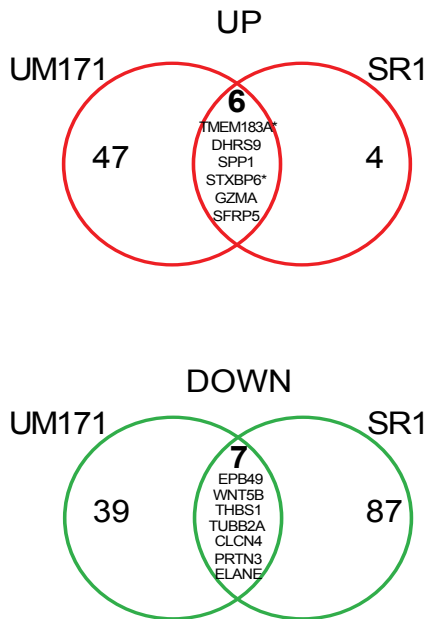


Fig. S2.11. Comparative transcriptome analysis of CD34+ cells exposed to UM171 or to SR1.

SR1/DMSO (A) or UM171/DMSO (B) gene expression (Y axis SR1 or UM171 vs X axis DMSO) presented in scatterplots. Only genes for which RPKM values are >1 are shown. Genes with highest levels of up- or down-regulation are labeled (complete list in fig. S7). Genes coding for cell surface receptors are indicated in red. (C) Waterfall bar graphs showing UM171/DMSO (red) or SR1/DMSO (blue) values (Y axis) for each gene (X axis). Upper and lower graphs show highest to lowest gene expression ratio for UM171/DMSO and SR1/DMSO, respectively.

A



B

UM171		SR1	
Up by 2 fold	Down by 1.5 fold	Up by 2 fold	Down by 1.5 fold
TMEM183A*	AHSP	TMEM183A*	CYP1B1*
NTS	UCA1*	DHRS9*	CYP1A1*
GZMA	HBG1*	SPP1*	CTTNBP2*
DHRS9	HBBP1	STXBP6*	AHRR*
ITGAM	HBB	TRY6	PRSS23*
RTN4RL2	HBG2*	CH25H	GPR68*
TNNT1	SPTA1	GZMA	TIPARP*
WNT11	ELANE	CLEC7A	FAM171A1
MS4A4A	HBD*	SIGLECP3	S100A9
ALOX5	PRTN3	PRSS1	EPB49
GLYATL2	FN3K	PRSS3	F2RL3*
PROCR*	PF4	PRSS2	LOC100128098*
GDF3	PNMT	SFRP5	MMP2
KRT1	LY6G6F		NCALD*
PLVAP	LOC388588		SEMA3C*
MF12	C5orf4		ANPEP
LY96*	RPL21		LOC386597*
TSPAN7*	SELP		CNR2
RMRP	PPBP		WASF3*
TRH	FAM178B		EPB41L3*
PHLDA2	MFSD2B		SAMSN1
MDFI	RHAG		IGFBP4
LILRB2	CLCN4		ARL4C*
ANGPT2	OSBP2		C1orf150
STXBP6*	C9orf116		RAB6B*
HDC	TUBB2A		RNF144A*
RNASE4	SNORD18A*		CLCN4
FSD1	SNORD1A		IL8
SFRP5	THBS1		FAM83F
CKAP4	ANK1		THBS1
SPP1	CD36*		CD96
LOC100271874*	AZU1		KIAA0087
LIF	WNT5B		RGS1
PTPRF*	ZFPM1		TUBB2A
TLL7	EPB49		RSAD2
SIRPB2	CD38*		AB13*
PFN2	GP1BA		CMTM5
RPPH1	LY6G6D		ARHGAP6
TNFSF10	KLF1		PRTN3
GBP1	BLVRB		GPR183
ENPP3	LTBP1		LPAR6
IER3	MIR4292		MMP14
CBR3*	GP9		ELANE
MFAP2	GYPB*		SOS1*
KCNMB1*	ATP7B		LMNA
CD72*	LRP11		RARG
TIAM1			IL4R
C16orf45*			ABCC4*
SCD5*			LOC401097
B3GNT3			BCL2L11
C18orf32*			AMICA1
C2orf82*			FUT7
C19orf38			CCR2
			LPXN
			MMP17
			CMPK2
			IZUMO4*
			MYO1G
			ADAP1
			ITGAL
			NCF4*
			RC3TB2
			ST8SIA6
			MGAT3
			ALOX5AP
			WNT5B
			DDIT4
			ID2
			LCN2
			MPZL2
			MIR93
			MTSS1
			CD9
			ETS2
			RAB27B
			SCARNA15
			PMP22
			GNG11
			FCER1A
			ALDH3B1
			PPP1R15A
			ARID5B
			BMF
			S100B
			GALNT2
			NQO1
			LAT

Fig. S2.12. List of differentially expressed genes in CD34+ CB cells exposed to UM171 or to SR1.

RNA-Seq experiments were performed using cells exposed for 12, 24, 48 and 72 hours to either DMSO (control), UM171[35nM] or SR1[500nM]. Results are expressed as most up (2x) or down (1.5x) regulated genes for which median RPKM values were >1. Venn diagram (A) and gene list (B) of up- or down-regulated genes which are specific or shared in both treatments. The asterisks indicate the genes that have p value of <0.05 (Mann Whitney test) where different time point treatments are considered as replicates.

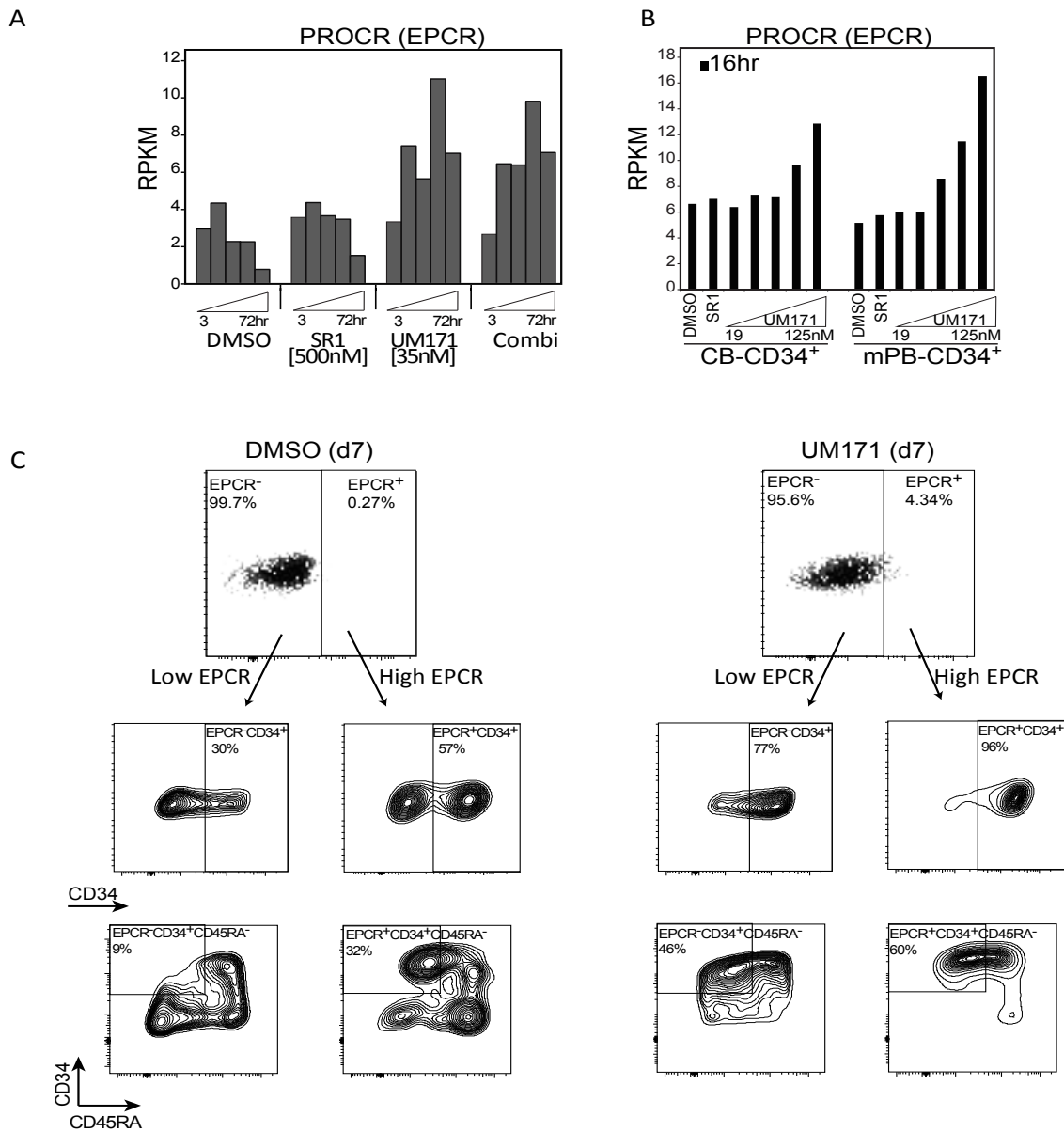


Fig. S2.13. PROCR (EPCR or CD201) gene and protein expression in response to UM171.

(A) RNA-Seq data, expressed in RPKM, showing the changes in EPCR expression in cells exposed 3, 12, 24, 48 and 72 hours to DMSO (control) or to UM171 [35 nM]. (B) Similar experiments were performed using increasing amount of UM171 [19, 30, 48, 78 and 125 nM] on CD34⁺ CB or mPB cells. (C) CD34⁺ CB cells cultured for 7 days with DMSO controls (right) or UM171 [35 nM] (left) were stained with EPCR, CD34 and CD45RA antibody for FACS analysis. See also supplementary text for fig. S13.

Determination of day 0 equivalent frequencies of LT-HSCs in various cultures					
Condition	Cell dose equivalent to d0	No. 1ry recipients reconstituted / transplanted	Reconstitution levels of 1ry recipients (Mean +/- SD)	1/SRC frequency per starting cell (20 wks post transplant)	95% confidence of interval (upper-lower)
Fresh					
	25000	5/5	39.2±20.58	883	(474-1647)
	10000	11/11	41.6±19.18		
	5000	4/4	6.2±3.43		
	1000	7/10	4.7±8.42		
	500	2/5	0.9±1.73		
	100	1/9	0.1±0.06		
	50	0/5	0.00±0.01		
DMSO					
	10000	14/14	32.3±19.23	976	(576-1653)
	1000	10/14	3.6±8.53		
	500	3/7	0.3±0.37		
	200	1/6	0.0±0.05		
	100	0/13	0.0±0.04		
	70	0/6	0.0±0.01		
SR1					
	10000	14/14	15.1±11.45	406	(259-635)
	1000	13/14	2.4±3.67		
	500	7/8	2.3±5.08		
	200	1/6	0.1±0.09		
	100	2/14	0.1±0.12		
	70	1/6	0.1±0.22		
UM171					
	10000	14/14	45.1±22.19	66	(40-108)
	1000	14/14	6.2±9.29		
	500	8/8	5.0±6.87		
	200	5/6	0.3±0.28		
	100	12/14	0.4±0.61		
	70	4/6	0.1±0.05		
Combi					
	10000	11/11	31.3±19.93	31	(17-60)
	1000	13/13	6.7±6.40		
	500	7/7	2.6±3.15		
	200	6/6	1.2±1.06		
	100	11/12	0.8±1.76		
	70	6/6	0.6±0.32		

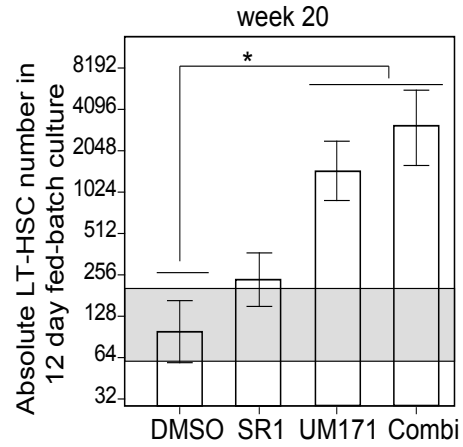


Table S2.1. Limit dilution analysis of NSG engraftment at 20 weeks post-transplantation.

Summary of primary transplantations performed to determine d0 equivalent frequencies (left panels) and numbers (right panels) of LT-HSCs in fresh (uncultured) or cultured (12 days) CB cells. Significance level: *p<0.05 (Mann Whitney test). Gray shade shows 95% CI for fresh cells.

Determination of day 0 equivalent frequencies of LT-HSCs in various cultures					
Condition	Cell dose equivalent to d0	No. 1ry recipients reconstituted / transplanted	Reconstitution levels of 1ry recipients (Mean +/- SD)	1/SRC frequency per starting cell (30 wks post transplant)	95% confidence of interval (upper, lower)
Fresh					
	25000	5/5	36.3±30.55	416	(192-901)
	5000	4/4	6.8±6.22		
	1000	4/5	6±6.92		
	500	4/5	1.9±3.15		
	50	1/4	0.1±0.05		
DMSO					
	10000	6/6	25±15.16	451	(223-911)
	1000	5/6	0.2±0.13		
	200	2/6	1.6±3.10		
	100	2/6	0.0±0.05		
	70	1/6	0.0±0.03		
SR1					
	10000	6/6	19.6±7.84	173	(84.3-354)
	1000	6/6	1.1±0.82		
	200	4/5	0.1±0.12		
	100	2/5	0.4±0.56		
	70	1/5	0.0±0.05		
UM171					
	10000	6/6	39.6±24.55	32	ND
	1000	5/5	2.9±0.47		
	200	6/6	0.8±0.47		
	100	5/5	1.0±0.56		
	70	6/6	0.4±0.19		
Combi					
	10000	4/4	29.8±20.05	33	ND
	1000	5/5	4.3±2.80		
	200	5/5	1.5±1.41		
	100	4/4	0.5±0.24		
	70	6/6	0.7±0.32		

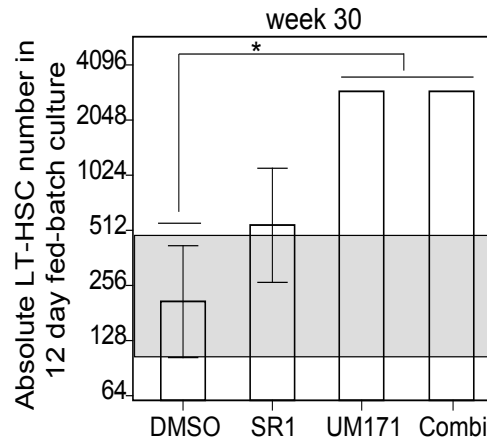


Table S2.3. Limit dilution analysis of NSG engraftment at 30 weeks post-transplantation.

Summary of primary transplantations performed to determine d0 equivalent frequencies (left panels) and numbers (right panels) of LT-HSCs in fresh (uncultured) or cultured (12 days) CB cells. Significance level: *p<0.05 (Mann Whitney test). Gray shade shows 95% CI for fresh cells.

Conditions	1ary mouse ID No.	Reconstitution levels of 1ry recipients (Mean +/- SD)	Total number of BM cells injected per secondary recipient	Human BM cells transplanted	No. 2ary recipients reconstituted / transplanted	Reconstitution levels of 2ary recipients (Mean +/- SD)	1/SRC frequency (18 wks post tranplantation)	95% Confidence of interval (upper, lower)	
Fresh									
	(13668, 13669, 13670, 13672)	38±27.65	10,000,000	3,800,000	2/4	7.43±12.40	2319481	1059149	5079542
			6,600,000	2,508,000	3/4	2.28±2.41			
			1,320,000	501,600	2/4	0.2±0.24			
			660,000	250,800	1/4	0.03±0.04			
			120,000	45,600	0/4	0.00±0.00			
DMSO									
	(13725, 13726, 13727, 13737, 13738, 13739)	21.37±13.12	10,000,000	2,136,667	4/6	0.3±0.19	1799526	908225	3565517
			6,600,000	1,410,200	3/6	0.13±0.08			
			1,320,000	282,040	2/6	0.08±0.08			
			660,000	141,020	0/6	0.00±0.00			
			120,000	25,640	0/6	0.00±0.00			
UM171									
	(13785, 13786, 13787, 13800, 13801)	33.54±26.59	10,000,000	3,354,000	4/4	3.05±5.11	509336	225339	1151258
			6,600,000	2,213,640	5/5	0.82±1.07			
			1,320,000	442,728	3/4	0.32±0.54			
			660,000	221,364	1/5	0.02±0.04			
			120,000	40,248	0/5	0.00±0.00			

Table S2.4. Results from secondary transplantation experiments.

Secondary NSG recipient mice were injected with bone marrow cells harvested from primary recipients sacrificed 30 weeks post-transplantation. Note that primary recipients received different cell doses: 25,000 for fresh (uncultured) cells and 10,000 day 0 equivalent DMSO and UM171 cultured cells.

Chapter 3: EPCR expression defines the most primitive subset of expanded human HSPCs and is required for their in vivo activity

Manuscript in Nature medicine-under revision (Number: NMED-L80529-T)

Synopsis:

Most of the surface markers that differentiate fresh (uncultured) hematopoietic stem cell (HSC) from more committed progenitor are not reliable in detecting HSC in culture. Using UM171, a small molecule previously described in chapter 2, we were able to identify endothelial protein c receptor (EPCR) as a first surface marker that enriches for human HSC in culture.

Contribution:

All the data in **Figure 3.1, 3.2, 3.3, 3.4 B-C, 3.5 D- E, S3.1-3.6, S3.8C, and Table S3.1-S3.6** were generated by **Iman Fares (100%)**

Data in **Figure 3.4A and S3.7** were generated by **Jalila Chagraoui**

Data in **Figure 3.5A-C and S3.8A-B** were plotted using R by **Bernhard Lehnertz**

EPCR Expression Defines the Most Primitive Subset of Expanded Human HSPCs and Is Required for Their *In Vivo* Activity

Iman Fares¹, Jalila Chagraoui¹, Bernhard Lehnertz¹, Tara MacRae¹, Nadine Mayotte¹, Guy Sauvageau^{1,2,3}

¹Molecular Genetics of Stem Cells Laboratory, Institute of Research in Immunology and Cancer (IRIC), University of Montreal, Montreal, QC, Canada.

²Division of Hematology, Maisonneuve-Rosemont Hospital, Montreal, QC, Canada.

³Department of Medicine, Faculty of Medicine, University de Montreal, Montreal, QC, Canada.

Corresponding Author:

Guy Sauvageau M.D., Ph.D.

Institut de Recherche en Immunologie et Cancérologie

C.P. 6128, succursale Centre-Ville, Montréal, Québec

Canada H3C 3J7

Telephone: (514) 343-7134

Facsimile: (514) 343-7379

E-mail: guy.sauvageau@umontreal.ca

Abstract

Cell purification technology combined with transcriptome sequencing and a small molecule agonist of hematopoietic stem cell self-renewal have allowed us to identify the endothelial protein c receptor (EPCR) as a surface marker that defines a rare subpopulation of human cells highly enriched for stem cell activity *in vivo*. EPCR-positive cells exhibit robust multi-lineage differentiation potential and serial reconstitution ability in immunocompromised mice. Following *ex vivo* stem cell expansion, HSC activity is detected in EPCR⁺ subpopulations, arguing for the stability of this marker on the surface of cultured cells, a feature not commonly observed with other recently described markers. Functionally, EPCR is essential for human HSC activity *in vivo*. Cells engineered to express low EPCR levels lack the ability to confer long-term reconstitution. EPCR is a highly performant marker for human HSCs and its exploitation should open new possibilities in our effort to understand the molecular bases behind HSC self-renewal.

3.1 Introduction

Human hematopoietic stem cells (HSC) constitute a rare sub-population of cells with the unique ability to self-renew and differentiate into all blood lineages. Human cord blood (CB) is one of the most accessible sources for HSCs and is frequently used in clinical and research settings. HSCs in CB samples can be prospectively identified with high confidence using antibodies that detect the combinatorial surface expression of CD34, CD38, CD90, CD45RA and CD49f¹⁻⁴. With this approach, HSCs can be isolated to up to 10% purity from human CB units. Although representing several orders of magnitude of enrichment, the scarcity of HSCs in purified CB samples hampers the functional dissection of the molecular mechanisms underlying HSC self-renewal. One possible avenue to overcome this hurdle is to expand such rare cells *ex vivo* using recently developed tools such as the UM171 and SR1 small molecules or fed batch bioreactor systems⁵⁻⁸. Unfortunately, another issue associated with this strategy is the fact that several of the HSC markers described, for example CD38⁹ and CD49f (Fig. S3.1), are no longer reliable once HSCs are cultured. This significantly restricts our ability to assess the frequency and purity of HSCs in *ex vivo* culture conditions.

We have previously developed the pyrimido-indole derivative UM171, which stimulates human hematopoietic stem and progenitor cell (HSPC) expansion *in vitro*. Transcriptome analysis of CD34-enriched human CB cells expanded *ex vivo* revealed the Endothelial Protein C Receptor (EPCR) gene as one of the best determinants of HSPCs response to UM171⁷. Given the known function of EPCR as a highly discriminatory surface antigen on mouse HSCs¹⁰, we reasoned that this receptor might also be selectively associated with human HSCs and that it may be stable in expanded HSC cultures.

3.2 Results

3.2.1 EPCR⁺ population exhibits a robust multi-lineage differentiation potential

To evaluate if EPCR expression correlates with HSC activity, UM171-treated cultures initiated 7 and 12 days earlier with CD34⁺CD45RA⁻ CB cells were sorted based on EPCR expression levels (EPCR⁻, EPCR^{low} and EPCR⁺) and their HSPC content was monitored (Fig. 3.1a, b). At day 7 and 12, the EPCR⁺ subpopulation represented 5±3% and 1.8±0.4% of the culture, respectively, and showed elevated CD34 expression (red peak in Fig. 3.1b). The EPCR⁺ population was less clonogenic than the EPCR^{low} and EPCR⁻ populations, as illustrated by the difference in frequencies of CFU-GEMM between these subsets (Fig. 3.1c). In sharp contrast, the long-term

reconstitution activity of the cultured cells was essentially restricted to the EPCR⁺ subpopulation both at day 7 and at day 12 (Fig. 3.1d, e). The strength of this marker to identify expanded LT-HSCs in culture is further highlighted by the relative enrichment of these cells as the culture progresses, from 20-fold enrichment at day 7 to 56-fold by day 12 (Fig. 3.1d, e and Table S3.1). Not only does EPCR expression correlate with LT-HSC activity *in vivo* at 24 weeks, it also identifies LT-HSCs with multi-lineage potential (Fig. 3.1f, g). These results were reproduced in a second series of experiments in which similar EPCR-based cell sorting was performed from CD34⁺CD45RA⁻ cells as compared to bulk cultures (Fig. 3.1d, e).

We next examined if EPCR is also a reliable HSC marker in experimental conditions where CB cells are not exposed to UM171. For these experiments, CD34⁺CD45RA⁻ CB cells were sorted based on EPCR expression after 3 days in culture, at which time LT-HSCs are still detectable and EPCR expression is maximal (Fig. S3.2a). Consistent with our findings with UM171 treated cells, EPCR⁺ cells from DMSO-treated cultures were characterized by long-term repopulating activity and multi-lineage potential similar to bulk cells (Fig. S3.2c, d and Table S3.2). Based on these results, we hypothesized that EPCR can be used as a surrogate marker to predict LT-HSC enrichment in different culture conditions. To test this, we monitored EPCR⁺CD34⁺ cells in UM171 or SR1-treated cultures after 12-day expansion where LT-HSC frequency was previously shown to be 13-fold higher in UM171-treated cultures compared to SR1⁷. Interestingly, EPCR⁺CD34⁺ cells were up to 10 times more abundant in cultures treated with UM171 when compared to those supplemented with SR1 (Fig. S3.3). Altogether, these results suggest that EPCR is a suitable marker to identify HSCs, irrespective of the culture condition.

3.2.2 EPCR⁺ cells provide multi-lineage reconstitution in secondary mice

To further evaluate the self-renewal potential of each EPCR subset, we performed secondary transplantation experiments in which cells collected 24 weeks post transplantation from BM of primary mice were transplanted into secondary recipients and monitored for an additional 18 weeks. As shown in Fig. 3.1h, reconstitution of secondary recipients was limited to mice transplanted with grafts originating from either unsorted cells or EPCR⁺ cells derived from the day 7 or day 12 cultures (Fig. 3.1h and Table S3.3). Secondary recipients of the marrow from EPCR⁻ or EPCR^{low} primary donors showed very low levels of engraftment, which was frequently undetectable. These findings suggest that only EPCR⁺ cells possess the required self-renewal potential to provide long-term multipotent reconstitution in serial transplantation settings.

3.2.3 High frequency of human LT-HSCs in EPCR⁺ fraction

Using limiting dilution analysis (LDA), we estimated that one per 68 EPCR⁺ cells was a multipotent LT-HSC in UM171 supplemented cultures harvested at day 7. The LT-HSC frequency was lower in all other fractions ranging from 1 per 2016 cells in EPCR^{low} to 1 per 4240 cells in EPCR⁻ subpopulations (Fig. 3.2a, b). Considering the LT-HSC frequency in the unsorted expanded CD34⁺CD45RA⁻ culture, we calculated that sorting on EPCR alone provided a 12-fold net enrichment in LT-HSCs (Fig. 3.2a, b, Fig. S3.4, and Table S3.4).

3.2.4 EPCR best discriminates expanded CD34⁺ HSPC

Although some of the most critical markers of human LT-HSCs are unreliable once cells are expanded (e.g. CD38 and CD49f), others seem to retain prospective value. These include CD90 and CD45RA^{1,3}. We hypothesized that a combinatorial surface marker-based sorting approach might improve our ability to isolate LT-HSCs, and thus analyzed EPCR expression in combination with these other markers. To this end, CD34⁺CD45RA⁻ CB cells were kept in UM171-supplemented culture for 7 days and then sorted into 7 different fractions based on CD34, EPCR, CD45RA and CD90 expression (Fig. S3.5a). Each fraction was then transplanted in NSG mice and reconstitution was analyzed at early (3 weeks) and late (24 weeks) time points (Fig. S3.5b).

With this approach, we observed that selection of CD34⁺ cells among the EPCR⁺ population further enriched the sample in LT-HSCs (Fig. S3.5b). Importantly, CD90 expression or lack of CD45RA did not allow for a significant additional subdivision of the EPCR⁺CD34⁺ population since this subfraction is largely CD90⁺CD45RA⁻. Conversely, selection of EPCR⁺ cells from the CD34⁺CD45RA⁻ and CD34⁺CD90⁺ populations enriched these samples in LT-HSCs by approximately 8- and 3- fold respectively, indicating that EPCR expression marks a subfraction of CD34⁺/CD90⁺/CD45RA⁻ cells.

To further evaluate the importance of EPCR expression on *ex vivo* expanded LT-HSCs and determine the value of additional markers such as CD133^{11,12}, we sorted EPCR⁺ and EPCR^{Low/-} populations from CD34⁺ CB cells following a 3-day culture with UM171 and expanded them separately for an additional 7 days at which time phenotypical analyses were conducted prior to transplantation in NSG mice (Fig. 3.3a, b). Results confirm that most of the LT-HSC activity resides in the EPCR⁺ population (Fig. 3.3, C and D). Most interestingly, in cultures initiated with CD34⁺EPCR^{low/-} cells, we noticed a large expansion of CD34⁺CD90⁺ and CD34⁺CD133⁺ cells (Fig. 3.3c) which contributed poorly to *in vivo* reconstitution (Fig. 3.3d) once again highlighting that a subset of EPCR-negative cells which remain positive for CD34, CD90, CD133

and depleted of CD45RA expression show modest repopulation activity.

3.2.5 EPCR as a marker of non-expanded LT-HSC

We next determined if EPCR can identify LT-HSCs from non-expanded samples (Extended Data Fig. 3.6a). Frequencies of multilineage progenitors were similar between CD34⁺CD45RA⁻EPCR^{low}, CD34⁺CD45RA⁻EPCR⁺ and unfractionated CD34⁺CD45RA⁻ populations (Fig. S3.6b). At a non-limiting cell dose, we observed that all LT-HSC activity is correlated to the EPCR^{low} or EPCR⁺ fractions (Fig. S3.6c) clearly documenting the relevance of this marker for fresh CB LT-HSCs. Strikingly and in contrast to cultured HSPC, recipients of CD34⁺CD45RA⁻EPCR^{low} and CD34⁺CD45RA⁻EPCR⁺ cells had similar levels of human chimerism and lineage distribution (Extended Data Fig. 3.6c-e and Supplementary Table S5). However, we noticed that long-term reconstitution was mostly observed in secondary recipients of a graft originating from CD34⁺CD45RA⁻EPCR⁺ cells (Fig. S3.6f). Based on this it appears that the EPCR⁺ subset of fresh human HSC is more primitive than the EPCR⁻ one.

3.2.6 EPCR expression is critical for HSPC function

To determine if EPCR expression is essential for HSPC activity, we identified 2 effective EPCR-targeting shRNA vectors which enabled different levels of knockdown (Fig. 3.4 a, b). CD34⁺CB cells transduced with the indicated shEPCR-GFP vectors were transplanted into NSG mice whose reconstitution by human cells was analyzed 20 weeks post-transplantation (Fig. 3.4c and Fig. S3.7). Results show that HSPC activity is inversely proportional to the magnitude of EPCR knockdown- the most efficient shEPCR (sh2) significantly reduces the engraftment levels. These results indicate that EPCR levels are critical for the *in vivo* activity of human HSPCs.

3.2.7 HSPC gene signature characterizes EPCR⁺ cells

In order to analyse the transcriptional landscape of EPCR⁺ cells, we performed mRNA profiling experiments using EPCR⁻, EPCR^{low} and EPCR⁺ populations sorted from expanded CD34⁺CD45RA⁻ CB cells (Fig. 3.1b, day7). Using a minimum of 2-fold difference in expression as a selection criterion, a total of 1,048 differentially expressed genes (597 up- and 451 down-regulated genes) were identified between the EPCR⁺ and EPCR^{-/low} populations (Fig. 3.5 a and Table S3.6). Gene set enrichment analysis (GSEA) shows that the differentially expressed genes of EPCR⁺ population are significantly overlapped with genes associated with HSPC derived from uncultured human CB and fetal liver¹³⁻¹⁵, providing evidence for a stem cell signature (Fig. 3.5b and Fig. S3.8). Manual curation and GSEA identified a marked underrepresentation of differen-

tiation-related genes in the EPCR⁺ population, namely genes associated with erythroid and myeloid differentiation (Fig. 3.5a and Fig. S3.8b, c). Intersecting our data with that of others^{13, 15}, we were able to refine a 120 HSPC gene signature (Fig. 3.5c and Fig. S3.8a). This signature is mostly comprised of either well-known transcriptional regulators of HSC self-renewal/function such as HLF, PRDM16, and MECOM or genes encoding cell surface markers typically used to enrich for HSC (CD90, CD133, CD143, CD318, CD93 and GPR56)^{1, 12, 16-19} (Fig. 3.5 a, d). We further validated the overlapping expression patterns of these cell surface markers with that of EPCR by flow cytometry (Fig. 3.5e).

3.3 Discussion

Our data suggests that EPCR represents a new robust marker of expanded human LT-HSCs. Accordingly; expanded human LT-HSPCs could be defined by the expression of a single gene product rather than group of receptors. Indeed in UM171-supplemented culture conditions, EPCR cell surface expression on its own identifies functional HSPC at a frequency which cannot be further improved by any of the previously defined cell surface markers such as CD34, CD90, CD49f or CD133.

ShRNA-mediated EPCR knockdown studies suggest that EPCR plays a crucial role for the *in vivo* activity of HSPCs. This observation is consistent with mouse studies in which EPCR expression was shown to confer a cytoprotective role in HSPC thus contributing to their maintenance²⁰. Interestingly, mice genetically engineered to express low levels of EPCR (*Procr^{low}*) showed defects in HSPC bone marrow retention and limited long-term reconstitution potential, strengthening the idea that EPCR is an important regulator of HSPC²¹.

3.4 Conclusion

Identifying surface makers that enrich for cultured human HSPC such as EPCR will allow for a better understanding of HSPC self-renewal mechanisms that in turn will facilitate the manipulation and expansion of human HSPC *ex vivo* for clinical applications.

Acknowledgments

The authors acknowledge the help of Marie-Eve Bordeleau and Keith Humphries for critical reading of this manuscript. We thank D. Gagné at IRIC for technical support with flow cytometry sort, and M. Frechette and V. Blouin-Chagnon for assistance with mouse experiments. We also thank Héma-Québec for providing human umbilical CB units, and our research assistants,

Corneau and I. Boivin, for purifying CD34⁺ CB cells. Financial support was from a CIHR foundation grant to GS and from the Stem Cell Network of Canada. Authors reported no conflict of interest.

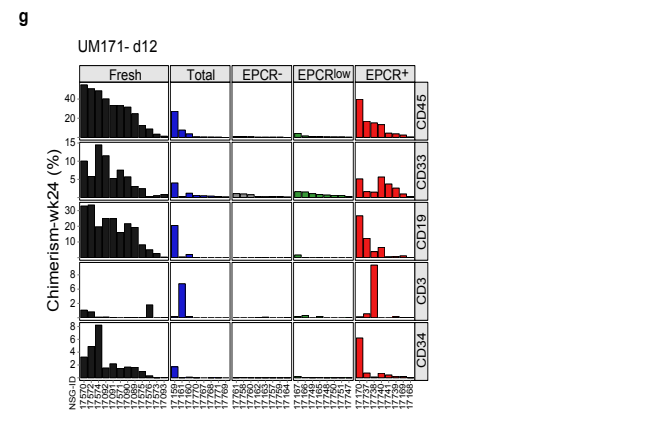
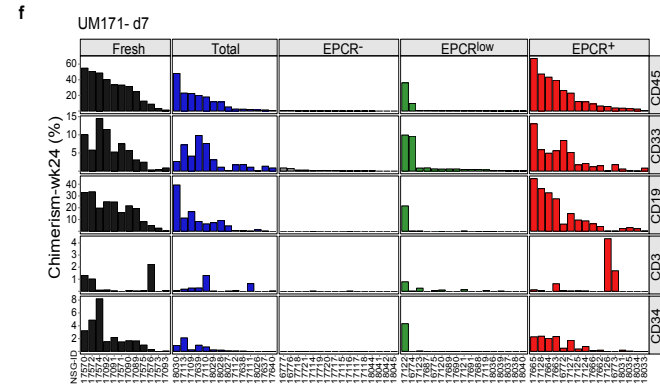
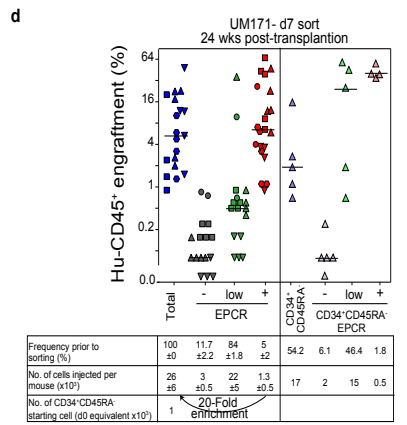
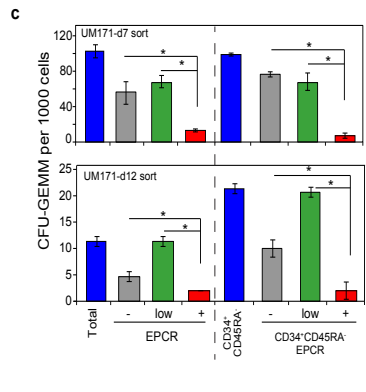
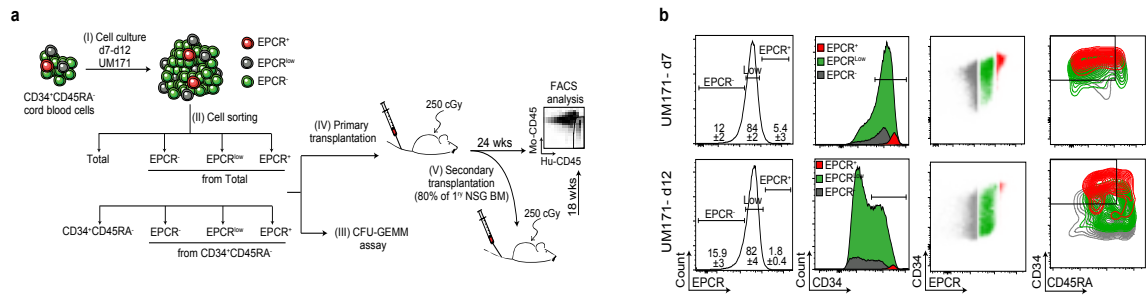


Fig. 3.1. EPCR+ population is enriched with LT-HSC in culture.

a, Schematic representation of EPCR sort after 7 and 12-day culture in UM171 (38 nM). **b**, FACS plot showing the percentage of EPCR subsets and their distribution in CD34+ and CD34+CD45RA- cells after culture (mean \pm s.d, 5 biological replicates). **c**, CFU-GEMMs count for EPCR sorted subsets after culture (mean \pm s.d, n= 3 wells counted per condition of 2 biological replicates); significance level *P<0.05 (Mann-Whitney test, one-sided). Human (Hu) CD45 engraftment and lineage potential of the indicated sorted cells assessed for each NSG recipient mouse identified as NSG-ID after 7- (**d, f**) and 12- (**e, g**) day culture; n= 3-20 mice per condition (each geometric shape corresponds to a biological replicate). **h**, Primary NSG mice, receiving the indicated sorted population after 7 and 12 day culture from 3×10^3 CD34+CD45RA- starting cell (d0 equivalent), were transplanted into 2ry NSG recipients. Hu-CD45 cell chimerism was analyzed in the 1ry and 2ry mice at 24 and 18 weeks post-transplantation respectively by flow cytometry; n= 4-5 mice per condition, technical replicates. The horizontal bars in (**d**), (**e**), and (**h**) indicate median values.

a

Sorted population (% at d7 prior to sorting)	Cell dose at d7	%Avg. Hu-CD45 ± STD (wk24)	(E/T)	Frequency of LT-HSC		Number (population %) of LT-HSC at d7 per 10 ³ CD34 ⁺ CD45RA ⁻ starting cell
				Estimate	(95% CI)	
Total (100%)	75,000	56.7±21	(5/5)	1: 828	(1,973 ; 347)	30.2 (100%)
	25,000	6.2±8.1	(4/4)			
	8,333	3.7±4	(5/5)			
	2,778	1.7±2.5	(5/5)			
	926	0.1±0.2	(3/5)			
EPCR ⁺ (6%)	4,500	54.1±18	(5/5)	1: 68	(155 ; 30)	22 (73%)
	1,500	33±22.7	(5/5)			
	500	14.2±13.2	(5/5)			
	167	0.3±0.1	(5/5)			
	56	0.1±0.1	(2/5)			
EPCR ^{low} (84%)	62,775	3.4 ±6.4	(5/5)	1: 2,016	(4,406 ; 923)	10.4 (34%)
	20,925	0.6±0.1	(5/5)			
	6,975	0.4±0.2	(5/5)			
	2,325	0.1±0.1	(4/5)			
	775	0.1±0.0	(0/4)			
EPCR ⁻ (10%)	7,575	0.1 ±0.1	(3/5)	1: 4,240	(8,824 ; 2,037)	0.6 (2%)
	2,525	0.2±0.0	(5/5)			
	842	0.1±0.0	(4/5)			
	281	0.0±0.0	(1/5)			

b

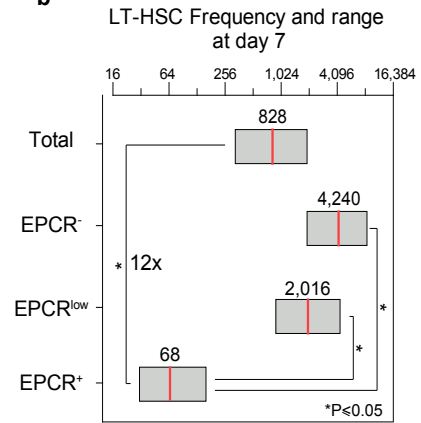


Fig. 3.2. Frequency of LT-HSC within EPCR-, EPCR^{low} and EPCR⁺ populations.

a, Table summarizing limit dilution analysis of the indicated sorted populations. CD34⁺CD45RA⁻ cells were expanded for 7 days in the presence of UM171 (38 nM). Five cell doses and their respective fractions based on EPCR expression (-, low and +) were sorted and transplanted in NSG (n= 5 mice per dose, technical replicates). The number of engrafted/ transplanted mice (E/T) with the average of human CD45 reconstitution is presented. Number of LT-HSCs per 10³ CD34⁺CD45RA⁻ starting cells based on the estimated LT-HSC frequencies and 95% clearance (CI). **b**, Estimated LT-HSC frequencies (red lines) and 95% CI (gray boxes) presented as 1/number of sorted cells at day 7; significance level *P < 0.05 (Mann-Whitney test, one-sided).

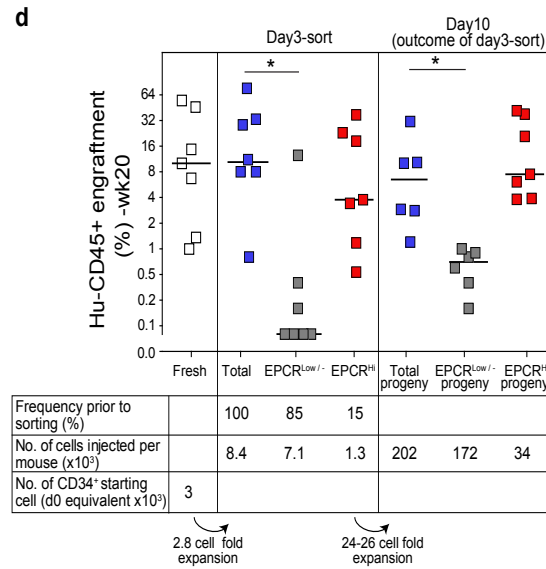
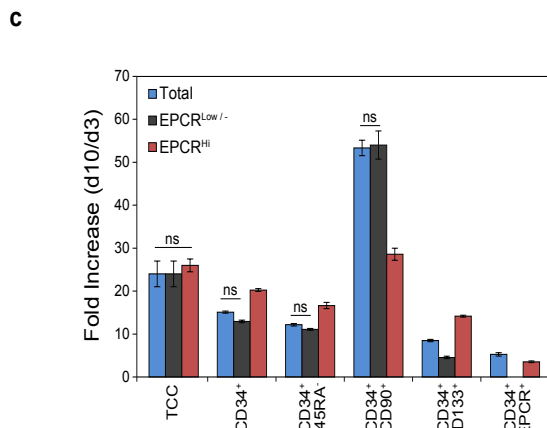
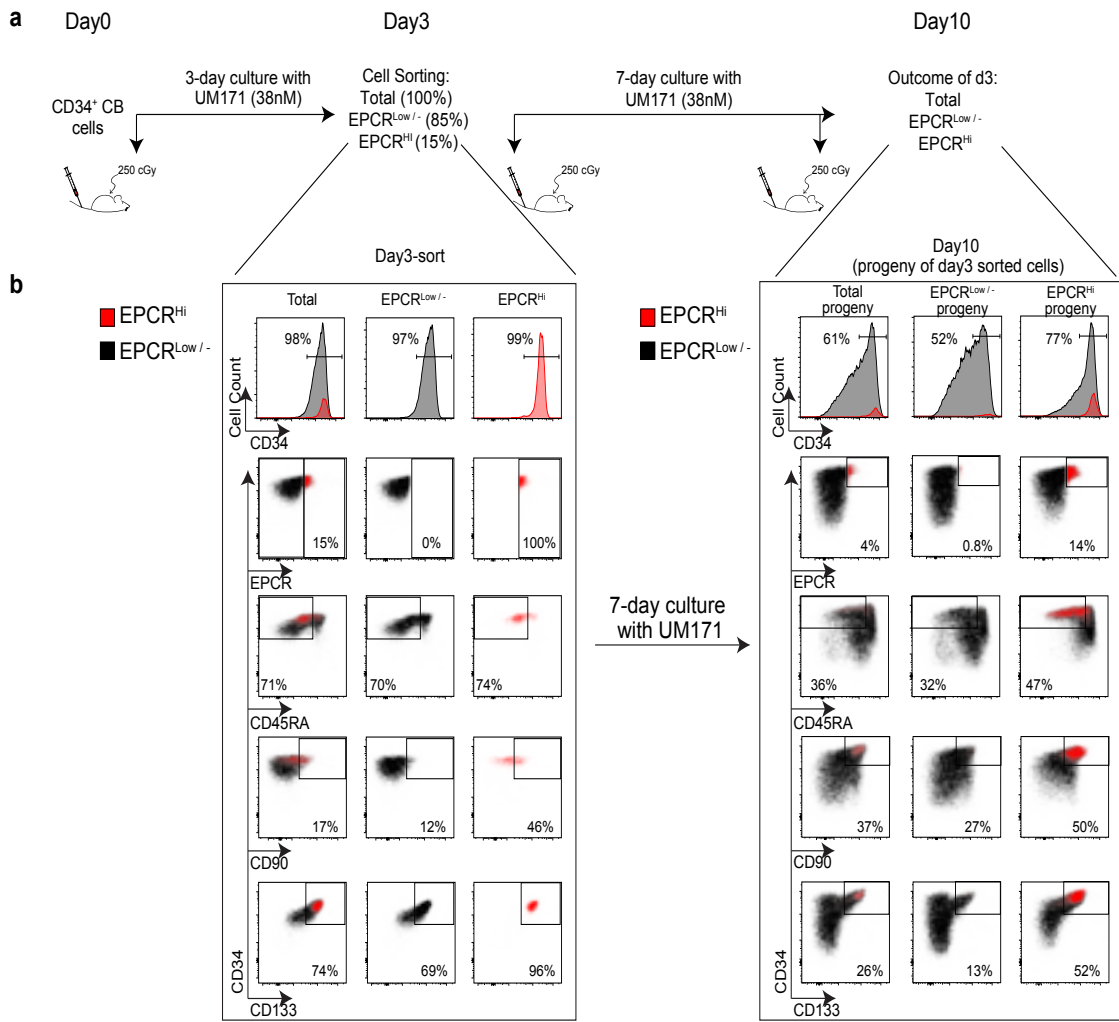


Fig. 3.3 | Expanded EPCR+ progeny retains the most of the ex vivo HSPC expanded cells.

a, Schematic presentation for EPCR sort and transplantation strategy. CD34⁺ cord blood (CB) cells were expanded for 3 days in UM171 (38 nM) before they were sorted on EPCR expression (EPCR⁺ and EPCR^{Low} / -) where they proliferated in UM171-cultures for additional 7 days. EPCR subsets in addition to unpurified cells were stained for HSC phenotype and transplanted in NSG mice to determine their in vivo proliferative potential at the day of the sort (day3) and after 7 day expansion (day10). **b**, Flow cytometry of HSCP phenotype at day3 and day10 culture. **c**, Fold-expansion of the indicated HSPCs population from day3 to day10 of the expanded progenies (unpurified, EPCR⁺ and EPCR^{Low} / -cells), (mean ± s.d, n= 3 technical replicates. Differences between conditions are statistically significant, unless specified ns: not significant (Mann-Whitney test, one-sided). **d**, Human CD45 engraftment in NSG mice receiving the indicated sorted population at day 3 or their outputs after 7-day expansion. The horizontal bars indicate median values (n= 7 mice per condition, technical replicates); significance level *P < 0.05 (Mann-Whitney test, one-sided).

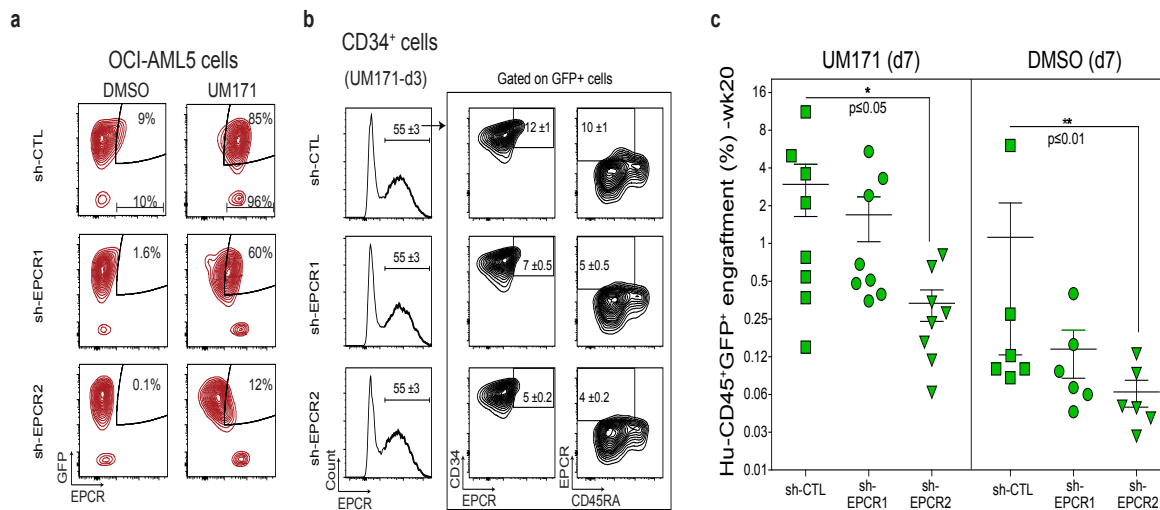


Fig. 3.4 | Loss of EPCR expression in CD34⁺ cells compromise their engraftment ability in NSG mice.

a, EPCR knockdown validation in OCI-AML5 cell line. UM171 treatment induces the EPCR surface expression up to 85% in OCI-AML5 cell line (upper panel). OCI-AML5 cells were transduced with lentiviral sh-EPCR-GFP (sh1 or 2) vs controls (sh-Renilla) at MOI 3 for 16 hours before they washed and cultured for 2 additional days with vehicle (DMSO) or UM171 (250 nM). OCI-AML5 cells were then collected and stained for EPCR. The knockdown of EPCR was assessed in GFP⁺ cells using flow cytometry. **b**, Representative FACSplots of CD34⁺ CB cells after EPCR knockdown (mean ± s.d, n= 3 technical replicates). Pre-stimulated CD34⁺ CB cells were infected with lentiviral sh-EPCR-GFP (sh1 or 2) vs controls (sh-Renilla) at MOI 100 for 16 hours. Transduced CD34⁺ CB cells were washed and cultured with or without UM171 (38 nM) for 3 days where the knockdown of EPCR surface expression in GFP⁺ cells was monitored using flow cytometry. Cells then were kept in culture for total of 7 days before they were injected in NSG mice to monitor their in vivo activity. **c**, Human (Hu)-CD45 engraftment in GFP⁺ populations in bone marrow of NSG at 20 weeks post-transplantation (mean with s.e.m, n= 4-5 mice per condition, technical replicates). Two different sh-EPCR are shown; significance level *P<0.5 (Mann-Whitney test, one-sided).

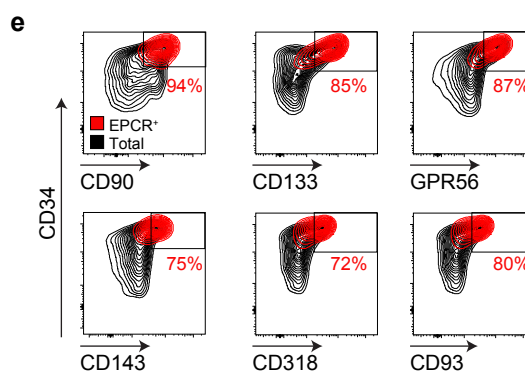
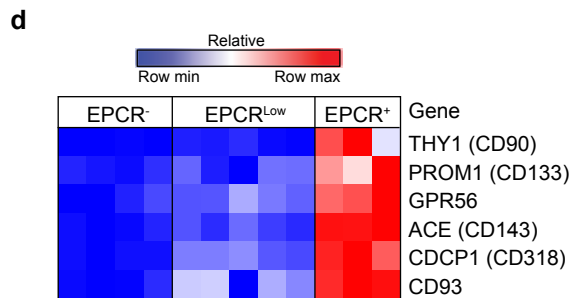
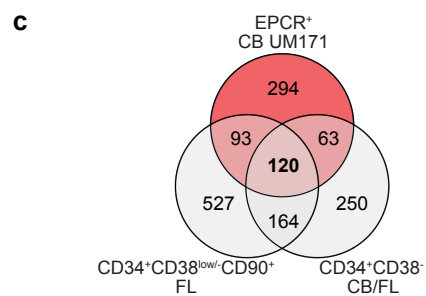
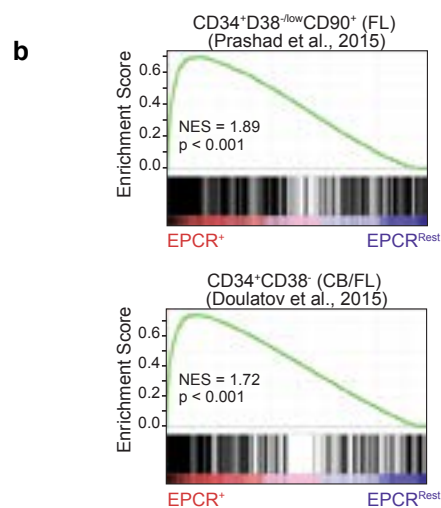
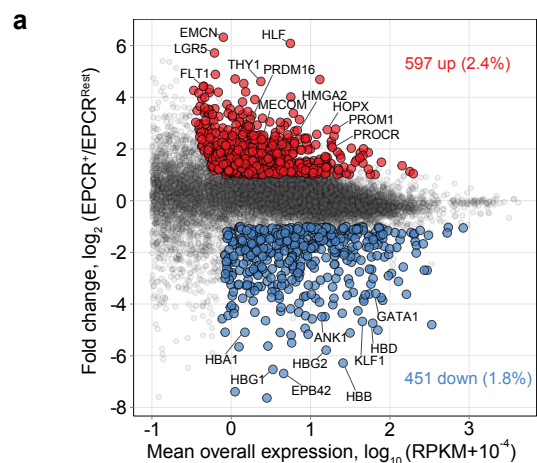


Fig. 3.5. Gene expression profiling of cultured EPCR⁺ population strongly correlates with uncultured HSC-related genes.

a, Scatterplot representation of global mRNA profiling showing upregulated (red) and down-regulated (blue) genes in EPCR⁺ versus EPCR^{Rest} (- and low) populations ($p \leq 0.01$, mean expression ≥ 1 RPKM; ≥ 2 -fold up or down). **b**, GSEA plot showing enrichment for HSC-related genes in the EPCR⁺ population. Gene expression of uncultured purified human HSC derived from cord blood (CB) and fetal liver (FL) from two independent data set were used for the GSEA analysis; NES= normalized enrichment score; all comparisons were significant. **c**, Venn diagram plot showing the number of common and distinct up-regulated genes in EPCR⁺ population, CD34⁺CD38^{low/-}CD90⁺ (FL) cells, and CD34⁺CD38⁻ (FL and CB) cells. mRNA **(d)** and protein **(e)** levels of known HSC surface markers in various cellular population.

Reference

1. C. M. Baum, I. L. Weissman, A. S. Tsukamoto, A. M. Buckle, B. Peault, Isolation of a candidate human hematopoietic stem-cell population. *Proceedings of the National Academy of Sciences of the United States of America* **89**, 2804-2808 (1992).
2. M. Bhatia, J. C. Wang, U. Kapp, D. Bonnet, J. E. Dick, Purification of primitive human hematopoietic cells capable of repopulating immune-deficient mice. *Proceedings of the National Academy of Sciences of the United States of America* **94**, 5320-5325 (1997).
3. R. Majeti, C. Y. Park, I. L. Weissman, Identification of a hierarchy of multipotent hematopoietic progenitors in human cord blood. *Cell stem cell* **1**, 635-645 (2007).
4. F. Notta *et al.*, Isolation of single human hematopoietic stem cells capable of long-term multilineage engraftment. *Science* **333**, 218-221 (2011).
5. H. E. Broxmeyer, L. M. Pelus, Inhibition of DPP4/CD26 and dmPGE(2) treatment enhances engraftment of mouse bone marrow hematopoietic stem cells. *Blood cells, molecules & diseases* **53**, 34-38 (2014).
6. A. E. Boitano *et al.*, Aryl hydrocarbon receptor antagonists promote the expansion of human hematopoietic stem cells. *Science* **329**, 1345-1348 (2010).
7. I. Fares *et al.*, Cord blood expansion. Pyrimidoindole derivatives are agonists of human hematopoietic stem cell self-renewal. *Science* **345**, 1509-1512 (2014).
8. P. Chaurasia, D. C. Gajzer, C. Schaniel, S. D'Souza, R. Hoffman, Epigenetic reprogramming induces the expansion of cord blood stem cells. *The Journal of clinical investigation* **124**, 2378-2395 (2014).
9. C. Dorrell, O. I. Gan, D. S. Pereira, R. G. Hawley, J. E. Dick, Expansion of human cord blood CD34(+)/CD38(-) cells in ex vivo culture during retroviral transduction without a corresponding increase in SCID repopulating cell (SRC) frequency: dissociation of SRC phenotype and function. *Blood* **95**, 102-110 (2000).
10. A. B. Balazs, A. J. Fabian, C. T. Esmon, R. C. Mulligan, Endothelial protein C receptor (CD201) explicitly identifies hematopoietic stem cells in murine bone marrow. *Blood* **107**, 2317-2321 (2006).
11. A. C. Drake *et al.*, Human CD34+ CD133+ hematopoietic stem cells cultured with growth factors including Angptl5 efficiently engraft adult NOD-SCID Il2rgamma-/- (NSG) mice. *PloS one* **6**, e18382 (2011).
12. A. H. Yin *et al.*, AC133, a novel marker for human hematopoietic stem and progenitor cells. *Blood* **90**, 5002-5012 (1997).
13. S. Doulatov *et al.*, Induction of multipotential hematopoietic progenitors from human pluripotent stem cells via respecification of lineage-restricted precursors. *Cell stem cell* **13**, 459-470 (2013).
14. E. Laurenti *et al.*, The transcriptional architecture of early human hematopoiesis identifies mul-

- tilevel control of lymphoid commitment. *Nature immunology* **14**, 756-763 (2013).
15. S. L. Prashad *et al.*, GPI-80 defines self-renewal ability in hematopoietic stem cells during human development. *Cell stem cell* **16**, 80-87 (2015).
 16. V. J. Jokubaitis *et al.*, Angiotensin-converting enzyme (CD143) marks hematopoietic stem cells in human embryonic, fetal, and adult hematopoietic tissues. *Blood* **111**, 4055-4063 (2008).
 17. T. Conze *et al.*, CDCP1 is a novel marker for hematopoietic stem cells. *Annals of the New York Academy of Sciences* **996**, 222-226 (2003).
 18. G. H. Danet *et al.*, C1qRp defines a new human stem cell population with hematopoietic and hepatic potential. *Proceedings of the National Academy of Sciences of the United States of America* **99**, 10441-10445 (2002).
 19. Y. Saito *et al.*, Maintenance of the hematopoietic stem cell pool in bone marrow niches by EVI1-regulated GPR56. *Leukemia* **27**, 1637-1649 (2013).
 20. H. Iwasaki, F. Arai, Y. Kubota, M. Dahl, T. Suda, Endothelial protein C receptor-expressing hematopoietic stem cells reside in the perisinusoidal niche in fetal liver. *Blood* **116**, 544-553 (2010).
 21. S. G. Cohen *et al.*, PAR1 signaling regulates the retention and recruitment of EPCR-expressing bone marrow hematopoietic stem cells. *Nature medicine* **21**, 1307-1317 (2015).
 22. Csaszar, E. *et al.* Rapid expansion of human hematopoietic stem cells by automated control of inhibitory feedback signaling. *Cell stem cell* **10**, 218-229, doi:10.1016/j.stem.2012.01.003 (2012).
 23. Logan, A. C. *et al.* Factors influencing the titer and infectivity of lentiviral vectors. *Human gene therapy* **15**, 976-988, doi:10.1089/hum.2004.15.976 (2004).
 24. Fellmann, C. *et al.* An optimized microRNA backbone for effective single-copy RNAi. *Cell reports* **5**, 1704-1713, doi:10.1016/j.celrep.2013.11.020 (2013).
 25. Hu, Y. & Smyth, G.K. ELDA: extreme limiting dilution analysis for comparing depleted and enriched populations in stem cell and other assays. *Journal of immunological methods* **347**, 70-78 (2009).

Supporting Material

Material and methods

Figures S1 to S8

Tables S1 to S6

METHODS

Human CD34⁺ cord blood cell collection

Umbilical cord blood units were collected from consenting mothers according to ethically approved protocol at CHU Sainte-Justine, Montreal, QC, Canada. Human CD34⁺ cord blood (CB) cells were isolated using The EasySep™ positive selection kit (StemCell Technologies Cat # 18056). Sorting for more primitive phenotypes was done in additional step using BD Aria II sorter.

Flow cytometry and sorting

Fresh or cultured hematopoietic cord blood cells were sorted for different HSPC phenotypes. Mouse anti-human antibodies were used to detect CD34 (FITC- BD Biosciences Cat # 555821 or BV421- BD Biosciences Cat #562577), CD45RA (PE- BD Biosciences Cat #555489, CD90 (PECY7- BioLegend Cat # 328124), CD49f (PECY5- BD Biosciences Cat #551129), and EPCR (APC- BioLegend Cat # 351906). Cells were analyzed on BD Canto flow cytometer, and cell sorting (low pressure) was conducted on BD Aria II. Cell sort recovery was estimated to be 50% post-sort.

HSPC cell culture

Human CB-derived CD34⁺ or CD34⁺CD45RA⁻ cells were cultured in HSC expansion media consisting of StemSpan SFEM (StemCell Technologies Cat # 09650) supplemented with human 100 ng/ml stem cell factor (SCF, R&D Systems_Cat # 255-SC), 100 ng/ml FMS-like tyrosine kinase 3 ligand (FLT3, R&D Systems Cat # 308-FK), 50 ng/ml thrombopoietin (TPO, R&D Systems Cat # 288-TP), and 10 µg/ml low-density lipoproteins (StemCell Technologies Cat # 02698). Cells were seeded at density of 1 x10³ cells/ml and fresh HSC expansion media supplemented with UM171 (StemCell Technologies Cat # 72914) (38nM), SR1 (Alichem Cat # 41864) (750 nM) or vehicle (0.1 % DMSO) was added to keep the cell density around 3-6 x10⁵ cells/ml. For transplantation experiments, the fed-batch culture system was used as previously described²². 1x10⁵ CD34⁺ or CD34⁺CD45RA⁻ CB cells/ml were injected into 25 ml bags (American Fluoroseal Corporation Cat # 2 PF-0025) connected to a syringe loaded pumping system and maintained on an orbital shaker at 37°C and 5% CO₂ in air. The pump was set to

continuously deliver HSC expansion media supplemented with vehicle (0.1% DMSO), UM171 (38 nM), or combination of UM171 (38 nM) and SR1 (750nM) at a flow rate of 0.7 μ l/min.

Colony-forming assay

Frequencies of colony-forming cells were estimated by plating 250-1000 EPCR⁻, EPCR^{low}, EPCR⁺ cell subsets sorted from uncultured CD34⁺CD45RA⁻ or their expanded progeny after 7 and 12 day culture with UM171 (38 nM). Cells were cultured in 2% methylcellulose-based media in Iscove's Modified Dulbecco's Medium (IMDM, GIBCO Cat #12440053), supplemented with 20% heat inactivated fetal bovine serum (FBS, WISENT Cat #115681), 1% bovine serum albumin (BSA, WISENT Cat #800-195-LG), 2 mM L-glutamine, 100 ng/ml SCF, 10 ng/ml IL3, 10 ng/ml IL6, 3 U/ml erythropoietin, 200 μ g/ml holo-transferrin Cat #T4132 Sigma, 10ng/ml GM-CSF (Shenandoah Biotechnology, Inc Cat #100-08), 50 ng/ml Tpo (Shenandoah Biotechnology, Inc Cat # 100-05) and 10⁻⁴ M 2-mercaptoethanol. After 14 days culture, plates were then scored for CFU-multilineage colonies containing granulocyte and erythroid.

Culture of EPCR progeny

Human CB-derived CD34⁺ cells were expanded for 3 days with UM171 (38nM) before they were stained with mouse anti-human EPCR antibody (APC-BioLegend Cat # 351906). Total (unpurified), EPCR^{-/low} and EPCR^{Hi} cells were sorted and placed in culture for additional 7 days in UM171 (38nM). HSC phenotype staining and transplantation assays were then performed.

Transplantation Assays

All experiments with animals were conducted under protocols approved by the University of Montreal Animal Care Committee. EPCR cell subsets purified from uncultured or expanded CD34⁺CD45RA⁻ CB cells were transplanted by tail vein injection into sub-lethally irradiated (250 cGy, <24 hr before transplantation) 8 to 16-week-old female NSG (NOD-Scid IL2R γ null, Jackson Laboratory) mice. The animal technicians performed blindly the transplantation experiments since they were not informed about the experimental conditions.

Human cells in NSG bone marrow (BM) was monitored by flow cytometry 12 and 24 weeks post-transplantation. NSG-BM cells were collected by femoral aspiration (at week 12) or by flushing the two femurs, tibias and hips when animals were sacrificed at week 24. For the limiting dilution analysis (LDA), cells were transplanted at 3-5 different cell doses in group of 5-8 mice.

For secondary transplantations, 80% of total BM cells from primary NSG recipients (24 weeks

post-transplantation) were injected into secondary sub-lethally irradiated NSG mice. BM cells of the secondary mice were harvested and analyzed 18 weeks post-transplantation. Flow cytometry analysis was performed on freshly collected BM cells. Cells were treated with 1x red blood cell lysis buffer (StemCell Technologies Cat # 20110), washed and stained with pacific blue-labelled anti-human CD45 (BioLegend Cat # 304029), APC-eFluor 780-labelled anti-mouse CD45 (eBioscience Cat # 47-0453-82), PE-labelled anti-human CD33 (BD Biosciences Cat #555450), PE-Cy7 labelled anti-human CD19 (BD Biosciences Cat #557835), FITC-labelled anti-human CD3 (BD Biosciences Cat # 555332). Cells then were washed and analyzed using a FACSCanto II (BD Biosciences). BD FACSDiva software was used to analyze the flow cytometry data.

Mice that show only human lymphoid engraftment (n=3) were not taken into consideration in LDA assessment because human lymphoid cells are long-lived cells and not necessary HSC-derived.

RNA sequencing and data analysis:

3-5 x 10⁵ cells were FACS sorted from day 7 cultured cord blood derived CD34⁺ HSPCs and preserved at -80C in TRIzol Reagent (Thermo Fisher Scientific Cat # 15596026). cDNA libraries were constructed according to TruSeq Protocols (Illumina) and sequencing was performed using an Illumina HiSeq 2000 instrument. We used the Casava pipeline (Illumina) and Refseq release 63 for subsequent mapping and quantification of gene expression. RPKM values were loaded into R and differential expression was tested using Wilcoxon rank sum statistics. We selected differentially expressed genes based on significance ($p \leq 0.01$, Mann-Whitney test), their mean expression values in at least one of the comparison groups (≥ 1 RPKM) and a minimum twofold expression difference. We converted all gene names using the HGNC helper package in R to facilitate comparisons with external datasets. GSEA analyses were done using the GSEA desktop application (Broad Institute). We performed analyses using the GSEA hallmark gene set collection and two curated HSC gene sets^{13, 15} using standard settings. Overlaps between EPCR⁺ associated genes and published HSC signatures were determined using the intersect command in R. Heat maps and clustering generated using the GENE-E (Broad Institute).

Gene expression Omnibus (GSO) Accession number

GSE77128

<http://www.ncbi.nlm.nih.gov/geo/query/acc.cgi?token=cfmxesswhfwnhkb&acc=GSE77128>

Construction of shEPCR lentiviral vectors

The MNDU-GFP -miRE vector was constructed by PCR amplification of a GFP-miR30 (shRenilla) cassette with EcoRI overhangs, and cloning into pCCL-c-MNDU3-eGFP (kindly provided by Donald Kohn²³), replacing the GFP cassette of the parental vector. GFP-miR is thus expressed from the MNDU promoter. The shRenilla-miR30 was converted to miRE by PCR as described by Fellman et al²⁴. A stuffer sequence was added between the XhoI and EcoRI sites (replacing the shRNA) to facilitate cloning of subsequent shRNAs.

Cloning of shRNAs for EPCR into the MNDU-GFP -miRE vector was performed as described by Fellmann et al²⁴, with minor modifications. Briefly, 97mer miR template oligos were amplified with common primers which add the XhoI and EcoRI restriction sites, using Phusion polymerase (Thermo Fisher Scientific Cat # *F-530*) supplemented with GC buffer and DMSO for 18 cycles. PCR products as well as MNDU-miRE-GFP vector were digested with FastDigest XhoI and EcoRI (Thermo Fisher Scientific Cat #FD0694 and FD0274, respectively), gel purified using the QIAQuick Gel extraction kit (Qiagen Cat #28704), then ligated together using T4 DNA ligase (Thermo Fisher Scientific Cat # [EL0011](#)) without addition of PEG 8000 to the ligase buffer, and transformed into Stbl4 bacteria by heat shock. Colonies were screened for multiple insertions by digestion with HpaI + EcoRI (Thermo Fisher Scientific, Cat # ER1031 and FD0274, respectively), then sequence verified. Oligonucleotide sequences for PCR amplification:

miRE-Xho-fw-long: TGTGTGTGTGTGAACCTCGAGAAGGTATATTGCTGTTGACAGT-GAGCG miRE-EcoRI-rev-long: TCTCTCTCTCTCTCGAATTCTAGCCCCTTGAAGTC-CGAGGCAGTAGGC

Templates from Fellman et al²⁴:

PROCR.1364 (shEPCR#1) TGCTGTTGACAGTGAGCGATGGTGGAAATGTAAAATC-CAATAGTGAAGCCACAGATGTATTGGATTTTACATTTCCACCACTGCCTACTG-CCTCGGA

PROCR.1240 (shEPCR#2) TGCTGTTGACAGTGAGCGCTCAAAGATATAACCAAATA-ATAGTGAAGCCACAGATGTATTATTGGTTATATCTTTTGAATGCCTACTGCCTCGGA

shEPCR lentiviral production:

HEK 293 cells were transfected with lenti-viral plasmid: 15 µg MNDU-GFP -miRE, packaging plasmids: 9 µg pLP1 and 4 µg pLP2 and envelope plasmid: 3 µg VSV-G using Lipofectamine

2000 (Thermo Fisher Scientific Cat #12566-014). Viral supernatant was collected after 48 hours and concentrated using PEG precipitation method (SBI, System Biosciences Cat # LV810A-1). Viral titers were determined to be $\sim 1 \times 10^9$ TU/ml using HEK293 cells.

Lentiviral transduction of OCI-AML5 cells

To validate EPCR knockdown, OCI-AML5 cells (DSMZ Cat #ACC 247) were used. As for any cell line imported in our laboratory, they were treated upon arrival for possible mycoplasma contamination. For viral transduction, the cells were pre-treated with protamine sulfate (10 μ g/ml) for 30 min at 37°C in 5% CO₂ before the viral supernatant was added for 16 hours at a MOI of 3. The transduced cells were then washed and cultured in the presence of vehicle (DMSO) or UM171 (250 nM) for 2 additional days. Transduction (assessed via GFP) and surface EPCR knockdown efficiency were measured by flow cytometry.

Lentiviral transduction of CD34⁺ CB cells

CD34⁺ cells were pre-stimulated for 24 hours in HSC expansion media. Cells were then transduced for 16 hours on retronectin (TaKaRa Cat #T100A) coated plates (20 μ g/cm²) at an MOI of 100 in HSC expansion media supplemented with polybrene (3 μ g/ml). Transduced CD34⁺ cells were washed and cultured in HSC expansion media in the presence of vehicle (DMSO) or UM171 (38nM). Transduction efficiency (assessed via GFP expression) and the expression of HSC cell surface markers were analyzed after 3 (Fig. 3.4) or 7 days (Fig. S3.7) post transduction.

shRNA transplantation assay

Outcome of 5 $\times 10^3$ CD34⁺ cells (d0 equivalent) cultured for 6 (Fig. 3.4) or 7 days (Fig. S3.7) post-transduction were transplanted by tail vein injection into sub-lethally irradiated (250 cGy, <24 hr before transplantation) 8 to 16 week-old female NSG (NOD-Scid IL2R γ null, Jackson Laboratory) mice. Bone marrow analysis was performed after 24 week post-transplantation to determine the percentage of human engraftment.

Statistical analysis

Statistical analyses of all in vitro experiments were done using GraphPad Prism v 6.01. Mann-Whitney test was used after confirming normal distribution to compare fold change between the conditions tested. Bars and error bars represent means or medians and s.d. or s.e.m., as specified.

Extreme limiting dilution analysis²⁵software (<http://bioinf.wehi.edu.au/software/elda/>) was used to estimate LT-HSC frequencies with 95% confidence intervals. Differences in LT-HSC frequencies were analyzed by Mann-Whitney test. $P < 0.05$ was considered significant.

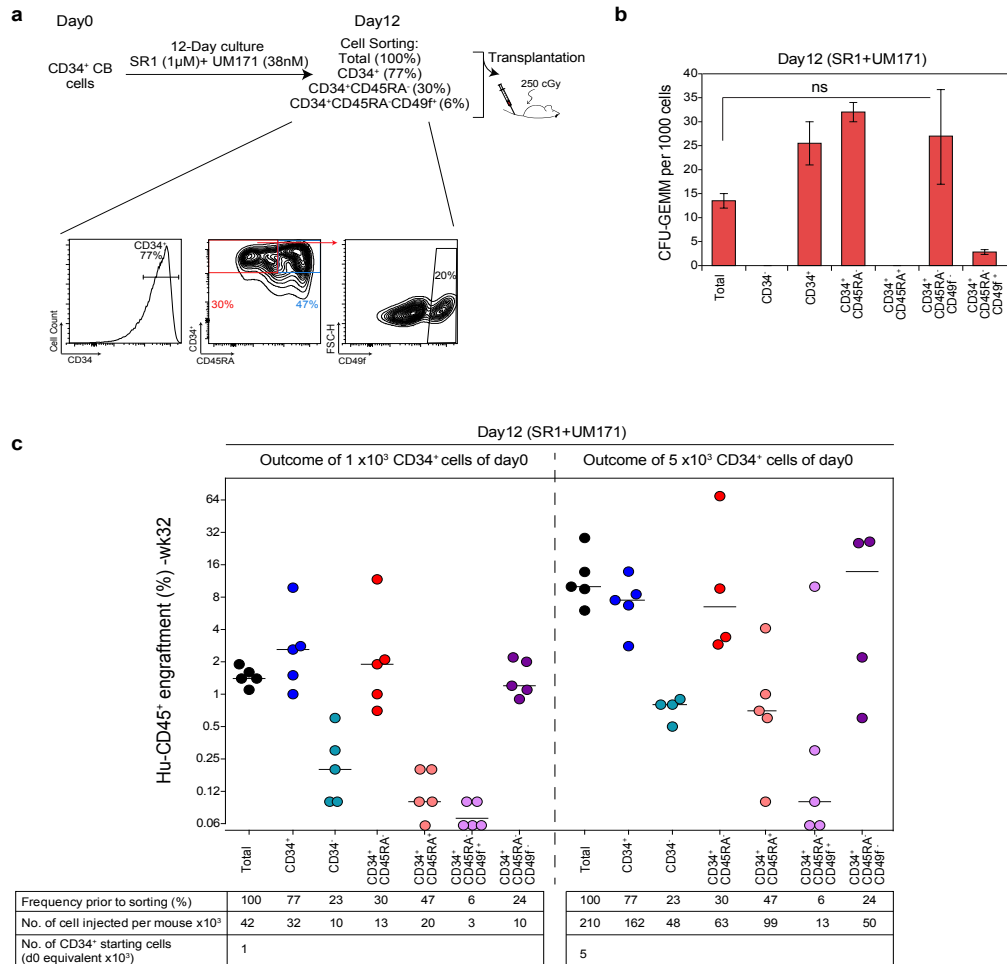


Fig. S3.1. Cultured CD49f^{high} CD34⁺CD45RA⁻ cells lack in vivo repopulation potential.

a, Schematic presentation of HSPC phenotype sort and transplantation strategy. CD34⁺ cord blood (CB) cells were expanded for 12 days in SR1(1 μM) + UM171(38 nM) before they were sorted for the indicated populations. **b**, CFU-GEMMs count for different cellular subsets after culture (mean ± s.d, n= 3 wells counted per condition, technical replicates). Comparison between various sorted populations to Total sorted cells is statistically significant difference unless specified ns: not significant (Mann-Whitney test, one-sided). **c**, Representative FACS purified populations were transplanted in NSG mice for outcome of 1 and 5x10³ CD34⁺ CB starting cell. Proportion of cultured cells transplanted for each cellular subset was adjusted based on their frequency at day12 and indicated in the table of panel (c). Bone marrow analysis was performed at 32 weeks post-transplantation (n=5 mice per condition, technical replicates). The horizontal bars indicate median values.

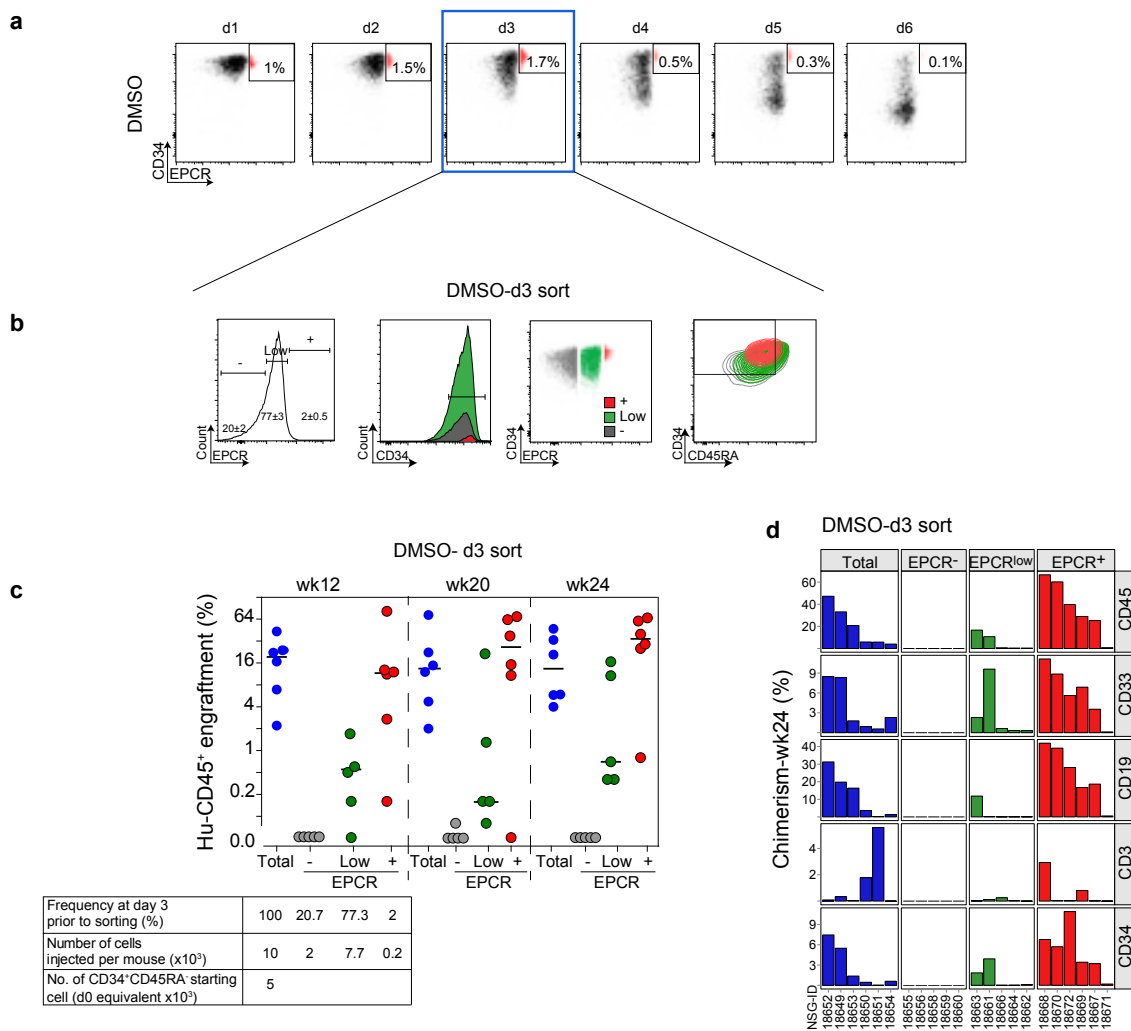


Fig. S3.2. EPCR is a universal surface marker for LT-HSC in culture.

a, CD34⁺CD45RA⁻ CB cells were cultured in DMSO for 6 days. FACS analysis of EPCR kinetic expression was monitored during the culture period where the highest level of EPCR was attained at day3. **b**, EPCR cell sorting scheme and phenotype after 3 day culture in DMSO controls (mean \pm s.d, 3 biological replicates). **(c, d)** Human (Hu) CD45 engraftment and lineage potential of the indicated sorted cells assessed in NSG mice at 12, 20, and 24 weeks post-transplantation; n= 5-6 mice per condition, technical replicates. The horizontal bars indicate median values.

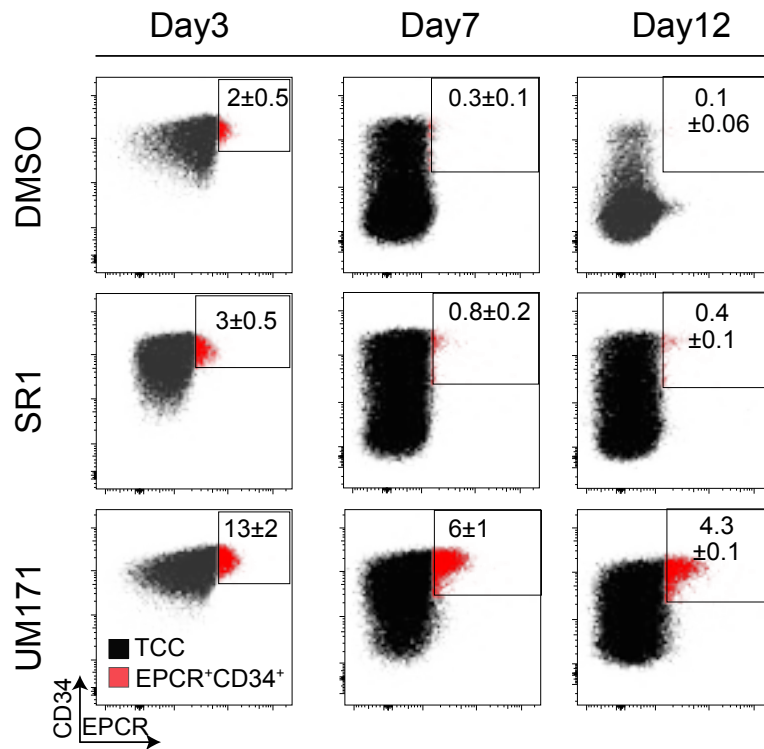


Fig. S3.3. CD34⁺ CB cells expanded with UM171 retain higher levels of EPCR surface marker expression than those expanded with SR1.

Representative flow cytometry plots of CD34 and EPCR of CD34⁺ CB cells after 3, 7 and 12 days in the presence of vehicle (DMSO), UM171 (38 nM), and SR1 (1000 nM) (mean ± s.d, 3 technical replicates).

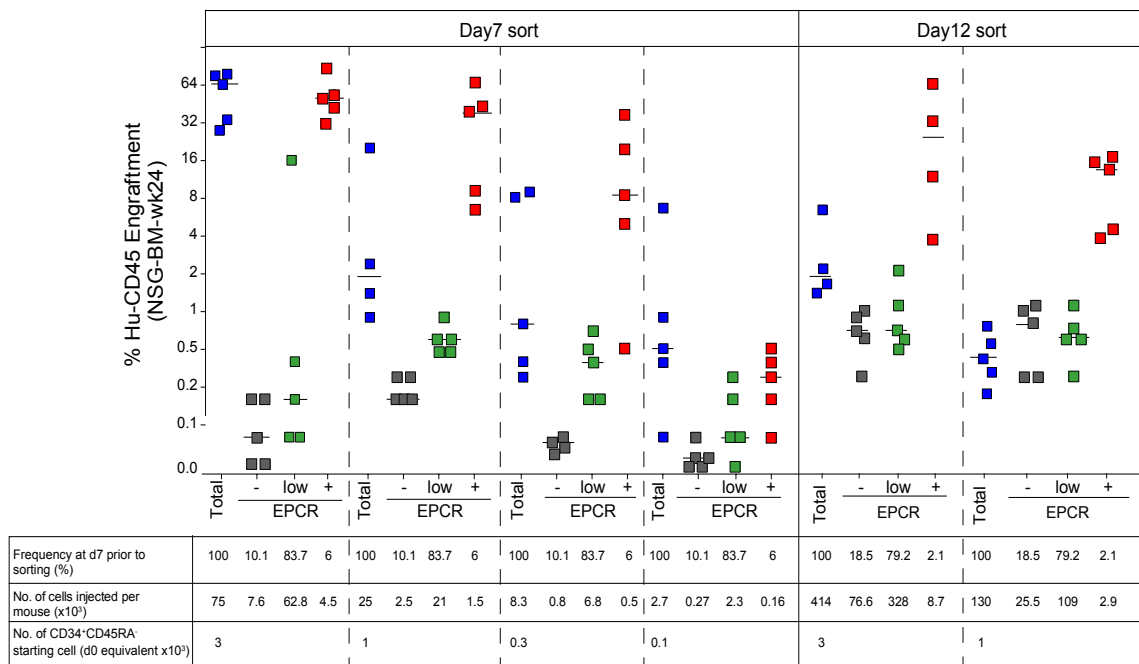


Fig. S3.4. Limit dilution assay performed on different EPCR cellular fractions (-, low, and +).

CD34⁺CD45RA⁻ (d0 starting) cells were cultured for 7 and 12 days in the presence of UM171. Cells then were sorted based on EPCR expression at the day of culture. Outcome of 4 and 2 doses of the d0 starting cells were used after 7 and 12 day culture, respectively. The sorted cells were injected in sublethally irradiated NSG mice (n=5 mice per dose, technical replicates). Levels of human (Hu) CD45 engraftment in NSG bone marrow (BM) at 24 weeks post-transplantation is shown. The horizontal bars indicate median values.

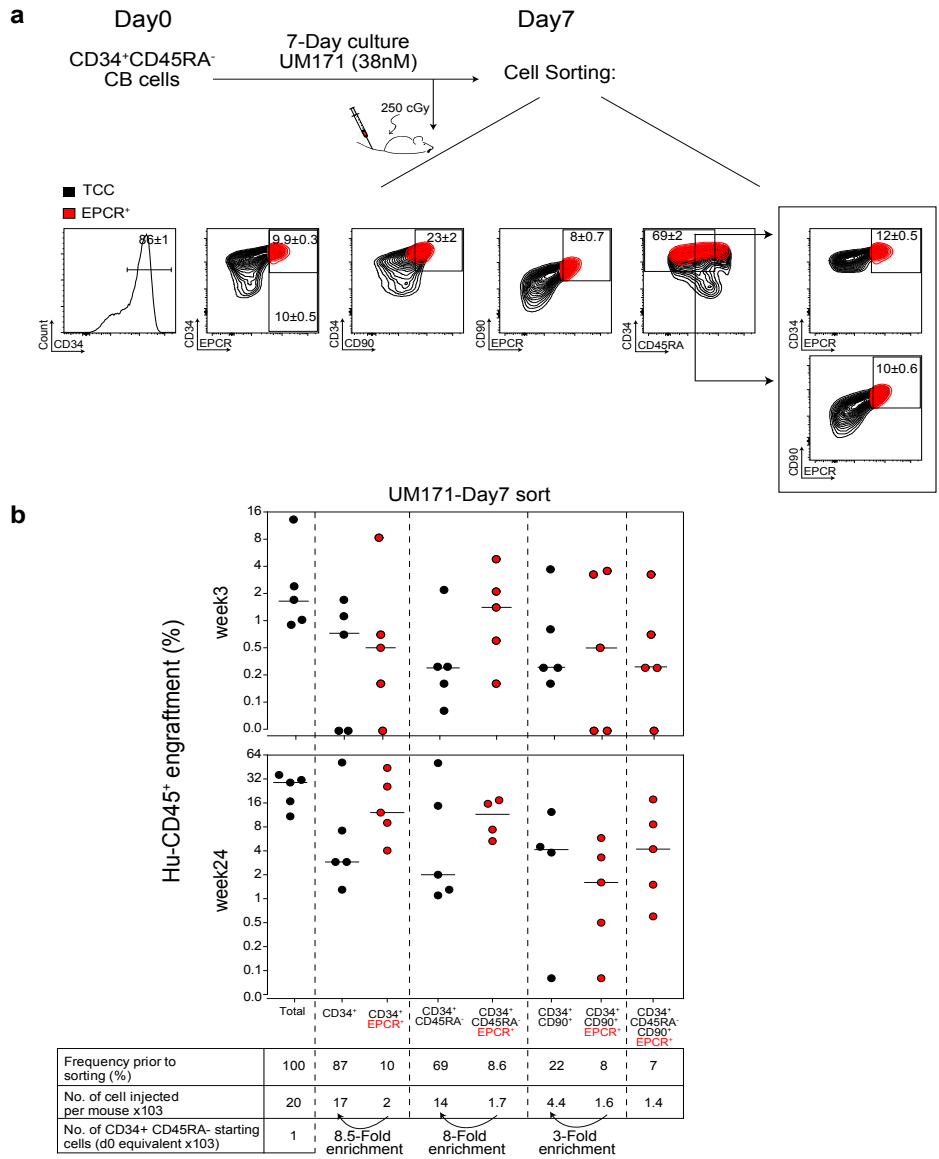
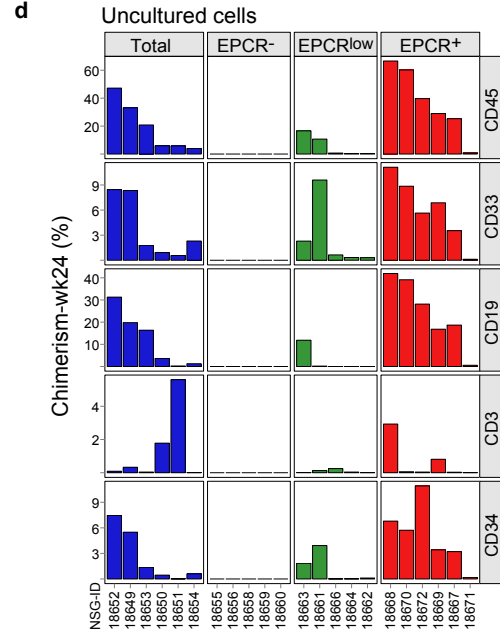
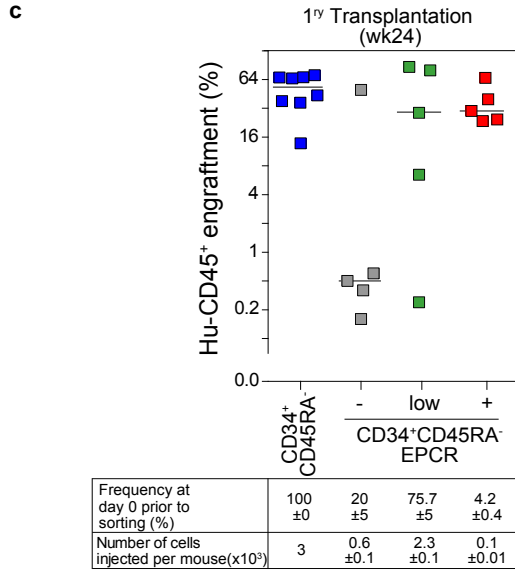
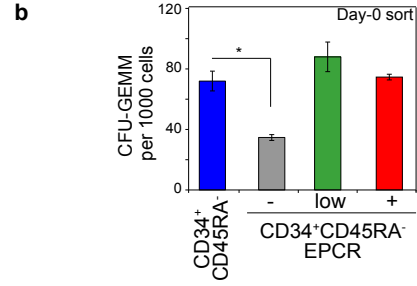
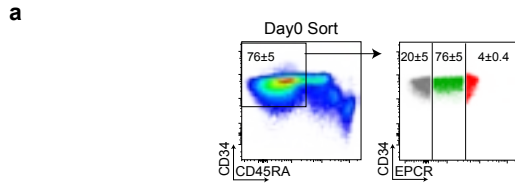


Fig. S3.5. In vivo proliferative outcome of different HSPC populations sorted after culture.

a, Schematic presentation of HSPC phenotype sort and transplantation strategy. CD34⁺CD45RA⁻ cord blood (CB) cells were expanded for 7 days in UM171 (38 nM) before they were sorted for the indicated HSPC population (mean ± s.d, 3 technical replicates). **b**, Respective HSPC populations based on their frequency at day 7 were sorted and transplanted in NSG mice for outcome of 1 x10³ CD34⁺ CD45RA⁻ CB starting cell. Bone marrow analysis was performed at 3 and 20 weeks post-transplantation to determine the short and long- term engraftment respectively; n=5 mice per condition, technical replicates. The horizontal bars indicate median values.



e

Sorted population (% at d0)	Cell dose at d0	Avg. Hu-CD45 (%) ± STD (wk24)	(E/T)	Frequency of LT-HSC at d0	
				Estimate	(95% confidence of interval)
CD34 ⁺ CD45RA ⁻ (100%)	3000 1000 333 111 37	50±19 27±19 3.1±4.6 0.5±0.9 1.3±3.3	(8/8) (13/13) (8/8) (3/7) (1/8)	142	(260 ; 78)
CD34 ⁺ CD45RA ⁻ EPCR ⁻ (4.2%)	138 46 39	36.6±16 0.4±0.6 2.3±4.5	(5/5) (3/5) (3/5)	42	(84 ; 20)
CD34 ⁺ CD45RA ⁻ EPCR ^{low} (76%)	2118 808 706	40±35 6.8±6 3.8±5.5	(5/5) (4/4) (5/5)	>706	
CD34 ⁺ CD45RA ⁻ EPCR ⁺ (20%)	739 246 152	10.5±20 0.2±0.1 0.1±0.1	(5/5) (5/5) (2/5)	144	(302 ; 69)

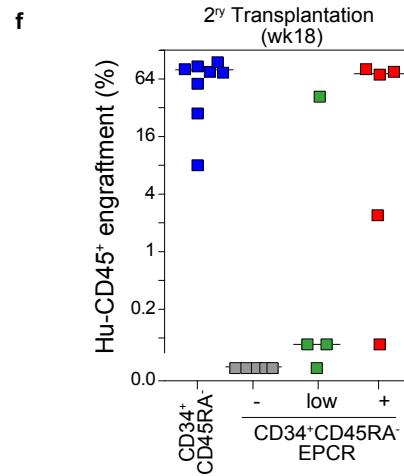


Fig. S3.6. Uncultured EPCR^{low} and EPCR⁺ population are the fractions enriched with LT-HSC.

a, FACS representation of different EPCR subsets sorted from uncultured CD34⁺CD45RA⁻ cells. **b**, CFU-GEMMs count per 1x10³ sorted population described in (a) (mean ± s.d, n= 3 wells counted per condition of 2 biological replicates); significance level *P<0.05 (Mann-Whitney test, one-sided). **c, d**, Human (Hu) CD45 engraftment and lineage potential of the sorted cells assessed in NSG mice at 24 weeks post-transplantation, (n=5-8 mice per dose, technical replicates). **e**, Summary of limit dilution analysis of uncultured CD34⁺CD45RA⁻ and CD34⁺CD45RA⁻ EPCR⁻, low, and + populations. Different doses of the indicated sorted population were transplanted in sublethally irradiated NSG recipients (n= 5-13 mice per dose). Twenty four weeks post-transplantations, the mice were sacrificed and the bone marrow cells were collected and checked for Hu-CD45 engraftment. The number of engrafted / transplanted mice (E/T) with the average of human (Hu) CD45 reconstitution is shown. The estimated LT-HSC frequency for each population is presented as 1/ number of sorted cells. The estimated frequency of CD34⁺CD45RA⁻ EPCR^{low} could not be exactly determined since all the mice were positive for Hu-CD45 reconstitution. **f**, Primary NSG recipients injected with uncultured indicated population were sacrificed at 24 weeks post-transplantation (n=5 mice, technical replicates). Eighty percent of the collected bone marrow cells from the 1ry NSG recipients presented in (c) were transplanted into 2ry recipients. Human (Hu) CD45 cell chimerism was analyzed in the secondary mice at 18 weeks post-transplantation by flow cytometry.

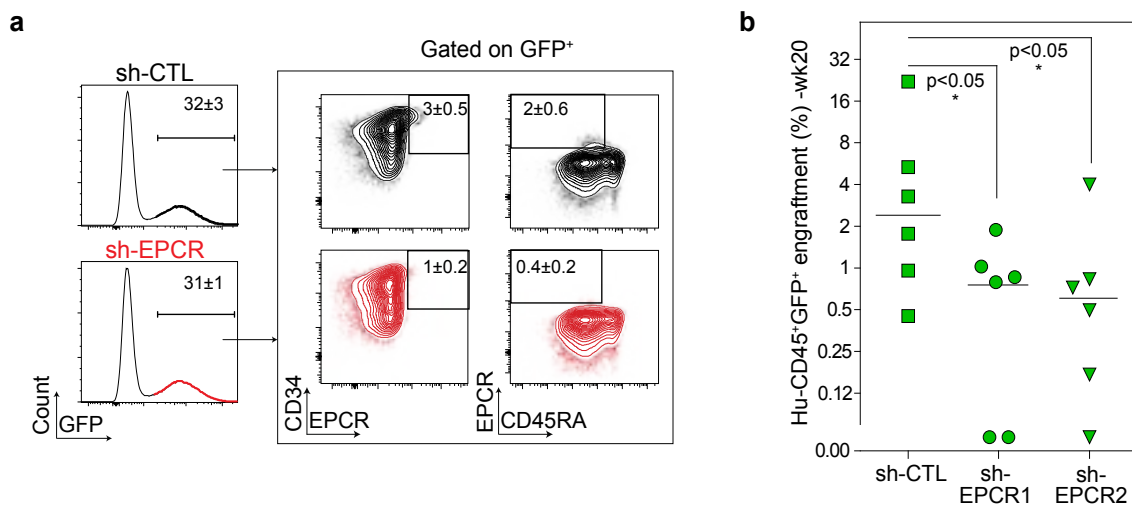


Fig. S3.7. Loss of EPCR expression in CD34⁺ cells compromise their engraftment ability in NSG mice.

a, Pre-stimulated CD34⁺ CB cells were infected with lentiviral sh-EPCR-GFP (sh1 or 2) vs controls (sh-Renilla) at MOI 100 for 16 hours. Transduced cells were washed and expanded in the presence of UM171 (38 nM) for a total of 8 day-culture. FACS analysis was then performed to assess the EPCR knockdown in GFP⁺ cells (mean ± s.d, n= 3 technical replicates). **b**, Human (Hu)-CD45 engraftment in GFP⁺ populations in bone marrow of NSG at 20 weeks post-transplantation (n=4-5 mice per condition, technical replicates). Two different sh-EPCR are shown. The horizontal bars indicate median values, significance level *P<0.5 (Mann-Whitney test, one-sided).

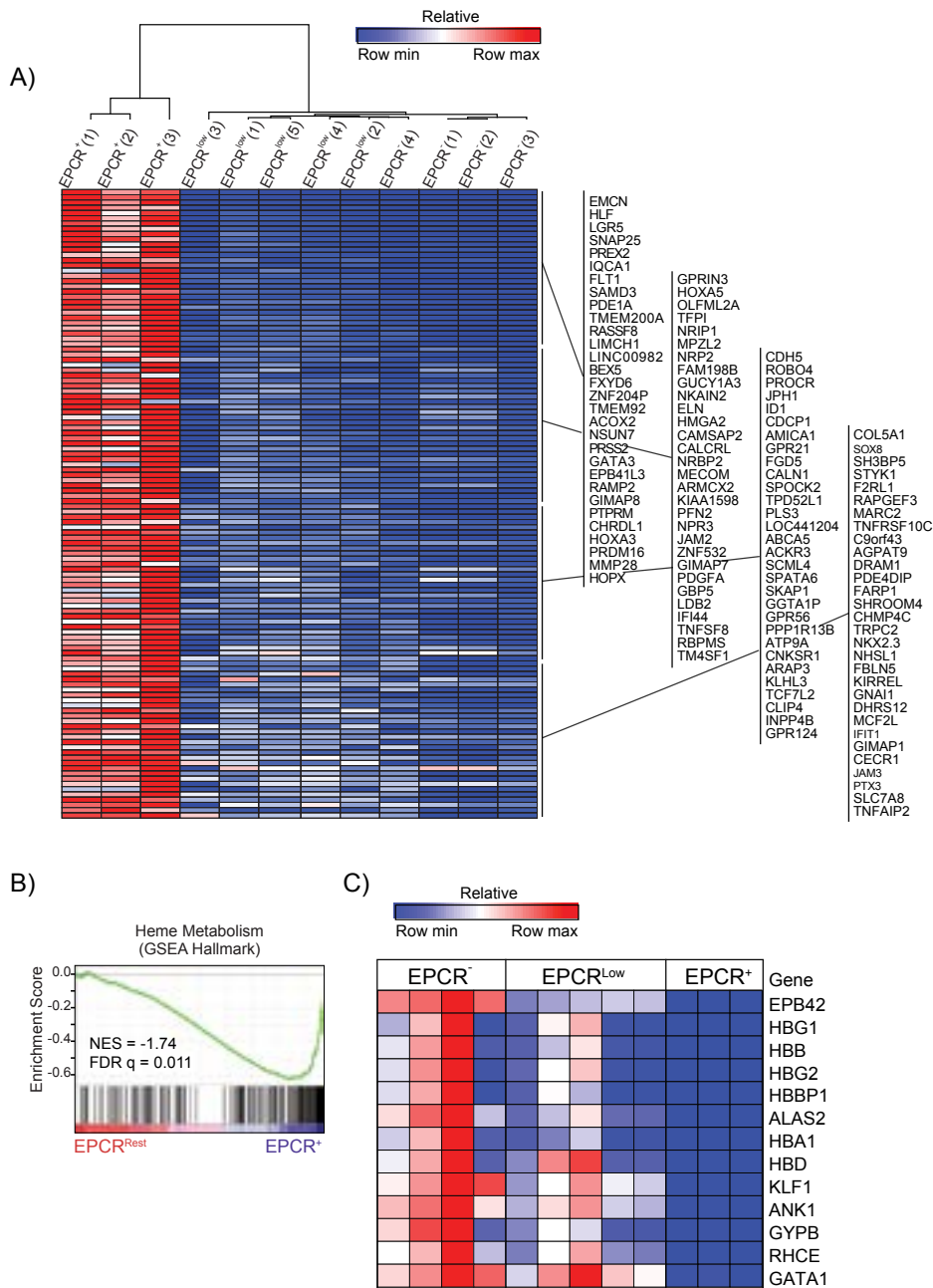


Fig. S3.8. EPCR⁺ population shares genetic features with highly purified primitive hematopoietic cells.

a, Heat map showing relative expression patterns of 120 common up-regulated genes in EPCR⁺ population, CD34⁺CD38^{low/-}CD90⁺ fetal liver (FL) cells, and CD34⁺CD38⁻ FL and cord blood cells. **b**, GSEA plot shows downregulation of hemoglobin levels. **c**, Heat map showing marked suppression of transcripts associated with erythroid development/differentiation in EPCR⁺ cells.

wk12 (BM aspiration)									
Sorted population	NSG-ID	Percentages at d0	Sorted cells transplanted at d0 per NSG	%CD45	%CD33	%CD19	%CD3	%CD34	
1,000 CD34+CD45RA- at day0									
Day0 CD34+ CD45RA-	17089	100	1,000	12.2	2.54	4.61	0.01	0.49	
Day0 CD34+ CD45RA-	17090			5.7	3.00	1.24	0.02	0.33	
Day0 CD34+ CD45RA-	17091			9.7	2.89	3.54	0.01	0.37	
Day0 CD34+ CD45RA-	17092			5.2	2.46	1.34	0.01	0.34	
Day0 CD34+ CD45RA-	17093			8.2	2.97	2.89	0.02	0.69	
1,000 CD34+CD45RA- at day7									
Sorted population	NSG-ID	Percentages at d0	Sorted cells transplanted at d0 per NSG	%CD45	%CD33	%CD19	%CD3	%CD34	
Day0 CD34+ CD45RA-	17570	100	1,000	8.2	2.08	5.56	0.02	0.45	
Day0 CD34+ CD45RA-	17572			77.9	4.44	66.14	0.00	4.91	
Day0 CD34+ CD45RA-	17574			5.9	2.02	3.06	0.01	0.37	
Day0 CD34+ CD45RA-	17571			5.2	2.31	2.59	0.02	0.36	
Day0 CD34+ CD45RA-	17575			16.5	3.98	11.09	0.02	0.74	
Day0 CD34+ CD45RA-	17576			6.9	1.22	5.39	0.01	0.10	
Day0 CD34+ CD45RA-	17573			4.3	0.61	3.41	0.01	0.05	
Outcome of 1,000 CD34+CD45RA- at day7									
Sorted population	NSG-ID	Percentages at d7	Sorted cells transplanted at d7 per NSG	%CD45	%CD33	%CD19	%CD3	%CD34	
Day7 EPCR+	16772	2.2	440	0.8	0.17	0.34	0.00	0.00	
Day7 EPCR+	16773			69.5	9.04	40.31	0.00	0.00	
Day7 EPCRlow	16774	82.3	16,460	2.3	2.17	0.04	0.00	0.00	
Day7 EPCRlow	16775			0.8	0.33	0.02	0.26	0.00	
Day7 EPCR-	16776	15.4	3,080	0.0	0.00	0.00	0.00	0.00	
Day7 EPCR-	16777			0.1	0.02	0.00	0.01	0.00	
1,000 CD34+CD45RA- at day7									
Sorted population	NSG-ID	Percentages at d7	Sorted cells transplanted at d7 per NSG	%CD45	%CD33	%CD19	%CD3	%CD34	
Day7 Total	17109	100	35,294	0.7	0.00	0.14	0.28	0.00	
Day7 Total	17110			3.6	2.97	0.16	0.05	0.27	
Day7 Total	17111			8.6	3.16	1.66	0.00	1.36	
Day7 Total	17112			14.5	13.49	0.51	0.00	0.68	
Day7 Total	17113			20.7	24.00	1.37	0.50	5.46	
Day7 EPCR+	17124	2	847	3.8	2.01	1.14	0.00	0.14	
Day7 EPCR+	17125			3.1	0.53	2.26	0.01	0.03	
Day7 EPCR+	17126			1.8	0.50	0.91	0.00	0.07	
Day7 EPCR+	17127			0.4	0.23	0.08	0.01	0.03	
Day7 EPCR+	17128			82.1	10.02	54.84	0.41	1.64	
Day7 EPCRlow	17119	87	30,706	0.1	0.09	0.00	0.01	0.00	
Day7 EPCRlow	17120			0.2	0.20	0.00	0.01	0.00	
Day7 EPCRlow	17121			0.6	0.30	0.19	0.02	0.02	
Day7 EPCRlow	17122			5.5	1.38	3.15	0.01	0.08	
Day7 EPCRlow	17123			0.1	0.08	0.01	0.01	0.00	
Day7 EPCR-	17114	10	3,600	0.0	0.00	0.00	0.00	0.00	
Day7 EPCR-	17115			0.0	0.00	0.00	0.00	0.00	
Day7 EPCR-	17116			0.0	0.00	0.00	0.00	0.00	
Day7 EPCR-	17117			0.0	0.00	0.00	0.00	0.00	
Day7 EPCR-	17118			0.0	0.00	0.00	0.00	0.00	
1,000 CD34+CD45RA- at day7									
Sorted population	NSG-ID	Percentages at d7	Sorted cells transplanted at d7 per NSG	%CD45	%CD33	%CD19	%CD3	%CD34	
Day7 Total	17639	100	25,000	9.9	5.67	3.55	0.04	0.37	
Day7 Total	17638			1.0	0.47	0.49	0.02	0.01	
Day7 Total	17637			2.6	0.22	2.20	0.01	0.02	
Day7 Total	17640			1.9	0.50	1.30	0.01	0.01	
Day7 Total	17641			15.3	2.56	8.31	3.14	0.18	
Day7 EPCR+	17665	6	1,500	22.2	6.04	13.59	0.00	0.89	
Day7 EPCR+	17664			47.0	10.29	34.17	0.00	1.03	
Day7 EPCR+	17663			55.4	3.93	46.65	0.00	2.33	
Day7 EPCR+	17666			2.9	0.14	2.44	0.00	0.04	
Day7 EPCR+	17662			1.9	0.33	1.44	0.00	0.01	
Day7 EPCRlow	17687	83.7	20,925	0.4	0.37	0.01	0.00	0.00	
Day7 EPCRlow	17689			0.1	0.09	0.00	0.00	0.00	
Day7 EPCRlow	17690			0.2	0.17	0.01	0.00	0.00	
Day7 EPCRlow	17691			0.3	0.28	0.01	0.00	0.00	
Day7 EPCRlow	17688			0.2	0.17	0.01	0.00	0.00	
Day7 EPCR-	17718	10.1	2,525	0.1	0.06	0.00	0.00	0.00	
Day7 EPCR-	17721			0.0	0.00	0.00	0.00	0.00	
Day7 EPCR-	17719			0.0	0.00	0.00	0.00	0.00	
Day7 EPCR-	17720			0.0	0.00	0.00	0.00	0.00	
Day7 EPCR-	17717			0.0	0.00	0.00	0.00	0.00	
1,000 CD34+CD45RA- at day7									
Sorted population	NSG-ID	Percentages at d7	Sorted cells transplanted at d7 per NSG	%CD45	%CD33	%CD19	%CD3	%CD34	
Day7 Total	18026	100	23,000	5.3	0.52	4.20	0.01	0.03	
Day7 Total	18027			0.6	0.30	0.21	0.00	0.05	
Day7 Total	18028			2.6	1.35	0.99	0.01	0.05	
Day7 Total	18029			0.7	0.37	0.24	0.00	0.04	
Day7 Total	18030			12.0	0.62	9.61	0.00	0.20	
Day7 EPCR+	18031	6	1,380	41.1	9.86	23.39	0.00	4.36	
Day7 EPCR+	18032			D/D					
Day7 EPCR+	18033			2.2	1.18	0.72	0.00	0.07	
Day7 EPCR+	18034			0.1	0.02	0.06	0.00	0.00	
Day7 EPCR+	18035			1.9	0.19	1.50	0.00	0.01	
Day7 EPCRlow	18036	83	19,091	0.4	0.39	0.00	0.00	0.01	
Day7 EPCRlow	18037			0.2	0.19	0.00	0.01	0.00	
Day7 EPCRlow	18038			0.2	0.19	0.00	0.00	0.00	
Day7 EPCRlow	18039			0.4	0.39	0.00	0.01	0.00	
Day7 EPCRlow	18040			0.5	0.49	0.00	0.00	0.00	
Day7 EPCR-	18041	11	2,530	0.0	0.00	0.00	0.00	0.00	
Day7 EPCR-	18042			0.1	0.10	0.00	0.00	0.00	
Day7 EPCR-	18043			0.0	0.00	0.00	0.00	0.00	
Day7 EPCR-	18044			0.3	0.30	0.00	0.00	0.00	
Day7 EPCR-	18045			0.0	0.00	0.00	0.00	0.00	
1,000 CD34+CD45RA- at day7									
Sorted population	NSG-ID	Percentages at d7	Sorted cells transplanted at d7 per NSG	%CD45	%CD33	%CD19	%CD3	%CD34	
Day7 Total	18402	100	20,000	10.2	2.61	6.50	0.01	0.12	
Day7 Total	18403			3.2	1.78	0.89	0.01	0.16	
Day7 Total	18404			4.9	1.18	3.25	0.00	0.04	
Day7 Total	18405			1.3	0.20	0.99	0.00	0.01	
Day7 Total	18406			5.4	1.97	2.96	0.01	0.09	
Day7 EPCR+	18412	10.4	2,080	6.1	1.32	4.15	0.00	0.08	
Day7 EPCR+	18413			1.1	0.27	0.71	0.01	0.01	
Day7 EPCR+	18414			3.2	1.50	1.29	0.00	0.13	
Day7 EPCR+	18415			7.0	2.56	3.84	0.01	0.22	
Day7 EPCR+	18416			1.1	0.35	0.59	0.02	0.06	

Table S3.1: Bone marrow aspiration data of NSG mice injected with different EPCR subsets sorted at day7 from UM171 cultures (page 1/3).

wk24 (BM Flush)									
1,000 CD34+CD45RA - at day0	Sorted population	NSG-ID	Percentages at d0	Sorted cells transplanted at d0 per NSG	%CD45	%CD33	%CD19	%CD3	%CD34
	Day0 CD34+ CD45RA-	17089		100	1,000	24.8	3.10	19.27	0.02
Day0 CD34+ CD45RA-	17090				31.6	5.69	21.65	0.06	1.67
Day0 CD34+ CD45RA-	17091				33.5	5.26	24.89	0.03	2.18
Day0 CD34+ CD45RA-	17092				40.2	11.50	25.08	0.12	1.53
Day0 CD34+ CD45RA-	17093				1.3	0.88	0.32	0.06	0.05
Sorted population	NSG-ID	Percentages at d0	Sorted cells transplanted at d0 per NSG	%CD45	%CD33	%CD19	%CD3	%CD34	
Day0 CD34+ CD45RA-	17570		100	1,000	54.8	10.03	32.93	1.32	3.23
Day0 CD34+ CD45RA-	17572				50.8	5.79	33.58	1.02	4.88
Day0 CD34+ CD45RA-	17574				48.6	14.48	19.68	0.10	8.21
Day0 CD34+ CD45RA-	17571				33.2	7.54	16.10	0.00	1.49
Day0 CD34+ CD45RA-	17575				12.7	2.46	8.18	0.05	0.99
Day0 CD34+ CD45RA-	17576				8.8	0.34	5.02	2.24	0.31
Day0 CD34+ CD45RA-	17573				3.4	0.53	2.63	0.00	0.01
Outcome of 1,000 CD34+CD45RA - at day7	Sorted population	NSG-ID	Percentages at d7	Sorted cells transplanted at d7 per NSG	%CD45	%CD33	%CD19	%CD3	%CD34
	Day7 EPCR+	16772	2.2	440	26.4	8.45	6.07	0.05	0.50
Day7 EPCR+	16773				4.0	1.30	0.09	1.70	0.00
Day7 EPCRlow	16774	82.3	16,460		9.8	9.61	0.02	0.01	0.00
Day7 EPCRlow	16775				0.7	0.62	0.00	0.05	0.00
Day7 EPCR-	16776	15.4	3,080		0.8	0.78	0.00	0.00	0.00
Day7 EPCR-	16777				0.9	0.88	0.00	0.00	0.00
Sorted population	NSG-ID	Percentages at d7	Sorted cells transplanted at d7 per NSG	%CD45	%CD33	%CD19	%CD3	%CD34	
Day7 Total	17109		100	35,294	22.5	4.14	16.72	0.27	0.25
Day7 Total	17110				18	7.61	6.28	1.31	0.70
Day7 Total	17111				2	1.09	0.03	0.64	0.02
Day7 Total	17112				2.6	1.76	0.65	0.05	0.06
Day7 Total	17113				23	7.25	11.25	0.18	2.12
Day7 EPCR+	17124	2	847		11.9	2.14	8.82	0.02	0.77
Day7 EPCR+	17125				12.2	1.74	9.52	0.04	0.38
Day7 EPCR+	17126				5.9	0.07	0.12	4.35	0.02
Day7 EPCR+	17127				22.9	5.18	15.05	0.02	1.74
Day7 EPCR+	17128				47.3	5.91	36.28	0.05	2.37
Day7 EPCRlow	17119	87	30,706		0.4	0.38	0.01	0.07	0.01
Day7 EPCRlow	17120				0.6	0.57	0.01	0.11	0.01
Day7 EPCRlow	17121				0.5	0.44	0.03	0.14	0.02
Day7 EPCRlow	17122				36.1	9.93	21.55	0.79	4.33
Day7 EPCRlow	17123				0.9	0.85	0.02	0.26	0.05
Day7 EPCR-	17114	10	3,600		0.2	0.16	0.01	0.01	0.01
Day7 EPCR-	17115				0.1	0.09	0.00	0.00	0.00
Day7 EPCR-	17116				0.1	0.08	0.01	0.01	0.01
Day7 EPCR-	17117				0.1	0.07	0.00	0.00	0.01
Day7 EPCR-	17118				0.1	0.09	0.00	0.00	0.01
Sorted population	NSG-ID	Percentages at d7	Sorted cells transplanted at d7 per NSG	%CD45	%CD33	%CD19	%CD3	%CD34	
Day7 Total	17639		100	25,000	20.2	9.82	8.32	0.28	0.97
Day7 Total	17638				2.4	1.81	0.48	0.00	0.03
Day7 Total	17637				1.4	1.36	0.03	0.00	0.02
Day7 Total	17640				0.9	0.88	0.00	0.02	0.01
Day7 Total	17641				DCD				
Day7 EPCR+	17665	6	1,500		67.2	13.04	44.76	0.13	2.28
Day7 EPCR+	17664				43.3	4.94	32.73	0.00	2.04
Day7 EPCR+	17663				39.4	5.63	27.62	0.63	2.32
Day7 EPCR+	17666				9.2	1.23	6.39	0.00	0.13
Day7 EPCR+	17662				6.5	1.51	4.11	0.00	0.19
Day7 EPCRlow	17687	83.7	20,925		0.9	0.90	0.00	0.00	0.02
Day7 EPCRlow	17689				0.6	0.60	0.00	0.00	0.01
Day7 EPCRlow	17690				0.6	0.60	0.00	0.00	0.01
Day7 EPCRlow	17691				0.5	0.49	0.00	0.00	0.01
Day7 EPCRlow	17688				0.5	0.49	0.01	0.00	0.02
Day7 EPCR-	17716	10.1	2,525		0.3	0.30	0.00	0.00	0.01
Day7 EPCR-	17721				0.3	0.30	0.00	0.00	0.01
Day7 EPCR-	17719				0.2	0.20	0.00	0.00	0.00
Day7 EPCR-	17720				0.2	0.20	0.00	0.00	0.00
Day7 EPCR-	17717				0.2	0.20	0.00	0.00	0.00
Sorted population	NSG-ID	Percentages at d7	Sorted cells transplanted at d7 per NSG	%CD45	%CD33	%CD19	%CD3	%CD34	
Day7 Total	18026		100	23,000	1.5	0.11	1.28	0.00	0.00
Day7 Total	18027				5.3	0.18	4.61	0.01	0.08
Day7 Total	18028				11.7	1.09	9.37	0.00	0.20
Day7 Total	18029				11.9	3.13	7.33	0.01	0.24
Day7 Total	18030				48.1	2.69	39.35	0.05	0.96
Day7 EPCR+	18031	6	1,380		3.7	0.60	2.43	0.00	0.19
Day7 EPCR+	18032				DCD				
Day7 EPCR+	18033				1.0	0.84	0.14	0.00	0.02
Day7 EPCR+	18034				2.6	0.03	2.22	0.00	0.01
Day7 EPCR+	18035				3.6	0.13	3.08	0.00	0.03
Day7 EPCRlow	18036	83	19,091		0.2	0.18	0.01	0.00	0.00
Day7 EPCRlow	18037				0.1	0.10	0.00	0.00	0.00
Day7 EPCRlow	18038				0.1	0.10	0.00	0.00	0.00
Day7 EPCRlow	18039				0.2	0.19	0.00	0.01	0.00
Day7 EPCRlow	18040				0.1	0.10	0.00	0.00	0.00
Day7 EPCR-	18041	11	2,530		0.0	0.00	0.00	0.00	0.00
Day7 EPCR-	18042				0.0	0.00	0.00	0.00	0.00
Day7 EPCR-	18043				DCD				
Day7 EPCR-	18044				0.1	0.09	0.00	0.00	0.00
Day7 EPCR-	18045				0.0	0.00	0.00	0.00	0.00
Sorted population	NSG-ID	Percentages at d7	Sorted cells transplanted at d7 per NSG	%CD45	%CD33	%CD19	%CD3	%CD34	
Day7 Total	18402		100	20,000	32.5	8.26	21.52	0.11	0.35
Day7 Total	18403				35.0	10.26	22.19	0.01	0.31
Day7 Total	18404				40.5	3.16	34.26	0.04	0.50
Day7 Total	18405				18.9	1.91	15.63	0.00	0.24
Day7 Total	18406				12.2	2.37	8.88	0.07	0.09
Day7 EPCR+	18412	10.4	2,080		12.1	2.57	8.55	0.10	0.11
Day7 EPCR+	18413				3.8	1.06	2.48	0.03	0.03
Day7 EPCR+	18414				44.0	13.99	26.05	0.02	0.64
Day7 EPCR+	18415				25.7	8.43	14.57	0.02	0.47
Day7 EPCR+	18416				9.0	5.81	0.36	0.95	0.19

Table S3.1: Bone marrow aspiration data of NSG mice injected with different EPCR subsets sorted at day7 from UM171 cultures (page 2/3).

wk12 (BM aspiration)									
Outcome of 1,000 CD34+CD45RA- at day12	Sorted population	NSG-ID	Percentages at d12	Sorted cells transplanted at d12 per NSG	%CD45	%CD33	%CD19	%CD3	%CD34
	Day12 Total	17159	100	150,000	5.7	1.00	3.50	0.33	0.01
	Day12 Total	17160			0.7	0.39	0.26	0.03	0.00
	Day12 Total	17161			1.3	0.67	0.20	0.34	0.02
	Day12 EPCR+	17168	1.2	1,800	3.5	0.96	2.10	0.01	0.04
	Day12 EPCR+	17169			3.0	1.22	1.46	0.01	0.11
	Day12 EPCR+	17170			8.7	0.32	7.57	0.01	0.09
	Day12 EPCRlow	17165	87.2	130,800	0.3	0.28	0.01	0.05	0.00
	Day12 EPCRlow	17166			1.0	0.98	0.01	0.19	0.01
	Day12 EPCRlow	17167			0.2	0.19	0.00	0.02	0.00
	Day12 EPCR-	17162	11.5	17,250	0.1	0.08	0.00	0.01	0.00
	Day12 EPCR-	17163			0.1	0.10	0.00	0.01	0.00
	Day12 EPCR-	17164			0.1	0.10	0.00	0.03	0.00
	Sorted population	NSG-ID	Percentages at d12	Sorted cells transplanted at d12 per NSG	%CD45	%CD33	%CD19	%CD3	%CD34
	Day12 Total	17770	100	138,000	0.5	0.30	0.10	0.06	0.01
	Day12 Total	17767			0.7	0.46	0.11	0.07	0.01
	Day12 Total	17768			0.1	0.08	0.00	0.01	0.00
	Day12 Total	17771			0.3	0.20	0.06	0.01	0.00
	Day12 Total	17769			0.7	0.47	0.17	0.02	0.01
	Day12 EPCR+	17737	2.1	2,898	74.3	25.48	39.16	0.07	3.57
	Day12 EPCR+	17738			1.1	0.23	0.56	0.01	0.04
	Day12 EPCR+	17740			0.3	0.11	0.13	0.01	0.01
	Day12 EPCR+	17741			2.3	0.72	1.05	0.00	0.04
	Day12 EPCR+	17739			2.4	1.08	1.00	0.02	0.03
Day12 EPCRlow	17749	79.2	109,296	0.6	0.54	0.01	0.11	0.02	
Day12 EPCRlow	17748			0.2	0.18	0.00	0.02	0.00	
Day12 EPCRlow	17750			0.2	0.18	0.00	0.02	0.00	
Day12 EPCRlow	17751			0.3	0.29	0.00	0.03	0.00	
Day12 EPCRlow	17747			0.1	0.08	0.00	0.01	0.00	
Day12 EPCR-	17761	18.5	25,530	0.2	0.18	0.00	0.03	0.01	
Day12 EPCR-	17758			0.5	0.46	0.00	0.03	0.01	
Day12 EPCR-	17760			0.2	0.19	0.00	0.02	0.00	
Day12 EPCR-	17757			0.1	0.08	0.00	0.01	0.00	
Day12 EPCR-	17759			0.1	0.08	0.00	0.01	0.00	

wk24 (BM Flush)									
Outcome of 1,000 CD34+CD45RA- at day12	Sorted population	NSG-ID	Percentages at d12	Sorted cells transplanted at d12 per NSG	%CD45	%CD33	%CD19	%CD3	%CD34
	Day12 Total	17159	100	150,000	27.3	4.01	20.53	0.22	1.72
	Day12 Total	17160			3.8	1.19	2.03	0.22	0.10
	Day12 Total	17161			7.7	0.29	0.46	5.95	0.02
	Day12 EPCR+	17168	1.2	1,800	0.5	0.28	0.17	0.01	0.01
	Day12 EPCR+	17169			2.5	0.99	1.16	0.03	0.20
	Day12 EPCR+	17170			39.8	5.13	26.71	0.16	6.21
	Day12 EPCRlow	17165	87.2	130,800	0.9	0.86	0.01	0.23	0.04
	Day12 EPCRlow	17166			1.6	1.54	0.02	0.40	0.05
	Day12 EPCRlow	17167			4.3	1.63	1.70	0.22	0.22
	Day12 EPCR-	17162	11.5	17,250	0.3	0.27	0.01	0.06	0.01
	Day12 EPCR-	17163			0.3	0.25	0.01	0.10	0.01
	Day12 EPCR-	17164			0.2	0.17	0.01	0.06	0.01
	Sorted population	NSG-ID	Percentages at d12	Sorted cells transplanted at d12 per NSG	%CD45	%CD33	%CD19	%CD3	%CD34
	Day12 Total	17770	100	138,000	0.7	0.62	0.07	0.00	0.01
	Day12 Total	17767			0.5	0.50	0.00	0.00	0.00
	Day12 Total	17768			0.4	0.40	0.00	0.00	0.01
	Day12 Total	17771			0.3	0.30	0.00	0.00	0.01
	Day12 Total	17769			0.2	0.20	0.00	0.00	0.00
	Day12 EPCR+	17737	2.1	2,898	16.9	1.64	12.32	0.69	0.74
	Day12 EPCR+	17738			15.2	1.49	3.85	9.21	0.12
	Day12 EPCR+	17740			13.4	5.65	6.54	0.00	0.71
	Day12 EPCR+	17741			4.5	3.73	0.60	0.00	0.44
	Day12 EPCR+	17739			3.8	2.60	0.82	0.19	0.23
Day12 EPCRlow	17749	79.2	109,296	1.1	1.09	0.00	0.00	0.02	
Day12 EPCRlow	17748			0.7	0.70	0.00	0.00	0.01	
Day12 EPCRlow	17750			0.6	0.60	0.00	0.00	0.01	
Day12 EPCRlow	17751			0.6	0.60	0.00	0.00	0.01	
Day12 EPCRlow	17747			0.3	0.30	0.00	0.01	0.01	
Day12 EPCR-	17761	18.5	25,530	1.1	1.09	0.00	0.00	0.02	
Day12 EPCR-	17758			1.0	1.00	0.00	0.00	0.04	
Day12 EPCR-	17760			0.8	0.80	0.00	0.00	0.02	
Day12 EPCR-	17757			0.3	0.30	0.00	0.00	0.01	
Day12 EPCR-	17759			0.3	0.30	0.00	0.00	0.01	

Table S3.1: Bone marrow aspiration data of NSG mice injected with different EPCR subsets sorted at day7 from UM171 cultures (page 3/3).

wk12 (BM aspiration)										
Outcome of 5,000 CD34+CD45RA- at day3	Sorted population	NSG-ID	Percentages at d3	Sorted cells transplanted at d3 per NSG	%CD45	%CD33	%CD19	%CD3	%CD34	
	Day3 Total	18649		100	10,000	23.9	12.48	9.49	0.00	0.19
	Day3 Total	18650				22.1	6.19	11.93	0.00	0.24
	Day3 Total	18651				43.4	13.67	24.13	0.01	0.53
	Day3 Total	18652				16.7	7.15	5.11	0.00	0.90
	Day3 Total	18653				2.2	0.66	1.27	0.00	0.05
	Day3 Total	18654				6.9	0.32	5.88	0.00	0.02
	Day3 EPCR+	18667		2	200	2.7	1.24	1.08	0.00	0.05
	Day3 EPCR+	18668				12.8	8.03	2.82	0.00	0.46
	Day3 EPCR+	18669				82.2	18.00	48.17	0.02	2.02
	Day3 EPCR+	18670				11.2	3.63	5.28	0.00	0.45
	Day3 EPCR+	18671				0.2	0.13	0.02	0.00	0.01
	Day3 EPCR+	18672				12.0	1.91	8.11	0.00	0.13
	Day3 EPCRlow	18661		77.3	7,730	0.20	0.17	0.00	0.00	0.00
	Day3 EPCRlow	18662				1.70	0.79	0.74	0.00	0.01
	Day3 EPCRlow	18663				0.60	0.18	0.30	0.00	0.01
	Day3 EPCRlow	18664				0.50	0.10	0.35	0.00	0.00
	Day3 EPCRlow	18666				0.00	0.00	0.00	0.00	0.00
	Day3 EPCR-	18655		20.7	2,070	0.00	0.00	0.00	0.00	0.00
	Day3 EPCR-	18656				0.00	0.00	0.00	0.00	0.00
Day3 EPCR-	18658				0.00	0.00	0.00	0.00	0.00	
Day3 EPCR-	18659				0.00	0.00	0.00	0.00	0.00	
Day3 EPCR-	18660				0.00	0.00	0.00	0.00	0.00	

wk24 (BM Flush)										
Outcome of 5,000 CD34+CD45RA- at day3	Sorted population	NSG-ID	Percentages at d0	Sorted cells transplanted at d0 per NSG	%CD45	%CD33	%CD19	%CD3	%CD34	
	Day3 Total	18649		100	10,000	33.1	8.34	19.79	0.33	5.49
	Day3 Total	18650				5.9	0.92	3.66	1.78	0.45
	Day3 Total	18651				5.8	0.57	0.23	5.60	0.01
	Day3 Total	18652				47.2	8.45	31.29	0.09	7.46
	Day3 Total	18653				20.8	1.79	16.37	0.04	1.37
	Day3 Total	18654				4.0	2.30	1.26	0.01	0.60
	Day3 EPCR+	18667		2	200	25.30	3.54	18.67	0.03	3.21
	Day3 EPCR+	18668				66.60	11.12	41.96	2.93	6.79
	Day3 EPCR+	18669				29.00	6.87	16.82	0.81	3.42
	Day3 EPCR+	18670				60.20	8.85	39.13	0.06	5.72
	Day3 EPCR+	18671				0.80	0.12	0.55	0.01	0.19
	Day3 EPCR+	18672				39.70	5.64	28.15	0.04	10.92
	Day3 EPCRlow	18661		77.3	7,730	10.70	9.59	0.18	0.13	3.92
	Day3 EPCRlow	18662				0.40	0.31	0.04	0.01	0.11
	Day3 EPCRlow	18663				16.60	2.29	11.85	0.02	1.84
	Day3 EPCRlow	18664				0.40	0.33	0.06	0.04	0.02
	Day3 EPCRlow	18666				0.70	0.64	0.03	0.25	0.01
	Day3 EPCR-	18655		20.7	2,070	0.00	0.00	0.00	0.00	0.00
	Day3 EPCR-	18656				0.00	0.00	0.00	0.00	0.00
Day3 EPCR-	18658				0.00	0.00	0.00	0.00	0.00	
Day3 EPCR-	18659				0.00	0.00	0.00	0.00	0.00	
Day3 EPCR-	18660				0.00	0.00	0.00	0.00	0.00	

Table S3.2: Bone marrow aspiration data of NSG mice injected with different EPCR subsets sorted at day3 from DMSO cultures

		week24 (1ry trsp)					week18 (2nd trsp)						
Mouse ID	Sorted population	Cell no. injected/NSG	%Hu CD45	%Hu-CD33	%Hu-CD19	%Hu-CD3	%Hu-CD34	Mouse ID	%Hu CD45	%Hu-CD33	%Hu-CD19	%Hu-CD3	%Hu-CD34
17562	CD34+ CD45RA- (100%)	3,000	38.1	6.63	22.71	0.04	4.31	18763	87.6	12.53	66.14	0.63	1.94
17563	CD34+ CD45RA- (100%)	3,000	43.6	12.21	23.76	0.31	4.05	18764	55.8	5.64	47.65	0.06	0.54
17564	CD34+ CD45RA- (100%)	3,000	65.8	18.16	32.70	1.51	7.70	18765	78.5	14.44	57.07	2.10	0.95
17565	CD34+ CD45RA- (100%)	3,000	67.7	29.72	27.22	1.22	6.03	18766	80.9	21.60	53.64	0.16	1.00
17566	CD34+ CD45RA- (100%)	3,000	13.8	6.20	3.68	1.88	0.73	18767	28.4	6.36	20.99	0.01	0.15
17567	CD34+ CD45RA- (100%)	3,000	72.1	15.36	42.97	0.36	5.05	18768	86.6	10.57	70.41	0.43	1.55
17568	CD34+ CD45RA- (100%)	3,000	62.9	24.66	23.96	2.45	3.02	18769	82.6	10.99	64.02	0.86	1.61
17569	CD34+ CD45RA- (100%)	3,000	36.6	14.24	6.99	11.09	0.84	18770	7.9	1.78	0.65	4.84	0.02
17602	CD34+ CD45RA-EPCR+ (4.6%)	138	30	1.59	3.18	24.69	0.09	18733	0.1	0.09	0.00	0.00	0.00
17603	CD34+ CD45RA-EPCR+ (4.6%)	138	39.8	29.93	7.32	0.04	1.55	18734	72.8	62.39	7.43	0.01	0.44
17604	CD34+ CD45RA-EPCR+ (4.6%)	138	23.5	2.59	13.54	3.06	1.36	18735	2.4	0.45	1.76	0.00	0.03
17605	CD34+ CD45RA-EPCR+ (4.6%)	138	24.4	2.12	4.93	15.23	0.22	18736	76.1	5.17	65.52	0.01	1.04
17606	CD34+ CD45RA-EPCR+ (4.6%)	138	65.5	12.51	45.92	0.26	5.24	18737	83.2	10.23	65.40	0.01	2.74
17612	CD34+ CD45RA-EPCRlow (70.6%)	2,118	83.8	4.69	71.73	0.42	4.61	18738	Dead				
17613	CD34+ CD45RA-EPCRlow (70.6%)	2,118	79.6	6.37	66.23	0.40	3.66	18739	41.7	4.38	33.86	0.13	0.40
17614	CD34+ CD45RA-EPCRlow (70.6%)	2,118	29.2	0.61	0.50	28.27	0.03	18740	0.1	0.01	0.08	0.00	0.00
17615	CD34+ CD45RA-EPCRlow (70.6%)	2,118	0.3	0.28	0.01	0.00	0.00	18741	0.0	0.00	0.00	0.00	0.00
17616	CD34+ CD45RA-EPCRlow (70.6%)	2,118	6.6	0.90	5.28	0.01	0.08	18742	0.1	0.08	0.01	0.00	0.00
17622	CD34+ CD45RA-EPCR- (24.6%)	738	0.5	0.49	0.00	0.01	0.01	18743	0.0	0.00	0.00	0.00	0.00
17623	CD34+ CD45RA-EPCR- (24.6%)	738	0.4	0.35	0.04	0.00	0.00	18744	0.0	0.00	0.00	0.00	0.00
17624	CD34+ CD45RA-EPCR- (24.6%)	738	50.9	1.53	43.47	0.20	1.83	18745	0.0	0.00	0.00	0.00	0.00
17625	CD34+ CD45RA-EPCR- (24.6%)	738	0.2	0.14	0.01	0.00	0.01	18746	0.0	0.00	0.00	0.00	0.00
17626	CD34+ CD45RA-EPCR- (24.6%)	738	0.6	0.53	0.01	0.00	0.00	18747	0.0	0.00	0.00	0.00	0.00
17632	Day7 Total (100%)	75,000	34.2	3.76	26.85	0.00	0.86	18748	0.1	0.09	0.00	0.00	0.00
17633	Day7 Total (100%)	75,000	76.1	8.98	55.78	3.35	3.27	18749	26.9	2.74	22.49	0.00	0.23
17634	Day7 Total (100%)	75,000	66.5	9.44	49.94	0.07	3.92	18750	21.2	2.31	16.41	1.43	0.11
17635	Day7 Total (100%)	75,000	78.9	11.84	56.97	0.87	4.10	18751	47.6	14.18	29.61	0.03	0.63
17636	Day7 Total (100%)	75,000	27.9	1.26	1.48	24.69	0.03	18752	0.5	0.39	0.01	0.08	0.00
17657	Day7 EPCR+ (6%)	4,500	53.3	8.58	36.51	0.96	2.88	18753	6.3	1.59	4.39	0.00	0.02
17658	Day7 EPCR+ (6%)	4,500	49.9	7.73	13.27	26.75	0.50	18754	0.6	0.33	0.15	0.00	0.00
17659	Day7 EPCR+ (6%)	4,500	31.4	3.80	20.57	0.88	2.54	18755	12.2	3.90	7.63	0.00	0.08
17660	Day7 EPCR+ (6%)	4,500	86.5	7.09	67.64	0.35	8.48	18756	4.0	0.86	3.00	0.00	0.02
17661	Day7 EPCR+ (6%)	4,500	49.6	8.58	31.55	0.50	1.84	18757	4.1	1.01	2.87	0.00	0.02
17682	Day7 EPCRlow (83.7%)	62,775	0.1	0.08	0.01	0.00	0.00	18758	0.0	0.00	0.00	0.00	0.00
17683	Day7 EPCRlow (83.7%)	62,775	0.2	0.06	0.12	0.00	0.00	18759	0.0	0.00	0.00	0.00	0.00
17684	Day7 EPCRlow (83.7%)	62,775	0.1	0.09	0.01	0.00	0.00	18760	0.0	0.00	0.00	0.00	0.00
17685	Day7 EPCRlow (83.7%)	62,775	0.4	0.27	0.10	0.00	0.00	18761	0.0	0.00	0.00	0.00	0.00
17686	Day7 EPCRlow (83.7%)	62,775	16.1	1.19	12.88	0.00	0.45	18762	5.1	0.88	3.48	0.00	0.18
17712	Day7 EPCR- (10.1%)	7,575	0.0	0.00	0.00	0.00	0.00	18771	Dead				
17713	Day7 EPCR- (10.1%)	7,575	0.2	0.19	0.00	0.01	0.00	18772	0.0	0.00	0.00	0.00	0.00
17714	Day7 EPCR- (10.1%)	7,575	0.1	0.09	0.00	0.00	0.00	18773	0.0	0.00	0.00	0.00	0.00
17716	Day7 EPCR- (10.1%)	7,575	0.2	0.19	0.00	0.00	0.00	18774	0.0	0.00	0.00	0.00	0.00
17762	Day12 Total (100%)	414,000	2.1	1.89	0.14	0.01	0.06	18775	0.1	0.09	0.00	0.00	0.00
17763	Day12 Total (100%)	414,000	1.4	1.37	0.01	0.01	0.02	18776	0.1	0.09	0.00	0.00	0.00
17764	Day12 Total (100%)	414,000	6.4	4.09	1.70	0.01	0.35	18777	0.2	0.18	0.01	0.00	0.00
17765	Day12 Total (100%)	414,000	1.7	1.64	0.04	0.01	0.04	18778	0.0	0.00	0.00	0.00	0.00
17732	Day12 EPCR+ (2.1%)	8,694	11.8	6.12	3.69	0.09	0.71	18779	13.1	1.45	11.08	0.00	0.10
17733	Day12 EPCR+ (2.1%)	8,694	63.7	7.84	43.19	0.00	4.08	18780	72.0	28.15	38.66	0.26	0.76
17734	Day12 EPCR+ (2.1%)	8,694	3.7	0.20	0.09	3.35	0.01	18781	1.7	0.62	0.85	0.09	0.02
17735	Day12 EPCR+ (2.1%)	8,694	32.6	6.13	17.86	0.03	2.93	18782	37.9	3.26	32.14	0.00	0.75
17742	Day12 EPCRlow (79.2)	327,888	0.5	0.48	0.00	0.00	0.01	18783	0.0	0.00	0.00	0.00	0.00
17743	Day12 EPCRlow (79.2)	327,888	1.1	1.08	0.01	0.00	0.02	18784	0.0	0.00	0.00	0.00	0.00
17744	Day12 EPCRlow (79.2)	327,888	2.1	2.08	0.00	0.00	0.04	18785	0.0	0.00	0.00	0.00	0.00
17745	Day12 EPCRlow (79.2)	327,888	0.6	0.56	0.01	0.00	0.02	18786	0.1	0.08	0.00	0.00	0.00
17746	Day12 EPCRlow (79.2)	327,888	0.7	0.69	0.00	0.00	0.01	18787	Dead				
17752	Day12 EPCR- (18.5%)	76,590	0.3	0.29	0.00	0.00	0.01	18788	0.0	0.00	0.00	0.00	0.00
17753	Day12 EPCR- (18.5%)	76,590	0.6	0.59	0.00	0.00	0.02	18789	0.0	0.00	0.00	0.00	0.00
17754	Day12 EPCR- (18.5%)	76,590	1.0	0.99	0.00	0.00	0.02	18790	0.0	0.00	0.00	0.00	0.00
17755	Day12 EPCR- (18.5%)	76,590	0.7	0.63	0.00	0.00	0.02	18791	0.0	0.00	0.00	0.00	0.00
17756	Day12 EPCR- (18.5%)	76,590	0.9	0.89	0.00	0.00	0.03	18792	0.0	0.00	0.00	0.00	0.00

Table S3.3: EPCR⁺ cells provide multi-lineage reconstitution in secondary mice.

Bone marrow aspiration data of 1ry and 2nd NSG recipients.

wk12 (BM Aspiration)								
Sorted population	NSG-ID	Percentages at d7	Sorted cells transplanted at d7 per NSG	%CD45	%CD33	%CD19	%CD3	%CD34
Total	17632	100	75,000	1.5	0.24	1.20	0.00	0.01
Total	17633			26.0	1.77	23.06	0.05	0.29
Total	17634			58.1	6.16	48.98	0.00	2.21
Total	17635			14.2	2.46	10.69	0.01	0.23
Total	17636			22.5	2.59	18.61	0.23	0.16
Total	17637	100	25,000	2.6	0.22	2.20	0.01	0.02
Total	17638			1.0	0.47	0.49	0.02	0.01
Total	17639			9.9	5.67	3.55	0.04	0.37
Total	17640			1.9	0.50	1.30	0.01	0.01
Total	17641			15.3	2.56	8.31	3.14	0.18
Total	17642	100	8,325	0.0	0.00	0.00	0.00	0.00
Total	17643			1.5	0.35	0.91	0.00	0.08
Total	17644			5.2	1.61	2.95	0.01	0.31
Total	17645			0.0	0.00	0.00	0.00	0.00
Total	17646			49.3	5.23	40.33	0.05	1.68
Total	17647	100	2,775	0.0	0.00	0.00	0.00	0.00
Total	17648			0.5	0.26	0.22	0.01	0.01
Total	17649			1.9	0.26	1.57	0.01	0.02
Total	17650			0.1	0.09	0.00	0.00	0.00
Total	17651			0.1	0.07	0.03	0.01	0.00
Total	17652	100	925	0.0	0.00	0.00	0.00	0.00
Total	17653			0.0	0.00	0.00	0.00	0.00
Total	17654			0.2	0.03	0.16	0.00	0.00
Total	17655			0.7	0.12	0.55	0.00	0.01
Total	17656			0.0	0.00	0.00	0.00	0.00
EPCR+	17657	6	4,500	13.7	3.51	9.10	0.01	0.16
EPCR+	17658			17.0	3.59	11.80	0.02	0.58
EPCR+	17659			15.3	1.87	12.45	0.02	0.28
EPCR+	17660			9.8	1.94	7.14	0.04	0.17
EPCR+	17661			6.9	1.19	4.91	0.03	0.08
EPCR+	17662	6	1,500	1.9	0.33	1.44	0.00	0.01
EPCR+	17663			55.4	3.93	46.65	0.00	2.33
EPCR+	17664			47.0	10.29	34.17	0.00	1.03
EPCR+	17665			22.2	6.04	13.59	0.00	0.89
EPCR+	17666			2.9	0.14	2.44	0.00	0.04
EPCR+	17667	6	500	6.6	0.68	5.16	0.01	0.11
EPCR+	17668			0.9	0.25	0.56	0.00	0.05
EPCR+	17669			62.2	9.95	46.09	0.06	1.62
EPCR+	17670			8.3	2.33	5.49	0.02	0.06
EPCR+	17671			0.2	0.13	0.06	0.00	0.00
EPCR+	17672	6	175	27.1	2.20	22.33	0.00	0.54
EPCR+	17673			0.1	0.01	0.08	0.00	0.00
EPCR+	17674			0.0	0.00	0.00	0.00	0.00
EPCR+	17675			0.0	0.00	0.00	0.00	0.00
EPCR+	17676			0.0	0.00	0.00	0.00	0.00
EPCR+	17677	6	50	0.0	0.00	0.00	0.00	0.00
EPCR+	17678			0.0	0.00	0.00	0.00	0.00
EPCR+	17679			0.0	0.00	0.00	0.00	0.00
EPCR+	17680			0.0	0.00	0.00	0.00	0.00
EPCR+	17681			0.0	0.00	0.00	0.00	0.00
EPCRlow	17682	83.7	62,775	1.4	1.35	0.02	0.00	0.00
EPCRlow	17683			2.1	2.02	0.03	0.01	0.01
EPCRlow	17684			0.3	0.27	0.01	0.00	0.00
EPCRlow	17685			2.2	2.16	0.01	0.00	0.00
EPCRlow	17686			1.4	1.36	0.01	0.00	0.01
EPCRlow	17687	83.7	20,925	0.4	0.37	0.01	0.00	0.00
EPCRlow	17688			0.2	0.17	0.01	0.00	0.00
EPCRlow	17689			0.1	0.09	0.00	0.00	0.00
EPCRlow	17690			0.2	0.17	0.01	0.00	0.00
EPCRlow	17691			0.3	0.28	0.01	0.00	0.00
EPCRlow	17692	83.7	6,975	0.1	0.06	0.01	0.00	0.00
EPCRlow	17693			0.1	0.09	0.00	0.00	0.00
EPCRlow	17694			0.1	0.07	0.01	0.00	0.00
EPCRlow	17695			0.2	0.18	0.01	0.00	0.00
EPCRlow	17696			0.1	0.08	0.00	0.00	0.00
EPCRlow	17697	83.7	2,325	0.0	0.00	0.00	0.00	0.00
EPCRlow	17698			0.0	0.00	0.00	0.00	0.00
EPCRlow	17699			0.0	0.00	0.00	0.00	0.00
EPCRlow	17700			0.0	0.00	0.00	0.00	0.00
EPCRlow	17701			0.0	0.00	0.00	0.00	0.00
EPCRlow	17702	83.7	775	0.0	0.00	0.00	0.00	0.00
EPCRlow	17703			0.0	0.00	0.00	0.00	0.00
EPCRlow	17704			0.0	0.00	0.00	0.00	0.00
EPCRlow	17705			0.0	0.00	0.00	0.00	0.00
EPCRlow	17706			Dead				
EPCR-	17707	10.1	22,725	0.8	0.77	0.01	0.00	0.00
EPCR-	17708			Dead				
EPCR-	17709			0.0	0.00	0.00	0.00	0.00
EPCR-	17710			0.1	0.09	0.00	0.00	0.00
EPCR-	17711			0.2	0.19	0.00	0.00	0.00
EPCR-	17712	10.1	7,575	0.3	0.28	0.01	0.00	0.00
EPCR-	17713			0.1	0.09	0.00	0.00	0.00
EPCR-	17714			0.0	0.00	0.00	0.00	0.00
EPCR-	17715			0.1	0.09	0.00	0.00	0.00
EPCR-	17716			0.2	0.19	0.00	0.00	0.00
EPCR-	17717	10.1	2,525	0.0	0.00	0.00	0.00	0.00
EPCR-	17718			0.1	0.09	0.00	0.00	0.00
EPCR-	17719			0.0	0.00	0.00	0.00	0.00
EPCR-	17720			0.0	0.00	0.00	0.00	0.00
EPCR-	17721			0.0	0.00	0.00	0.00	0.00
EPCR-	17722	10.1	850	0.0	0.00	0.00	0.00	0.00
EPCR-	17723			0.0	0.00	0.00	0.00	0.00
EPCR-	17724			1.0	0.87	0.05	0.06	0.04
EPCR-	17725			0.0	0.00	0.00	0.00	0.00
EPCR-	17726			0.0	0.00	0.00	0.00	0.00
EPCR-	17727	10.1	275	0.0	0.00	0.00	0.00	0.00
EPCR-	17728			0.0	0.00	0.00	0.00	0.00
EPCR-	17729			0.0	0.00	0.00	0.00	0.00
EPCR-	17730			0.0	0.00	0.00	0.00	0.00
EPCR-	17731			0.0	0.00	0.00	0.00	0.00

Table S3.4: Limit dilution experiment of different EPCR subsets sorted at day7 (page 1/4).

wk24 (BM Flush)										
Sorted population	NSG-ID	Percentages at d7	Sorted cells transplanted at d7 per NSG	%CD45	%CD33	%CD19	%CD3	%CD34		
Total	17632	100	75,000	34.2	3.76	26.85	0.00	0.86		
Total	17633			76.1	8.98	55.78	3.35	3.27		
Total	17634			66.5	9.44	49.94	0.07	3.92		
Total	17635			78.9	11.84	56.97	0.87	4.10		
Total	17636			27.9	1.26	1.48	24.69	0.03		
Total	17637	100	25,000	1.4	1.36	0.03	0.00	0.02		
Total	17638			2.4	1.81	0.48	0.00	0.03		
Total	17639			20.2	9.82	8.32	0.28	0.97		
Total	17640			0.9	0.88	0.00	0.02	0.01		
Total	17641			Dead						
Total	17642	100	8,325	0.4	0.40	0.00	0.00	0.00		
Total	17643			9.0	5.42	2.88	0.00	0.45		
Total	17644			8.1	0.65	6.27	0.00	0.24		
Total	17645			0.3	0.29	0.01	0.00	0.00		
Total	17646			0.8	0.63	0.14	0.00	0.02		
Total	17647	100	2,775	6.7	1.15	5.09	0.00	0.02		
Total	17648			0.4	0.12	0.25	0.00	0.00		
Total	17649			0.5	0.24	0.23	0.00	0.01		
Total	17650			0.1	0.10	0.00	0.00	0.00		
Total	17651			0.9	0.31	0.49	0.00	0.02		
Total	17652	100	925	0.1	0.10	0.00	0.00	0.00		
Total	17653			0.1	0.10	0.00	0.00	0.00		
Total	17654			0.0	0.00	0.00	0.00	0.00		
Total	17655			0.5	0.14	0.31	0.00	0.01		
Total	17656			0.0	0.00	0.00	0.00	0.00		
EPCR+	17657	6	4,500	53.3	8.58	36.51	0.96	2.88		
EPCR+	17658			49.9	7.73	13.27	26.75	0.50		
EPCR+	17659			31.4	3.80	20.57	0.88	2.54		
EPCR+	17660			86.5	7.09	67.64	0.35	8.48		
EPCR+	17661			49.6	8.58	31.55	0.50	1.84		
EPCR+	17662	6	1,500	6.5	1.51	4.11	0.00	0.19		
EPCR+	17663			39.4	5.63	27.62	0.63	2.32		
EPCR+	17664			43.3	4.94	32.73	0.00	2.04		
EPCR+	17665			67.2	13.04	44.76	0.13	2.28		
EPCR+	17666			9.2	1.23	6.39	0.00	0.13		
EPCR+	17667	6	500	19.7	2.44	14.91	0.00	0.45		
EPCR+	17668			37.4	7.44	25.13	0.00	2.24		
EPCR+	17669			5.0	0.41	0.19	3.96	0.02		
EPCR+	17670			8.5	2.63	5.13	0.00	0.44		
EPCR+	17671			0.5	0.47	0.01	0.00	0.01		
EPCR+	17672	6	175	0.4	0.39	0.01	0.00	0.01		
EPCR+	17673			0.2	0.11	0.08	0.00	0.00		
EPCR+	17674			0.5	0.19	0.28	0.00	0.01		
EPCR+	17675			0.1	0.09	0.00	0.00	0.00		
EPCR+	17676			0.3	0.29	0.00	0.00	0.01		
EPCR+	17677	6	50	0.2	0.20	0.00	0.00	0.00		
EPCR+	17678			0.0	0.00	0.00	0.00	0.00		
EPCR+	17679			0.2	0.04	0.00	0.03	0.02		
EPCR+	17680			0.0	0.00	0.00	0.00	0.00		
EPCR+	17681			0.0	0.00	0.00	0.00	0.00		
EPCRlow	17682	83.7	62,775	0.1	0.08	0.01	0.00	0.00		
EPCRlow	17683			0.2	0.06	0.12	0.00	0.00		
EPCRlow	17684			0.1	0.09	0.01	0.00	0.00		
EPCRlow	17685			0.4	0.27	0.10	0.00	0.00		
EPCRlow	17686			16.1	1.19	12.88	0.00	0.45		
EPCRlow	17687	83.7	20,925	0.9	0.90	0.00	0.00	0.02		
EPCRlow	17688			0.5	0.49	0.01	0.00	0.02		
EPCRlow	17689			0.6	0.60	0.00	0.00	0.01		
EPCRlow	17690			0.6	0.60	0.00	0.00	0.01		
EPCRlow	17691			0.5	0.49	0.00	0.00	0.01		
EPCRlow	17692	83.7	6,975	0.4	0.39	0.00	0.00	0.04		
EPCRlow	17693			0.7	0.69	0.00	0.00	0.01		
EPCRlow	17694			0.2	0.20	0.00	0.00	0.00		
EPCRlow	17695			0.5	0.49	0.00	0.00	0.01		
EPCRlow	17696			0.2	0.19	0.00	0.00	0.00		
EPCRlow	17697	83.7	2,325	0.1	0.10	0.00	0.00	0.00		
EPCRlow	17698			0.1	0.10	0.00	0.00	0.00		
EPCRlow	17699			0.2	0.19	0.00	0.00	0.01		
EPCRlow	17700			0.3	0.30	0.00	0.00	0.01		
EPCRlow	17701			0.0	0.00	0.00	0.00	0.00		
EPCRlow	17702	83.7	775	0.0	0.00	0.00	0.00	0.00		
EPCRlow	17703			0.0	0.00	0.00	0.00	0.00		
EPCRlow	17704			0.0	0.00	0.00	0.00	0.00		
EPCRlow	17705			0.0	0.00	0.00	0.00	0.00		
EPCRlow	17706			Dead						
EPCR-	17707	10.1	22,725	1.5	1.49	0.01	0.00	0.03		
EPCR-	17708			Dead						
EPCR-	17709			0.0	0.00	0.00	0.00	0.00		
EPCR-	17710			0.7	0.70	0.00	0.00	0.01		
EPCR-	17711			0.7	0.70	0.00	0.00	0.01		
EPCR-	17712	10.1	7,575	0.0	0.00	0.00	0.00	0.00		
EPCR-	17713			0.2	0.19	0.00	0.01	0.00		
EPCR-	17714			0.1	0.09	0.00	0.00	0.00		
EPCR-	17715			0.0	0.00	0.00	0.00	0.00		
EPCR-	17716			0.2	0.19	0.00	0.00	0.00		
EPCR-	17717	10.1	2,525	0.2	0.20	0.00	0.00	0.00		
EPCR-	17718			0.3	0.30	0.00	0.00	0.01		
EPCR-	17719			0.2	0.20	0.00	0.00	0.00		
EPCR-	17720			0.2	0.20	0.00	0.00	0.00		
EPCR-	17721			0.3	0.30	0.00	0.00	0.01		
EPCR-	17722	10.1	850	0.1	0.10	0.00	0.00	0.00		
EPCR-	17723			0.1	0.10	0.00	0.00	0.00		
EPCR-	17724			0.1	0.09	0.00	0.00	0.00		
EPCR-	17725			0.1	0.09	0.00	0.00	0.00		
EPCR-	17726			0.0	0.00	0.00	0.00	0.00		
EPCR-	17727	10.1	275	0.0	0.00	0.00	0.00	0.00		
EPCR-	17728			0.1	0.09	0.00	0.00	0.01		
EPCR-	17729			0.0	0.00	0.00	0.00	0.00		
EPCR-	17730			0.0	0.00	0.00	0.00	0.00		
EPCR-	17731			0.0	0.00	0.00	0.00	0.00		

Table S3.4: Limit dilution experiment of different EPCR subsets sorted at day7 (page 2/4).

wk12 (BM Aspiration)								
Sorted population	NSG-ID	Percentages at d12	Sorted cells transplanted at d12 per NSG	%CD45	%CD33	%CD19	%CD3	%CD34
Total	17762	100	414,000	0.6	0.31	0.16	0.04	0.01
Total	17763			2.0	1.34	0.06	0.60	0.11
Total	17764			69.4	9.37	47.61	0.07	2.15
Total	17765			1.7	1.27	0.30	0.26	0.03
Total	17767	100	138,000	0.7	0.46	0.11	0.07	0.01
Total	17768			0.1	0.08	0.00	0.01	0.00
Total	17769			0.7	0.47	0.17	0.02	0.01
Total	17770			0.5	0.30	0.10	0.06	0.01
Total	17771			0.3	0.20	0.06	0.01	0.00
Total	17772	100	45,954	0.0	0.00	0.00	0.00	0.00
Total	17773			0.1	0.09	0.00	0.01	0.00
Total	17774			0.1	0.09	0.00	0.01	0.00
Total	17775			0.2	0.19	0.00	0.02	0.00
Total	17776			0.1	0.08	0.00	0.01	0.00
Total	17777	100	15,318	0.0	0.00	0.00	0.00	0.00
Total	17778			0.2	0.19	0.00	0.02	0.00
Total	17779			0.0	0.00	0.00	0.00	0.00
Total	17780			0.0	0.00	0.00	0.00	0.00
Total	17781			0.0	0.00	0.00	0.00	0.00
Total	17782	100	5,106	0.0	0.00	0.00	0.00	0.00
Total	17783			0.0	0.00	0.00	0.00	0.00
Total	17784			0.0	0.00	0.00	0.00	0.00
Total	17785			0.1	0.04	0.02	0.01	0.00
Total	17786			0.0	0.00	0.00	0.00	0.00
EPCR+	17732	2.1	8,694	1.0	0.38	0.41	0.01	0.04
EPCR+	17733			63.3	16.46	35.89	0.19	5.32
EPCR+	17734			3.3	1.17	1.08	0.84	0.08
EPCR+	17735			42.4	11.91	26.16	0.08	1.74
EPCR+	17736			6.4	4.60	0.77	0.01	0.76
EPCR+	17737	2.1	2,898	74.3	25.48	39.16	0.07	3.57
EPCR+	17738			1.1	0.23	0.56	0.01	0.04
EPCR+	17739			2.4	1.08	1.00	0.02	0.03
EPCR+	17740			0.3	0.11	0.13	0.01	0.01
EPCR+	17741			2.3	0.72	1.05	0.00	0.04
EPCRlow	17742	79.2	327,888	0.4	0.36	0.00	0.04	0.01
EPCRlow	17743			0.4	0.39	0.00	0.05	0.00
EPCRlow	17744			1.4	1.35	0.00	0.16	0.02
EPCRlow	17745			0.2	0.19	0.00	0.02	0.00
EPCRlow	17746			0.4	0.36	0.01	0.04	0.00
EPCRlow	17747	79.2	109,296	0.1	0.08	0.00	0.01	0.00
EPCRlow	17748			0.2	0.18	0.00	0.02	0.00
EPCRlow	17749			0.6	0.54	0.01	0.11	0.02
EPCRlow	17750			0.2	0.18	0.00	0.02	0.00
EPCRlow	17751			0.3	0.29	0.00	0.03	0.00
EPCR-	17752	18.5	76,590	0.1	0.08	0.00	0.01	0.00
EPCR-	17753			0.2	0.19	0.00	0.01	0.00
EPCR-	17754			0.2	0.18	0.00	0.02	0.00
EPCR-	17755			0.1	0.09	0.00	0.01	0.00
EPCR-	17756			0.5	0.46	0.00	0.05	0.01
EPCR-	17757	18.5	25,530	0.1	0.08	0.00	0.01	0.00
EPCR-	17758			0.5	0.46	0.00	0.03	0.01
EPCR-	17759			0.1	0.08	0.00	0.01	0.00
EPCR-	17760			0.2	0.19	0.00	0.02	0.00
EPCR-	17761			0.2	0.18	0.00	0.03	0.01

Table S3.4: Limit dilution experiment of different EPCR subsets sorted at day7 (page 3/4).

wk24 (BM Flush)									
Sorted population	NSG-ID	Percentages at d12	Sorted cells transplanted at d12 per NSG	%CD45	%CD33	%CD19	%CD3	%CD34	
Total	17762	100	414,000	2.1	1.89	0.14	0.01	0.06	
Total	17763			1.4	1.37	0.01	0.01	0.02	
Total	17764			6.4	4.09	1.70	0.01	0.35	
Total	17765			1.7	1.64	0.04	0.01	0.04	
Total	17767	100	138,000	0.5	0.50	0.00	0.00	0.00	
Total	17768			0.4	0.40	0.00	0.00	0.01	
Total	17769			0.2	0.20	0.00	0.00	0.00	
Total	17770			0.7	0.62	0.07	0.00	0.01	
Total	17771			0.3	0.30	0.00	0.00	0.01	
Total	17772	100	45,954	0.1	0.10	0.00	0.00	0.00	
Total	17773			0.3	0.30	0.00	0.00	0.01	
Total	17774			0.4	0.40	0.00	0.00	0.02	
Total	17775			0.5	0.50	0.00	0.01	0.01	
Total	17776			0.3	0.30	0.00	0.00	0.01	
Total	17777	100	15,318	0.1	0.10	0.00	0.00	0.00	
Total	17778			0.2	0.20	0.00	0.00	0.01	
Total	17779			0.3	0.29	0.00	0.01	0.01	
Total	17780			0.1	0.10	0.00	0.00	0.00	
Total	17781			0.3	0.30	0.00	0.01	0.01	
Total	17782	100	5,106	0.1	0.09	0.00	0.00	0.00	
Total	17783			0.2	0.19	0.00	0.00	0.01	
Total	17784			0.0	0.00	0.00	0.00	0.00	
Total	17785			0.6	0.60	0.00	0.00	0.02	
Total	17786			0.2	0.20	0.00	0.00	0.00	
EPCR+	17732	2.1	8,694	11.8	6.12	3.69	0.09	0.71	
EPCR+	17733			63.7	7.84	43.19	0.00	4.08	
EPCR+	17734			3.7	0.20	0.09	3.35	0.01	
EPCR+	17735			32.6	6.13	17.86	0.03	2.93	
EPCR+	17736			Dead					
EPCR+	17737	2.1	2,898	16.9	1.64	12.32	0.69	0.74	
EPCR+	17738			15.2	1.49	3.85	9.21	0.12	
EPCR+	17739			3.8	2.60	0.82	0.19	0.23	
EPCR+	17740			13.4	5.65	6.54	0.00	0.71	
EPCR+	17741			4.5	3.73	0.60	0.00	0.44	
EPCRlow	17742	79.2	327,888	0.5	0.48	0.00	0.00	0.01	
EPCRlow	17743			1.1	1.08	0.01	0.00	0.02	
EPCRlow	17744			2.1	2.08	0.00	0.00	0.04	
EPCRlow	17745			0.6	0.56	0.01	0.00	0.02	
EPCRlow	17746			0.7	0.69	0.00	0.00	0.01	
EPCRlow	17747	79.2	109,296	0.3	0.30	0.00	0.01	0.01	
EPCRlow	17748			0.7	0.70	0.00	0.00	0.01	
EPCRlow	17749			1.1	1.09	0.00	0.00	0.02	
EPCRlow	17750			0.6	0.60	0.00	0.00	0.01	
EPCRlow	17751			0.6	0.60	0.00	0.00	0.01	
EPCR-	17752	18.5	76,590	0.3	0.29	0.00	0.00	0.01	
EPCR-	17753			0.6	0.59	0.00	0.00	0.02	
EPCR-	17754			1.0	0.99	0.00	0.00	0.02	
EPCR-	17755			0.7	0.63	0.00	0.00	0.02	
EPCR-	17756			0.9	0.89	0.00	0.00	0.03	
EPCR-	17757	18.5	25,530	0.3	0.30	0.00	0.00	0.01	
EPCR-	17758			1.0	1.00	0.00	0.00	0.04	
EPCR-	17759			0.3	0.30	0.00	0.00	0.01	
EPCR-	17760			0.8	0.80	0.00	0.00	0.02	
EPCR-	17761			1.1	1.09	0.00	0.00	0.02	

Table S3.4: Limit dilution experiment of different EPCR subsets sorted at day7 (page 4/4).

		wk12 (BM aspiration)							
Day0	Name	NSG-ID	percentages at d0	Sorted cells transplanted at d0/NSG	%CD45	%CD33	%CD19	%CD3	%CD34
		CD34+CD45RA-	17562	100	3,000	3.9	1.08	2.26	0.01
	CD34+CD45RA-	17563			31.0	27.25	1.43	0.06	3.26
	CD34+CD45RA-	17564			11.9	3.65	7.50	0.01	0.64
	CD34+CD45RA-	17565			86.5	22.32	56.23	0.09	5.62
	CD34+CD45RA-	17566			6.8	1.05	5.21	0.02	0.32
	CD34+CD45RA-	17567			8.2	1.52	6.13	0.02	0.34
	CD34+CD45RA-	17568			28.3	10.53	15.20	0.06	2.60
	CD34+CD45RA-	17569			80.9	17.64	53.15	0.16	4.37
	CD34+CD45RA-	17570	100	1,000	8.2	2.08	5.56	0.02	0.45
	CD34+CD45RA-	17571			5.2	2.31	2.59	0.02	0.36
	CD34+CD45RA-	17572			77.9	4.44	66.14	0.00	4.91
	CD34+CD45RA-	17573			4.3	0.61	3.41	0.01	0.05
	CD34+CD45RA-	17574			5.9	2.02	3.06	0.01	0.37
	CD34+CD45RA-	17575			16.5	3.98	11.09	0.02	0.74
	CD34+CD45RA-	17576			6.9	1.22	5.39	0.01	0.10
	CD34+CD45RA-	17577			34.7	4.68	27.97	0.07	0.66
	CD34+CD45RA-	17578	100	333	0.2	0.12	0.04	0.02	0.03
	CD34+CD45RA-	17579			0.8	0.77	0.01	0.01	0.02
	CD34+CD45RA-	17580			0.2	0.18	0.01	0.00	0.00
	CD34+CD45RA-	17581			1.7	0.43	1.14	0.01	0.06
	CD34+CD45RA-	17582			0.0	0.00	0.00	0.00	0.00
	CD34+CD45RA-	17583			0.3	0.05	0.21	0.01	0.00
	CD34+CD45RA-	17584			0.0	0.00	0.00	0.00	0.00
	CD34+CD45RA-	17585			0.8	0.09	0.64	0.01	0.02
	CD34+CD45RA-	17586	100	111	3.9	0.59	2.68	0.01	0.33
	CD34+CD45RA-	17587			Dead				
	CD34+CD45RA-	17588			0.9	0.16	0.66	0.00	0.03
	CD34+CD45RA-	17589			0.0	0.00	0.00	0.00	0.00
	CD34+CD45RA-	17590			0.0	0.00	0.00	0.00	0.00
	CD34+CD45RA-	17591			0.0	0.00	0.00	0.00	0.00
	CD34+CD45RA-	17592			0.1	0.05	0.04	0.01	0.00
	CD34+CD45RA-	17593			0.0	0.00	0.00	0.00	0.00
	CD34+CD45RA-	17594	100	37	0.0	0.00	0.00	0.00	0.00
	CD34+CD45RA-	17595			0.0	0.00	0.00	0.00	0.00
	CD34+CD45RA-	17596			0.1	0.03	0.06	0.00	0.00
	CD34+CD45RA-	17597			0.0	0.00	0.00	0.00	0.00
	CD34+CD45RA-	17598			0.0	0.00	0.00	0.00	0.00
	CD34+CD45RA-	17599			0.0	0.00	0.00	0.00	0.00
	CD34+CD45RA-	17600			0.0	0.00	0.00	0.00	0.00
	CD34+CD45RA-	17601			0.1	0.06	0.03	0.01	0.01
	CD34+CD45RA-EPCR+	17602	4.6	138	11.9	6.02	4.94	0.00	0.37
	CD34+CD45RA-EPCR+	17603			1.8	0.48	1.08	0.00	0.04
	CD34+CD45RA-EPCR+	17604			5.1	0.66	3.87	0.01	0.12
	CD34+CD45RA-EPCR+	17605			3.5	1.08	1.61	0.08	0.14
	CD34+CD45RA-EPCR+	17606			29.3	5.92	21.01	0.00	0.50
	CD34+CD45RA-EPCR+	17607	4.6	46	0.0	0.00	0.00	0.00	0.00
	CD34+CD45RA-EPCR+	17608			0.1	0.03	0.06	0.01	0.01
	CD34+CD45RA-EPCR+	17609			38.8	29.72	4.07	0.00	2.95
	CD34+CD45RA-EPCR+	17610			0.0	0.00	0.00	0.00	0.00
	CD34+CD45RA-EPCR+	17611			0.0	0.00	0.00	0.00	0.00
	CD34+CD45RA-EPCRlow	17612	70.6	2,118	29.8	3.34	23.24	0.00	0.54
	CD34+CD45RA-EPCRlow	17613			12.3	1.02	10.38	0.00	0.12
	CD34+CD45RA-EPCRlow	17614			10.6	0.94	8.75	0.00	0.25
	CD34+CD45RA-EPCRlow	17615			2.2	0.51	1.44	0.00	0.04
	CD34+CD45RA-EPCRlow	17616			13.0	1.37	10.35	0.00	0.25
	CD34+CD45RA-EPCRlow	17617	70.6	706	4.4	3.96	0.22	0.02	0.28
	CD34+CD45RA-EPCRlow	17618			0.3	0.10	0.18	0.00	0.00
	CD34+CD45RA-EPCRlow	17619			31.7	2.88	25.55	0.00	0.32
	CD34+CD45RA-EPCRlow	17620			34.8	5.19	26.31	0.00	0.70
	CD34+CD45RA-EPCRlow	17621			0.8	0.08	0.66	0.00	0.01
	CD34+CD45RA-EPCR-	17622	24.6	739	0.2	0.18	0.00	0.01	0.00
	CD34+CD45RA-EPCR-	17623			0.3	0.19	0.09	0.00	0.01
	CD34+CD45RA-EPCR-	17624			8.1	0.59	6.80	0.00	0.07
	CD34+CD45RA-EPCR-	17625			0.1	0.09	0.01	0.00	0.00
	CD34+CD45RA-EPCR-	17626			0.0	0.00	0.00	0.00	0.00
	CD34+CD45RA-EPCR-	17627	24.6	246	0.0	0.00	0.00	0.00	0.00
	CD34+CD45RA-EPCR-	17628			0.0	0.00	0.00	0.00	0.00
	CD34+CD45RA-EPCR-	17629			0.0	0.00	0.00	0.00	0.00
	CD34+CD45RA-EPCR-	17630			0.1	0.09	0.00	0.00	0.00
	CD34+CD45RA-EPCR-	17631			0.0	0.00	0.00	0.00	0.00

Table S3.5: Limit dilution experiment of uncultured sorted cells (page 1/2).

		wk24 (BM Flush)							
Day0	Name	NSG-ID	percentages at d0	Sorted cells transplanted at d0/NSG	%CD45	%CD33	%CD19	%CD3	%CD34
		CD34+CD45RA-	17562	100	3,000	38.1	6.63	22.71	0.04
	CD34+CD45RA-	17563			43.6	12.21	23.76	0.31	4.05
	CD34+CD45RA-	17564			65.8	18.16	32.70	1.51	7.70
	CD34+CD45RA-	17565			67.7	29.72	27.22	1.22	6.03
	CD34+CD45RA-	17566			13.8	6.20	3.68	1.88	0.73
	CD34+CD45RA-	17567			72.1	15.36	42.97	0.36	5.05
	CD34+CD45RA-	17568			62.9	24.66	23.96	2.45	3.02
	CD34+CD45RA-	17569			36.6	14.24	6.99	11.09	0.84
	CD34+CD45RA-	17570	100	1,000	54.8	10.03	32.93	1.32	3.23
	CD34+CD45RA-	17571			33.2	7.54	16.10	0.00	1.49
	CD34+CD45RA-	17572			50.8	5.79	33.58	1.02	4.88
	CD34+CD45RA-	17573			3.4	0.53	2.63	0.00	0.01
	CD34+CD45RA-	17574			48.6	14.48	19.68	0.10	8.21
	CD34+CD45RA-	17575			12.7	2.46	8.18	0.05	0.99
	CD34+CD45RA-	17576			8.8	0.34	5.02	2.24	0.31
	CD34+CD45RA-	17577			2.1	1.02	0.87	0.00	0.02
	CD34+CD45RA-	17578	100	333	15.2	6.16	7.33	0.02	0.71
	CD34+CD45RA-	17579			0.1	0.09	0.01	0.00	0.00
	CD34+CD45RA-	17580			0.3	0.28	0.01	0.01	0.00
	CD34+CD45RA-	17581			3.1	2.22	0.67	0.02	0.06
	CD34+CD45RA-	17582			1.9	1.88	0.00	0.01	0.01
	CD34+CD45RA-	17583			1.7	1.68	0.00	0.02	0.01
	CD34+CD45RA-	17584			1.0	0.99	0.00	0.00	0.01
	CD34+CD45RA-	17585			1.8	1.78	0.00	0.01	0.02
	CD34+CD45RA-	17586	100	111	1.1	1.06	0.00	0.03	0.02
	CD34+CD45RA-	17587			Dead				
	CD34+CD45RA-	17588			2.6	0.76	1.35	0.00	0.07
	CD34+CD45RA-	17589			0.0	0.00	0.00	0.00	0.00
	CD34+CD45RA-	17590			0.0	0.00	0.00	0.00	0.00
	CD34+CD45RA-	17591			0.0	0.00	0.00	0.00	0.00
	CD34+CD45RA-	17592			0.0	0.00	0.00	0.00	0.00
	CD34+CD45RA-	17593			0.1	0.10	0.00	0.00	0.00
	CD34+CD45RA-	17594	100	37	0.0	0.00	0.00	0.00	0.00
	CD34+CD45RA-	17595			0.0	0.00	0.00	0.00	0.00
	CD34+CD45RA-	17596			10.0	3.20	4.82	0.00	0.36
	CD34+CD45RA-	17597			0.0	0.00	0.00	0.00	0.00
	CD34+CD45RA-	17598			0.0	0.00	0.00	0.00	0.00
	CD34+CD45RA-	17599			0.0	0.00	0.00	0.00	0.00
	CD34+CD45RA-	17600			0.0	0.00	0.00	0.00	0.00
	CD34+CD45RA-	17601			0.0	0.00	0.00	0.00	0.00
	CD34+CD45RA-EPCR+	17602	4.6	138	30.0	1.59	3.18	24.69	0.09
	CD34+CD45RA-EPCR+	17603			39.8	29.93	7.32	0.04	1.55
	CD34+CD45RA-EPCR+	17604			23.5	2.59	13.54	3.06	1.36
	CD34+CD45RA-EPCR+	17605			24.4	2.12	4.93	15.23	0.22
	CD34+CD45RA-EPCR+	17606			65.5	12.51	45.92	0.26	5.24
	CD34+CD45RA-EPCR+	17607	4.6	46	0.0	0.00	0.00	0.00	0.00
	CD34+CD45RA-EPCR+	17608			0.1	0.07	0.02	0.00	0.00
	CD34+CD45RA-EPCR+	17609			1.7	1.38	0.07	0.00	0.07
	CD34+CD45RA-EPCR+	17610			0.0	0.00	0.00	0.00	0.00
	CD34+CD45RA-EPCR+	17611			0.3	0.30	0.00	0.00	0.00
	CD34+CD45RA-EPCRlow	17612	70.6	2,118	83.8	4.69	71.73	0.42	4.61
	CD34+CD45RA-EPCRlow	17613			79.6	6.37	66.23	0.40	3.66
	CD34+CD45RA-EPCRlow	17614			29.2	0.61	0.50	28.27	0.03
	CD34+CD45RA-EPCRlow	17615			0.3	0.28	0.01	0.00	0.00
	CD34+CD45RA-EPCRlow	17616			6.6	0.90	5.28	0.01	0.08
	CD34+CD45RA-EPCRlow	17617	70.6	706	1.7	1.65	0.04	0.00	0.01
	CD34+CD45RA-EPCRlow	17618			0.4	0.39	0.00	0.01	0.01
	CD34+CD45RA-EPCRlow	17619			14.7	7.22	6.20	0.06	0.46
	CD34+CD45RA-EPCRlow	17620			1.3	1.05	0.18	0.02	0.01
	CD34+CD45RA-EPCRlow	17621			0.7	0.27	0.38	0.00	0.00
	CD34+CD45RA-EPCR-	17622	24.6	739	0.5	0.49	0.00	0.01	0.01
	CD34+CD45RA-EPCR-	17623			0.4	0.35	0.04	0.00	0.00
	CD34+CD45RA-EPCR-	17624			50.9	1.53	43.47	0.20	1.83
	CD34+CD45RA-EPCR-	17625			0.2	0.14	0.01	0.00	0.01
	CD34+CD45RA-EPCR-	17626			0.6	0.53	0.01	0.00	0.00
	CD34+CD45RA-EPCR-	17627	24.6	246	0.3	0.29	0.00	0.00	0.00
	CD34+CD45RA-EPCR-	17628			0.2	0.20	0.00	0.00	0.00
	CD34+CD45RA-EPCR-	17629			0.1	0.10	0.00	0.00	0.01
	CD34+CD45RA-EPCR-	17630			0.2	0.20	0.00	0.00	0.00
	CD34+CD45RA-EPCR-	17631			0.1	0.10	0.00	0.00	0.00

Table S3.5: Limit dilution experiment of uncultured sorted cells (page 2/2).

Chapter 4: Discussion and Future Perspective

Contribution: All the data presented in this chapter was generated by Iman Fares except Figure S4.5 which was provided by Jalila Chagraoui.

4.1 Limitation of cord blood HSC transplantation

Allogeneic hematopoietic stem cell (HSC) transplantation is a life-saving procedure for patients with various hematopoietic malignancies. Unfortunately, 30-40% of patients will not have a peripheral blood (PB), or bone marrow (BM) matched donor¹. Cord blood (CB) is a very attractive alternative source of stem cells due to its unique properties resulting in permissive human leukocyte antigen (HLA) mismatches, low incidence of chronic graft-versus-host disease (GVHD) and rapid accessibility². However, the use of CB is limited by the low number of HSCs and progenitors per unit which is frequently insufficient for adult patients, leading to delayed engraftment, increased infections, prolonged hospitalization and early mortality³. Thus, there is a clinical need to define culture conditions that would lead to the expansion of CB-derived stem and progenitor cells.

4.2 UM171 mediates expansion of LT- HSC independent of AhR inhibition

We have identified UM171, a novel small molecule that expands by about one log the long-term-HSCs (LT-HSCs), which repopulate NSG mice up to 30 weeks post-transplantation⁴. This expansion is independent of aryl hydrocarbon receptor (AhR) suppression and requires the continuous presence of UM171 in the growing culture. We also showed that AhR inhibition maintains rather than expands LT-HSCs. This data seems to contrast the results of Boitano et al.⁵ who claims an expansion in LT-HSCs after evaluating NSG repopulation cells at 16 weeks post transplantation, a time frame possibly compatible with cells having short-term repopulating potential⁶. Consistently, we observe that SR1 treatment is as potent as UM171 in expanding CD34⁺ cells and multipotent progenitors but less active in retaining a more primitive phenotype, namely the CD34⁺CD45RA⁻ fraction⁷. Consistent with our findings, SR1 preferentially stimulates the expansion of CD34⁺CD45RA⁺ cells (reference⁸ and Figure 2.2 B) - a progenitor population that lacks long-term repopulating activity (Figures S3.1). Moreover, co-treatment of SR1 and UM171 shows an additive effect on expanding multipotent progenitor cells while the primitive LT-HSCs are mostly responsive to UM171. Transcription profiling of HSPC exposed to SR1 or UM171 reveals only a few commonly regulated genes suggesting that the two molecules differ in their mechanism of action. Unlike SR1, UM171 treatment does not suppress the AhR downstream targets and uniquely shows downregulation of transcripts associated with erythroid and megakaryocyte differentiation. Based on this, we propose a model in which UM171 triggers a pathway that stimulates self-renewal of human LT-HSCs independent of AhR inhibition that is essential for short-term HSCs (Figure 4.1). Of interest, and in line with these results, our group have reported that human leukemia stem cells, believed to be derived from

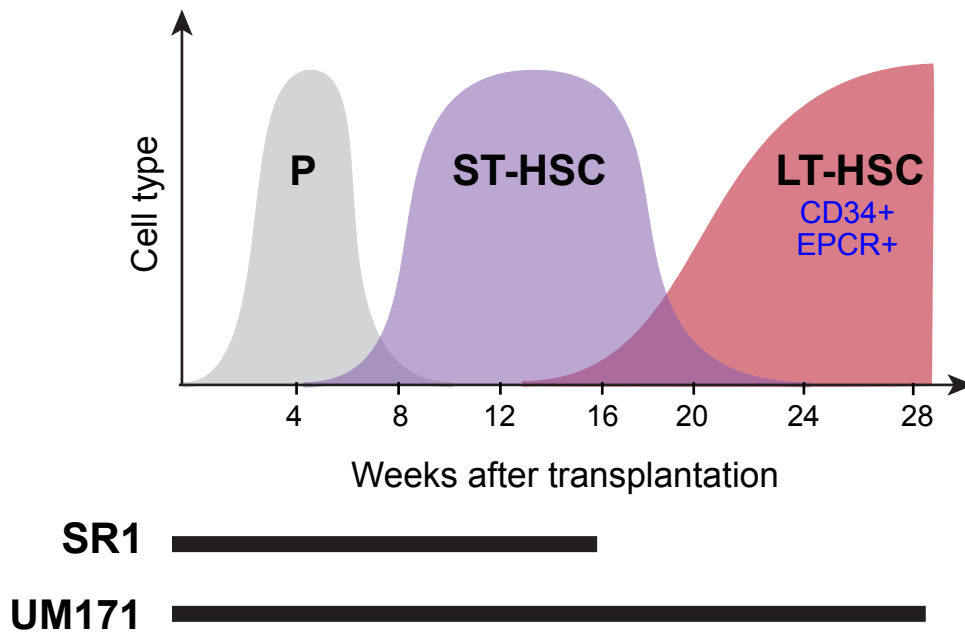


Figure 4.1. Schematic representation showing effects of UM171 and SR1 on different cell population.

UM171 treatment retains the EPCR+HSC phenotype and expands the long-term human engraftment analyzed up to 30 weeks post transplantation. SR1 expands multipotent progenitor cells that sustain blood production up to 16-20 weeks post transplantation. Short-term hematopoietic stem cell (ST-HSC), long-term hematopoietic stem cell (LT-HSC).

a limited pool of self-renewing stem cells or progenitors⁹ mostly respond to SR1 and poorly to a UM171 analog (UM729)¹⁰ (Figure 4.2). A clinical trial of SR1-expanded CB cells has been recently performed. The patients show a faster hematopoietic reconstitution compared to that in the historical cohort (Figure 4.3 C); yet, the SR1 treated unit does not demonstrate any significant improvement in hematopoietic recovery when compared with parallel infused unmanipulated unit in their double CB transplant setting (Figure 4.3 D). Although several molecules besides SR1 have been identified to expand human HSPCs *ex vivo* (Tables 1.5 and 1.6), there remains a need to enhance the efficacy of the expanded graft.

4.3 UM171 applications

The LT-HSC expansion achieved in the cultures supplemented with UM171 could reduce by 10 times the minimal number of cells needed for CB transplantation (CBT)¹¹ (for example lowering cell dose from 2.5×10^7 to 0.25×10^7 nucleated cell/ kg of recipient weight). Thus, CB transplantation of a single unit with the best HLA-matched score will be more feasible after *ex vivo* cell expansion with UM171 and more favorable than the use of two CB units that usually show higher rates of GVHD^{12,13}. This approach will increase the size of the available CB bank inventories and therefore the chance to have a compatible HLA-matched unit, which is associated with favorable clinical outcomes^{1,14}.

HSC gene therapy is one of the most attractive treatments for numerous genetic and acquired disorders. Unfortunately, such treatment shows modest clinical success due to low numbers of transduced stem cells as a result of poor gene transfer or compromised transduced cells^{15,16}. Our group shows that UM171 treatment improves the yield of the transduced CD34⁺CD45RA⁻ cells without losing their long-term repopulating potential (Figure 4.4). Thus, our optimized culture condition may prove useful for HSC transduction in therapeutic gene delivery.

4.4 Chemical manipulation of the hematopoietic system is a powerful tool

Small molecules are very efficient in regulating proteins and pathways at low cost, reduced variability, and minimal risk of tumorigenesis when compared with gene modification, recombinant proteins, and growth factors. The biological activity of small molecules can be (i) tuned by adjusting the concentrations and (ii) optimized by enhancing their stability, solubility, and efficacy^{17,18}. Indeed, UM structure-activity relationship (SAR) analysis allows us to identify more potent analogs achieving similar HSPC expansion with 10-20x less of the initial concentration used. Dropping the dose of UM compound to low nM range (5nM of newly tested analogs) reduces its off-target effects thereby improving its clinical use. Also, small molecules can

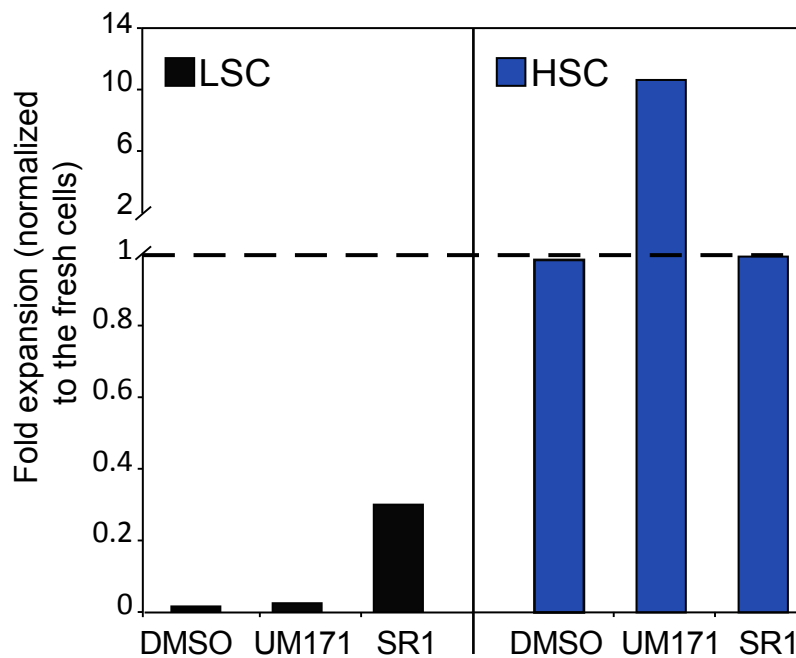


Figure 4.2. Comparing effect of UM171, SR1 and DMSO on hematopoietic stem cell (HSC) and leukemia stem cell (LSC) expansion.

SR1 treatment partially rescues number of LSC compared to their counterparts in fresh (uncultured) cells while UM171 treatment expands HSC. Data of this figure was extrapolated from Pabst et al., 2014 and Fares et al., 2014.

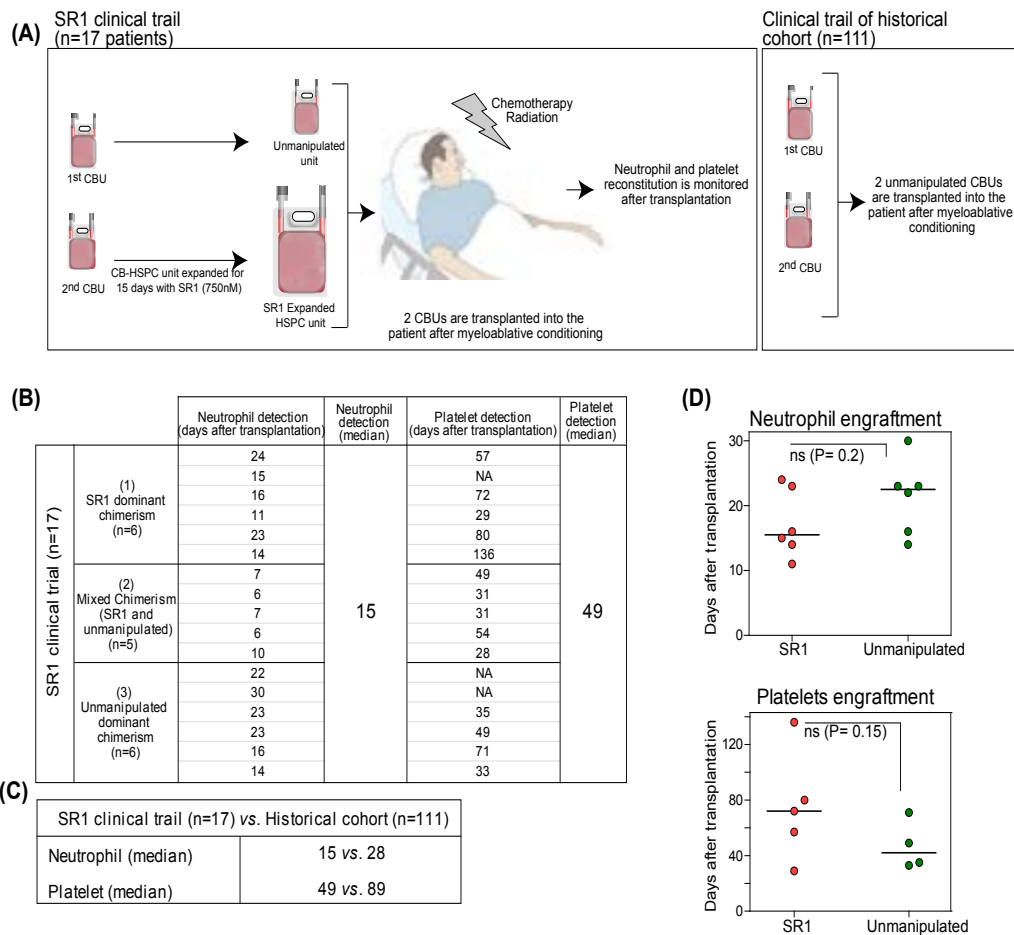


Figure 4.3. Phase I/II trial of StemRegenin-1 (SR1) expanded cord blood HSPC.

(A) Clinical design: 17 patients received double cord blood units (CBU), one expanded by SR1 and another left unmanipulated. Both units were infused into patients with hematological malignancy after receiving myeloablative conditioning. The historical cohort represents patients (n=111) who received two unmanipulated CBUs. (B) Early detection of the donor neutrophil and platelet engraftment in the patients' peripheral blood. Patients were classified into 3 groups: patients who have (1) SR1 dominant chimerism (n=6), (2) mixed chimerism derived from SR1 expanded and unmanipulated unit (n=5), and (3) unmanipulated dominant chimerism (n=6). (C) Comparing hematopoietic engraftment between SR1 clinical trial (n=17) and historical cohort (n=111). When compared with historical cohort, SR1 trial shows faster hematopoietic recovery. (D) Comparing time of neutrophils and platelets engraftment of expanded CBU vs. unmanipulated CBU within SR1 clinical trial, no significant difference between the two units (Mann-Whitney test, one-sided). The horizontal bars represent median values. Each circle represents a patient. Data in this figure was taken from Wagner et al., 2016, Cell Stem Cell 18, 144–155.

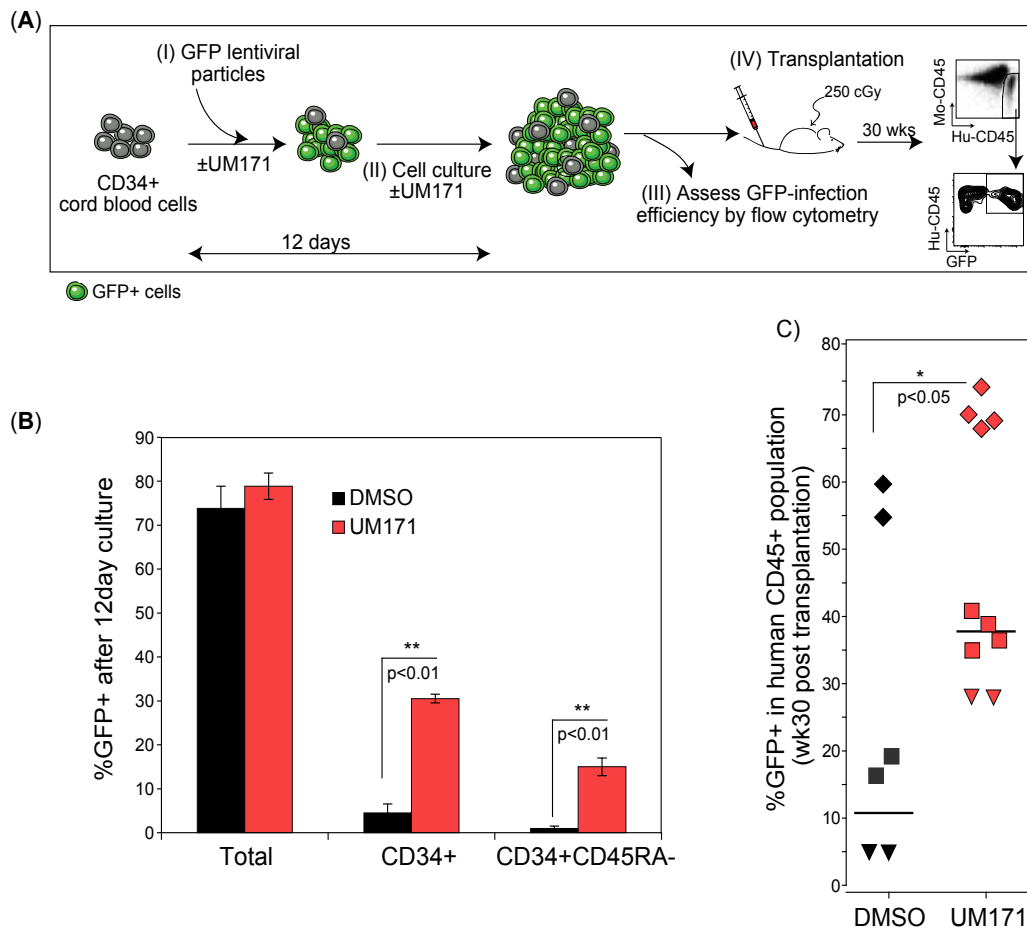


Figure 4.4. UM171 increases lentiviral vector transduction efficiency in human HSPC cells.

(A) CD34+ cord blood cells were pre-stimulated for 48 hours and transduced with GFP lentiviral particles (MOI: 50 or 100 viral particles/ cell) for 12 hours in the presence of vehicle (DMSO) or UM171 (35 nM). Cells then were washed and cultured again in the presence or absence of UM171. Flow cytometry analysis was performed to determine the GFP positive cells within the indicated populations 10 days post-transduction (a total of 12 day-culture). The transduced cells were transplanted into NSG mice to determine their in vivo proliferative potential. Mouse (Mo), human (Hu). (B) Flow cytometry results showing frequency of transduced cells before transplantation experiment. (C) In vivo data showing the frequency of GFP transduced repopulating cells in the NSG bone marrow recipients after 30 weeks of transplantation. Each geometric shape represents different viral envelop and the horizontal bar indicates the median values; significance level * $P < 0.05$ and ** $P < 0.01$ (Mann-Whitney test, one-sided). The complete study is published in a patent application WO2016041080A1.

be combined to enhance the expansion and engraftment of repopulating cells without increasing the culture media and cytokine usage^{19,20}. Although a significant enhancement in HSC activity is observed when these compounds are added, their early hematopoietic recovery is still compromised compared with uncultured cells²¹ suggesting that further HSPC culture optimization is needed.

Transcriptome profiling and functional studies of newly identified HSPC agonists reveal new targets and pathways that regulate stem cell fate²². Although the UM171 mechanism of action is currently under investigation using proteomic and genomic studies, the compound discovery allows us to define the LT-HSCs in culture and determine critical factors for their self-renewal (Chapter 3).

4.5 UM171 treatment induces expression of EPCR, a surface marker that enrich for LT-HSC

EPCR is one of the genes preferentially up-regulated upon UM171 treatment. Cell sorting followed by xenograft transplantations identified EPCR as the first marker that enables the isolation of human LT-HSC in culture. EPCR was previously reported to enrich uncultured mouse bone marrow HSC²³; however, nothing had been described on its application as a method to isolate fresh human HSC. Our data shows that EPCR expression is more efficient in isolating the cultured LT-HSC rather than the fresh LT-HSC.

4.6 EPCR, a stable and reliable LT-HSC surface marker

Most of the HSC surface makers discussed in section 1.5 are not reliable in culture. Their expression changes dramatically upon culturing the cells thus jeopardizing their correlation with HSC activity. For example, cultured cells show dissociation between the expansion of CD34⁺CD38⁻ phenotype and increase in NOD/SCID repopulating cell (SRC) numbers. Moreover, sorted CD34⁺ CD38⁺ cells that contain no SRC activity can become CD34⁺CD38⁻ during *ex vivo* culture leading to a false HSC phenotype read²⁴. CD90 is another example; cells depleted from CD90 acquire expression of this receptor upon culture and show a robust repopulating activity²⁵. Remarkably, EPCR expression is stable in culture and correlates to LT-HSC outputs. EPCR depleted (EPCR^{low/-}) cells do not gain EPCR expression after culture and still poorly engraft immunocompromised mice (Figure 3.3D). Although EPCR depleted cells show similar expansion of CD34⁺ CD45RA⁻CD90⁺ as EPCR⁺ cells, only the latter is enriched with LT-HSC population suggesting that EPCR expression is the most relevant read for HSC activi-

ty. Accordingly, expanded human LT-HSC could be defined by the expression of a single gene product rather than a group of receptors. However, since EPCR is also expressed on differentiated hematopoietic cells such as monocytes and lymphocytes, co-staining with CD34 marker is still mandatory to assure the primitive EPCR cell phenotype. Furthermore, the small fraction of EPCR⁺HSPC shows similar UM171-mediated LT-HSC expansion as unsorted HSPCs (Figure 3.3D) suggesting that the EPCR⁺ population is the major cell subset that responds to HSC expansion *ex vivo*. Consequently, purifying HSC population based on EPCR expression from early-expanded cultures could allow the development of a cost-effective HSPC expansion protocol where less culture media and cytokines are required.

Identifying EPCR as a surrogate surface maker for LT-HSC could replace xenograft transplantation as the gold standard for assaying HSC function, which is labor and time intensive. This discovery could allow not only for quick detection but also for better quantification of LT-HSC since the expansion fold of EPCR⁺ CD34⁺ cells correlates with the numbers of LT-HSC in culture. Accordingly, we expect that EPCR assessment will optimize the high-throughput screen readouts for uncovering novel self-renewing agonists.

4.7 Human and mouse HSCs, similar need during *ex vivo* culture

In chapter 2, we claimed that UM171 at 35 nM-optimal dose used for human HSCs *ex vivo* expansion-does not expand mouse HSCs (Figure S2.4). However, RNA profiling of UM171-treated cells showed an up-regulation of EPCR, one of the most important surface markers that define mouse HSCs. This made us question if the dose of UM171 used was optimal for mouse HSCs *ex vivo* expansion. Indeed, transplantation experiments showed that UM171 has to be used at higher dose (500nM) to be efficient for mouse HSC *ex vivo* expansion (Figure 4.5). This data suggests that mechanism of action of UM171 in expanding HSC is conserved between mice and human.

4.8 Role of EPCR in HSC activity

Functional studies performed with shRNA vectors suggest that EPCR is functionally important for the *in vivo* activity of human HSCs. This observation is consistent with mice studies where EPCR, which is used as a marker to isolate HSC²³, regulates HSC anti-apoptotic activity through EPCR/PAR1 signaling ²⁶. Recent studies show that EPCR/PAR1 pathway regulates EPCR⁺HSC retention and long-term potential in the bone marrow by restricting nitric oxide (NO) production and increasing integrin VLA4 expression. In line with this, mice genetically modified to express low levels of EPCR surface expression (Procr^{low} mice) show defects in HSC

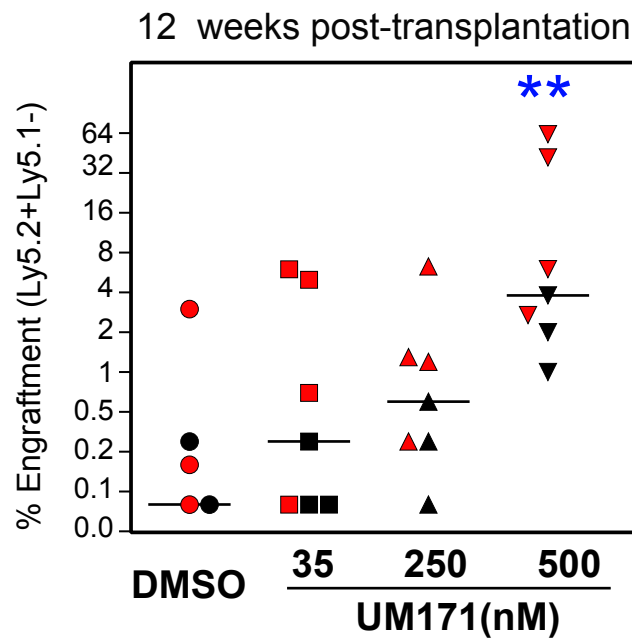


Figure 4.5. UM171 expands mouse HSCs.

KLS-SLAM cells from Ly5.2 mice were expanded for 7 days in the presence of different doses of UM171 (35, 250, 350 nM). Outcome of 15 KLS-SLAM cells were injected into Ly5.1 recipient mice. Engraftment levels were monitored 12 weeks post-transplantation.

bone marrow homing where most of HSCs are detected in blood circulation²⁷. All these findings suggest that EPCR expression is crucial for HSC activity.

4.9 Endothelial-related markers of EPCR⁺ population and origin of HSC

The discovery of EPCR as a human LT-HSC surface marker will have great impact on the study of HSC biology. Recently Prasad et al. showed that EPCR is expressed in human fetal liver HSCs²⁸; thus EPCR expression might be used as a tool to trace the origin of HSCs and reveal their localization in different hematopoietic organs (Figure 1.3). This may highlight the presence of specialized microenvironments that provide vital factors or signals essential for human HSC survival and maintenance. Dissecting these cues may help in generating a further optimized HSC culture condition.

Endothelial antigens mark HSCs particularly at early developmental stages possibly because HSC and endothelial cells emerge from a common precursor, the hemangioblast/ hemogenic endothelium. The expression level of some of these endothelial antigens declines during HSC development especially when they migrate to BM where they become mostly quiescent²⁹. VE-cadherin (CD144) is one example of endothelial specific marker that is expressed transiently in human fetal liver HSCs but not adult bone marrow HSCs³⁰ with an extensive self-renewal hematopoietic potential³¹. Studies in mice revealed that VE-cadherin is predominantly expressed in the fetal liver EPCR⁺HSC and is significantly down-regulated after culture when long-term reconstitution activity of EPCR⁺HSC is lost, suggesting that the self-renewal potential of these cells rely on their surrounding environment, particularly the endothelial microenvironment²⁶. Remarkably, EPCR⁺ fraction retains the expression of numerous endothelial cell molecules including VE-cadherin (Figure 4.6); thus raising the question of whether the endothelial phenotype is crucial for human HSC self-renewal.

4.10 Stemness genetic feature of EPCR population

Transcription profiling shows a striking molecular difference between EPCR^{-low} and EPCR⁺ cells. The genetic makeup that governs the HSC specification and function is highly enriched in EPCR⁺ fraction. Our analysis uncovered the expression of potential stem cell surface marker genes including EMCN³² and LGR5³³ in EPCR⁺ fraction (Table 4.1). These newly identified markers could further enrich for LT-HSC frequency within EPCR⁺ population, possibly achieving LT-HSC detection at single cell resolution. Studying the up-regulated transcription factors in extensive self-renewing EPCR⁺ population (Figure S3.8 and Table S3.6) will provide an

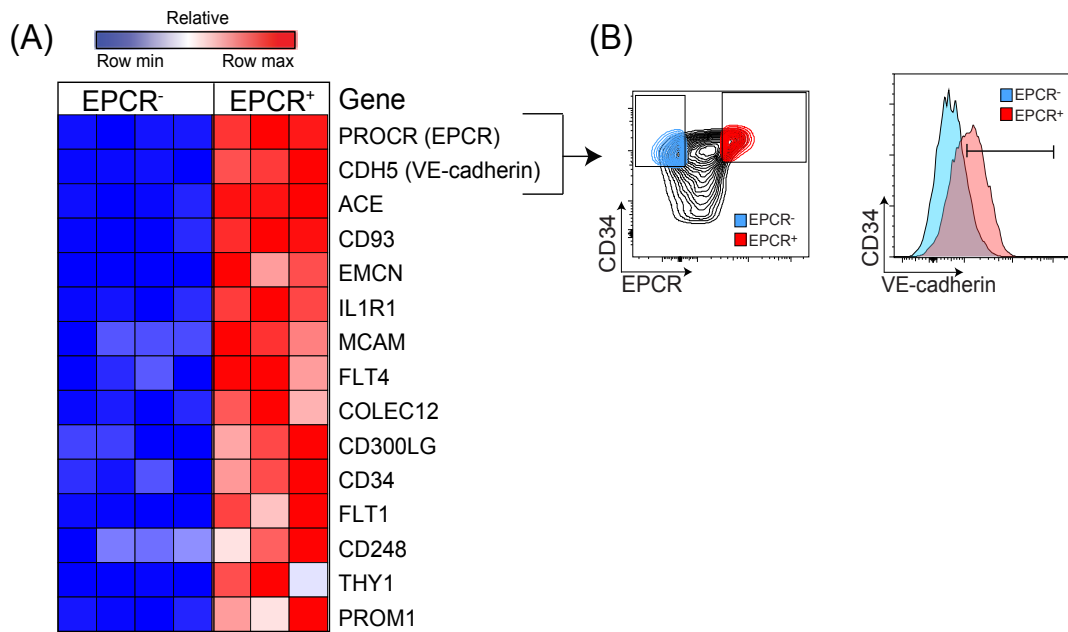


Figure 4.6. EPCR⁺ population retains endothelial phenotype.

(A) Heat map showing relative expression patterns of genes coding for endothelial surface markers. VE-cadherin is up-regulated at mRNA and protein (B) level in EPCR⁺ cells.

Cellular location	Gene	Log ₂ FC (EPCR ⁺ vs EPCR ^{Rest})	Hu-HSC	Mo-HSC	Study	Reference (PMID no.)
Cell membrane	EMCN	6.32	■	■	Endomucin, a CD34-like sialomucin, marks HSCs throughout development.	16314436
	LGR5	5.72	■	■	LGR5-protein-coupled Receptor 5 marks short-term HSPCs during mouse embryonic development.	24966324
	THY1	4.61	■	■	Isolation of a candidate human HSC population.	1372992
	FLT1	4.41	■	■	Autocrine-paracrine VEGF loops potentiate the maturation of megakaryocytic precursors through Flt1 receptor.	12406876
	PROM1	2.77	■	■	AC133, a novel marker for human HSPCs.	9389720
	ITGA3	2.75	■	■	Intermediate-term hematopoietic stem cells with extended but time-limited reconstitution potential.	20074534
	CDH2	2.58	■	■	N-cadherin+ HSCs in fetal liver exhibit higher long-term BM reconstitution activity than N-cadherin- HSCs.	23092738
	TFPI	2.50	■	■	Glypican-3-mediated inhibition of CD26 by TFPI: a novel mechanism in HSC homing and maintenance.	23327927
	DLL1	2.40	■	■	Delta-1 enhances marrow and thymus repopulating ability of human CD34(+)CD38(-) cord blood cells.	12393852
	ACE	2.31	■	■	Angiotensin-converting enzyme (CD143) marks HSCs in human embryonic, fetal, and adult hematopoietic tissues.	17993616
	CDH5	2.10	■	■	VE-cadherin expression allows identification of a new class of HSCs within human embryonic liver.	20693433
PROCR	2.07	■	■	Endothelial protein C receptor (PROCR/ CD201) explicitly identifies hematopoietic stem cells in murine bone marrow.	16304059	
CDCP1	2.03	■	■	CDCP1 is a novel marker for hematopoietic stem cells.	12799299	
Nucleus	HLF	6.08	■	■	Hierarchical and ontogenic positions serve to define the molecular basis of human HSC behavior.	1586615
	PRDM16	2.88	■	■	Prdm16 is a physiologic regulator of HSC. Prdm16 promotes stem cell maintenance in multiple tissues, partly by regulating oxidative stress.	21343612 20835244
	HOPX	2.74	■	■	The genetic landscape of HSC frequency in mice	26050929
	HOXA6	2.72	■	■	Hoxa6 potentiates short-term hemopoietic cell proliferation and extended self-renewal	19157684
	HMGGA2	2.42	■	■	The Lin28b-let-7-Hmga2 axis determines the higher self-renewal potential of fetal HSCs.	23811688
	MECOM	2.36	■	■	Evi1 is essential for HSC self-renewal, & its expression marks hematopoietic cells with LT- multilineage repopulating activity	22084405
	LDB2	2.23	■	■	Nuclear adaptor Ldb1 regulates a transcriptional program essential for the maintenance of HSCs.	21186366
	FGD5	2.00	■	■	Fgd5 identifies HSCs in the murine bone marrow.	24958848

Table 4.1. EPCR+ population is enriched with transcripts coding for surface markers and transcription factors that define and regulate HSC activity.

Fold enrichment of the presented transcripts in the EPCR+ population with reported studies supporting their role in human (Hu) and Mouse (Mo) HSCs. Fold change (FC).

invaluable resource for the genetic program that govern “stemness” in HSCs. Inducing these transcriptional programs in a variety of human cells including hematopoietic progenitor cells, embryonic stem cells, and induced pluripotent cells may convert their fate to fully functional HSCs compatible with therapeutic applications (Figure 1.7).

References

- 1 Ballen, K. K., Gluckman, E. & Broxmeyer, H. E. Umbilical cord blood transplantation: the first 25 years and beyond. *Blood* **122**, 491-498, doi:10.1182/blood-2013-02-453175 (2013).
- 2 Broxmeyer, H. E. Insights into the biology of cord blood stem/progenitor cells. *Cell Prolif* **44 Suppl 1**, 55-59, doi:10.1111/j.1365-2184.2010.00728.x (2011).
- 3 Gluckman, E. History of cord blood transplantation. *Bone Marrow Transplant* **44**, 621-626, doi:10.1038/bmt.2009.280 (2009).
- 4 Fares, I. *et al.* Cord blood expansion. Pyrimidoindole derivatives are agonists of human hematopoietic stem cell self-renewal. *Science* **345**, 1509-1512, doi:10.1126/science.1256337 (2014).
- 5 Boitano, A. E. *et al.* Aryl hydrocarbon receptor antagonists promote the expansion of human hematopoietic stem cells. *Science* **329**, 1345-1348, doi:10.1126/science.1191536 (2010).
- 6 Cheung, A. M. *et al.* Analysis of the clonal growth and differentiation dynamics of primitive barcoded human cord blood cells in NSG mice. *Blood* **122**, 3129-3137, doi:10.1182/blood-2013-06-508432 (2013).
- 7 Majeti, R., Park, C. Y. & Weissman, I. L. Identification of a hierarchy of multipotent hematopoietic progenitors in human cord blood. *Cell stem cell* **1**, 635-645, doi:10.1016/j.stem.2007.10.001 (2007).
- 8 Bouchez, L. C. *et al.* Small-molecule regulators of human stem cell self-renewal. *Chembiochem : a European journal of chemical biology* **12**, 854-857, doi:10.1002/cbic.201000734 (2011).
- 9 Krivtsov, A. V., Feng, Z. & Armstrong, S. A. Transformation from committed progenitor to leukemia stem cells. *Ann N Y Acad Sci* **1176**, 144-149, doi:10.1111/j.1749-6632.2009.04966.x (2009).
- 10 Pabst, C. *et al.* Identification of small molecules that support human leukemia stem cell activity ex vivo. *Nature methods* **11**, 436-442, doi:10.1038/nmeth.2847 (2014).
- 11 Barker, J. N., Scaradavou, A. & Stevens, C. E. Combined effect of total nucleated cell dose and HLA match on transplantation outcome in 1061 cord blood recipients with hematologic malignancies. *Blood* **115**, 1843-1849, doi:10.1182/blood-2009-07-231068 (2010).
- 12 Wagner, J. E., Jr. *et al.* One-unit versus two-unit cord-blood transplantation for hematologic cancers. *The New England journal of medicine* **371**, 1685-1694, doi:10.1056/NEJMoa1405584 (2014).
- 13 Wagner, J. E., Jr., Eapen, M. & Kurtzberg, J. One-unit versus two-unit cord-blood transplantation. *The New England journal of medicine* **372**, 288, doi:10.1056/NEJMc1414419 (2015).

- 14 Gluckman, E. *et al.* Factors associated with outcomes of unrelated cord blood transplant: guidelines for donor choice. *Experimental hematology* **32**, 397-407, doi:10.1016/j.exphem.2004.01.002 (2004).
- 15 Barquinero, J. *et al.* Efficient transduction of human hematopoietic repopulating cells generating stable engraftment of transgene-expressing cells in NOD/SCID mice. *Blood* **95**, 3085-3093 (2000).
- 16 Glimm, H., Oh, I. H. & Eaves, C. J. Human hematopoietic stem cells stimulated to proliferate in vitro lose engraftment potential during their S/G(2)/M transit and do not reenter G(0). *Blood* **96**, 4185-4193 (2000).
- 17 Davies, S. G. *et al.* Stemistry: the control of stem cells in situ using chemistry. *Journal of medicinal chemistry* **58**, 2863-2894, doi:10.1021/jm500838d (2015).
- 18 Xu, T., Zhang, M., Laurent, T., Xie, M. & Ding, S. Concise review: chemical approaches for modulating lineage-specific stem cells and progenitors. *Stem cells translational medicine* **2**, 355-361, doi:10.5966/sctm.2012-0172 (2013).
- 19 Broxmeyer, H. E. & Pelus, L. M. Inhibition of DPP4/CD26 and dmpGE(2) treatment enhances engraftment of mouse bone marrow hematopoietic stem cells. *Blood cells, molecules & diseases* **53**, 34-38, doi:10.1016/j.bcmd.2014.02.002 (2014).
- 20 Chen, X. *et al.* G9a/GLP-dependent histone H3K9me2 patterning during human hematopoietic stem cell lineage commitment. *Genes & development* **26**, 2499-2511, doi:10.1101/gad.200329.112 (2012).
- 21 Miller, P. H. *et al.* Early production of human neutrophils and platelets posttransplant is severely compromised by growth factor exposure. *Experimental hematology*, doi:10.1016/j.exphem.2016.04.003 (2016).
- 22 Lyssiotis, C. A. *et al.* Chemical control of stem cell fate and developmental potential. *Angewandte Chemie* **50**, 200-242, doi:10.1002/anie.201004284 (2011).
- 23 Balazs, A. B., Fabian, A. J., Esmon, C. T. & Mulligan, R. C. Endothelial protein C receptor (CD201) explicitly identifies hematopoietic stem cells in murine bone marrow. *Blood* **107**, 2317-2321, doi:10.1182/blood-2005-06-2249 (2006).
- 24 Dorrell, C., Gan, O. I., Pereira, D. S., Hawley, R. G. & Dick, J. E. Expansion of human cord blood CD34(+)CD38(-) cells in ex vivo culture during retroviral transduction without a corresponding increase in SCID repopulating cell (SRC) frequency: dissociation of SRC phenotype and function. *Blood* **95**, 102-110 (2000).
- 25 Notta, F. *et al.* Isolation of single human hematopoietic stem cells capable of long-term multilineage engraftment. *Science* **333**, 218-221, doi:10.1126/science.1201219 (2011).
- 26 Iwasaki, H., Arai, F., Kubota, Y., Dahl, M. & Suda, T. Endothelial protein C receptor-expressing hematopoietic stem cells reside in the perisinusoidal niche in fetal liver. *Blood* **116**, 544-553, doi:10.1182/blood-2009-08-240903 (2010).
- 27 Gur-Cohen, S. *et al.* PAR1 signaling regulates the retention and recruitment of EPCR-expressing

- bone marrow hematopoietic stem cells. *Nature medicine* **21**, 1307-1317, doi:10.1038/nm.3960 (2015).
- 28 Prashad, S. L. *et al.* GPI-80 defines self-renewal ability in hematopoietic stem cells during human development. *Cell stem cell* **16**, 80-87, doi:10.1016/j.stem.2014.10.020 (2015).
- 29 Mikkola, H. K. & Orkin, S. H. The journey of developing hematopoietic stem cells. *Development* **133**, 3733-3744, doi:10.1242/dev.02568 (2006).
- 30 Kim, I., Yilmaz, O. H. & Morrison, S. J. CD144 (VE-cadherin) is transiently expressed by fetal liver hematopoietic stem cells. *Blood* **106**, 903-905, doi:10.1182/blood-2004-12-4960 (2005).
- 31 Oberlin, E. *et al.* VE-cadherin expression allows identification of a new class of hematopoietic stem cells within human embryonic liver. *Blood* **116**, 4444-4455, doi:10.1182/blood-2010-03-272625 (2010).
- 32 Matsubara, A. *et al.* Endomucin, a CD34-like sialomucin, marks hematopoietic stem cells throughout development. *The Journal of experimental medicine* **202**, 1483-1492, doi:10.1084/jem.20051325 (2005).
- 33 Barker, N. *et al.* Identification of stem cells in small intestine and colon by marker gene Lgr5. *Nature* **449**, 1003-1007, doi:10.1038/nature06196 (2007).

Conclusion

We identified a small molecule named UM171 that expands human cord blood hematopoietic stem cell (HSC) *ex vivo* by more than 10-folds. This expansion is independent of aryl hydrocarbon suppression, a pathway that is implicated in expanding hematopoietic cells with less extensive self-renewal ability.

Using UM171, we were able to identify endothelial protein c receptor (EPCR) as a first reliable surface marker that enriches for human HSC in culture. We showed that EPCR⁺ cells selectively exhibit a robust multi-lineage and serial reconstitution capacity in immune-compromised mice, demonstrating the high reliability of this stem cell marker on the surface of cultured HSCs, a feature not found with previously described markers. Remarkably, although EPCR⁻ subsets exhibit striking similarity with the bulk expanded cells in displaying a surface immunophenotype associated with human HSC such as CD45RA⁻ CD34⁺ CD90⁺ CD133⁺, they are functionally different and show poor *in vivo* proliferative outcomes confirming that EPCR expression is restricted to HSC compartment.

In summary, the UM171 expanded-HSC population retains EPCR expression, a unique surface marker that correlates with HSC activity in culture. These findings are valuable for clinical and research applications to optimize further the HSPC purification and expansion protocols and understand the molecular machinery that governs the HSC self-renewal. Finally, our data open new avenues for the therapeutic use of stem cell transplantation providing hope for patients with detrimental blood disorders.